LASI | VI | Neuquén Basin

THE PHYSICAL GEOLOGY OF SUBVOLCANIC SYSTEMS – LACCOLITHS, SILLS AND DYKES

Malargüe, Argentina – November 25-29, 2019

ABSTRACTS

CONICET · AGA · CHOIQUE TURISMO ALTERNATIVO E.V.y T. Leg. 12997. Res. 0389/06 · Y-TEC YPF TECNOLOGÍA · MALARGÜE · FUNDACIÓN WILLIAMS · AGENCIA NACIONAL DE PROMOCIÓN CIENTÍFICA Y TECNOLÓGICA · NJORD

Cover photographs

Top: andesitic sills (brown cliffs) emplaced in organic-rich shale, El Manzano, Mendoza, Argentina (O. Galland)

Bottom: oil pump of the Río Grande Valley oil field, Mendoza, Argentina (O. Galland)

LASI | VI | Neuquén Basin

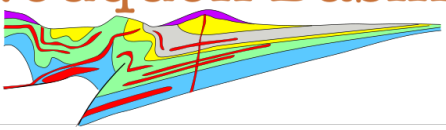

LASI6 – The Physical Geology of Subvolcanic Systems – Laccoliths, Sills and Dykes

Malargüe, Argentina –
November 25th-29th, 2019

Edited by
Olivier Galland, José Mescua, Octavio Palma

LASI | VI | Neuquén Basin

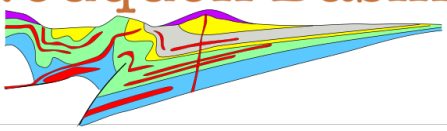

Organizing committee

Chair: Olivier Galland

Members: Héctor A. Leanza, Karen Mair, Graciela Marín, José Mescua, Octavio Palma

Scientific committee

Steffi Burchardt, Dougal Jerram, Sverre Planke, Patricia Sruoga

Foreword

The LASI conferences gather scientists in volcanology, tectonics, structural geology, petrology, geochemistry, geochronology, geophysics, exploration geology, and modelers. Since 2002, the open LASI community gathers scientists interested in shallow-level tabular igneous intrusions. Five international conferences have been held since then, each one with 40-50 participants from 10-17 countries, presenting papers and attending a field trip on tabular intrusions. The conferences highlighted the vitality of this research community as well as the relevance of the topic to societal needs such as hydrocarbon and ore mineral exploration, natural hazards, and climate change.

It has been already seven years since the former LASI meeting, held in the Karoo Basin, South Africa, during October 2012. It was a very successful meeting followed by an exceptional field trip through the extensive doleritic sills of the Karoo Large Igneous Province and their associated hydrothermal vent complexes. Back then, there were discussions about where the 6th LASI meeting would take place. Among several ideas, the Neuquén Basin already appeared as a potentially highly relevant localion. Nevertheless, even if there was overall knowledge about potential outcrops to visit during a field excursion, we lacked robust research results to make a scientifically relevant and coherent field excursion. It was thus too premature to plan a meeting in a part of the world that is so far away from Europe and North America.

Fortunately from 2014, several research projects involving fieldwork in the Neuquén Basin were funded. The first of all was a CONICET PhD grant to Juan Spapacan, followed a year later by a Y-TEC PhD grant to Octavio Palma, thanks to the great efforts of Héctor A. Leanza. In parallel, two large projects were funded by the Norwegian Research Council, each of them involving a PhD student and a postdoc. This building team of talented and enthusiastic young scientists has been the foundation of ambitious field expeditions in several parts of the Neuquén Basin.

In addition, the Neuquén Basin is a peculiar part of the world were volcanic plumbing systems are essential components of producing hydrocarbon fields. This has been known for many years, but very few research results were available in the literature. However, from 2015 the impacts of volcanism on petroleum systems became a highly relevant theme among the national Argentinian oil company YPF and a brand-new national petroleum-related research institute Y-TEC. Since then, we established research collaborations with YPF and Y-TEC, with access to scientifically invaluable subsurface data of oil-producing sills in the southern Malargüe area.

The LASI6 meeting builds on these recent research results, which considerably expanded our knowledge of the geology of volcanic plumbing systems in the Neuquén Basin and their petroleum implications. We feel very happy and proud to welcome you all in Malargüe, the northern gate to the wonderful geology of the Neuquén Basin, and to share the recent scientific knowledge we built since the LASI V meeting.

Olivier Galland, Octavio Palma, José Mescua, Karen Mair, Héctor Leanza

LASI VI Conference Program – Neuquén Basin 2019

"The physical geology of subvolcanic systems: laccoliths, sills and dykes"

Malargüe, Mendoza province (24-29.11)

Sunday 24 November

08.00	*Departure from Malargüe for the Payunia pre-conference excursion for registered participants.*
20.00	*Icebreaker and diner at the hotel.*

Monday 25 November

08.30-09.00	Galland – Welcome, introduction and logistics of LASI6 in the Neuquén Basin
09.00-10.30	***Case studies - Dykes, sills laccoliths and sub-volcanic complexes (chair: J. Mescua)***
Sigmundsson	Studies of active volcanic plumbing systems: Lessons learned from recent magmatic activity in Iceland (*keynote*)
Rivas Dorado	Subsurface geometry and emplacement conditions of a giant dike system in the Elysium Volcanic Province, Mars
Browning	Influence of normal-faults on magma propagation with examples from the Hafnarfjall caldera, Iceland, and Santorini, Greece
Waitchel	The Taió plumbing system (Paraná-Etendeka igneous province, Southern Brazil)-Mapping, petrography and geochemistry
Oliveira	Structural framework of the tholeiitic and alkaline intrusive bodies on the onshore border of the Campos and Santos basins
10.30-11.00	*Break*
11.00-12.30	***Case studies - Dykes, sills laccoliths and sub-volcanic complexes (chair: O. Palma)***
Dini	Emplacement of multiple granite intrusions and triggering of geothermal systems (Larderello, Tuscany): new insights from zircon petrochronology
Mattsson	Magmatic fabrics related to different growth stages of the Cerro Bayo Cryptodome, Chachahuén volcano, Argentina
Rhodes	Insights into the magmatic processes of shallow, silicic storage zone: Reyðarártindur Pluton, Iceland
Ruz Ginouves	Field observations and numerical models of a Pleistocene-Holocene feeder dike swarm associated with a fissure complex to the east of the San Pedro-Pellado complex, Southern Volcanic Zone, Chile
Galetto	Structural characterization of the western flank of Domuyo volcano and its relationship with Neogene to Quaternary magmatic activity (Neuquén, Argentina)

Millet	Top down or bottom up: identification and implications of invasive lavas versus shallow intrusions in sedimentary basins
12.30-13.30	*Lunch break*
13.30-15.30	***Poster session (chair: C. Breitkreuz)***
15.30-16.00	*Break*
16.00-17.30	***Subsurface imaging of plumbing systems (chair: S. Planke)***
Bischoff	Seismic Reflection Imaging of Volcano Plumbing Systems in Sedimentary Basins (*keynote*)
Köpping	Sill emplacement in the Exmouth Basin, NW Australia: The influence of host rock lithology and pre-existing structures on sill segmentation
Oliveira	Sill emplacement mechanisms and their relationship with the Pre-Salt stratigraphic framework of the Libra Area (Santos Basin, Brazil)
Michelon	Distribution and volume of Mesozoic intrusive rocks in the Parnaíba Basin constrained by well data
Manton	Hydrothermal venting in sedimentary basins: similarities between ancient and modern (Møre Basin, Norway and Java, Indonesia)

Tuesday 26 November

09.00-10.30	***Modelling sub-volcanic systems (chair: A. Zanella)***
Kavanagh	Laboratory modelling of sill and dyke emplacement (*keynote*)
Poppe	Magma-induced deformation of the Earth's upper crust in nature and in laboratory experiments scanned by X-ray Computed Tomography
Schmiedel	Coulomb failure of Earth's brittle crust controls growth, emplacement and shapes of igneous sills, saucer-shaped sills and laccoliths
Wallner	Numerical modelling towards fast melt transport in magmatic continental crust via dykes
Annen	Volcano plumbing systems envisioned as complex dynamic networks
10.30-11.00	*Break*
11.00-12.15	***Contact metamorphism and associated mineralization (chair: G. Marín)***
Rubinstein	Controls on porphyry style mineralization in continental arc settings *(keynote)*
Gaspar	Complex metamorphic and metasomatic processes and products: preliminary mineralogical assemblages from Irati Fm and Serra Geral intrusions (Stavias Quarry, Rio Claro SP, Brazil)
Kangxu	Metamorphism of pre-salt limestones produced by Santonian-Campanian alkaline sills in the Libra Block, Santos Basin
Iyer	Sill driven fluid circulation and hydrothermal venting in sedimentary basins
12.15-13.30	*Lunch*
13.30-15.30	***Poster sessions (chair: S. Rocchi)***
15.30-16.00	*Break*

16.00-16.30	***Contact metamorphism and associated mineralization (chair: D. Jerram)***
Paez	When mining saves the day: Studying emplacement processes of subvolcanic bodies in poorly outcropping volcanic terrains (*keynote*)
16.30-17.45	***Petroleum implications of sub-volcanic complexes (chair: D. Jerram)***
Aragao	Intrusion-Related Source Rock Maturation in the Parnaíba Basin, Brazil, and Implications for the Petroleum System
Lopez	Geochemical and mineralogical effects of basic sills on siliciclastic sediments of the Palaeozoic Parnaíba basin: implications for hydrocarbon reservoirs (NE, Brazil)
D'Angiola	Subsurface identification and characterization of volcanic bodies in non-conventional Vaca Muerta reservoir using borehole resistive images, Neuquen Basin, Argentina
Palma	The atypical igneous Petroleum System of the Cara Cura range, southern Mendoza province, Argentina
Rebori	An Exploratory History of Igneous Reservoirs in the Rio Grande Valley, Malargüe, Argentina
17.45-20.00	***More poster sessions, empanadas and vino***

Wednesday 27 November

Field excursion Day 1. Departure from and return to Malargüe.

Thursday 28 November

Field excursion Day 2. Departure from and return to Malargüe.

Friday 29 November

Field excursion Day 3. Departure from Malargüe, arrival at San Rafael at ca. 18:00.

LASI VI Poster Program

"The physical geology of subvolcanic systems: laccoliths, sills and dykes"

Malargüe, Mendoza province (24-29.11)

Case studies - Dykes, sills laccoliths and sub-volcanic complexes

Almeida et al.	Kinematic and dynamic criteria for dyke emplacement: the case of Early Cretaceous dykes swarms in southeastern Brazil and southwestern Africa
Araujo et al.	Mode of emplacement of shallow igneous bodies in the Malargüe fold and thrust belt, Mendoza
Benítez et al.	Geochemistry of igneous silicic rocks of the Martín García Island, Río de la Plata Craton, Argentina
Benitez	Emplacement mechanism of igneous sheet intrusions: A case study in the Malargüe Fault and Thrust Belt and analogue modeling
Brauner and Breitkreuz	Caldera-forming magmatic systems in Late Paleozoic Central Europe – the subvolcanic perspective
Browning et al.	Insights on carbonatite-related magma propagation, degassing and conduit conditions from an exponentially well-exposed dike swarm in Catalão, Brazil
Cellier and Juliani	Characterization of the Paleoproterozoic volcanism in the south area of Tapajós Mineral Province, Amazonian Craton
Chistyakova et al.	Did dolerite sill emplacement pre-date basaltic volcanism in the Karoo Igneous Province, South Africa?
Clunes et al.	Interactions between folded crustal segments and magma propagation with examples from the Central Andes
Espinosa Leal and Salas	Cenozoic Basement and its relationship with the emplacement of mafic monogenetic volcanoes, Cerro Negro: A structural view (TSVZ, Chile)
Galland et al.	Laccolith-induced deformation – A case study integrating field mapping, 3D seismic and well data at Pampa Amarilla, Neuquén Basin, Argentina
Gauer Pascualon et al.	Alkaline dykes of the Trindade Complex (Trindade Island, Brazil): field and petrographic aspects
Giro Cardoso et al.	The Gondwana break-up interpreted by tectonics emplacements of tholeiitic dykes in the central segment of the South American continental margin
Gomez Figueroa	Sills in the evaporites of the Miembro Troncoso Superior, Neuquén Basin, Malargüe, Argentina
Gorden and Cruden	Where did the Jurassic dolerites of Tasmania come from?
Gressier et al.	Two case studies of peperites from Chile: Los Molles, V Región de Valparaíso, (~32°14′S) y Puerto Ingeniero Ibañez (~46°17'S), Región de Aysén
Kjenes et al.	Architecture and morphology of mafic sills: Field observations from San Rafael Swell, Utah, US

Contact metamorphism and associated mineralization

Petroleum implications of sub-volcanic complexes

About Malargüe Area

The Pierre Auger Astrophysics Observatory

Malargüe hosts the international **Pierre Auger Observatory,** which is a cosmic ray observatory in Argentina designed to detect ultra-high-energy cosmic rays: sub-atomic particles traveling nearly at the speed of light and each with energies beyond 10^{18} eV. In Earth's atmosphere such particles interact with air nuclei and produce various other particles. These effect particles (called an "air shower") can be detected and measured. But since these high energy particles have an estimated arrival rate of just 1 per km^2 per century, the Auger Observatory has created a detection area of 3,000 km^2 — the size of Rhode Island, or Luxembourg — in order to record a large number of these events. It is located in the western Mendoza Province, Argentina, near the Andes.

The road between San Rafael and Malargüe crosses a 1500 m high, almost perfectly flat plateau, called Pampa Amarilla (the Yellow Flat). This flat plateau is the pillar of the detection area, on which 1660 particle detector stations have been deployed along a giant regular array. The detector stations are about 1.5 km apart. Each surface detector consists of a water tank of 12,000 liters. The high energy particles interact with water, which produces Cherenkov light as a result of electromagnetic shock waves, which can be measured by photomultipliers tubes mounted on the tanks. Other detectors are “fluorescence detectors”, which pick up on the ultraviolet light emitted when cosmic particles interact with nitrogen in the Earth’s atmosphere.

On both sides of the road from San Rafael, it is possible to spot the detectors, which extends over long lines through the Pampa. In Malargüe, the observatory is located just in front of the conference center that hosts the LASI6 meeting, and it can be visited. We recommend taking a few minutes to go and have a look. This year, the observatory celebrates its 20th anniversary, and the festivities will take place a few days before LASI6. More infor on the observatory can be found here: https://www.auger.org.

Uruguayan Air Force Flight 571

The Malargüe area hosted a dramatic event of human history with the crash of the Uruguayan Air Force Flight 571 on the flanks of Cerro Sosneado. **Uruguayan Air Force Flight 571** was a chartered flight that crashed on a glacier in the remote Andes in 1972. Among the 45 people on board, 28 survived the crash. Facing starvation and death, the survivors reluctantly resorted to cannibalism. After 72 days on the glacier, 16 people were rescued.

The flight, carrying 19 members of the Uruguayan rugby team, family, supporters, and friends originated in Montevideo, Uruguay and was headed for Santiago, Chile. While crossing the Andes, the inexperienced co-pilot who was in command mistakenly believed they had reached Curicó, Chile, despite instrument readings that indicated otherwise.

On the tenth day after the crash, the survivors learned from a transistor radio that the search had been called off. Faced with starvation and death, those still alive agreed that should they die, the others might consume their bodies in order to live. With no choice, the survivors ate the bodies of their dead friends. Seventeen days after the crash, 27 remained alive when an avalanche filled the rear of the broken fuselage they were using as shelter, killing eight more survivors.

The survivors had little food and no source of heat in the harsh conditions. They decided that a few of the strongest people would hike out to seek rescue. Sixty days after the crash, passengers Nando Parrado and Roberto Canessa, lacking mountaineering gear of any kind, climbed from the glacier at 3,570 metres (11,710 ft) to the 4,670 metres (15,320 ft) peak blocking their way west. Over 10 days they trekked about 38 miles (61 km) seeking help. The first person they saw was Chilean *arriero* Sergio Catalán, who gave them food and then rode for ten hours to alert authorities. The story of the passengers' survival after 72 days drew international attention. The remaining 14 survivors were rescued on 23 December 1972, more than two months after the crash.

The survivors were concerned about what the public and family members of the dead might think about their acts of eating the dead. There was an initial public backlash, but after they explained the pact the survivors made to sacrifice their flesh if they died to help the others survive, the outcry diminished and the families were more understanding. The incident was later known as the **Andes flight disaster** and, in the Hispanic world, as *El Milagro de los Andes* (**The Miracle of the Andes**).

View of Cerro El Sosneado (left peak, 5169 m) from National Road 40 between San Rafael and Malargüe. The Uruguayan Air Force Flight 571 crashed behind the mountain, where remnants of the plane can be found. El Sosnenado is the southernmost “5000 m” peak in the world.

Information about the conference

Date	Travel information	Comments
Sat 23 Nov	Arrival, Malargüe (optional)	Optional: Payunia pre-conference trip (departure 8:30 am)
Sun 24 Nov	Arrival, Malargüe	Ice breaker and dinner from 20.00
Mon 25 Nov	Conference day 1	Conference and meals at conference center, conference diner outside town
Tue 26 Nov	Conference day 2	Conference and meals at conference center, diner outside restaurant
Wed 27 Nov	Field trip day 1	Departure 8.30. Return to Malargüe in the evening
Thu 28 Nov	Field trip day 2	Departure 8.30. Return to Malargüe in the evening
Fri 29 Nov	Field trip day 3	Departure 9.30 from Malargüe with luggages. Drive to San Rafael late afternoon (18:00). Each individual has to organize own accommodation and/or travel in San Rafael.

Accommodation information

Hotel Malargüe Inn & Suite
Av. San Martin norte 1230
5613 Malargüe, Mendoza
Web: http://hotelmalarguesuite.com
Email: reservas@hotelmalarguesuite.com
Tel.: +54 9 0260-4472300

Facilities: swimming pool, sauna, gym, bar, restaurant, landry

Conference center information

Conference and Exhibition Center Thesaurus
Pasaje la Orteguina
Av. San Martín Norte
Malargüe, Argentina

The Thesaurus center is at walking distance (10 min) from the hotel. There is no shuttle scheduled between hotel and conference center, unless special needs.

General information

- At Buenos Aires airport, do not use random taxi. Instead, use what is called “servicio de remis” desks, which are the exit of the luggage claim at the airport. There, you pay in advance after giving the address of the hotel, and the driver brings you to his car.
- Check ***vaccination*** guidelines provided by your own countries. However, we have not experienced problems with sickness or food poisoning on previous

field trips.

- Field trip will be by a minibus with driver that fits 20 people. All food and accommodation is provided during the trip. Please pack in soft bags, which make it easier to pack the cars.
- Olivier Galland is responsible for logistics and safety during the trip. Please notify him if you have any safety concerns or require specific medication or diet (and especially if you are ***vegetarian or vegan***!). Olivier will bring first aid equipment. No difficult hikes or climbs will be attempted. Wild animals and snakes are rarely encountered in the field area. There is no aware human safety problem in the field area. In Buenos Aires, conversely, be particularly aware of fast traffic, and never walk alone at night.
- The ***weather conditions*** will hopefully be nice, but may change rapidly: expect any weather, from snow to very warm. Please bring warm and waterproof cloths, good hiking boots, a small day pack, and sun hat and sun screen. If you are sensitive to wind, bring painkillers for headaches. Importantly, the soils are very loose and sandy with small gravels. Because there will be walks, please make sure that your trousers cover your boots to avoid having sand and gravels in them. If not, think of brining ***gaiters***.
- Electricity: 220V, 50 Hz. European plugs normally cannot be used, so should you can buy adaptors in Buenos Aires or at the airport.
- GSM mobile phones can be used in most of Argentina, but commonly not in the field.

Conference participants

Participants	Affiliation	COUNTRY	Email
Almeida, Julio	Rio de Janeiro State University	BRAZIL	jchalmeida@gmail.com
Alvarez, Pablo Fernando	YPF	ARGENTINA	pablo.alvarez@ypf.com
Annen, Catherine	Université Savoie Mont-Blanc	FRANCE	Catherine.Annen@univ-savoie.fr
Aragao, Fernando	Eneva S.A.	BRAZIL	fernando.aragao@eneva.com.br
Arai, Mitsuru	UNESP/UNESPetro	BRAZIL	arai2015sp@yahoo.com.br
Araujo, Vanesa	Universidad Nacional del Sur	ARGENTINA	vane32.va@gmail.com
Argento, Jorge	UNCUYO	ARGENTINA	jorge.a.argento@gmail.com
Barandica, Martin	Crown Point Energy	ARGENTINA	mbarandica@crownpointenergy.com
Bischoff, Alan	University of Canterbury	NEW ZEALAND	alan.bischoff@canterbury.ac.nz
Brauner, Jacob	TU Bergakademie Freiberg	GERMANY	Jacob.Brauner1@geo.tu-freiberg.de
Breitkreuz, Christoph	TU Bergakademie Freiberg	GERMANY	Christoph.Breitkreuz@geo.tu-freiberg.de
Browning, John	Pontificia Universidad Catolica de Chile	CHILE	jbrowning@ing.puc.cl
Candido, Aladino	Eneva S.A.	BRAZIL	alexandre.vilela@eneva.com.br
Castaño, Ana Rosa	ICES Malargüe	ARGENTINA	anaro95@hotmail.com
Castresana, Clemente Perez	Crown Point Energy	ARGENTINA	cpcastresana@crownpointenergy.com
Cattaneo, Diego	YPF/UNC	ARGENTINA	diego.m.cattaneo@ypf.com
Chiacchiera, Sabina	Universidad Nacional de Río Negro	ARGENTINA	sabina.chiacchiera@gmail.com
Chistyakova, Sofia	Wits University	SOUTH AFRICA	Sofia.Chistyakova@wits.ac.za
Clunes, Matías	Pontificia Universidad Catolica de Chile	CHILE	mclunes@uc.cl
Costa de Oliveira, Leonardo	Petrobras	BRAZIL	leogeo.oliveira@petrobras.com.br
D'Angiola, Marta	Weatherford Argentina - IES	ARGENTINA	marta.dangiola@weatherford.com
De la Cal, Hernán	Roch S.A.	ARGENTINA	hdelacal@roch.com.ar
Del Mouro, Lucas	Universidade de Santa Catarina	BRAZIL	lucas.delmouro@gmail.com
Dering, Gregory	University of Western Australia	AUSTRALIA	gregory.dering@research.uwa.edu.au
Dini, Andrea	Istituto di Geoscienze e Georisorse-CNR	ITALY	a.dini@mac.com
Espinosa Leal, Javier Andrés	University of Concepción	CHILE	jaespinosa@udec.cl
Fernandes Lima, Evandro	Federal University of Rio Grande do Sul	BRAZIL	eflgeologo@gmail.com
Galetto, Antonella	Universidad de Buenos Aires	ARGENTINA	antogaletto@gmail.com
Galland, Olivier	University of Oslo	NORWAY	olivier.galland@geo.uio.no
Gaspar, Jose Carlos	UNESP RC	BRAZIL	josecarlosgaspar@gmail.com
Giro Cardoso, João	Universidade do estado do Rio de Janeiro	BRAZIL	jp.geol2012@gmail.com
Gordon, Andrés	AGGEO & UERJ	BRAZIL	acgordon@ymail.com
Gressier, Jean-Baptiste	Universidad Andrés Bello de Santiago	CHILE	jean.b.gressier@gmail.com
Guedes, Eliane	Museu Nacional/UFRJ	BRAZIL	eguedes@mn.ufrj.br
Guldstrand, Frank	University of Oslo	NORWAY	f.b.b.guldstrand@geo.uio.no
Homewood, Peter	UNESPetro	FRANCE	pwhomewood@yahoo.fr
Iyer, Karthik	GeoModelling Solutions GmbH	SWITZERLAND	karthik.iyer@geomodsol.com
Jerram, Dougal	University of Oslo/DougalEarth	UNITED KINGDOM	dougal@dougalearth.com
Kangxu, Ren	CNODC Brasil	CHINA	renkangxu@cnpcla.com.br
Kavanagh, Janine	University of Liverpool	UNITED KINGDOM	Janine.Kavanagh@liverpool.ac.uk
Kjenes, Martin	University of Bergen	NORWAY	Martin.Kjenes@uib.no

Kjøll, Hans Jørgen	University of Oslo	NORWAY	h.j.kjoll@geo.uio.no
Köpping, Jonas	Monash University	AUSTRALIA	jonas.kopping@monash.edu
Latypov, Rais	Wits University	SOUTH AFRICA	Rais.Latypov@wits.ac.za
Licitra, Diego Tomas	YPF	ARGENTINA	diego.licitra@ypf.com
Lombardo, Ezequiel	Chevron	ARGENTINA	EzequielLombardo@chevron.com
Lopes, Henrique Araujo	Eneva S.A.	BRAZIL	lopes.henrique04@gmail.com
Manton, Ben	VBPR	NORWAY	ben@vbpr.no
Marín, Graciela	Asociación Geológica Argentina	ARGENTINA	gramarin2018@gmail.com
Masarik, Maria Christina	Chevron	ARGENTINA	mmsr@chevron.com
Mattsson, Tobias	Uppsala University	SWEDEN	tobias.mattsson@geo.uu.se
Medialdea, Adrian	YPF	ARGENTINA	adrian.medialdea@ypf.com
Mescua, Jose	CONICET	ARGENTINA	jmescua04@yahoo.com.ar
Mettraux, Monique	UNESPetro	FRANCE	moho1959@yahoo.fr
Michelon, Diogo	Eneva S.A.	BRAZIL	diogo.michelon@eneva.com.br
Millet, John	VBPR UK	UNITED KINGDOM	john.millett@vbpr.no
Oliveira, Maria Jose Resende	Petrobras	BRAZIL	mjoliveira@petrobras.com.br
Orozco, Paola	Universidad Nacional de San Juan	ARGENTINA	paola.orozco@unsj-cuim.edu.ar
Páez, Gerardo	CONICET	ARGENTINA	gerardo.paez.unlp@gmail.com
Palma, Octavio	Y-TEC	ARGENTINA	octavio.palma@ypftecnologia.com
Pedró, Estefania	Y-TEC	ARGENTINA	estefania.pedro@ypftecnologia.com
Planke, Sverre	VBPR	NORWAY	planke@vbpr.no
Poppe, Sam	Vrije Universiteit Brussel	BELGIUM	Sam.Poppe@vub.be
Rabbel, Ole	University of Oslo	NORWAY	ole.rabbel@geo.uio.no
Reborí, Luis	Searcher Seismic	ARGENTINA	l.rebori@searcherseismic.com
Rhodes, Emma	Uppsala University	SWEDEN	emma.rhodes@geo.uu.se
Rivas Dorado, Samuel	Universidad Complutense de Madrid	SPAIN	samuelrivas@ucm.es
Rocchi, Sergio	Università di Pisa	ITALY	sergio.rocchi@unipi.it
Rubinstein, Nora	University of Buenos Aires	ARGENTINA	narubinstein@gmail.com
Ruz Ginouves, Javiera	Pontificia Universidad Católica de Chile	CHILE	jnruz@uc.cl
Salvioli, Melisa	Universidad Nacional de La Plata	ARGENTINA	melisa_salvioli@hotmail.com.ar
Sanchez, Natalia	Universidad Nacional del Sur	ARGENTINA	natalia.sanchez@uns.edu.ar
Scaglia, Fernando	Universidad de la República	URUGUAY	scagliageo@gmail.com
Schmiedel, Tobias	Uppsala University	SWEDEN	tobias.schmiedel@geo.uu.se
Senger, Kim	University Centre in Svalbard	NORWAY	Kim.Senger@UNIS.no
Serra Varela, Samanta	Universidad Nacional de Río Negro	ARGENTINA	s.serravarela@gmail.com
Sigmundsson, Freysteinn	University of Iceland	ICELAND	fs@hi.is
Silveira de Miranda, Frederico	Eneva S.A.	BRAZIL	frederico.miranda@eneva.com.br
Souza de Silveira, Lilan	Eneva S.A.	BRAZIL	lilian.souza@eneva.com.br
Suarez, Manuel	Universidad Andrés Bello de Santiago	CHILE	suarezpatagonia@gmail.com
Vallejo, Maria Dolores	Chevron	ARGENTINA	MDVallejo@chevron.com
Vigide, Nicolas	Universidad de Buenos Aires	ARGENTINA	nicolas.vigide@gmail.com
Waichel, Breno Leitão	Federal University of Rio Grande Do Sul	BRAZIL	breno@cfh.ufsc.br
Wallner, Herbert	Goethe-Universität Frankfurt	GERMANY	wallner@geophysik.uni-frankfurt.de
Walwer, Damian	École Normale Supérieure de Lyon	FRANCE	damianwalwer@gmail.com

Westerman, David	Norwich University	UNITED STATES	westy@norwich.edu
Witcher, Taylor	Uppsala University	SWEDEN	taylor.witcher@geo.uu.se
Yao, Zewe	Zhejiang University	CHINA	everydaygood@163.com
Zanella, Alain	Le Mans Université	FRANCE	zanella.alain@gmail.com

Table of Sessions

Session on Case Studies – Dykes, Sills, Laccoliths, Volcanic Feeders

Contents

Kinematic and dynamic criteria for dyke emplacement: the case of Early Cretaceous dykes swarms in southeastern Brazil and southwestern Africa

Almeida, J.[1], McMaster, M.[1], Giro, J.P.[2]

[1] *Rio de Janeiro State University, Rio de Janeiro, Brazil* – jchalmeida@gmail.com, [2] *Graduate Program on Geoscience, Rio de Janeiro State University, Rio de Janeiro, Brazil*

Keywords: Dyke Swarms, Brazilian Continental Margin, Kinematic criteria.

The emplacement of dykes is controlled by a number of different factors related to temperature, fluid pressure, regional and local stress tensors, and the rheology of magma and country rocks. If we consider specific dyke swarms that intruded crystalline host rocks with a regular geometry, we observe that some of these conditioning factors can be considered as homogeneous or without influence on the structures that result from the interaction between dyke and host-rock. Asymmetrical features can be used as indicators of the kinematics and/or dynamics of dyke emplacement (Correa-Gomes et al. 2001, McMaster et al. 2019). In this work we summarize the criteria used to evaluate the external stress field in a crystalline host rock intruded by a mafic dyke swarm in the interior of West Gondwana prior to its breakup.

The Serra do Mar Dyke Swarm (SMDS - Almeida, 1976, Almeida et al., 2013) extends for ~700 km along the coast of São Paulo and Rio de Janeiro states of southeastern Brazil. The conjugate margin of this portion of Brazil is represented by the Benguela region of Angola. The dyke swarm intruded crystalline rocks (mainly gneisses, granites and schists) in early Cretaceous times (Almeida et al., 2013). The majority of the dykes are subalkaline, tholeiitic basalts, but other compositions can be found (alkali basalts, lamprophyre) in minor quantities. AFT measurements and other methods have estimated dyke emplacement depths of around four to five kilometres. The dominant direction of the dykes is around N40-50E, although there are other modal directions such as N10-30E and N0-20W. These dykes are steeply dipping (>70°) and conspicuously regular in thickness and orientation along their length. Faults along the host-rock/dyke boundary are common.

Features that can be used as kinematic indicators can be divided into three types: host-rock markers (HRM), dyke markers (DM) and host-rock/dyke boundary markers (DBM). HRM are structures observed in the host-rock such as lithological contacts, veins, faults, folds and enclaves. Horizontal planar markers are ideal dip-slip movements, whilst meanwhile vertical planar markers are the best indicators for strike-slip movements. Care should be taken when using oblique planar makers. Linear markers are the most precise gauge for the evaluation of offset. DM are internal features such as preferred orientation of crystals, magnetic foliation and lineation, fractures and gashes. Most of these internal markers can be related to magma flow, as such they are usually inconclusive for external stress field measurements. Symmetry can be helpful to determine if there is lateral movement combined with extension (Correa-Gomes et al., 2001, Spacapan et al., 2016, Dering, et al., 2019). DBM include features such as zig-zags, steps, bridges and branches, which can be indicative of magma flow direction as well as being utilized for the external stress field evaluation.

The kinematic analysis of asymmetrical features, such as branching dykes, zigzags and en-echelon dykes, demonstrates that the SMDS was emplaced under predominantly sinistral oblique extension, with a resultant mean extension direction of N50-60°W (Almeida et al., 2013b).

Within the Cabo Frio Terrane, and in the Angolan Craton, the tholeiitic dykes cut across the flat lying NW-SE trending basement structures (Figure 1) and vary in thickness from 10cm to 22m wide (Almeida et al., 2013a). The majority of dykes are linear but dykes in zigzags, stepped contacts and bridges between dyke segments also occur. The kinematic analysis of these elements and other asymmetrical features, such as curved cooling fractures, allows the estimation of the regional stress field active during the emplacement of the dykes. The dykes in the Cabo Frio Region registered a dominantly normal extension (perpendicular to the walls of the dykes) with a small strike-slip component (sinistral) related to NW-SE extension.

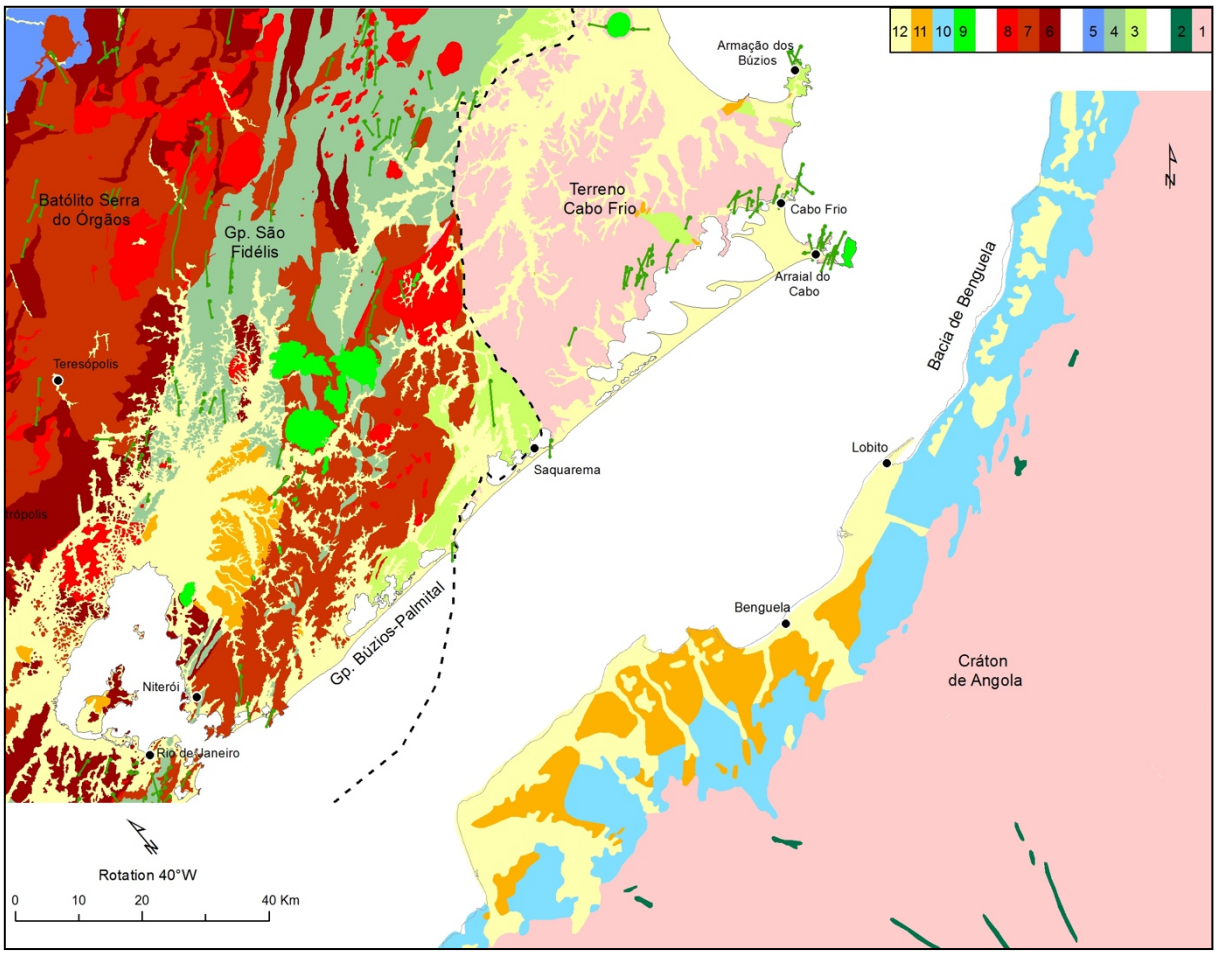

Fig. 1 – Simplified reconstructed geological map of southeastern Brazil and southwestern Africa with the Cretaceous tholeiitic dykes highlighted in green. 1) Paleoproterozoic basement, 2) Mesoproterozoic mafic intrusions, 3) Buzios-Palmital Gr., 4) São Fidelis Gr., 5) Raposos Gr., 6) Arc Granites, 7) Syn-collisional granites, 8) Post-orogenic granites, 9) Alkaline intrusions, 10) Cretaceous sediments - Benguela Basin, 11) Cenozoic sediments, 12) Quaternary - unconsolidated sediments.

Acknowledgements

FAPERJ, CAPES, CNPq and PETROBRAS have in many ways supported this research and supplied scholarships for Master students. The authors are also grateful to the assistance of Tektos Group researchers and technicians.

References

Almeida, F.F.M. (1976), The system of continental rifts bordering the Santos Basin, Brazil. Continental Margins of Atlantic Type, *Anais da Academia Brasileira de Ciências*, *48*, 14-26.

Almeida, J., Dios, F., Mohriak, W.U., Valeriano, C. M., Heilbron, M., Eirado, L. G., Tomazzoli, E. (2013), Pre-rift tectonic scenario of the Eo-Cretaceous Gondwana breakup along SE Brazil – SW Africa: insights from tholeiitic mafic dyke swarms, In: Mohriak, W. U., Danforth, A., Post, P. J., Brown, D. E., Tari, G. C., Nemčok, M. & Sinha, S. T. (eds) *Conjugate Divergent Margins. Geological Society, London, Special Publications, 369*, 11-40.

Correa-Gomes L.C., Souza-Filho, C.R., Martins, C.J.F.N., Oliveira, E.P. (2001), Development of symmetrical and asymmetrical fabrics in sheet-like igneous bodies: the role of magma flow and wall-rock displacements in theoretical and natural cases, *Journal of Structural Geology*, *23* (09), 1415-1428.

Dering, G.M., Micklethwaite, S., Cruden, A.R., Barnes, S.J., Fiorentini, M.L. 2019. Evidence for dyke-parallel shear during syn-intrusion fracturing, *Earth and Planetary Science Letters, 507*, 119–130.

McMaster, M., Almeida, J., Heilbron, M., Guedes, E., Mane, M. (2019), Characterisation and Tectonic Implications of the Early Cretaceous, Skeleton Coast Dyke Swarm, NW Namibia, *Journal of African Earth Science, 150,* 319-336.

Spacapan, J.B, Galland, O., Leanza, H.A., Planke, S. 2016. Control of strike-slip fault on dyke emplacement and morphology. Journal of the Geological Society, *173*, 573–576.

Mode of emplacement of shallow igneous bodies in the Malargüe fold and thrust belt, Mendoza

Araujo Vanesa S.[1], Sánchez Natalia P. [1], Frisicale María C. [1], Turienzo Martin M. [1], Lebinson Fernando[1] and Dimieri Luis V.[1]

[1] *INGEOSUR- CONICET, Departamento de Geología, Universidad Nacional del Sur, Bahía Blanca, Argentina* – vanesa.araujo@uns.edu.ar

Keywords: Shallow igneous bodies, Emplacement, Cordillera Principal.

It is considered that the rheological contrast between strata and tabular igneous bodies exert an important control on the emplacement and shape of magmatic bodies (Menand, 2011; Thomson and Schofield, 2008). Field observations and laboratory experiments regarding the location of sills and laccoliths indicate that some of these are formed when the feed channel reaches a layer whose rigidity does not allow to progress, thereby causing the lateral spread of magma (Kavanagh et al., 2006). There are several publications studying emplacement models of these bodies in compressive environments (Galland et al., 2007; Montanari et al., 2010; Menand, 2011; Ferre et al., 2012; Walker et al., 2016) which reveal that the bodies are constructed from amalgamation of successive pulses of tabular bodies, that are emplaced through fault systems under compressive stresses.

The Malargüe FTB is a suitable place to study the mode of emplacement of neogene shallow intrusives likes sills, dykes and laccoliths. Figure 1 shows the distribution of the main bodies exposed in our study area.

In the NE area (Fig. 1) the Laguna Amarga body and other shallow intrusive rocks are emplaced over a wide area coincident with a backthrusts system affecting basement rocks located in the hanging wall of the Carrizalito thrust (Turienzo et al., 2012). This relationship was also observed in seismic lines and exploration wells where it is possible to observed sills intruded in Late Jurassic-Early Cretaceous rocks at the footwall of the thin-skinned Sosneado and Mesón thrusts. This implies that the feed channels of intrusive bodies must be deeper than those thrusts. Therefore we consider that the emplacement of the Laguna Amarga laccolithic body may be associated with the underneath backthrust system generated in the hangingwall of the thick-skinned Carrizalito thrust (Araujo et al. 2013, 2019).

To the south of the Atuel river (Fig. 1) the Cerro Chivato body seems to be emplaced benefitting from the weakness of the Auquilco Formation gypsum. In its eastern edge the body shows structural complexity in the contact with La Manga and Lotena Formations, disrupting and folding the strata. In the western side is possible to recognize the Tordillo Formation clearly resting on the intrusive in a concordant manner. We interpret that this intrusive could have been emplaced through a north-south thrust fault within the Auquilco gypsum. This fault can be observed within the strata located at the south edge of the intrusive, verging to the east.

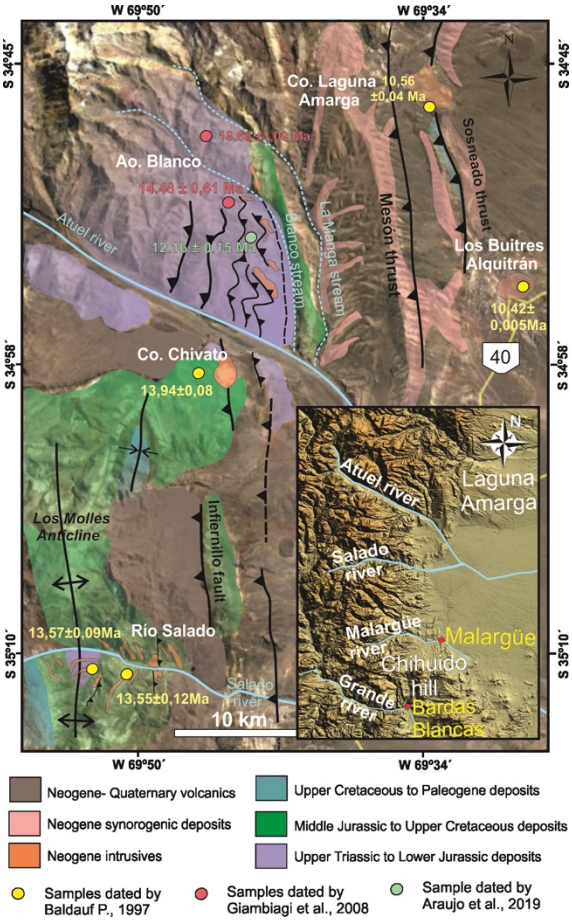

Figure 1: Satellite image with the distribution of the main bodies.

In the Chihuido area (Fig. 1), there are andesitic sills and dykes in contact with the Mendoza Group. In some sectors is possible to observe shales folded due to the intrusion of magma. On the floor of some of these sills there are ridge and groove structures parallel to the dip direction of the sedimentary layers. One of the intrusives has a thickness of about 15–20

cm and is located along the fault surface. The floor of this tabular body is concordant with the Mendoza Group sediments (footwall flat), and the roof is discordant with the same sediments (hangingwall ramp). This outcrop is evidence that the tabular body was emplaced through a thrust surface that was used as a feed channel (Fig. 2). On the other hand, in these areas there are some sills affected by faulting, indicating that some of them are pretectonic with the deformation produced by thrusts. Good evidence between the relation of emplacement and tectonics is founded in the Arroyo Blanco zone (Fig. 1), where the sills are intruded into the core of an anticline. There, an east dipping thrust (backthrust) duplicates the layers of the El Freno Formation. It is possible to interpret that this backthrust folded the sill. This igneous rock has an age $^{40}Ar/^{39}Ar$ on hornblende of 12.16 ± 0.15 Ma (Araujo et al. 2019). Therefore, this dating allows us to constrain the age of thrust deformation.

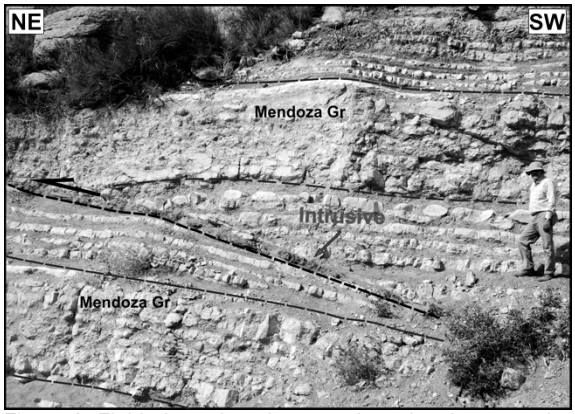

Figure 2: Field photo that shows an intrusive that uses the fault zone as a feed channel. Black dashed line indicates a thrust, blue dashed lines indicate top and bottom of strata on both hanging and footwall blocks.

Finally, the survey of the igneous bodies allowed us to define their morphology, thus helping to provide evidence on the mechanisms of emplacement in the upper crust and led us to establish the close relationship of these bodies with the Andean contractional fault systems.

It is interpreted that these thrusts have acted as feeding channels for the ascent of magma and therefore there is a direct link between the distribution of magmatism and fault systems. The igneous bodies are emplaced through low-angle faults and it results in longitudinal strips of intrusive bodies of younger ages towards the Andean foreland.

The expansion of the Andean magmatism may be based on the close relationship between the simultaneous progress towards the foreland of thrust systems and igneous bodies without necessity of considering significant displacement of the sources of magma

Acknowledgements

The authors would like to acknowledge the use of the material provided by Departamento de Geología, Universidad Nacional Del Sur and Instituto Geológico Del Sur, CONICET, Argentina.

References

Araujo, V. S., L. V. Dimieri, M. C. Frisicale, M. M., Turienzo, N. P. Sanchez (2013), Emplazamiento del cuerpo subvolcanico Laguna Amarga y su relacion con las estructuras tectonicas andinas, sur de la provincia de Mendoza, *Rev. Asoc. Geol. Argent*., 70 (1), 40‑52.

Araujo, V. S., M. C. Frisicale, N. P. Sanchez, M. M. Turienzo, F. Lebinson and L. V. Dimieri (2019), The relationship between Cenozoic shallow igneous bodies and thrust systems of the mountain front of the Cordillera Principal, Mendoza province, Argentina, *Journal of South American Earth Sciences,* 92, 531‑551.

Ferré, E. C., O. Galland, D. Montanari, T. Kalakay (2012), Granite magma migration and emplacement along thrusts. *International Journal of Earth Sciences* 101(7), 1673–1688.

Galland, O., P. R Cobbold, J. de Bremond d'Ars, E. Hallot (2007), Rise and emplacement of magma during horizontal shortening of the brittle crust: Insights from experimental modeling. Journal *of Geophysical Research: Solid Earth*, 112(6), 1–21.

Kavanagh J., T. Menand, R. Sparks (2006), An experimental investigation of sill formation and propagation in layered elastic media, *Earth Planetary Science Letters,* 245, 799-813.

Menand, T. (2011), Physical controls and depth of emplacement of igneous bodies: A review, *Tectonophysics* 500, 11-19.

Montanari, D., G. Corti, F. Sani, C. Del Ventisette, M. Bonini, G. Moratti (2010), Experimental investigation on granite emplacement during shortening, *Tectonophysics* 484(1-4), 147–155.

Thomson, K., N. Schofield (2008), Lithological and structural controls on the emplacement and morphology of sills in sedimentary basins, structure and emplacement of high-level magmatic systems, *Geol Soc Lond Spec Publ*, 302, 31‑44.

Turienzo M. M., L. V. Dimieri, M. C. Frisicale, V. S. Araujo, N. P. Sánchez (2012), Cenozoic structural evolution of the Argentinean Andes at 34º40'S: A close relationship between thick and thin-skinned deformation, *Andean Geology*, 39 (2), 317-357.

Walker, R., D. Healy, T. Kawanzaruwa, K. Wright, R. England, K. W. McCaffrey, A. Bubeck, T. Stephens, N. Farrell, T. Blenkinsop (2016), Igneous sills as a record of horizontal shortening: the San Rafael subvolcanic field, Utah. *Geol. Soc. Am. Bull*., 129 (9‑10), 1052‑1070. https://doi.org/10.1130/b31671.1.

Emplacement mechanism of igneous sheet intrusions: A case study in the Malargüe Fault and Thrust Belt and analogue modeling

Benitez, A.[1,2], Vigide, N.[2], Winocur, D.A.[1,2] and Yagupsky, D.L.[1,2]

[1] *Universidad de Buenos Aires, FCEYN. Depto. de Ciencias Geológicas. Pabellon II, Ciudad Universitaria, CABA, Argentina*
[2] *Instituto de Estudios Andinos Don Pablo Groeber (IDEAN)- (UBA-CONICET).*

Keywords: intrusion, rheology, sills.

The occurrence of intrusive bodies such as dikes and sills in sedimentary basins has been documented worldwide. In the northern sector of the Neuquén Basin in Mendoza, Argentina, intrusive bodies are recognized, preferably emplaced in shales, sandstones and limestones of the Cuyo and Mendoza groups and in the continental sedimentary rocks of the Neuquén Group.

The case study of this work corresponds to a sector of the Malargüe fold and thrust belt, in the south of Mendoza between 35º00' and 35°30' LS, where excellent outcrops of intrusive bodies are exhibited. We have recognized punched laccoliths up to 500 meters thick, which have elongated morphologies and are linked to linear structures, i.e. thrusts faults or large anticlines. There are also smaller igneous sheet intrusions corresponding to dikes and sills. The dykes are up to 20 meters thick, while the sills are up to 50 meters thick and 1000 meters long. In Los Blancos anticline core, shales and carbonates of the Cuyo Group are intruded by a sill ranging between 30 and 60 meters thick and 1400 m long (Fig. 1).

Fig. 1 – Field photograph of the transgressive sill emplaced in Cuyo Group.

Host rocks are mainly limestones (mudstones and wackestones) and shales. Limestones were previously fractured, so these rocks behaved as purely linear elastic solid. Magma propagated through some of these fractures, resulting in the irregular body in Figure 2a. On the other hand, inelastic deformation affected shale beds during sill intrusion. In some cases, the propagating magma seems to have pushed the host rock ahead like an indenter with a rectangular tip (Fig. 2b). These field observations suggest that the rheology of different host rocks defines the sill or dike geometry and the dominant intrusion mechanism.

Thus, factors such as differences in Young's module between successive layers control, at least partially, the intrusion mechanism. This is in good agreement with theoretical works (Kavanagh et al., 2006; Barnet and Gudmundsson, 2014). However, other mechanical aspects of the host rock can condition the propagation of sheet intrusions. In order to understand the influence of rock cohesion during the intrusive sill emplacement, simple analogue models were carried out.

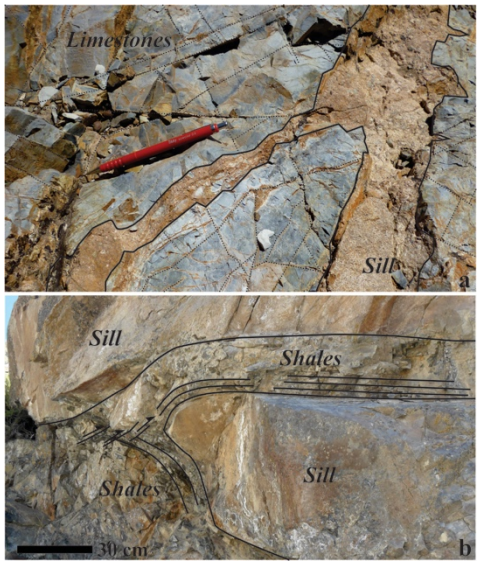

Fig. 2 – Close up photographs of the contacts between sills and different host rocks.

Glass microspheres (GM) and silica powder (SP) were used as interbedded host rocks analogue, given their contrasting cohesion (low and high respectively). GM with grain diameters of 70 µm have a density in a range of 1.5 – 1.9 g.cm^{-3}, a cohesion between 64 – 173 Pa, and an internal friction angle of 20º (Schellart, 2000). SP has grain diameters of 40 µm, a density of 1.3 g.cm^{-3}, cohesion of 38 Pa and an internal friction angle of 38º (Galland et al., 2006; Abdelmalak et al., 2016). Vegetal oil (VO) was used as magmatic analogue. This material can be injected as a viscous fluid, and it solidifies under the 32ºC. The used commercial vegetaline has a density of 0.9 g.cm^{-3} and a viscosity of 2x10-2 at 50ºC (Galland et al., 2006).

Mechanical properties for both, granular and viscous materials, are appropriate to simulate and scale different host rocks and low viscosity magmas

(see Galland et al., 2006 for experimental scaling complete analysis).

The experiments dimensions were 40 cm x15 cm x 4cm. Model 1 consists of a single homogeneous layer of glass microspheres (Fig 3a), and model 2 consists in four successive thin layers (0.3 cm) of GM-SP mix, interbedded with thicker (between 0.2 and 0.5 cm) SP layers. Melted VO was injected by a volumetric pump at a rate of 10 cm^3min^{-1}. After the vegetal oil gets cold, the granular material was extracted to recover the resultant intrusive body, allowing its tridimensional analysis.

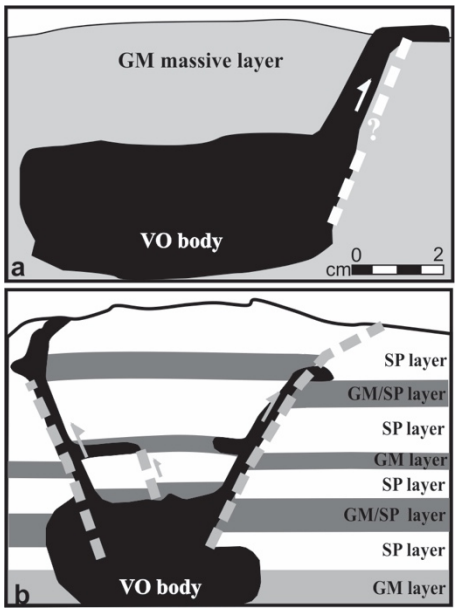

Fig. 3a.b. – Photographs and corresponding drawing of cross-sections of the experiments Models 1 and 2.

In the not layered model (1), the VO accumulates at the base of the model, pushing upwards the host material until a branch propagates through, reaching the surface. This results in an oblate spheroid basal body, with an arm plunging from the surface towards the body margin (Fig. 3a). The low cohesion of the GM volume allows a remarkable propagation of the viscous material both laterally and vertically.

In the layered model (2), the basal layer of GM allows the formation of a spheroidal body that pushes the sequence upwards. VO raises along reverse faults, forming dykes (Fig 3b). Sills propagate laterally from these dikes through the interfaces between GM-SP mix layers and SP layers.

Our experiments show that the intrusion geometry is conditioned by the existence of layers with different rheological properties. In a homogeneous medium of GM, i.e. a low cohesion material, massive lacoliths are formed, as previously suggested by Schmiedel et al. (2017). In contrast, the SP layers are elastically fractured by the stresses resulting from the propagation of the VO, generating annular dikes or cone sheets. The existence of interfaces with less cohesive layers (GM or GM-SP mix) favors the formation of sills that extend from the dykes towards the interior of the cone in the deep levels, while they extend outwards in the upper levels.

These results constitute an approximation to understand the intrusion geometry of tertiary volcanic rocks in southern Mendoza. Sills and dikes are formed between units or layers with rheological contrast, as in the Los Blancos anticline. There, sills are emplaced in shale layers or in the interfaces between shales and limestones, in good correlation with results of model 2. On the other hand, punched laccoliths described in La Valenciana anticline are emplaced in a ~700 m thick shales sequence, with subordinate limestones and silty sandstones. Well data in the Altiplano del Payun and Los Cavaos oil fields located south of the Rio Grande Valley show similar intrusion geometries, affecting shales of the Mendoza Group (Rodriguez Monreal et al., 2009; Witte et al., 2012). Model 1 results present a good correlation with this prototype, being the massive and low cohesive host material a determining factor to the intrusion mechanism and the resulting body shape.

References

Abdelmalak, M, C. Bulois, R. Mourgues, O. Galland, J. Legland, and C. Gruber (2016). Description of new dry granular materials of variable cohesion and friction coefficient: Implications for laboratory modeling of the brittle crust. *Tectonophysics*, 684, 39–

Barnet, Z. and A. Gudmundsson (2014). Numerical modelling of dykes deflected into sills to form a magma chamber. *Journal of Volcanology and Geothermal research*, 15, 1-11.

Galland O, P. Cobbold, E. Hallot, J. de Bremond d'Ars and G. Delavaud (2006). Use of vegetable oil and silica powder for scale modelling of magmatic intrusion in a deforming brittle crust. *Earth Planet. Sci. Lett.*, 243, 786–804.

Kavanagh, J.L., T. Menand and R.S. Sparks (2006). An experimental investigation of sill formation and propagation in layered elastic media. *Earth Planet. Sci. Lett.*, 245, 799–813.

Rodriguez Monreal, F., H. J. Villar, R. Baudino, D. Delpino, and S. Zencich (2009). Modeling an atypical petroleum system: A case study of hydrocarbon generation, migration and accumulation related to igneous intrusions in the Neuquén Basin, Argentina. *Marine and Petroleum Geology*, 26, 590–605.

Schellart, W.P. (2000). Shear test results for cohesion and friction coefficients for different materials: scaling implications for their usage in analogue modelling. *Tectonophysics,* 324, 1–16.

Witte J., M. Bonora, C. Carbone, and O. Oncken (2012). Fracture evolution in oil-producing sills of the Rio Grande Valley, northern Neuquén Basin, Argentina. AAPG Bulletin, 96 (7), 1253–1277.

Geochemistry of igneous silicic rocks of the Martín García Island, Río de la Plata Craton, Argentina

Benítez M.E.[1, 2], Ballivián Justiniano C.A.[1, 3], Lanfranchini M.E.[1, 2] , Lajoinie M.F.[1, 4], Salvioli M.A.[1, 3]

[1]*Instituto de Recursos Minerales. Facultad de Ciencias Naturales y Museo, Universidad Nacional de La Plata. La Plata, Buenos Aires, Argentina – manuelaebenitez@hotmail.com*
[2]*Comisión de Investigaciones Científicas de la Provincia de Buenos Aires. La Plata, Buenos Aires, Argentina.*
[3]*Consejo Nacional de Investigaciones Científicas y Técnicas. Ciudad Autónoma de Buenos Aires, Argentina.*
[4]*Centro de Investigaciones Viales, Facultad Regional La Plata, Universidad Tecnológica Nacional.Berisso, Buenos Aires, Argentina.*

Keywords: granitoids, Martín García Complex, Buenos Aires Province

The Martín García Island (MGI, Buenos Aires Province, Argentina) is located in the Río de la Plata estuary, 44 km northeast of Buenos Aires city (Fig. 1). The MGI is composed of basement rocks partially covered by modern fluvial sediments. The basement rocks crop out mainly along the southern and southwestern coasts of the island and are constituted by metaultrabasites, metabasites, metagranitoids, and basic and acidic dykes. They correspond to the Martín García Complex, defined by Dalla Salda (1975), which together with the Buenos Aires Complex (Marchese and Di Paola 1975) of the Tandilia System, constitute part of the Río de la Plata Craton, assigned to the Transamazonian Orogenic Cycle (Dalla Salda et al. 2005 and references therein). The aim of this work is to determine the chemical features and petrogenesis of the silicic rocks of the MGI. A selection of samples was made in order to analyse them petrographically and geochemically (bulk rock by ICP-MS). The distribution of samples is shown in Fig. 1.

MGI granitoids outcrops have a N 35° E/40° NW foliation and occur as small and isolated bodies on the southwestern coast. These rocks show fine grained granoblastic (G1) and porphiroid (G2) textures in hand specimen which allow two igneous pulses to be differentiated. Also, they are cut by N-S granodioritic dykes. The rocks are granodioritic and tonalitic protomylonites composed of microcline, ortose, quartz, zoned plagioclase (An_{5-20}), biotite and hornblende. G1 and G2 show microcline crystals about 400-800 μm and 4 cm long, respectively, and a preferential orientation (Dip direction 273°/35°) in some sectors. Quartz with undulose extinction, oscillatory zoning in plagioclase, biotite fish surrounding K-feldspar and hornblende crystals, and biotite and hornblende fish were recognized. Additionally, zircon, apatite and titanite crystals were identified as accessory minerals.

MGI granitoids have high contents of SiO_2 (65.6-71.9 wt.%), Al_2O_3>15.00 wt.% and Mg# between 0.42 and 0.52. They plot within the granodiorite and tonalite fields of the Ab-An-Or diagram (Barker 1979). They also plot into the subalkaline and calc-alkaline fields of the SiO_2 vs. $Na_2O + K_2O$ (Irvine and Baragar 1971) and SiO_2 vs. K_2O (Peccerillo and Taylor 1976) diagrams, respectively. Regarding the alumina saturation, the analysed rocks plot within the metaaluminous field of the Al/(Ca + Na + K) vs. Al/(Na + K) diagram of Shand (1927). The Alumina Saturation Index (ASI) is between 0.85 and 0.97.

Regarding the incompatible elements, an enrichment in large ion lithophile elements and a decrease in high field straight elements can be observed as well as strong negative anomalies of Nb, Ti and Ta. Moreover, a high Sr/Y ratio (43.42-56.23) was observed.

The total rare-earth elements content of the MGI granitoids varies between 88 and 1046 ppm. In the chondrite-normalised spidergram (McDonough and Sun 1995), these rocks exhibit a marked enrichment in light rare-earth elements with respect to the heavy rare-earth elements (La_N/Yb_N= 14.25–30.24). Eu anomalies are slightly negative (Eu/Eu* = 0.85–0.95) and indicate scarce fractionation of plagioclase at the source (Fig. 2). When plotted in the tectonic discrimination diagram of Pearce et al. (1984), granitoid rocks plot within the VAG + syn-COLG field of the Y-Nb. Thus, the MGI granitoids have petrographical and geochemical characteristics of I-type rocks, related to a volcanic arc setting linked to a Rhyacian magmatism, according to the Paleoproterozoic U-Pb ages obtained by Santos et al. (2017). Also, MGI granitoids have remarkable geochemical coincidences with those defined for adakites, which would point out a low crust partial melting origin (Castillo 2012, Arndt 2013 and references therein).

Acknowledgements

This research has been funded by CICPBA and UNLP. We want to thank the support of Carlos Cingolani and also Micaela García, Facundo De Martino, Mercedes Carlini and Eugenia Giannoni for helping with the field work.

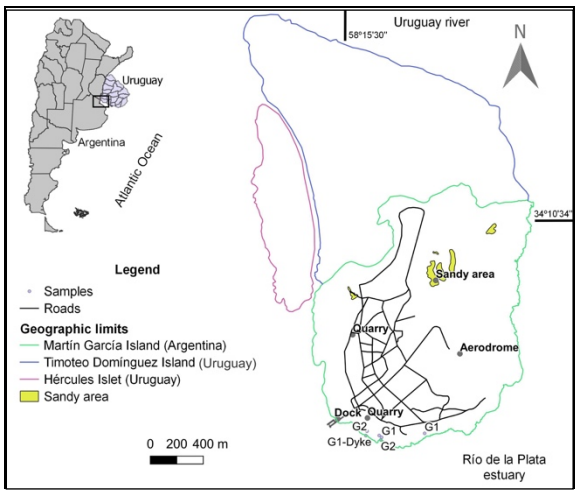

Fig. 1 –Location Map of the Martín García Island. Studied sectors and selected samples locations are shown.

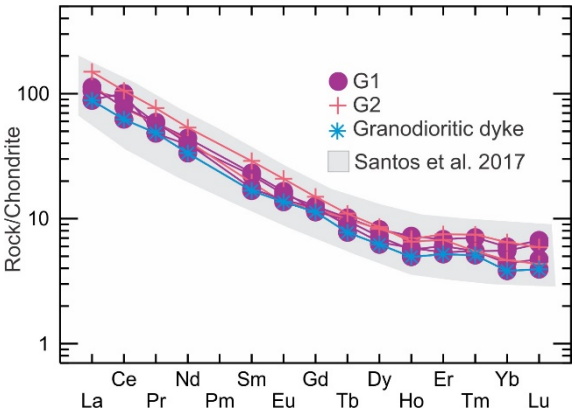

Fig. 2 –Chondrite-normalised spidergram according to McDonough and Sun (1995).

References

Arndt, N.T, 2013. Formation and evolution of continental crust. *Geochemical Perspectives*, European Association of Geochemistry. 2 (3): 405-530.

Barker, F., 1979. Trondhjemites: definition, environment and hypothesis of origin. In: Barker, F. (Ed.), *Trondhjemites, Dacites and Related Rocks*. Elsevier, Amsterdam, 1–12.

Castillo, P.R, 2012.Petrogenesis of adakites. *Lithos*, 134–135: 304–316

Dalla Salda, L.H., 1975. Geología y petrología del basamento cristalino en el área del Cerro El Cristo e Isla Martín García. Provincia de Buenos Aires, República Argentina. *Tesis Doctoral, inédito*. Facultad de Ciencias Naturales y Museo. Universidad Nacional de La Plata.

Dalla Salda, L., de Barrio R.E., Echeveste, H.J., Fernández, R.R., 2005. El Basamento de las Sierras de Tandilia. de Barrio, R., Etcheverry, R., Caballé, M. y Llambías, E. (eds.). *Geología y Recursos Minerales de la Provincia de Buenos Aires*. Relatorio XVI Congreso Geológico Argentino, 1-50.

Irvine, T.N., Baragar, W.R.A., 1971. A Guide to the Chemical Classification of the Common Volcanic Rocks. *Canadian Journal of Earth Sciences*, 8, 523–548.

Marchese, H., Di Paola, E. 1975. Reinterpretación estratigráfica de la perforación de Punta Mogotes I, Provincia de Buenos Aires. *Revista de la Asociación Geológica Argentina*, 30 (1): 44-52.

McDonough, W.F., Sun, S.-s., 1995. The composition of the Earth. *Chemical Geology*, 120, 223–253.

Pearce, J.A., Harris, N.B.W., Tindle, A.G., 1984. Trace Element Discrimination Diagrams for the Tectonic Interpretation of Granitic Rocks. *Journal of Petrology*, 25, 956–983.

Peccerillo, A., Taylor, S.R., 1976. Geochemistry of Eocene calc-alkaline volcanic rocks from the Kastamonu area, Northern Turkey. *Contributions to Mineralogy and Petrology*, 58, 63–81.

Santos, Joã O.S., Chernicoff, C.J., Zappettini, E.O., McNaughton, N.J., Greau, Y., 2017. U-Pb geochronology of Martín García, Sola, and Dos Hermanas Islands (Argentina and Uruguay): Unveiling Rhyacian, Statherian, Ectasian, and Stenian of a forgotten area of the Río de la Plata Craton, *Journal of South American Earth Sciences*, 80, 207-228.

Shand, S.J., 1927. On the Relations between Silica, Alumina, and the Bases in Eruptive Rocks, considered as a Means of Classification. *Geological Magazine*, 64, 446–449.

Caldera-forming magmatic systems in Late Paleozoic Central Europe – the subvolcanic perspective

Jacob Brauner[1], Christoph Breitkreuz[1]

[1] *Department of Geology and Paleontology, TU Bergakademie Freiberg, Freiberg, Germany* – brauner-j@web.de

Keywords: Deeply eroded calderas, syn- to post-climactic activity, caldera cycles

Studies on Cenozoic calderas like Yellowstone, Valles, Galan, Long Valley are crucial for a better understanding of continental magmatic plumbing systems (Cole et al. 2005; Cashman and Giordano 2014; Bachmann and Huber 2016; and references therein). Kennedy et al. (2012, 2018) and Galetto et al. 2017 shed light on the role of subvolcanic processes and their significance for the comprehension of caldera-forming magmatic systems. Investigation on Late Paleozoic caldera complexes in Central Europe (Fig. 1) can nourish the current debate because I) they are deeply eroded; II) the ancient centers, in contrast to Neogene systems, definitely finished activity: Thus we can differentiate between single- and multi-cycle complexes; III) Intensive exploration drilling and quarrying provide abundant out- and subcrops, in places; IV) to a certain degree, the geotectonic setting of the Central European systems is comparable to the well-studied Cenozoic calderas.

Caldera plumbing systems develop throughout caldera life cycle(-s). Pyroclastic dykes may represent feeding conduits active during climactic phases (Aguirre-Díaz and Labarthe-Hernández 2003). Post-climactic processes like resurgence or lava(dome) formation is mainly controlled by the dynamics and temporal evolution of the deeper crustal magma reservoir rather than by decompression due to climactic eruption (Kennedy et al. 2012, 2018). Life time and magma supply of the deep-seated system also controls single vs. multicycle caldera evolution.

Optimal conditions for resurgence are moderate magma supply rates into middle-sized to large reservoirs under moderate extension (Galetto et al. 2017). In contrast, high ascent rates favor dyking through rheological barriers, such as crystal mush domains or thick caldera-fill ignimbrites.

Large-scale resurgence is caused by the intrusion of shallow-level sills, dykes (e.g. into the caldera ring- faults) and laccoliths often accompanied by mixing and mingling (Kennedy et al. 2012; Galetto et al. 2017).

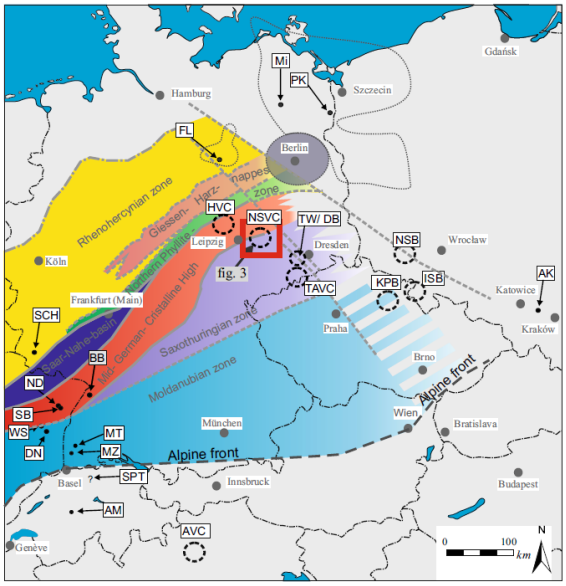

Fig. 1: Variscan tectonic units and Late Paleozoic magmatism in Central Europe – AK: Alwernia–Krzeszowice; AM: Aar massif; AVC: Arthesian volcanic complex: BB: Baden–Baden; CB: Chemnitz Basin; DB: Döhlen Basin; DN: Donon; FL: Flechtingen; HVC: Halle Volcanic Complex; ISB: Intra Sudetic Basin; KPB: Krkonoše-Piedmont Basin; Mi: well Mirow 1/74; Mt: Münstertal; Mz: Marzell; Nd: Niedeck; NSB: North Sudetic Basin; NSVC: North Saxon Volcanic Complex; PK: well Penkun 1/71; SB: Schieferberg; SCH: Schmelz; SPT: Swiss Permian Through; TAVC: Teplice–Altenberg Volcanic Complex; TW: Tharandt Wald Caldera; Ws: Wisches.(modified from Repstock et al. 2018).

The Late Paleozoic caldera-forming volcanic complexes in Central Europe show several of the aforementioned subvolcanic features (see also Table 1). The only known example that can be attributed to syn-climactic subvolcanic activity is a feeding fissure from the third caldera cycle of the TAVC. Although not every of the listed complexes show signs for large scale resurgence like sills and laccoliths, all of them reveal remnants of post-climactic activity. Ring dykes (TAVC and TW) and central intrusions (NSVC and TW) display post-collapse activity in close temporal proximity, involving residual and replenished magma provoking mingling and mixing. Larger bodies like sill complexes (FL) and laccoliths (NSVC) imply extended periods of emplacement. The observed compositional differences between the caldera fill and several subvolcanic bodies point towards the existence of newly ascending magmas in

Table 1: Late Paleozoic caldera complexes in Central Europe and related subvolcanic features. CR: crystal-rich; A: Andesite; B: Basalt; G: Granite; R: Rhyolite; *cogenetic to caldera fill; for location see Fig. 1.

Caldera (type / cyclicity / composition of caldera fill)	**Syn-climactic subvolcanic features**	**Post-climactic subvolcanic features**	**Magmatic system**	**References**
Flechtingen-Roßlau Complex – FL (sag caldera / single cycle / R)		Voluminous sill complex below caldera fill (A) and high-level intrusions (G*)	Deep-seated, separate SiO_2-rich and –poor reservoirs	Benek et al. 1996; Awdankiewicz et al. 2004; Geißler et al. 2008
North Saxonian Volcanic Complex – NSVC (sag caldera / two cycles / CR-R)	Fiamme of divers composition indicate magma mingling caused by dyke injection into crystal mush	Shallow intrusions into caldera-fill ignimbrite (G*); Laccolith (R*, Leisnig Porphyry); magmatic dykes (in parts with magma mingling; R+B); phreatic dykes	Reheated crystal mush / replenishment from deep-seated reservoir	Repstock et al. 2018, in revision
Tharandt Wald Caldera – TW (piston caldera / single cycle / R)		Ring dykes and intrusions into the central part of the caldera fill (R* - slightly depleted geochemistry)	Heterogeneous rhyolitic supracrustal magma chamber	Benek 1980; Alexowsky et al. 2012
Altenberg Teplice Volcanic Complex- TAVC (features of piecemeal + trapdoor caldera / three cycles / CR-R)	Feeding fissure of third cycle (R, Harter Stein)	High-volume microgranite* (ring dyke) mixed with less evolved melts; shallow-level plutons, G*	Deflation of stratified reservoir / replenishment from deep-seated reservoir	Müller et al. 2005; Casas García et al. (resubmitted)

places (FL, NSVC). Voluminous andesitic sills emplaced subsequent to the garnet-bearing ignimbrites implies co-existence of large, separate magma reservoirs in the lower crust (FL). The abundance of exotic fiamme and mingled andesitic to rhyolitic dykes in the Wurzen system (NSVC) proofs injection of melt into/through a crystallizing magma chamber. Dependent on the ascent rate and magmatic overpressure, the rheological barrier was unable to inhibit diking in terms of Galetto et al. (2017). In places, the melts reached the surface and formed lava domes (NSVC and FL) and thin tuff beds (FL).

At other locations like the TAVC, subvolcanic bodies and eruptive deposits are similar in composition implying a close relationship. Here the late ignimbrites and following granite porphyry ring dykes in TAVC, both with outsized feldspar crystals, suggest a co-genetic tapping of crystal mush. The multi-cyclicity of the NSVC and TAVC implies a long lasting magma supply in contrast to FL and TW. Regarding the similar setting, further investigations on the relationships between the caldera fill and post-climactic subvolcanics might help to answer the question why some caldera systems are resurgent and others not.

References

Aguirre-Díaz, G.J. and G. Labarthe-Hernández (2003), Fissure ignimbrites: Fissure-source origin for voluminous ignimbrites of the Sierra Madre Occidental and its relationship with Basin and Range faulting, *Geology, 31,* 773–776.

Alexowsky, W., et al. (2012), Geologische Karte des Freistaates Sachsen 1:25.000 – Erläuterungen zu Blatt 5047 Freital, *3. Auflage*, 180 pp, Sächsisches Landesamt für Umwelt und Geologie, Freiberg.

Awdankiewicz, M., et al. (2004), Emplacement textures in Late Palaeozoic andesite sills of the Flechtingen-Roßlau Block, north of Magdeburg (Germany), *Geological Society, London, Special Publications, 234,* 51-66.

Bachmann, O. and C. Huber (2016), Silicic magma reservoirs in the Earth's crust, *American Mineralogist, 101,* 2377-2404.

Benek, R. (1980), Geologisch-strukturelle Untersuchungen im Tharandter Vulkanitkomplex (Südteil der DDR), *Zeitschrift für geologische Wissenschaften, 8,* 627-643.

Benek, R., et al. (1996), Permo-Carboniferous magmatism of the Northeast German Basin, *Tectonophysics, 266 (1–4),* 379-404.

Casas García, R., et al. (resubmitted), Facies architecture, composition, and age of the Carboniferous Teplice Rhyolite (German-Czech border): Insights into the evolution of the Altenberg-Teplice Caldera, *Journal of Volcanology and Geothermal Research*.

Cashman, K.V. and G. Giordano (2014), Calderas and magma reservoirs, *Journal of Volcanology and Geothermal Research*, *288*, 28-45.

Cole, J.W., et al. (2005), Calderas and caldera structures: a review, *Earth-Science Reviews, 69,* 1-26.

Galetto, F., et al. (2017), Caldera resurgence driven by magma viscosity contrasts, *Nature Communications, 8,* 1750.

Geißler, M., et al. (2008), Late Paleozoic volcanism in the central part of the Southern Permian Basin (NE Germany, W Poland): facies distribution and volcano-topographic hiati, *International Journal of Earth Sciences, 97,* 973-989.

Kennedy, B.M., et al. (2012), Caldera resurgence during magma replenishment and rejuvenation at Valles and Lake City calderas, *Bulletin of Volcanology, 74,* 1833-1847.

Kennedy, B.M. et al. (2018), Magma plumbing beneath collapse caldera volcanic systems. *Earth-Science Reviews, 17,* 404-424.

Müller, A., et al. (2005), Quartz and feldspar zoning in the eastern Erzgebirge volcano-plutonic complex (Germany, Czech Republic): Evidence of multiple magma mixing, *Lithos, 80,* 201-227.

Repstock, A., et al. (2018), Voluminous and crystal-rich igneous rocks of the Permian Wurzen volcanic system, northern Saxony, Germany: physical volcanology and geochemical characterization, *International Journal of Earth Sciences, 107,* 1485-1513.

Repstock, A., et al. (in revision), The Early Permian Wurzen Caldera system of northern Saxony, Germany: Insights into the magma dynamics in an intra-plate setting and implications for the eruption of a crystal-rich monotonous intermediate ignimbrite, *Mineralogy and Petrology.*

Insights on carbonatite-related magma propagation, degassing and conduit conditions from an exponentially well-exposed dike swarm in Catalão, Brazil

John Browning[1], Pedro Cordeiro[1], Antonio Simonetti[2], Bruno Palhares Milanezi[3], Sergio Silva[3]

[1] *Department of Mining Engineering and Department of Structural and Geotechnical Engineering, Pontificia Universidad Católica de Chile, Santiago, Chile – jbrowning@ing.puc.cl*

[2] *University of Notre Dame, College of Engineering, USA*

[3] *CMOC International Brazil, Brazil*

Keywords: Inclined sheets, dikes, Carbonatite,

The mechanisms of emplacement and eruptive dynamics of very low viscosity magmas remain enigmatic, in part, because there are so few well-exposed sections. Questions remain regarding the propagation pathways, arrest and deflection mechanisms and dynamic changes in conduit processes associated with such magmas. For example, it is unclear what the dominant mechanisms that govern the change from highly effusive behaviour to explosive eruptive behaviour which are commonly observed at carbonatite volcanoes. Here we present preliminary field observations from a series of carbonatite-related dike swarms exposed in the walls of the Boa Vista mine in Catalão, Brasil.

The southern part of the Catalão II carbonatite complex contains a series of dike swarms of carbonatites and nelsonites hosted by basement metavolcano-sedimentary rocks. Geophysical modelling and dike emplacement style suggests that this system represents the roof of a much larger non-exposed magmatic system (Palmieri, 2011). The genesis of nelsonites, i.e. whether iron-phosphate melts or "cumulate dikes" from a carbonatite melt, is still poorly constrained.

Three populations of dikes can be observed within the walls of the open pit mine cutting through schists and metavolcanics rocks. The oldest populations, a series of carbonatite and nelsonite dikes emplaced in a complex radial pattern, exhibit a range of attitudes from shallow dipping to near vertical. This population also exhibits a complex array of geometrical interactions indicating a highly anisotropic or dynamic stress field throughout the emplacement. The latest population of dikes are a series of < 1m thick phlogopite-picrite dikes which strike dominantly N-S, cross-cut the older dike populations, are generally steeply dipping.

Similar nelsonites and carbonatites intrude the core of the Catalão I carbonatite complex where widespread dike and plug emplacement, in addition to brecciation, took place. Some plugs are documented to contain basal sections filled with particulate material with horizontal cross- and parallel bedding and upper brecciated sections (Ribeiro et al., 2011), which are interpreted as indicative of diluted particulate flows (i.e. surges).

In this presentation we present preliminary field observations and thin-section analysis with the aim of generating discussion and interest in the emplacement of carbonatite-type magmas. The work forms part of a new project with the larger aim of understanding the economic potential of such deposits.

References

Palmieri, M., 2011. Modelo Geológico e avaliação de recursos minerais do depósito de nióbio Morro do Padre, Complexo Alcalino-carbonatítico Catalão II, GO. Unpublished MSc thesis, University of Brasil.

Ribeiro, C.C., Brod, J.A., Junqueira-Brod, T.C., Gaspar, J.C. and Petrinovic, I.A., 2005. Mineralogical and field aspects of magma fragmentation deposits in a carbonate–phosphate magma chamber: evidence from the Catalão I complex, Brazil. Journal of South American Earth Sciences, 18 (3-4), pp.355-369.

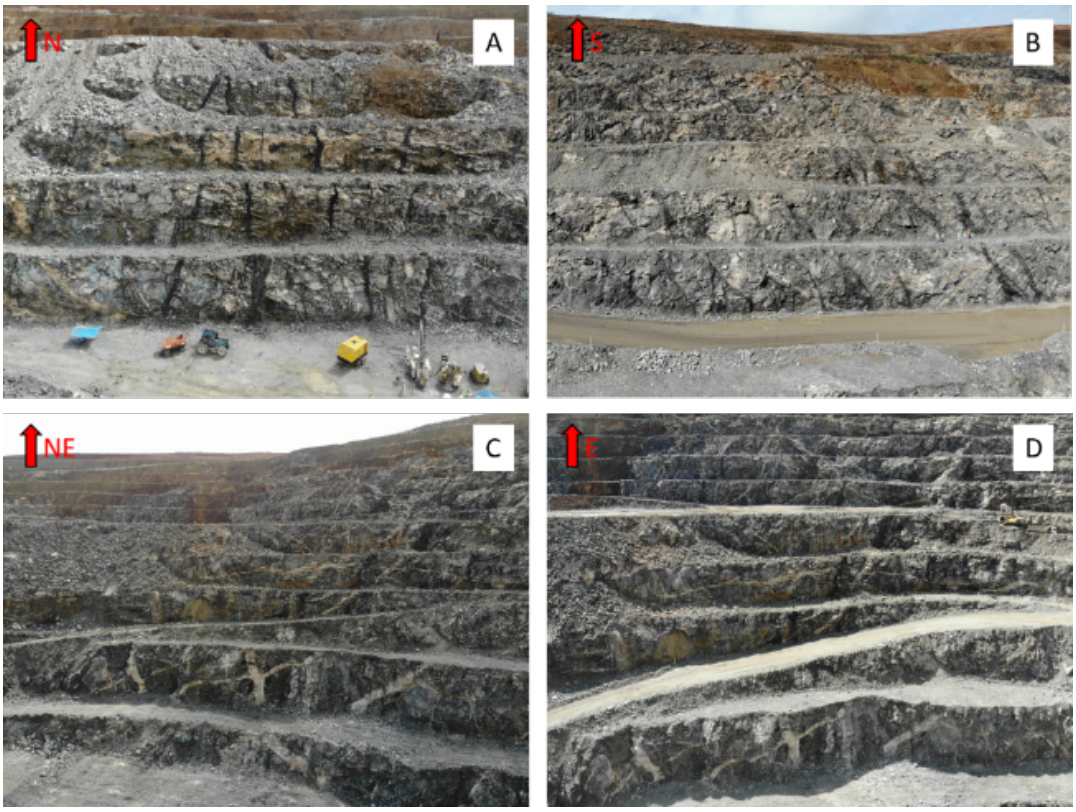

Fig. 1 – A and B) Series of near vertical picrite dikes that strike dominantly N-S and cut the older carbonatite dike sequences. C and D) Complex geometrical relationships between carbonatite and nelsonite dikes emplaced in a radial swarm.

Influence of normal-faults on magma propagation with examples from the Hafnarfjall caldera, Iceland, and Santorini, Greece

John Browning[1], Kyriaki Drymoni[2] and Agust Gudmundsson[2]

[1] *Department of Mining Engineering and Department of Structural and Geotechnical Engineering, Pontificia Universidad Católica de Chile, Santiago, Chile – jbrowning@ing.puc.cl*

[2] *Department of Earth Sciences, Royal Holloway University of London, Egham, United Kingdom*

Keywords: Inclined sheets, caldera faults, Iceland and Santorini

Here we present field observations of dike and fault interactions from two well-exposed calderas in Iceland and Greece. The Tertiary central volcano Hafnarfjall, in Southwest Iceland, exhibits a deeply eroded and uniquely well-exposed section of caldera ring-fault. The ring-fault represents the outermost fault complex of an elliptical caldera with an original diameter of approximately 5 km. Vertical displacement is estimated to be > 200 m on the steeply inward-dipping ring fault and several thin (< 1 m) dikes occupy an approximately 5 m thick section within a section of the ring-fault. We interpret the region containing multiple dykes to have once acted mechanically as a fault core with a lower stiffness or Young's modulus than the surrounding host rocks.

The volcano hosts a swarm of basaltic inclined sheets that all dip, by variable amounts, towards the centre of the volcano (Gautneb et al., 1989). The vast majority of the sheets do not interact, in any way, with the caldera fault or any other faults in or around the volcano. However, a number of the sheets on the downthrown block of the caldera are observed to abruptly change dip when they approach and come into contact with the caldera fault. We observe the inclined sheets, presumably originating from the part of the shallow magma chamber located the caldera margin, becoming either arrested or deflected upon contact with the ring fault.

The Holocene volcano of Santorini, Greece hosts a caldera 11 km in diameter formed over repeated collapse events (Druitt et al., 1999). The last caldera forming event (3.6 ka) scalped a section of the northern part of the island which exposed an intense dike swarm and a series of normal faults. Most of the dikes strike NW-SE and apparently follow the alignment of both the normal-faults and regional strike-slip faults. However, the dikes at Santorini were emplaced in a highly heterogeneous and anisotropic host rock consisting of both faults and numerous layers of different eruptive products, from lavas and tuffs to pyroclastic rocks.

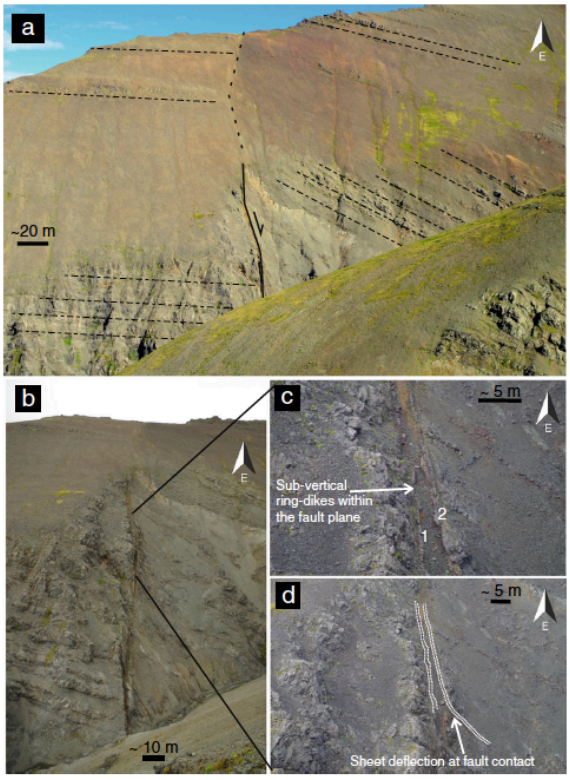

Fig. 1 – a) Caldera ring fault exhibits a general inward-dipping normal trend, although subtle variations in attitude occur throughout. The height from the base to the top of the fault is ~300 m. Lavas on the inner caldera margin dip more steeply than those outside, and generally dip increases with depth. Several markers are used to infer synclinal drag folding, perhaps the most prominent is a light white tuff which clearly bends into the fault. Displacement is greater than the vertical section, so no horizontal markers can be traced across the fault plane. b) Many individual lava layers with thicknesses between 1 and 2 m can be traced to the fault contact on the outer margin; however, most lavas on the inner margin are sufficiently deformed and not discernible. c, d) Section of the upper observable part of the fault. Individual dikes shown and numbered are around 1 m thick.

To test models on the interactions between the observed sheets and caldera fault at Hafnarfjall and the dikes and normal faults at Santorini, we built a suite of FEM numerical models. Many faults which have been active over an extended period develop a

damage zone around the fault core; this is a zone of high fracture frequency which is generally stiffer than the core but softer or more compliant than the surrounding host rock. In the numerical models we simulated the fault zones as regions with different Young's modulus to the host rock. Dikes or sheets were modelled as elliptical cavities with an applied internal magma pressure. The dikes were aligned at different angles with the fault to test the effect of the multiple dike populations observed in the field, at both Hafnarfjall and Santorini.

We suggest a series of mechanical explanations for the observed sheet and dike deflections at a mechanically stratified fault damage zone and core. In the numerical models we were able to test multiple fault properties and with combinations of different amounts of fault damage (or stiffness). We performed extra sensitivity tests to simulate the effect of tectonic loading (i.e. regional extension or compression), the thickness of the dyke and the fault, the length of the fault and the dyke-fault angle. Our models reviewed and explored the mechanical conditions and potential outcomes of those dyke-fault interactions. It was found that the stiffness of the fault core, the dike-fault geometry and the thickness of the fault were primary controls dike deflection in the crust.

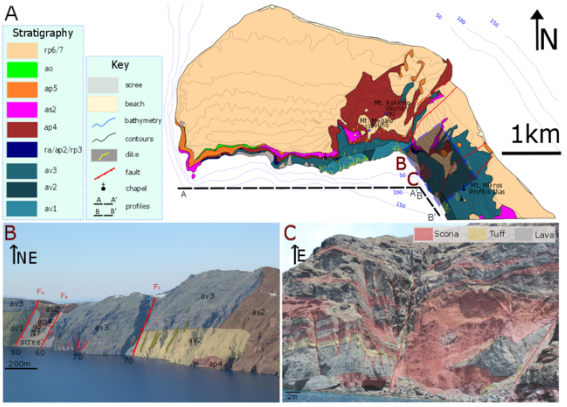

Fig. 2 – a) Simplified geological map of the northern section of Santorini. The now well-exposed section of caldera wall hosts a complex and highly heterogeneous stratigraphy and a series of dikes and faults (b and c).

We further propose a model whereby caldera ring-faults can act as a barrier for the propagation of inclined sheets away from a magma chamber within a caldera. Our findings provide an alternative mechanical explanation for magma channelling along caldera ring faults, which is a process likely to be fundamental in controlling the location of post-caldera volcanism (Browning and Gudmundsson., 2015).

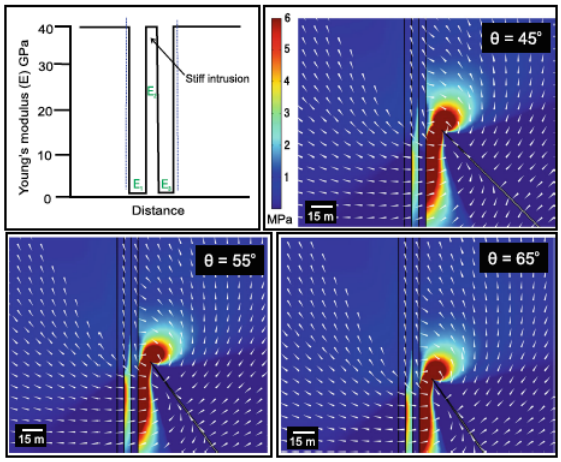

Fig. 3 – Example of FEM numerical models simulating a stiff layer (40 GPa) in the center of a fault zone to simulate a previous dike intrusion. Principal stress rotation at the sheet tip and stress concentration within the stiff layer favor fault capture, most likely along the nearside edge of the previous intrusion. Sheet approach angle has little effect on the stresses within the fault zone above 35°

References

Browning, J. and Gudmundsson, A., 2015. Caldera faults capture and deflect inclined sheets: an alternative mechanism of ring dike formation. *Bulletin of Volcanology*, *77*(1), p.4.

Browning, J., Drymoni, K. and Gudmundsson, A., 2015. Forecasting magma-chamber rupture at Santorini volcano, Greece. *Scientific reports*, *5*, p.15785.

Druitt, T.H., Edwards, L., Mellors, R.M., Pyle, D.M., Sparks, R.S.J., Lanphere, M., Davies, M. and Barreirio, B., 1999. Santorini volcano. *Geological Society Memoir*, *19*.

Gautneb, H., Gudmundsson, A. and Oskarsson, N., 1989. Structure, petrochemistry and evolution of a sheet swarm in an Icelandic central volcano. *Geological Magazine*, *126*(6), pp.659-673.

Did dolerite sill emplacement pre-date basaltic volcanism in the Karoo Igneous Province, South Africa?

Cawthorn, R. G.[1], **Chistyakova, S. Y.**[1], Latypov, R. M.[1] and Putirka, K. D.[2]

[1] *School of Geosciences, University of the Witwatersrand, Johannesburg, South Africa* - sofia.chistyakova@wits.ac.za
[2] *Department of Earth and Environmental Sciences, California University-Fresno 2345, California 93720, USA*

Keywords: Karoo Igneous Province, Al_2O_3 in clinopyroxene in sills, sills pre-date volcanism.

The Karoo Igneous Province and its sills have been extensively studied (e.g. Duncan and Marsh, 2006; Neumann et al., 2011; Svensen et al., 2015). Dolerite sill emplacement and basaltic lava eruption have generally been considered to have been contemporaneous in the evolution of large igneous provinces. Here we present data that challenges that assumption. A suite of 27 vertically-stacked sills from a borehole (Fig. 1) intersecting 2.5 km of sedimentary rocks in the Karoo Supergroup, South Africa, has been sampled. Of these, 13 of the chilled margins contain clinopyroxene phenocrysts showing a systematic increase in Al_2O_3 contents, from 2.0 to 2.8%, with increasing depth (= pressure) as shown in Fig. 2. Such a change (of 0.8% for a 0.75 kbar increase) is broadly consistent with experimental data (Putirka et al., 1996 and 2003). It is acknowledged that the Al_2O_3 content of clinopyroxene is dependent upon other factors apart from pressure, specifically liquid composition, but our data show that all these sills have the same composition, except for one at 1200 m depth that has a different liquid composition and an anomalously high Al_2O_3 content in clinopyroxene compared to all others (Fig. 2). However, if randomly-timed, concomitant sill emplacement and eruption had been contemporaneous such a relationship should not have developed, as illustrated in Fig. 3. We suggest that this systematic change in Al_2O_3 content in clinopyroxene with depth in the sedimentary package indicates that dolerite sill emplacement occurred immediately before lava eruption. Changes in minimum stress direction from vertical to horizontal as a result of the initiation of the breakup of Gondwana may explain such a relationship of early sill emplacement followed by dyke emplacement and consequent eruption, as shown in Fig. 4. Dolerite sills have been dated (at about 183 my; Svensen et al., 2015), but no zircon grains have so far been obtained from the lavas (as far as we are aware) and so this difference in age cannot be demonstrated, and may too small anyway.

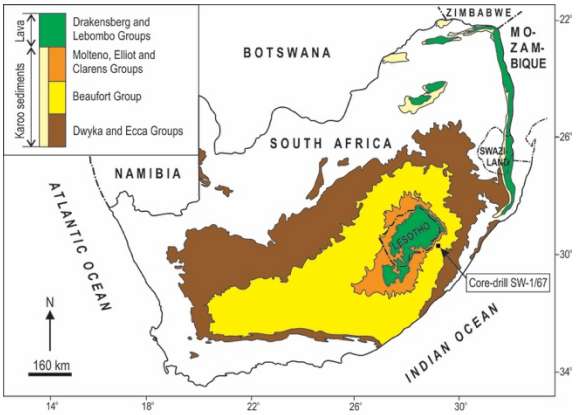

Fig. 1 – Map of the Karoo Igneous Province, in South Africa, showing the locality of the borehole used in this study.

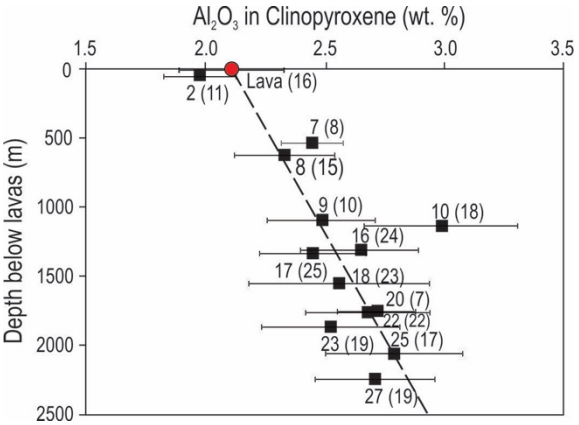

Fig. 2 - Plot of Al_2O_3 in clinopyroxene as a function of depth. We have found only one sample of Karoo lavas (red circle) for which an analysis of clinopyroxene exists (from A. A. Mitchell, in an unpublished thesis, Rhodes University) which is very close to that obtained for the shallowest sill. The number of each sill and number of analyses are indicated by values without and within brackets, respectively.

However, we note that Burgess et al. (2017) obtained small differences in ages between the lavas and sills of the Siberian Traps and suggested a similar evolution of stress directions to explain their observations.

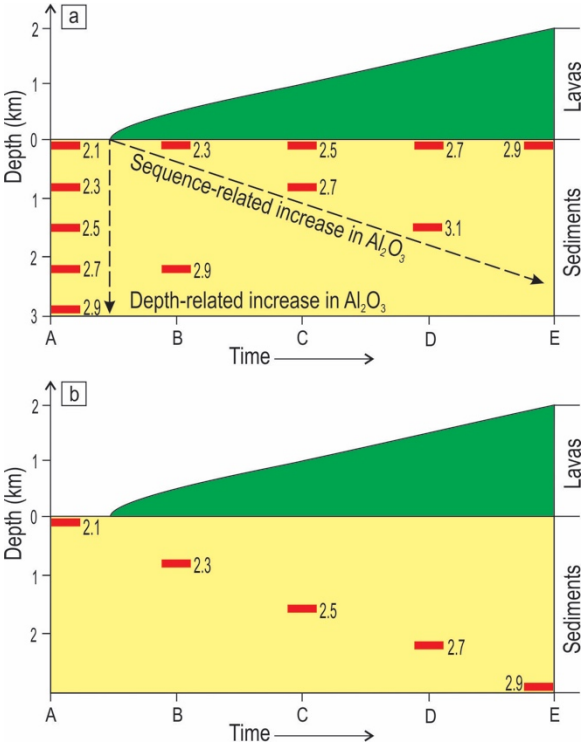

Fig. 3 - Time-depth relations in a developing sill-lava succession, illustrating how Al_2O_3 content in clinopyroxene may have been produced. (a) shows two possibilities of predicted Al_2O_3 content. The vertical column on the left shows changes in composition if all sills pre-dated the lavas. The values to the right show a random assortment of depths and timing of sills of intrusion and extrusion were contemporaneous. (b) shows relationship (considered very implausible) in which the observed correlation of Al_2O_3 with depth could have been achieved if emplacement of sills occurred concurrently with volcanic activity.

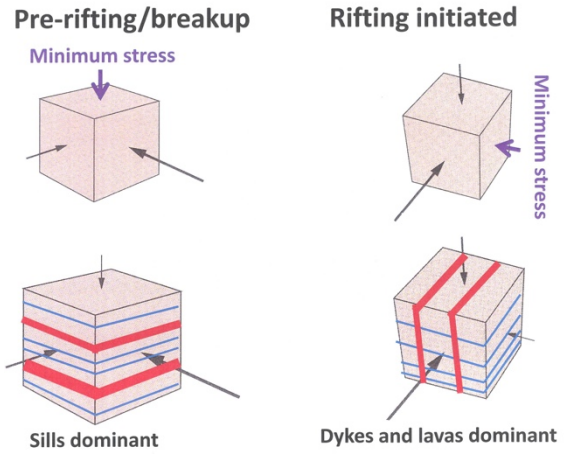

Fig. 4 - Development of stress directions illustrating why sill injection may have pre-dated volcanicity.

Acknowledgements

We are grateful to the staff at the Council for Geoscience, South Africa for access to their borehole store to collect these samples.

References

Burgess, S. D., Muirhead, J. D. and Bowring, S. A. (2017), Initial pulse of Siberian Trapp sills as the trigger of the end-Permian mass extinction, *Nature Communication, 8(1)* doi: 10.1038/s41467-017-00083-9.

Duncan, A. R. and Marsh, J. S. (2006), The Karoo Igneous Province, in *The Geology of South Africa,* edited by Johnson, M. R., Anhaeusser, C. R., Thomas, R. J., 501-520, Geological Society of South Africa, Johannesburg / Council for Geosciences, Pretoria.

Neumann, E.-R., Svensen, H., Galerne, C. Y. and Planke, S., (2011), Multistage Evolution of Dolerites in the Karoo Large Igneous Province, Central South Africa. *Journal of Petrology, 52,* 959–984.

Putirka, K. D., Johnson, M., Kinzler, R., Longhi, J. and Walker, D. (1996), Thermobarometry of mafic igneous rocks based on clinopyroxene-liquid equilibria, 0 – 30 kbar, *Contributions to Mineralogy and Petrology*, *123*, 92-108.

Putirka, K. D., Mikaelian, H., Ryerson, F. and Shaw, H. (2003), New clinopyroxene-liquid thermometers for mafic, evolved, and volatile-bearing lava compositions, with applications to lavas from Tibet and Snake River Plain, Idaho, *American Mineralogist, 88*, 1542-1554.

Svensen, H. H., Polteau, S., Cawthorn, R. G. and Planke, S. (2015), Sub-volcanic intrusions in the Karoo basin, South Africa, in *Physical Geology of Shallow Magmatic Systems,* edited by Breitkreuz, C. H. and Rocchi, S., pp. 1-14, Advances in Volcanology, Springer, Berlin, doi: 10.1007/11157_2014_7.

Characterization of the Paleoproterozoic volcanism in the south area of Tapajós Mineral Province, Amazonian Craton

Cellier, G.[1], Juliani, C.[1]

[1] *Institute of Geociences, University of São Paulo, São Paulo, Brazil* – gabrielcellier@usp.br; cjuliani@usp.br

Keywords: *Uatumã, Tapajós, Amazonian Craton.*

In the Tapajós Mineral Province area, located between the Xingu and Tapajós rivers in the SE portion of the Amazonian Craton occur extensive units of volcanic, volcanoclastic, porphyry and granite rocks. In general, those are linked to the Paleoproterozoic Uatumã magmatic event (ca. 1.88 Ga).

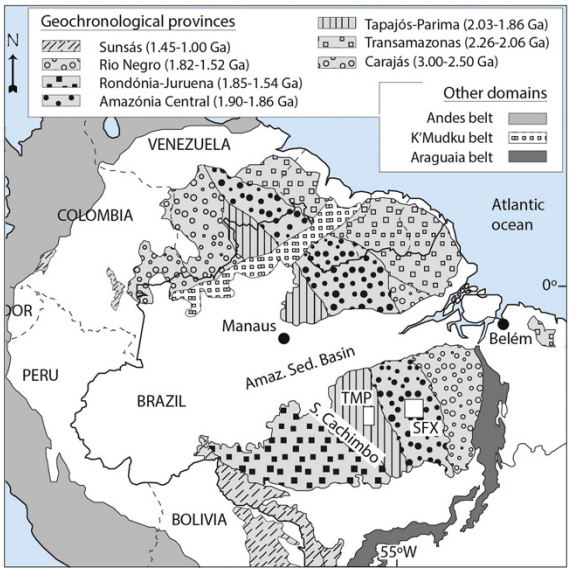

Fig. 1 – Geochronological provinces of Amazonian Craton and other domains according to Santos *et al.* (2000). TMP: Tapajós Mineral Province, SFX: São Felix do Xingu Mineral Province.

However, in the Tapajós area, calc-alkaline rocks similar to those typically linked to the Andean-type magmatic arc have been formed at least in three events, around 2.0, 1.96, and 1.88 Ga. These rocks range between basaltic andesite to rhyolitic composition, defining a magmatic series of medium to high-K calc-alkaline rocks, even reaching shoshonitic composition, related to continental magmatic arcs. Furthermore, in the area, ca. 1.87 Ga alkaline volcanic, sub-volcanic and intrusive A-type rocks, mostly represented by rhyolites with associated basalts and gabbros, are identified.

Older ca. 2.0–1.88 Ga calc-alkaline orogenic units are represented by the Vila Riozinho (ca. 2.0 Ga) and Novo Progresso (ca. 1.97–1.96 Ga) units, these related to older orogenic events in the area.

The ca. 1.89 to 1.87 Ga calc-alkaline volcanic event is associated with volcanic calderas, stratovolcanoes, and rhyolite domes described in the region.

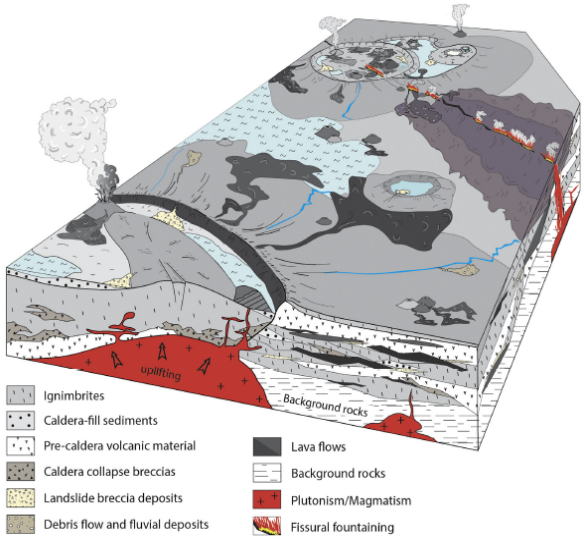

Fig. 2 – Paleogeographic reconstruction of the volcanic and fissural activity in the southern area of Amazonian Craton (Roverato *et al.*, 2019).

Recent studies have indicated different hydrothermal alteration zones and epithermal mineralization in the region. These high-, intermediate- and low-sulfidation mineralization are similar to those hosted in Phanerozoic volcanic rocks. At Tapajós, epithermal mineralization occurs in hydrothermal breccias in volcanic calderas, rhyolite domes and fault zones. In the region, rhyodacite to rhyolitic dykes and porphyry stocks with hydrothermal alteration and Cu-Mo-Au porphyry-type mineralization also occurs.

The improvement of the knowledge on the tectonic evolution and petrogenesis of the Uatumã magmatic event might be a key to elaborate high-impact metallogenetic models for base and precious metals deposits in the southern area of the Amazonian Craton.

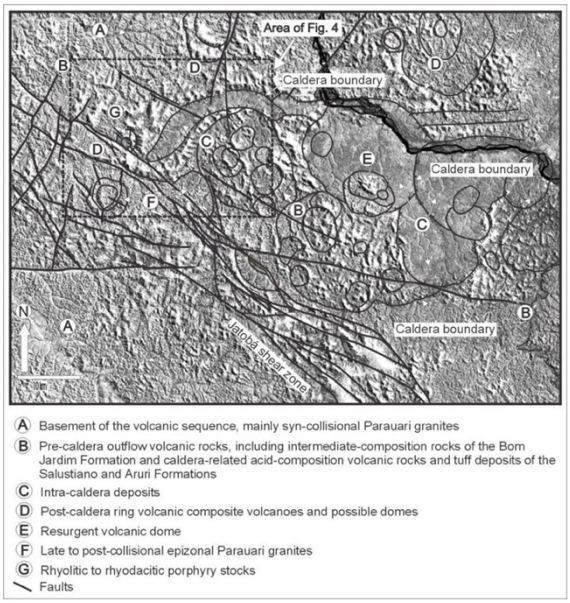

Fig. 3 – Landsat image of volcano calderas and associated volcanic units in the Tapajós Mineral Province (Juliani *et al.*, 2005).

Acknowledgements

The author would like to thank Lena Monteiro for the assistance and CAPES for the scholarship grant.

References

Bahia, R.B.C., M.L.E.S. Quadros (2000), Geologia e recursos minerais da Folha Caracol (SB.21-X-C). Estado do Pará. Escala 1:250.000. PROMIN Tapajós, CPRM, Brasília, Brazil (CD-ROM).

Juliani, C., R.O. Rye, C.M.D. Nunes, L.W. Snee, R.H. Correa-Silva, L.V.S. Monteiro, J.S. Bettencourt,, R. Neumann, A.A. Neto (2005), Paleoproterozoic high-sulfidation mineralization in Tapajós gold province, Amazonian Craton, Brazil: geology, mineralogy, alunite argon age, and stable-isotope constraints. Chemical Geology, 215(1-4): 95-215.

Juliani, C., C.C. Carneiro, C.M.D. Fernandes, L.V.S. Monteiro, A.P. Crosta, S.A. Carneiro-Araujo, C.M. Echeverri-Misas, C.C. Tokashiki, M.A. Aguja-Bocanegra (2014), Arcos magmáticos continentais paleoproterozoicos superposto na porção sul do Cráton Amazônico. In: 47º Congresso Brasileiro de Geologia, 2014, Salvador. Anais. Salvador: SBG.

Roverato, M., D. Giordano, T. Giovanardi, C. Juliani, L. Polo (2019), The 2.0–1,8 Ga Paleoproterozoic evolution of the southern Amazonian Craton (Brazil): An interpretation inferred by lithofaciological, geo-chemical and geochronological data. Gondwana Research, v. 70, p 1-24.

Tassinari, C.C.G., M.J.B. Macambira (1999), Geochronological Provinces of the Amazonian Craton. Episodes, 22(3): 174−182.

Interactions between folded crustal segments and magma propagation with examples from the Central Andes

Matías Clunes.[1], John Browning. [1, 2], José Cembrano.[1, 3] and Carlos Marquardt [1, 2]

[1] *Department of Structural and Geotechnical Engineering, School of Engineering, Pontificia Univesidad Católica de Chile, Vicuña Mackenna 4860, Macul, Santiago, Chile* – mclunes@uc.cl
[2] *Department of Mining Engineering, School of Engineering, Pontificia Universidad Católica de Chile, Vicuña Mackena 4860, Macul, Santiago, Chile.*
[3] *Andean Geothermal Centre of Excellence (CEGA), Universidad de Chile, Plaza Ercilla 803, Santiago, Chile.*

Keywords: Crustal heterogeneity, Dikes and Sills, Magma Storage.

The process of magma emplacement and storage in the upper crust is controlled, to a large extent, by the structure of the crust through which the magma propagates. Contrasts in the mechanical properties between different crustal lithologies can alter the distribution of crustal stresses and hence generate a stress field, which is favorable or unfavorable for magma propagation. It is the crustal stress field that largely determines if a dike will reach the surface to trigger a volcanic eruption or instead if it become arrested in the crust, or change its direction of propagation to form sheets or sills. The emplacement and growth of large intrusive bodies in the upper crust relies on the formation and growth of sills and hence understanding the process of sill formation is important for understanding the development of crustal magma chambers.

The interaction between magma emplacement and a vertically stratified heterogeneous crust, as hosts many volcanoes, is a problem that requires further attention. This is because many models of magma emplacement assume a homogeneous and isotropic crustal structure (Gudmundsson, 2006). The study of magma emplacement under transpresional tectonic conditions, as in the Andes (Cembrano & Lara, 2009), has received far less attention but can provide new ways of understanding the nature of interactions between magma and the crust. This is especially important because in the areas like the Andes, the crustal segments are both mechanically stratified and heterogeneous and the regional stresses are also highly anisotropic and hence the stress field is heterogeneous. As such, new models are needed, based on field evidence, to understand magma propagation and crustal storage in such region.

Any magma that forms a volcano must propagate through often highly heterogeneous successions. It is generally now well-understood how fractures can become arrested at interfaces between layers in heterogeneous successions, for example through the processes of, for example 1) stress barriers, 2) elastic mismatch, and 3) Cook-Gordon debonding (Gudmundsson, 2011). However, the fundamental concepts that derive these models are based on the contacts and layer interfaces being arranged normal to the fracture. This situation holds true for heterogeneous crustal segments which are layered sub-horizontally, such as lava piles in shallow dipping volcanic edifices. However, in regions that have experienced intense orogenesis the crustal layers are often intensely deformed and hence fractures meet the contacts and interfaces over a range of different angles. Also, the stresses in the layers are formed, not just by the regional tectonic forces or the material properties, they are also a function of the geometry of the system. Therefore, an assumption of isotropic material properties and horizontally stratification can lead to highly erroneous results. And again, in the Andean example both assumptions are likely invalid. Hence, new mechanical models are needed to understand the propagation of storage of magma beneath Andean volcanoes.

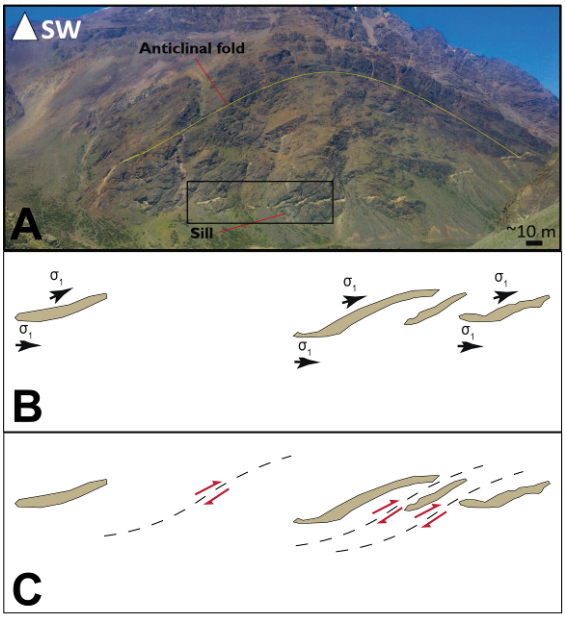

Fig. 1 – A. Sill emplaced in the core of an anticlinal fold. B. Sill rotation due to changes in the direction of maximum principal stress (σ_1). C. Sill rotation due to reverse faults.

Here we present preliminary field mapping of a series of magmatic plutons, sills and dikes in the central Andean cordillera. For example, in El Juncal, in the Chilean central Andes, near to the border with Argentina, a series of rhyodacitic sills were emplaced in the core of an anticlinal east vergence fold (Figure 1). They form rotated lenses about 10-50 m length (Piquer et al., 2015).

The objective of the research, which will be conducted as part of a PhD program, is to establish a link between how magma interacts with the host rock during its ascent to the surface within heterogeneous crustal segments, that is, mechanically stratified, and anisotropic, through the presence of structures such as folds and faults. Within other aspects to be examined, are the thermal effects and the deformation associated with the emplacement of intrusive bodies, as well as their connection with mineralizing processes. The results can be useful for aiding geophysical interpretations during periods of magma injection in Andean volcanoes.

References

Cembrano, J., and L. Lara (2009), The link between volcanism and tectonics in the southern volcanic zone of the Chilean Andes: A review, *Tectonophysics*, 471(1-2), 96-113.

Gudmundsson, A. (2006), How local stresses control magma-chamber ruptures, dyke injections, and eruptions in composite volcanoes, *Earth-Science Reviews*, 79(1-2), 1-31.

Gudmundsson, A. (2011), Deflection of dykes into sills at discontinuities and magma-chamber formation, *Tectonophysics*, 500(1-4), 50-64.

Piquer, J., J. Skarmeta, and D. R. Cooke (2015), Structural Evolution of the Rio Blanco-Los Bronces District, Andes of Central Chile: Controls on Stratigraphy, Magmatism, and Mineralization, *Economic Geology*, 110(8), 1995-2023.

Emplacement of multiple granite intrusions and triggering of geothermal systems (Larderello, Tuscany): new insights from zircon petrochronology

Dini A.[1] and Farina F.[2]

[1] *Istituto di Geoscienze e Georisorse-CNR, Pisa, Italy – a.dini@igg.cnr.it*
[2] *Dipartimento di Scienze della Terra, Università di Milano, Italy*

Keywords: *Granites, Zircon petrochronology, geothermal*

The Larderello geothermal field (Tuscany, Italy) is located in an area of ca. 200 km^2 that experienced multiple emplacement of peraluminous granite magmas during the last 4 My (Dini et al., 2005). At least four major pulses have been identified by ^{40}Ar-^{39}Ar dating: at ca. 3.8 Ma, 3.3 Ma, 2.5 Ma and 1.5 Ma (Dini et al. 2005 and references therein). Granite intrusions do not crop out and they were intersected by exploratory wells at depth ranging between 1500 and 5000 m. Petrological and geochronological studies of metasedimentary rocks hosting the intrusions, indicate that multiple contact aureoles developed through time reaching maximum temperatures of 600-650°C.

This intrusive complex is part of the Tuscan Magmatic Province (TMP): a large number of plutons, laccoliths and sills (from 8.5 Ma to present) that intruded the shallow crust (2-6 km depth) during the opening of the continental Northern Tyrrhenian back-arc basin (Dini et al., 2008). TMP intrusive bodies exhumed by tectonics and erosion have been intensively studied and they usually show a sub-horizontal, roughly tabular shape and maximum volumes of 120 km^3 (Dini et al., 2008; Rocchi et al., 2010). TMP magmatism is dominated by relatively "cold" (750-900°C) acidic peraluminous products derived by partial melting of the metasedimentary continental crust (Figure 1), while "hot" (900-1000°C) mantle-derived mafic products are rather rare.

The low temperature of the magma, the small size of the intrusion and their emplacement at shallow crustal levels are responsible for: i) the maximum temperature reached by host rocks (650°C), ii) the limited thickness of the contact aureoles (100-700 m for temperature ranging from 650 to ca. 400°C) and iii) the relatively short life time of the thermal anomaly (few 10^5 y).

Several petrological, geophysical and numerical constraints support the existence of an intermediate crustal level where TMP granite melts are collected reaching the critical volume size (magma chamber) for sustaining the final ascent to shallow crustal levels (Figure 1). The most striking evidence results from high precision ID-TIMS U-Pb dating of zircon from Tuscan granites showing a prolonged zircon crystallization time for each intrusive unit (200-400 ky; Caricchi et al., 2016; Farina et al., 2018). Following the approach of Caricchi et al. (2016), ranges of zircon ages, zircon saturation temperatures and magma fluxes can be integrated in a thermal model providing the size of the storage magma chambers. The numerical models of Caricchi et al. (2016) for the Monte Capanne pluton (Elba Island) estimate a volume of the intermediate magma chamber of 300-1000 km^3, larger than the volume of the pluton itself (ca. 100-150 km^3; Dini et al., 2008; Rocchi et al., 2010).

We combined high-precision CA-ID-TIMS U–Pb dates with stable and radiogenic isotope data from zircon crystals in the Larderello–Travale (Italy) shallow-level granites (Farina et al., 2018).

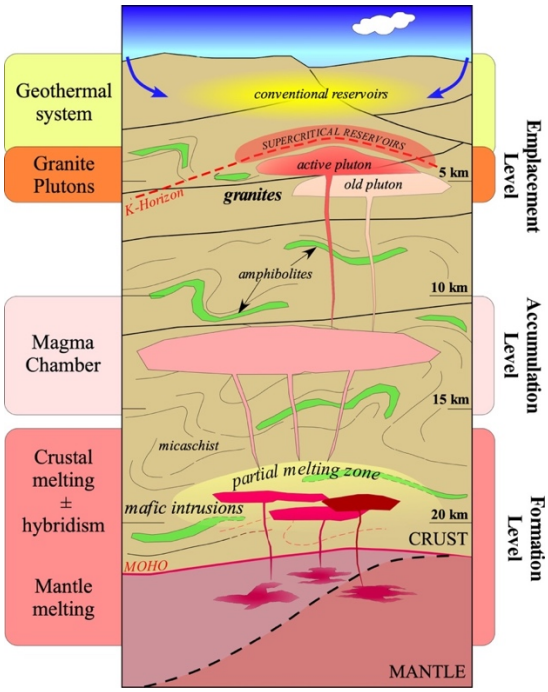

Fig. 1 – Interpretive, idealized cross section of the thinned Tuscan crust showing the different levels for generation, storage and final emplacement of TMP granite magmas.

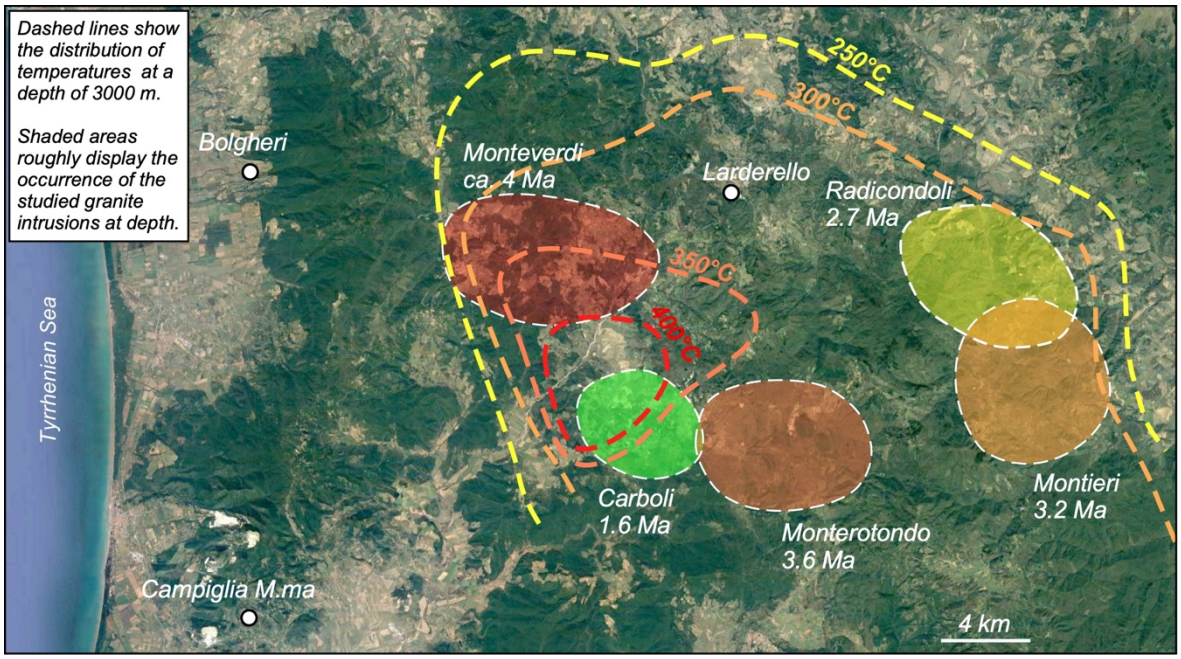

Fig. 2 –Distribution of the different granite intrusions cored in Larderello geothermal field at depth ranging from 2000 to 5000 m. The hottest isotherms (> 350°C) highlight the occurrence of the active intrusion triggering the present-day geothermal system

Magmatic zircon crystals from these granites contain $\delta^{18}O$ values ranging from 8.6 to 13.5‰ and crystals from individual samples exhibit inter- and intra-grain oxygen isotope variability exceeding 3‰.

The analyzed crystals have ε_{Hf} values ranging between −7.4 and −12.4, with moderate, intra-sample ε_{Hf} isotope variability. All CA-ID-TIMS (chemical abrasion isotope-dilution thermal ionization mass spectrometry) $^{206}Pb/^{238}U$ zircon ages range from 4.5 to 1.6 Ma and suggest five pulses of magmatic activity at ~4, 3.6, 3.2, 2.7 and 1.6 Ma in good agreement with previous ^{40}Ar-^{39}Ar ages. More importantly, zircon crystals from individual samples typically exhibit an age spread as large as 300–500 ka. This age dispersion suggests that most of the zircon did not crystallize at the emplacement level but in the middle crust (Farina et al., 2018).

These data coupled with previous petrological data (Dini et al., 2005) indicate that the intermittent magmatic activity triggered a long lived thermal anomaly. However, such "young" granites are still too old to sustain the present day geothermal system and the extremely high thermal gradient (up to ca. 150°C/km). The strongest temperature gradients occurring in the SW part of the geothermal field have been recently interpreted as the result of the recent emplacement (few thousands years) of granite magmas at a depth of ca 3300-3500 m (Bertani et al., 2018).

Acknowledgements

This work has been partly carried out as part of the "DESCRAMBLE" EU-H2020 Project (AD) and a Marie Curie Fellowship (FF).

References

Bertani, R., Büsing, H., Buske, S., Dini, A., Hjelstuen, M., Luchini, M., Manzella, A., Nybo, R., Rabbel, W. and Serniotti, L., 2018. The First Results of the DESCRAMBLE Project. *Proceedings, 43rd Workshop on Geothermal Reservoir Engineering, Stanford University*. SGP-TR-213.

Caricchi, L., Sympson, G., and Schaltegger, U., 2016. Estimates of Volume and Magma Input in Crustal Magmatic Systems from Zircon Geochronology: The Effect of Modeling Assumptions and System Variables, *Frontiers in Earth Science, 4*: 1-15.

Dini, A., Gianelli, G., Puxeddu, M. and Ruggieri, G., 2005. Origin and evolution of Pliocene – Pleistocene granites from the Larderello geothermal field (Tuscan Magmatic Province, Italy), *Lithos, 31*: 1-31.

Dini, A., Westerman, D.S., Innnocenti, F. and Rocchi, S., 2008a. Magma emplacement in a transfer zone: the Miocene mafic Orano dyke swarm of Elba Island (Tuscany), in *Structure and Emplacement of High-Level Magmatic Systems,* edited by K. Thomson and N. Petford, Geol. Soc. London Sp. Publ. 302, pp. 131-148.

Farina, F., Dini, A., Davies, J.H.F.L., Ovtcharova, M., Greber, N.D., Bouvier, A.S., Baumgartner, L., Ulianov, A., Schaltegger, U., 2018. Zircon petrochronology reveals the timescale and mechanism of anatectic magma formation, *Earth and Planetary Science Letters, 495*: 213-223.

Rocchi, S., D.S. Westerman, A. Dini and F. Farina (2010), Intrusive sheets and sheeted intrusions at Elba Island (Italy), *Geosphere, 6*(3): 225-236.

Cenozoic Basement and his relationship with the emplacement of mafic monogenetic volcanoes, Cerro Negro: A structural view (TSVZ, Chile)

Espinosa-Leal J.[1] and Salas P.[1]

[1] *Department of earth science, University of Concepción, Concepción, Chile* – jaespinosa@udec.cl

Keywords: TSVZ, monogenetic volcanoes, structural geology.

In the Transitional Southern Volcanic Zone of the Southern Andes (TSVZ, 34.5°-37°S; López-Escobar et al., 1995), it is possible to identify a large number of monogenic volcanoes (MV in Table 1) of varying compositions from basalts to rhyolites (Singer et al., 1997; Hildreth et al., 2010; Salas et al., 2016). Geochemical analyzes performed on olivines of some of these, indicate a short period of residence in the upper cortex (Salas et al., 2016). This contrasts with the fact that the crust in this segment has a high thickness (~ 45 km; Tassara and Echaurren, 2012), unlike the Central and South segment of the Southern Andes, in which the cortical thickness is low and there is also the presence of structures of regional scale, such as the Liquiñe-Ofqui Fault Zone and the Andean Transversal Fault System, which would control or even promote the location of the volcanism (Cembrano and Lara, 2009).

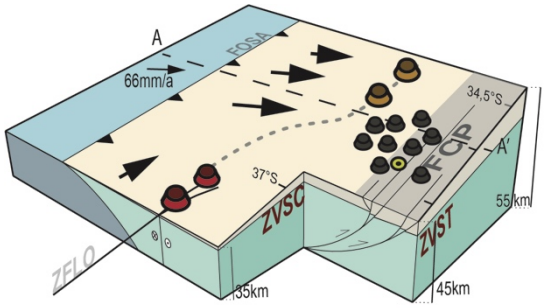

Fig. 1 – Tectonic setting of the TSVZ. Green dot shows the location of the Cerro Negro (36°01'S).

In this work, structural measurements are obtained in the field and from satellite images (morphometry and structures) in MVs that have similar lithological and age characteristics, with the objective of determine which conditions would be favorable for rapid transport of magma, which would allow the emplacement of poorly differentiated magmas in a segment with thick crust.

Of the large number of MVs identified by various authors in the ZVST (Singer et al., 1997; Hildreth et al., 2010; Salas et al., 2016), 50% have favorable lithological characteristics for this study (basal compositions) and 10% (10 MVs) present the well-preserved building, that is, they have not suffered erosion due to glacial processes (<25 Ka).

From the measurements, the maximum and minimum elongation parameters of the building are obtained, in order to determine the maximum elongation index (*ge*), which allows establishing if there is a tectonic (or structural) control over the emplacement of the MVs (Tibaldi, 1995; Table 1).

MV	ge	DE	Lineaments	Faults
LHC	0,85	NE	LI (NE)	N/F
BHC	0,87	NW	LF (NW)	LF (NW)
VSw	0,60	NW	LF (NW)	LF (NW)
MEB	0,90	EW	N/L	FB (EW)
VLP	0,76	NW	T2 (NE)	FT1 (NE)
MCRw	0,83	EW	T2 (NE)	N/F
MCRe	0,90	NW	T2 (NE)	N/F
MCTw	0,90	WNW	LF (NW)	LF (NW)
MCTe	0,96	WNW	LF (NW)	LF (NW)
VLF	0,80	NW	LF (NW)	LF (NW)

Tabla 1 – Correlations between structures and directions of the possible dike swarm of each MV. Dark grey, total correlation; Light grey, location only. N/F no faults measured; N/L no lineaments measured.

The values of *ge* range from 0, maximum elongation with structural control, to 1, without elongation. From the *ge* parameter, the directions of the possible dike swarm are obtained (DE in Table 1), which could also be related to the occurrence of structures. The data of *ge* are compared with the directions of the structures measured for each MV, to establish if there are relations (Table 1).

From this analysis, it is determined that all of the monogenic volcanoes have a correlation between location and structure, that is, are located over the trace of this lineaments, some of which also have faults measured in the field (Laguna Fea, Troncoso 1 and 2 and Invernada, LF, T1, T2 and LI lineaments, respectively). Regarding the orientations of the possible swarms of dikes, these also coincide with the orientation of the structures, so it can be said that

everyone would present a structural control in their emplacement.

Monogenic volcanoes are also located mainly on Cenozoic rocks, except for the LHC (Fig. 2.a).

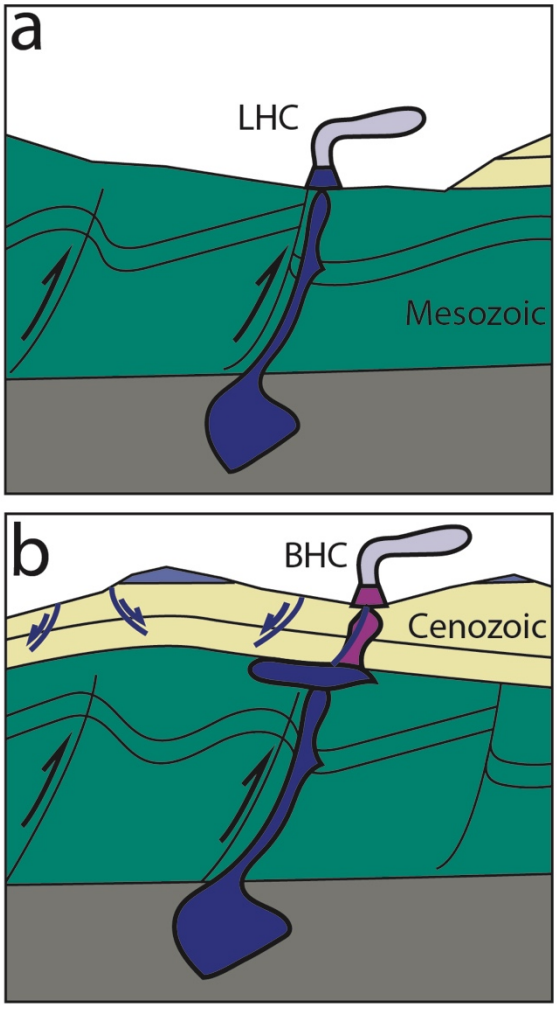

Fig. 2 – Cartoon that shows the relationship between MVs, structures and basement. a) Thrust faults on the Mesozoic basement transporting non differentiated magma (blue) to the upper crust; b) Cenozoic cover with normal faults and differentiated MVs (pink).

With respect to the compositions, LHC corresponds to the only pair of MVs with mantelic component. This can be attributed to the fact that this pair is located in the ancient Mesozoic basement, unlike the monogenetic volcanoes located to the south, located on the Cenozoic rocks, which leads us to think that the interaction of the magma rising with this, it allows a certain degree of differentiation. In addition, the tectonic characteristics in the ZVST would promote the development of NS orientation faults, due to the compressive subduction regime (Cembrano and Lara, 2009). These faults would not directly cut the Cenozoic rocks, but would control the development of normal faults on them, in directions between NW and NNE, as determined in this work (Fig. 2.b). Thus, the Cenozoic cover would function as a trap for rising magma, allowing an increase in the degree of differentiation of magmas.

In future works, we intend to analyze the totality of the monogenetic volcanoes of the TSVZ, in order to understand the tectonomagmatic significance of the occurrence of this type of volcanism.

Acknowledgements

The autors sincerely thank to Federica Mattioli for her contributions in the development of the illustrations and review of this manuscript.

References

Cardona, C., Tassara, A., Gil-Cruz, F., Lara, L., Morales, S., Kohler, P., and Franco, L. (2018), Crustal seismicity associated to rapid Surface uplift at Laguna del Maule Volcanic Complex, Southern Volcanic Zone of the Andes, *Journal of Volcanology and Geothermal Research*, 1-12.

Cembrano, J., and Lara, L. (2009), The link between volcanism and tectonics in the southern volcanic zone of the Chilean Andes: a review, *Tectonophysics*, (471)96-113.

Hildreth, W., Godoy, E., Fiertein, J., and Singer, B. (2010), Laguna del Maule Volcanic Field: Eruptive history of a Quaternary basalt-to rhyolite distributed volcanic field on the Andes rangecrest in central Chile, *Subdirección Nacional de Geología*. *Boletín* N°63.

López-Escobar, L., Cembrano, J., and Moreno, H. (1995), Geochemistry and tectonics of the Chilean Southern Andes basaltic Quaternary volcanism (37-46°S), *Revista Geológica de Chile*, 22(2), 219-234.

Salas, P., Rabbia, O., Hernández, L., and Ruprecht, P. (2016), Mafic monogenetic vents at the Descabezado Grando volcanic field (35.5°S-70.8°W): the northernmost evidence of regional primitive volcanism in the Southern Volcanic Zone of Chile, *International Journal of Earth Science (Geol Rundsch)*, 1-15.

Singer, B., Thompson, R., Dungan, M., Feeley, T., Nelson, S., Pickens, J., and Metzger, J. (1997), Volcanism and erosion during the past 930 ky at the Tatara–San Pedro complex, Chilean Andes, *Geological Society of America, Bulletin.* 109(2) 127-142.

Tassara, A., and Echaurren, A. (2012), Anatomy of the Andean subduction zone: three-dimensional density model upgraded and compared against global-scale models, *Geophysical Journal International*, (189)161-168.

Tibaldi, A. (1995), Morphology of pyroclastic cones and tectonics, *Journal of Geophysical Resaerch*, 100(B12) 24,521 - 24,535.

Structural characterization of the western flank of Domuyo volcano and its relationship with Neogene to Quaternary magmatic activity (Neuquén, Argentina)

Galetto Antonella T.[1], García Víctor H.[2,3], Yagupsky Daniel L.[1], Bechis Florencia[4]

[1] *CONICET-Laboratorio de Modelado Geológico (LaMoGe-IDEAN), Departamento de Ciencias Geológicas, Facultad de Ciencias Exactas y Naturales, Universidad de Buenos Aires (UBA), Pabellón II, Ciudad Universitaria, C1428EHA, Ciudad autónoma de Buenos Aires, Argentina – antogaletto@gmail.com*
[2] *Institut für Geowissenschaften, Universität Potsdam, Karl-Liebknecht-Str. 24-25, 14476, Potsdam-Golm, Germany.*
[3] *La.Te. Andes S. A. (GEOMAP-CONICET), Las Moreras 510, 4401, Vaqueros, Salta, Argentina.*
[4] *CONICET-IIDyPCA, Universidad Nacional de Río Negro (UNRN), Sarmiento Inferior 3974, CP 8400, San Carlos de Bariloche, Argentina.*

Keywords: structures, volcanism, Domuyo.

This study covers the structural analysis of the western flank of Domuyo volcano, located in the northwestern sector of the Chos Malal fold and thrust belt (36°38'15.10"S; 70°25'55.37"W) (Fig. 1). Based on detailed fracture analysis and kinematic study of mesoscale faults, combined with pre-existing geological, structural, and geophysical data, the structural configuration of this region is interpreted as directly conditioned by pre-existing basement structures (Galetto et al., 2018; Galetto, 2019). Late Triassic-Early Jurassic normal faulting conditioned the geometry of the sedimentary sequences of the Neuquén Basin, the location of compressive deformation during the Andean orogeny, and the emplacement of the Neogene to Quaternary magmatism. The Manchana Covunco N-S fault is the main partially inverted normal fault interpreted on the western flank of Domuyo volcano (Galetto et al., 2018). Unpublished thermo-chronological data obtained from samples of the structural basement, the Mesozoic sedimentary sequence, and the Neogene to Quaternary units, suggest that a compressive tectonic regime have taken place from Late Cretaceous to Paleogene times (Galetto, 2019; Galetto et al., in prep). This regime would have triggered the reactivation and partial inversion of the normal faults, together with the development of conjugated fractures sets (NW-SE/NE-SW) (Galetto et al., 2018; Galetto, 2019; Galetto et al., in prep). Evidences about the continuation of the compressive deformation during Middle Miocene to Late Miocene times are documented in numerous areas of the Chos Malal fold and thrust belt (Folguera et al., 2007; Sagripanti et al., 2011, 2012; Gürer et al., 2015; Sánchez et al., 2018; among others); nevertheless no evidence have been found in Domuyo area. The magmatic activity of Domuyo Volcanic Complex started between Late Miocene to Pliocene times, according to unpublished thermochronological data (Galetto, 2019; Galetto et al., in prep) and to observations made by Llambías et al. (1978). The intrusive phase of the Domuyo Volcanic Complex crops out in the southern flank of Domuyo volcano and in the core of a broad N-S anticline, developed during the Late Cretaceous-Paleogene compressive stage (Llambías et al., 1978; Galetto et al., 2018; Galetto, 2019). The stress regime identified through the measurement of normal kinematic indicators in mesoscale faults affecting Late Miocene to Pleistocene units, suggests that the emplacement of the Domuyo Volcanic Complex could have occurred under an extensional regime (Galetto et al., 2018). However, this not necessarily rejects the possibility of its emplacement during the lasting effects of the Middle-Late Miocene compression documented in the Chos Malal fold and thrust belt (Folguera et al., 2007; Sagripanti et al., 2011, 2012; Gürer et al., 2015; Sánchez et al., 2018; among others).

During Pleistocene times, the Magmatismo Dómico (Brousse and Pesce, 1982) is registered in the western flank of Cerro Domuyo. The location of the magmatism during this period could have been conditioned by the presence of the Manchana Covunco fault, as its distribution coincides with the interpreted trace of this structure at surface. Kinematic analyses carried out on Pleistocene units indicate that its activity could be related with a Pleistocene extensional regime (Galetto et al., 2018). The uncertainty regarding to the tectonic regime that conditioned the emplacement of the Domuyo Volcanic Complex, has encouraged the development of further studies. Therefore, analogue models simulating magmatic emplacement under contrasting structural and dynamic regimes are being performed in order to evaluate the possible scenarios, and compare the resulting experimental vs. natural geometries. This studies will not only shed light on the structural evolution of Domuyo area, but also contribute on the understanding of the relationships between volcanism within both compressive and extensional tectonic settings, when both are controlled by previous structures.

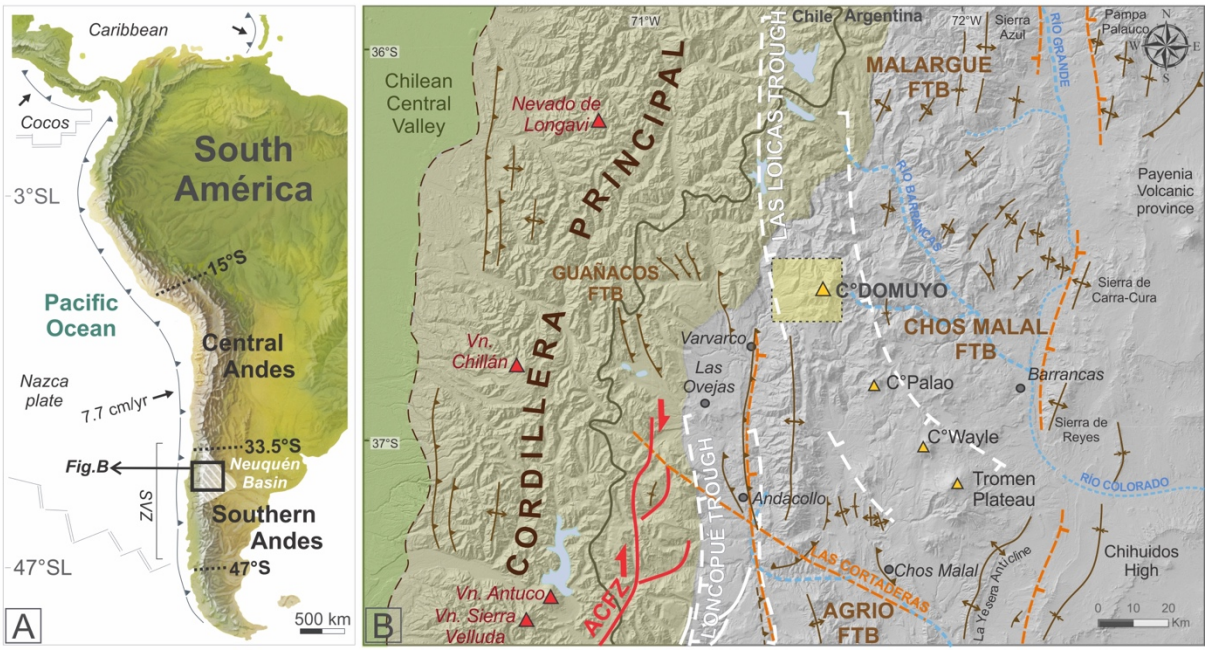

Fig. 1 – (A) Location of the Southern Andes between 33°30′ and 47°SL (Tassara and Yañez, 2003). The regional map of Fig. B is indicated with a box. The limit of the Neuquén basin is marked with a white dashed line. Southern Volcanic Zone (SVZ). (B) Regional map between 36° and 37°30′SL with the main morphostructural units present in the area, and the study area indicated with a yellow box. Upper Cretaceous-to-Miocene fold-and-thrust belts in brown (FTB); Plio-Pleistocene extensional basins (troughs) in white; active volcanoes (red triangles); and Antiñir-Copahue Fault Zone (ACFZ) in red. Upper Triassic to Lower Jurassic regional lineaments that conditioned the Precuyano depocenters are represented by orange dashed lines. Taken and modified from Galetto et al. (2018).

Acknowledgements

This work is based on part of Antonella Galetto's Ph.D. and post-PhD. research, which have been partially funded by CONICET, the YPF Foundation (FYPF), and the Scientific and Technological Promotion Agency, through a PhD and post-PhD grant, the PIO project 13320130100212CO and the PICT projects 2014-2240 / 2016-1407 / 2017-3259.

References

Brousse, R., and A. H. Pesce (1982). Cerro Domo. Un volcán Cuartario con posibilidades geotérmicas. Provincia del Neuquén, en los relatorios del 5to Congreso Latinoamericano de Geología, 4, 197-208.

Folguera, A., V. A. Ramos, T. Zapata, and M. Spagnuolo (2007). Andean evolution at the Guañacos and Chos Malal fold and thrust belts (36°30'-37°00'SL). Journal of Geodynamics 44, 129-148.

Galetto, A. T. (2019). Caracterización tectónica Plio-Cuaternaria de la vertiente occidental del Cerro Domuyo. Controles estructurales de las manifestaciones geotérmicas de alta entalpía asociadas. Tesis de doctorado. Universidad de Córdoba, 305 p.

Galetto, A. T., V. H. García, and A. T. Caselli (2018). Structural controls of the Domuyo geothermal field, Southern Andes (36°38´S), Argentina. Journal of Structural Geology 114, 76-94.

Gürer, D., O. Galland, F. Corfu, H. Leanza, and C. Sassier (2015). Structure and evolution of volcanic plumbing systems in fold-and-thrust belts: A case study of the Cerro Negro de Tricao Malal, Neuquén Province, Argentina. Geological Society of America Bulletin 128, 1-2.

Llambías, E. J., M. Palacios, J. C. Danderfer, and N. Brogioni (1978). Petrología de las rocas ígneas cenozoicas del Volcán Domuyo y áreas adyacentes, Provincia del Neuquén, en los relatorios del 7mo Congreso Geológico Argentino, Neuquén 2, 553-584.

Sagripanti, L., G. Bottesi, M. Naipauer, A. Folguera, and V. A. Ramos (2011). U/Pb ages on detrital zircons in the southern central Andes Neogene foreland (36°–37°S): Constraints on Andean exhumation. Journal South America Earth Science, 32, 555-566.

Sagripanti, L., G. Bottesi, D. Kietzmann, A. Folguera, and V. A. Ramos (2012). Mountain building processes at the orogenic front. A study of the unroofing in Neogene foreland sequence (37°S). Andean Geology 39, 201-219.

Sánchez, N., I. Coutand, M. Turienzo, F. Lebinson, V. Araujo, and L. Dimieri (2018). Middle Miocene to Early Pliocene Contraction in the Chos Malal Fold-and-Thrust Belt (Neuquén Basin, Argentina): Insights from Structural Analysis and Apatite Fission-Track Thermochronology. Tectonics 36 (10), 1966-1987.

Laccolith-induced deformation – A case study integrating field mapping, 3D seismic and well data at Pampa Amarilla, Neuquén Basin, Argentina

Galland O.[1], de la Cal H.[2], and Rabbel O.[1]

[1] *PGP, the NJORD Center, Department of Geosciences, University of Oslo, Oslo, Norway* – olivier.galland@geo.uio.no
[2] *ROCH S.A., Buenos Aires, Argentina*

Keywords: punched laccolith, overburden deformation, field-seismic data.

Magma transport and emplacement in the Earth's crust is a complex geological process that couples the flow of the magma and the deformation of the host rock. The dynamics of the system is to a great extent governed by the mechanical response of the host from the forceful intrusion of magma. In particular, the forceful emplacement of shallow tabular intrusions, such as sills and laccoliths, can trigger complex deformation patterns at several scales. In petroleum prospective basins, these complex magma-induced deformation patterns have tremendous implications for fluid trapping in dome and fluid flow through fractures and damage (Senger et al., 2017).

Most mechanical models of sill and laccolith emplacement account for pure elastic bending of the intrusion's overburden. In contrast, field observations highlight significant inelastic, plastic deformation accommodating, for instance, the emplacement of thick sills and laccoliths. The challenge of revealing the detailed deformation patterns in the field is that only parts of the intrusion/overburden systems are exposed or preserved, leading to substantial extrapolation of the subsurface or eroded parts. Finally, seismic data of buried sills and laccoliths provide unprecedented new insights on intrusion-induced deformation in volcanic basins. However, even if seismic imaging appears adequate for studying simple structures such as low amplitude, elastic bended domes, it reveals very limited to image complex structures induced by, e.g. punched laccoliths.

In this contribution we present an unprecedented case study of an intrusion-induced dome by integrating 3D seismic data, well data and detailed geological mapping. The structure is located at Pampa Amarilla area, in the Agua Botada block, south of Cuesta del Chihuido, 40 km south of Malargüe, Mendoza province, Argentina (Barrionuevo et al., 2019). There, Upper Cretaceous continental deposits of the Neuquén Gr. crop out regionally, with the exception of a sub-circular outcrop of deeper, marine sediments of the mid-Cretaceous-Lower Cretaceous formations of the Huitrín and Agrio Fms., respectively. Earlier geological mapping identified that the sedimentary formations exhibit concentric, shallow outward dipping directions around this structure. A well was drilled in 1938 near the centre of this structure: the last 120 meters of the well perforated andesitic rocks, strongly suggesting that this sub-circular structure is a dome induced by the emplacement of a laccolith thicker than 150 m. However, the shape of the intrusion, its thickness and lateral extent, and the deformation induced by the intrusion remained unconstrained.

In the Agua Botada block, a 3D seismic survey was conducted in the area. Half of the dome structure was included in the seismic block. Even if regional reflectors are perfectly imaged in the 3D seismic data, these reflectors are lost at the vicinity and in the centre of the dome, making it impossible to constrain its shape.

In March 2019, we performed a detailed mapping campaign of the dome structure. We identified clearly distinct formations, from deep to shallow: (1) marine pelite of the Agrio Fm., (2) gypsum of the Lower Huitrín Fm., (3) thin carbonate of the Upper Huitrín Fm. (La Tosca Mb.), (4) yellow to reddish clay of the Rayoso Fm., and (5) red sandstone and conglomerate of the Neuquén Gr. Each formation corresponded to clear geological markers to constrain the structure of the dome. The mapping highlights an asymmetric dome along an E-W transect, with a steeply dipping western margin and a very shallow dipping eastern margin. On the western margin, the deformed bedding exhibit dip angles as high as 70° to the west. Deformational foliation in the gypsum dipping to the west, with lineation also plunging to the west, strongly suggest that the western margin of the dome is faulted. A N-S transect exhibits a more symmetrical structure. In addition, several faults observed in the dome suggests significant deformation.

The geological map alone reveals not sufficient to estimate (1) the thickness of the subsurface intrusion, (2) the associated amplitude of the dome, and (3) the distribution of the intrusion-induced deformation. In addition, the study area is located in a fold-and-thrust belt, and deciphering between magma-induced deformation and tectonic structures can be challenging.

However, we built geological cross sections by integrating our geological map, the 3D seismic data and well data. The seismic data allow us to map the regional structures, which consist of large wavelength, low amplitude folding in the study area. In addition, the combination of well data and 3D seismic data shows that the exposed formations in the dome are much deeper in the surrounding areas. All this information show that the studied dome is a prominent structure that sticks out of the regional structures. We estimate that the dome amplitude is about 400 m, and we infer that the thickness of the underlying intrusion is also close to 400 m. The structural reconstruction in the geological cross sections implies that the intrusion is asymmetric and extends eastward over several kilometres, and that the associated overburden deformation is typical of trapdoor type.

Overall, our study shows that integrating surface geological mapping and subsurface 3D seismic and well data provides unprecedented insights on the complex dome structure of a punched laccolith.

Acknowledgements

The field work was funded by ROCH S.A. We gratefully thank ROCH S.A. for providing 3D seismic and well data.

References

Barrionuevo, M., Giambiagi, L., Mescua, J., Suriano, J., de la Cal, H., Soto, J.L. & Lossada, A.C. 2019. Miocene deformation in the orogenic front of the Malargüe fold-and-thrust belt (35°30′–36° S): Controls on the migration of magmatic and hydrocarbon fluids. *Tectonophysics*,

Senger, K., Millett, J., Planke, S., Ogata, K., Eide, C.H., Festøy, M., Galland, O. & Jerram, D.A. 2017. Effects of igneous intrusions on the petroleum system: a review. *First break*, **35**, 47-56.

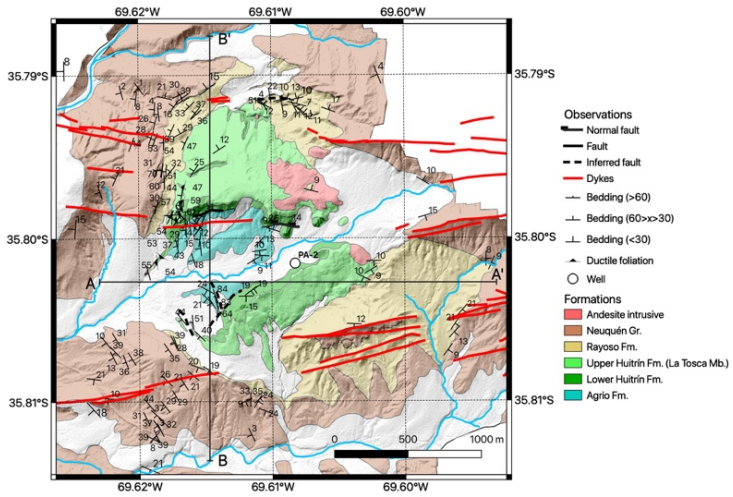

Fig. 1 – Geological map of dome structure of Pampa Amarilla, southern Mendoza province, Argentina. Straight black lines locate parts of cross sections of Fig. 2. The topography was calculated from a drone photogrammetric survey.

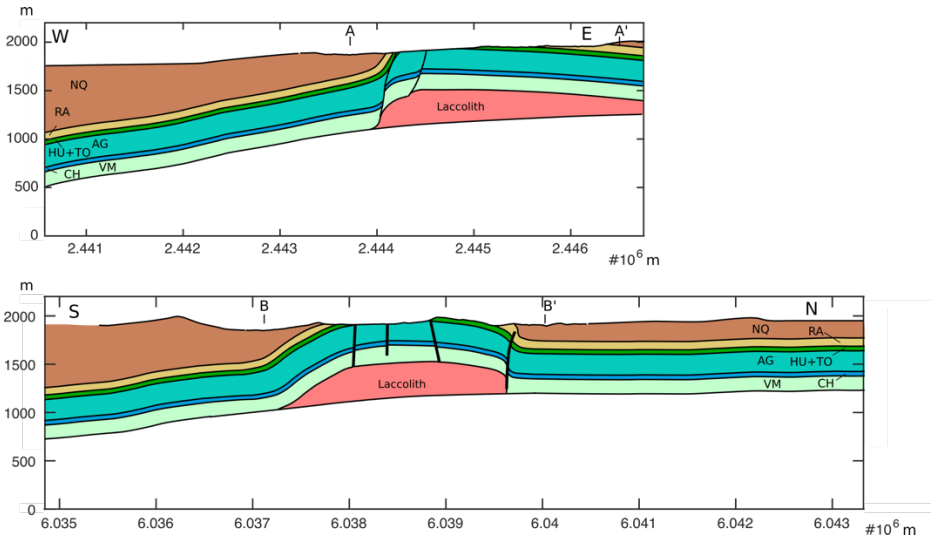

Fig. 2 – Geological cross sections built from integrated field mapping, well data and 3D seismic data. Top: E-W cross section; Bottom: N-S cross section. Notice that the cross sections extend much beyond the boundaries of the map of Fig. 1 (see letters). VM: Vaca Muerta Fm; CH: Chachao Fm.; AG: Agrio Fm.; HU+TO: Huitrín Fm.; RA: Rayoso Fm.; NQ: Neuquén Gr.

The Gondwana break-up interpreted by tectonics emplacements of tholeiitic dykes in the central segment of the South American continental margin

João Paulo Giro.[1,2], Julio Almeida.[2] and Eliane Guedes.[2,3]

[1] *PPGG- Graduate Program on Geoscience, Rio de Janeiro State University, Rio de Janeiro, Brazil – jp.geol2012@gmail.com*
[2] *TEKTOS – Geotectonics Research Group, Faculty of Geology, Rio de Janeiro State University, Rua Sao Francisco Xavier 524/4006-A, Rio de Janeiro, Brazil*
[3] *Museu Nacional/UFRJ, Quinta da boa Vista S/N, Rio de Janeiro, Brazil*

Keywords: Rio de Janeiro - Geology, Mafic Dyke Swarms, Gondwana break-up, Crustal Weakness Zones.

The Gondwana supercontinent was formed during the Neoproterozoic-Ordovician with the amalgamation of several continental and oceanic plates (Heilbron et al., 2004; Heilbron & Machado 2003). A geological framework composed of Paleoproterozoic-Archean basement rocks, Neoproterozoic metasedimentary units and granites configure an orogenic belt named Ribeira belt (Figure 1). The Ribeira belt displays a NE-SW conspicuous strike orientation with distinct lithological and structural contents separated in four domains or terranes (Heilbron et al., 2004).

The Gondwana break-up is marked by the Jurassic-Cretaceous swarm (Serra do Mar Dyke Swarm - SMDS) of tholeiitic dykes (dolerites) that intruded the crystalline rocks of Ribeira belt (Almeida et al., 2013).

The NE-trending dykes follow the general trend of the Ribeira Belt and cross-cut the variable dipping Brasiliano foliations (Almeida et al., 2013). Based on external and internal markers, the same authors consider that the SMDS was emplaced in a predominantly sinistral oblique extension, resulting in a mean extension vector of approximately N50W (Almeida et al., 2013). Besides the N40-50E dykes, other directions of intrusions, such as NW, N-S, and NNE also occur in the south of the Rio de Janeiro state, following the faults and the intense fracturing oblique to the NE trend of the basement (Guedes et al., 2016). These dykes are slightly older (Jurassic) than the SMDS and were named The Resende – Ilha Grande Dyke swarm (RIGDS).

The focus of this research is the dykes which occurs in the central part of Rio de Janeiro state, where N15-30E-striking dykes display a different orientation when compared with the SMDS (Figure 1). Although these dykes have been already recognized, none geochemical or structural studies were carried out until now. We carried out a close investigation on these dykes and compare with the previous data from the SMDS. The main objective to establish whether these dykes are geochemically and structurally consistent with the emplacement of SMDS or are superposed events as it is with the RIGDS.

These dykes are composed by high-TiO2 tholeiitic dolerites and microgabbros. The lithogeochemical data of these dykes are very similar to those high-TiO2 tholeiitic from the SMDS, especially in the REE elements and trace elements.

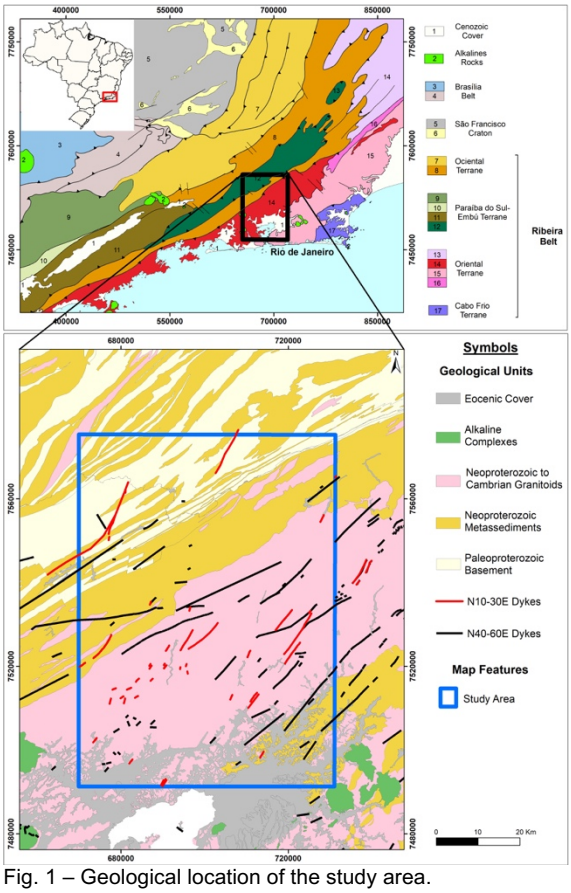

Fig. 1 – Geological location of the study area.

The preferential localization of the Mesozoic break-up lines was influenced by the differences between the rheology of distincts blocks of the Ribeira belt (Alkmim, 2004). The Atlantic rift system display several characteristics that are common in divergent margins, such as extensional normal faults

along the rift (Mohriak et al., 2013). However, the opening of the South Atlantic Ocean is marked by intraplate deformation which propagated northwards along the South American Plate (Moulin, 2010). The geometry of the continent-ocean boundary (COB) shows a ~N-S line from the south of the continental margin until the Rio de Janeiro coastline, where it turns ~E-W, and then turns again northward to the ~N-S direction.

Considering this line geometry and/or the movement of the Santos Block proposed for Moulin (2010), the Rio de Janeiro continental margin has undergone a transtensional sinistral deformation process during the Gondwana break-up. Considering this, we used the conjugate fractures Riedel model (1929) to understand the differences of the dyke orientations of the Serra do Mar Dyke Swarm. Assuming that the most ~N50E dykes are sinistral in oblique extension (Almeida et al., 2013), we concluded that these dykes are parallel to the R fracture of Riedel (sinistral). The N20-30E dykes studied in this work are parallel to the T fracture of Riedel (extensional) and the NNW fractures in the Rio de Janeiro State are parallel to the R' fracture (Figure 2). As the R' direction is an antithetical fracture, its development is more difficult than the others directions. The few numbers of NNW dykes (R') at the Rio de Janeiro state corroborates with this model. In this model, the main compression vector in the Rio de Janeiro state is parallel to the coast of Brazil and the main extension vector is at approximately N70W, different from N50W proposed by Almeida et al., 2013 and others authors.

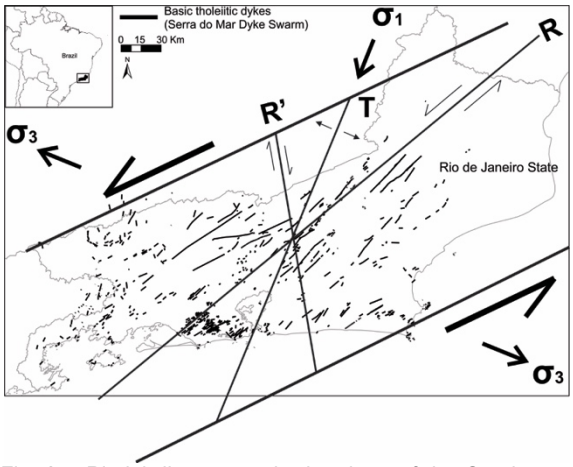

Fig. 2 – Riedel diagram to the break-up of the Gondwana superposed on the SMDS in the Rio de Janeiro state, southeastern of Brazil.

Acknowledgements

The first author is grateful for the Rio de Janeiro State agency - FAPERJ for financial support. Authors also acknowledgement for FGEL-UERJ to the infrastructure and all the Tektos group for the comments and suggestions.

References

Alkmim, F. F. 2004. Extensional collapse and the geologic architecture of Precambrian orogens. In: 32nd International Geological Congress, Florence, Italy, 20–28 August 2004, Abstracts Volume 2. APAT – Italian Agency for the Environmental Protection and Technical Services, Rome, 1254.

Almeida, J., Dios, F., Mohriak, W. U., Valeriano, C. D. M., Heilbron, M., Eirado, L. G., & Tomazzoli, E. (2013). Pre-rift tectonic scenario of the Eo-Cretaceous Gondwana break-up along SE Brazil–SW Africa: insights from tholeiitic mafic dyke swarms, Geological Society, London, Special Publications, 369(1), 11-40.

Guedes, E., Heilbron, M., de Morisson Valeriano, C., de Almeida, J. C. H., & Szatmari, P. (2016). Evidence of Gondwana early rifting process recorded by Resende-Ilha Grande Dike Swarm, southern Rio de Janeiro, Brazil, *Journal of South American Earth Sciences*, 67, 11-24.

Heilbron, M., and Machado, N. (2003). Timing of terrane accretion in the Neoproterozoic–Eopaleozoic Ribeira orogen (SE Brazil). *Precambrian Research*, 125(1-2), 87-112.

Heilbron, M., et al (2004), A Província Mantiqueira, in *O Desvendar de Um Continente: A Moderna Geologia da América do Sul e o Legado da Obra de Fernando Flávio Marques de Almeida*, edited by V. Mantesso-Neto, A. Bartorelli, C.D.R. Carneiro & B.B. Brito Neves, pp. 203-234.

Mohriak, W. U., & Leroy, S. (2013). Architecture of rifted continental margins and break-up evolution: insights from the South Atlantic, North Atlantic and Red Sea–Gulf of Aden conjugate margins, *Geological Society, London,* Special Publications, 369(1), 497-535.

Moulin, M., Aslanian, D., & Unternehr, P. (2010). A new starting point for the South and Equatorial Atlantic Ocean, *Earth-Science Reviews*, 98(1-2), 1-37.

Riedel, W., 1929. Zur mechanik geologischer brucherscheinungen, *Centralblatt fur Minerologie, Geologie, und Paleontologie*, 354.

Sills in the evaporites of the Miembro Troncoso Superior, Neuquén Basin, Malargüe, Argentina

Gomez Figueroa, Javier.[1]

[1] *Facultad de Ciencias Exactas y Naturales, UNCuyo, Mendoza, Argentina* – javi10gomez@hotmail.com

Keywords: *intrusions, evaporites, Neuquén basin*

The geology of the Neuquén basin is delineated by the interaction of its sedimentary cycles, with its heterogeneous deformation style. The presence of intense failure and permeable strata in contact with the source rock, has allowed the migration of hydrocarbons over long distances. In this sense, the filling of the traps from the depocenters towards the edge areas, preferably from the West to the East has contributed to the development of deposits of very varied size and dissimilar characteristics.

The sills in the Neuquén basin haves significant accumulations of hydrocarbons, mainly in the northern part of Neuquen province. They present abundant intrusions of andesitic dikes that accentuate the anticline structure and act as fluid barriers (Orchuela, 1975). The main sites where these igneous intrusions are found are Chihuido de la Sierra Negra (ChSN), Los Barriales, Pampa Negra, Filo Morado, Pampa de las Liebres and the southern area of the Salinas de Huitrín.

The purpose of this work is to provide a brief description of the igneous intrusions housed in the evaporites of the Miembro Troncoso Superior (MTS), their petrographic characteristics, structures and thermal effects of these intrusions.

The MTS is located within the Huitrin Formation (Barremian-aptian), which together with the Rayoso Formation (lower Albian-Cenomanian) (Uliana *et al*, 1975)) constitute up the Bajada del Agrio Group (Leanza *et al.,* 2001). This member has a purely evaporitic composition, mostly it is composed by halita with different facies and characteristics, to a lesser extent anhydrite is presented arranged in layers of different thickness and finally, significant horizons of silvite and carnalite, interspersed in this evaporitic package that generate an important deposit from the economic point of view

The MTS has a wide areal distribution and thicknesses that range from 20 meters to 180 meters. The tectonic participation of this evaporitic package, as a detachment level in the structure of the fold-and-thrust, is recognized throughout the entire Neuquén basin. (Fig 1).

According to the analysis and correlation of drill-cores obtained in the exploration of potassium salts of more than 100 surveys located in the Neuquen and Mendoza provinces, a series of intrusive bodies are defined within the MTS. One of the best examples is found in the POT-BNOR-DH00013 well, located in the Huantraico syncline area where two igneous intrusions are intercepted. (Fig. 2).

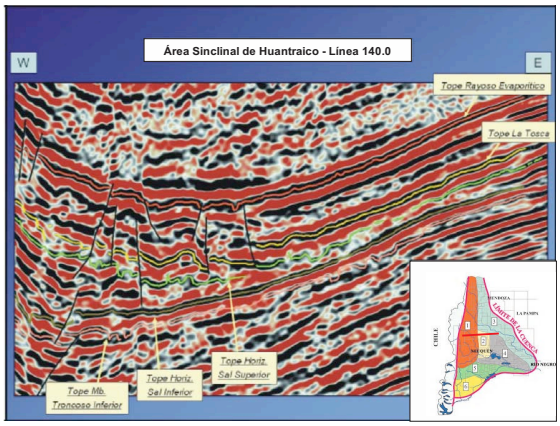

Fig. 1 – 3D seismic line in the W-E direction where the syncline structure can be observed. Note the deformation of the central sector of the structure and the western flank in the vicinity of the triangular zone, where the vertical black lines correspond to faults and fractures. The coloured lines follow the attitude of reflectors corresponding to different levels within the Miembro Troncoso Superior, Miembro La tosca and Rayoso evaporitico Formation.

These intrusions occur between 2018 and 2022 TVD. These are two sills of a dark black coloured, aphanitic texture rock, with eventual halite crystals. These crystals present flow lineations 70° / 80° with respect to the drill core axis. Halite veins 5 mm thick cross-cut the intrusive bodies. The contacts with the halite are of net type and concordant with the structure of the rock. Evaporites are white to gray, recrystallized, translucent, with subhedral crystals of 1 to 2 cm. Abundant cavities of 1 mm attributed to fluids of the igneous body, are very abundant throughout this area. Black clay disseminated with salt in aggregates of 2 to 5 mm.

Is important to note the presence of potassium horizons with igneous intrusions. There is recrystallization of salt mainly in the area of contact with these bodies. Fluid remobilization is evident, but not enough to make these potassium levels disappear.

The age (dated) of these intrusive bodies is 15.8-17.7 Ma (Miocene) (Gulisano et al, 1996, Orchuela et al., 2003) in drill-cores obtained by Chevron, as well as in outcrops (Cobbold and Rosello, 2003). The most

shallow (intruded in La Tosca and MTS) produce oil in ChSN (Comeron et al., 2001).

These data could indicate the accumulation of oil in different areas where the Miembro Troncoso Superior is in coexistence with these intrusive bodies. In the ChSN deposit, in 1993, oil was discovered in a thick igneous body located in the MTS evaporites, at a depth of 950 meters, achieving one of the largest production wells in the area with 750 m3 / day.

The reservoir rock is made up of andesites and trachites with a very low primary porosity, which are fractured giving a secondary permeability. The igneous body has a laccoliths shape. At the edges it is intensely fractured. Levels of anhydrite and clays of the Rayoso Formation constitute the seal for this accumulation (Valenzuela et al., 2011).

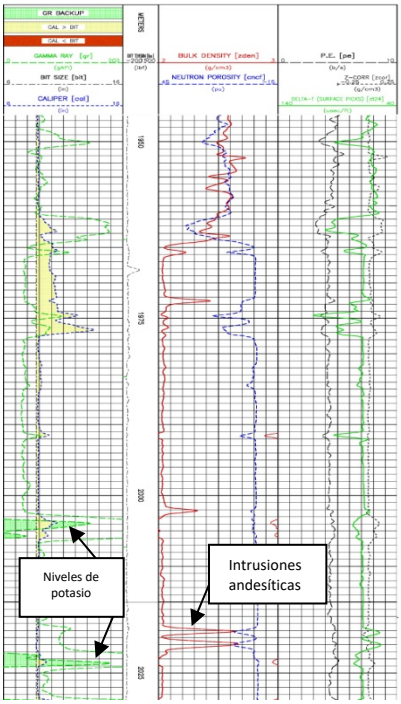

Fig. 2 – Electric profile of the POT-BNOR-DH0003 well. Igneous intrusions within the evaporitic levels of the MTS are marked. Observe how the porosity increases in the igneous levels.

References

Barrionuevo, M. (2002). Los reservorios de las formaciones Agrio-Huitrín. Simposio de Rocas Productivas, 5° Congreso de Exploración y Desarrollo de Hidrocarburos. Trabajos técnicos. Versión CD ROM. Mar del Plata.

Cobbold, P. & Rosello, E. (2003). Aptien to recent compressional deformation, foothills of the Neuquén Basin, Argentina. Marine and Petroleum Geology, 429-443.

Comeron, R.E., M.E. Valenzuela, & J.L. Ramirez, (2002). Chihuido de la Sierra Negra: Petróleo en reservorios no convencionales. Boletín de Informaciones Petroleras 69:70-75.

Frigerio M., A. Giusiano & C. Herrmann, (2003). Potasio en Neuquén. Evaluación del recurso en el área de exclusividad provincial. Subsecretaria de Energía y Minería de la provincia del Neuquén. Servicio Geológico Minero Argentino. Provincia de Neuquén. 45pp.

González, P. & E. Aragón, (2000). El Cerro Bayo de la Sierra Negra, Neuquén. un ejemplo de lacolito tipo arbol de Navidad. Revista de la Asociación Geológica Argentina, 55 (4): 363-377.

Gomez Figueroa, J. & Balod, M. (2016). Presencia de sales de potasio en el miembro Troncoso Superior (formación Huitrín, cretácico inferior, cuenca neuquina) en el yacimiento Chihuido de la Sierra Negra, provincia de Neuquén. Libro de Resúmenes del VII Congreso Latinoamericano de Sedimentología y XV Reunión Argentina de Sedimentología p, 89, Santa Rosa, La Pampa.

Leanza, H.A., C.A. Hugo y D. Repol, (2001). Hoja Geológica 3969-I- Zapala, provincia del Neuquén. Instituto de Geología y Recursos Naturales. SEGEMAR, Boletín 275: 1-128. Buenos Aires.

Legarreta, L. (2002). Eventos de desecación en la Cuenca Neuquina. Depósitos continentales y distribución de los hidrocarburos. 5° Congreso de Exploración y Desarrollo de Hidrocarburos. Trabajos técnicos. Versión CD ROM. Mar del Plata.

Orchuela, I. (1975). Los cuerpos andesíticos en el subsuelo del Chihuido de la Sierra Negra y distribución areal de la arenisca de Avilé. YPF SA Informe 1492 (informe inédito). Buenos Aires.

Orchuela, I., M. Lara & M. Suarez, (2003). Productive large scale holding associated with igneous intrusion: El trapial field, Neuquén Basin, Argentina. AAPG Internacional Conference, Barcelona.

Valenzuela, M. & Comeron, R. (2005). Yacimiento Chihuido de la Sierra Negra-Lomita, Mb. Avilé. Las trampas de hidrocarburos en las cuencas productivas de la Argentina. Mar del Plata.

Vergani G., C. Arregui, y O. Carbone, (2011). Sistemas petroleros y tipos de entrampamiento en la Cuenca Neuquina. Relatorio del XVIII Congreso Geológico Argentino. Neuquén 2011.

Uliana, M. A., D.A. Dellapé, & G.A. Pando, (1975a). Distribución y génesis de las sedimentitas rayosianas (Cretácico inferior de las provincias de Neuquén y Mendoza). 2º Congreso Ibero- Americano de Geología Económica. Actas 1: 151-176, Buenos Aires.

Where did the Jurassic dolerites of Tasmania come from?

Gordon, A.[1], Barter, J.[1] and **Cruden, A.**[1]

[1] *School of Earth, Atmosphere & Environment, Monash University, Melbourne, Australia* – sandy.cruden@monash.edu

Keywords: sills, AMS, Tasmania.

Jurassic dolerite sills dominate the landscape, and make up ~50% of the bedrock geology of Tasmania, SE Australia (Fig. 1a). The differentiated Red Hill sill in Tasmania yielded a U-Pb ID-TIMS zircon age of 182.540 ± 0.059 Ma, which overlaps within error with dolerite sills and basaltic lavas in the Ferrar province, Antarctica, and the Karoo, South Africa (Burgess et al., 2015). Hence, the Tasmanian dolerites have long been considered to be part of a major Large Igneous Province (LIP) that extended parallel to the Jurassic margin of Gondwana from what is now southern Africa, the Transantarctic Mountains, Tasmania and South Australia (Elliot and Fleming, 2004; Faure and Mensing, 2010).

Two hypotheses have been proposed for the Ferrar LIP and Tasmanian dolerites. 1) They are related to a mantle plume emplaced in the present-day Wedell Sea region, implying long-range, shallow-crustal transport of magmas in sills and dykes over distances of up to 4,000 km (Leat, 2008; Elliot and Fleming, 2004). 2) They are sourced from the mantle below Tasmania and Antarctica, implying only short-range lateral transport at the level of emplacement (Leaman, 1975). A local source for Ferrar-Tasmanian dolerites would be consistent with the suggestion that mafic magmatism is linked to back-arc rifting inboard of the Jurassic Gondwana subduction margin (Faure and Mensing, 2010; Choi et al. 2019). In order to evaluate these hypotheses, we have carried out a combined structural and anisotropy of magnetic susceptibility (AMS) study of the Tasmanian dolerites.

The aim of this study is to differentiate between flow patterns and structural architectures in sills that are indicative of local versus distal sources. The former should be associated with point magma sources feeding sills and radial flow patterns (Leaman, 1975). The latter would be indicated by uniform magma flow and sill propagation directions, and the absence of point sources (e.g. Palmer et al., 2007)).

We have carried out detailed structural mapping and 3D modelling of sills in the Hobart region, and a regional AMS sampling and analysis campaign that covers most of the outcrop of the dolerites in Tasmania (Fig. 1a). Structural mapping, 3D modelling and regional cross section analysis indicate that dolerite in Tasmania comprises no

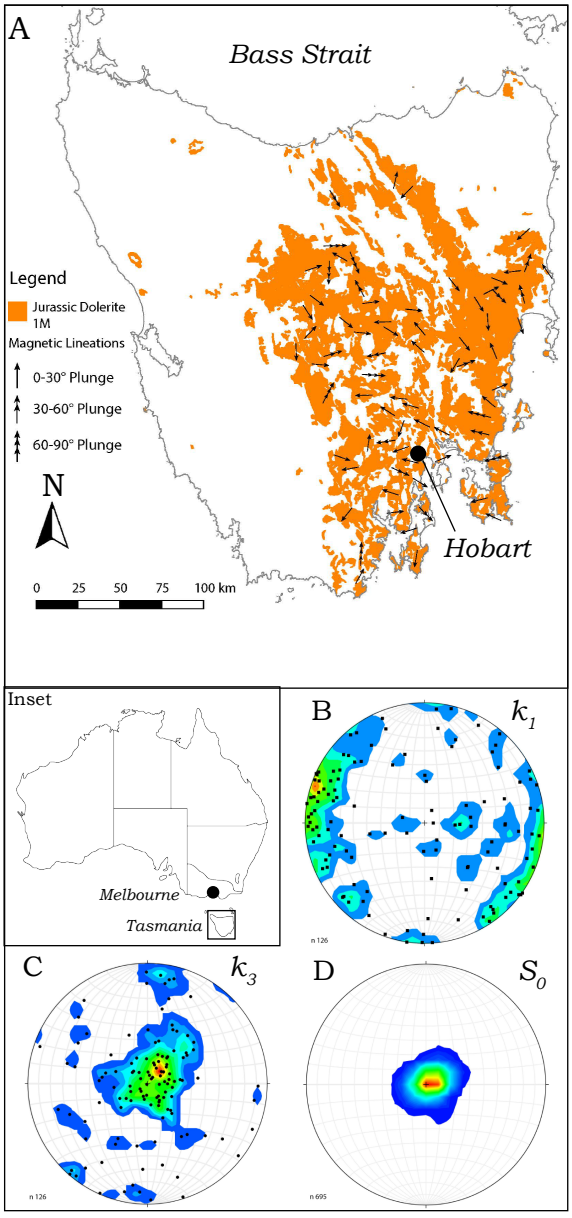

Fig. 1 – A. Map of Tasmania showing the outcrop of Jurassic dolerite, AMS sampling sites, and the trend and plunge of site mean magnetic lineations (k_1) in sills. See inset for location of Tasmania. B. Equal area, lower hemisphere stereonet plotting site mean magnetic lineations (k_1) in sills. C. Stereonet plotting poles to the site mean magnetic foliation (k_3) in sills. D. Stereonet plotting poles to bedding (S_0) in sedimentary rocks of the Parmeneer Supergroup, which host the dolerite sills. Contour intervals = 1% of 1% of area (B,C) and 2% of 1% of area (D).

more than a few sills, possibly only one. Large sub-horizontal dolerite sheets were emplaced parallel to bedding (Fig. 1d) in sedimentary host rocks of the Permian Parmeneer Group. These sheets are offset by steps that we interpret as NWE-trending, steeply dipping broken bridges, an observation that is also observed at outcrop scale.

The AMS of oriented dolerite samples collected from 126 sites across Tasmania was measured using a Kappabridge KLY-A susceptibility meter. Site mean orientations of the principal susceptibilities $k_1>k_2>k_3$ of specimens from each site were calculated by tensor averaging. The resulting magnetic fabrics display remarkably consistent orientations (Fig. 1b and c). Magnetic lineations, k_1 where $k_1>k_2>k_3$ are the principal susceptibilities, are dominantly subhorizontal trending mostly NW-SE with a dispersal of ~ 45º. Steeply-moderately inclined magnetic lineations are rare and most plunge SE. Subsets of shallow N-S and NE-SW lineations are associated with sites with subvertical E-W and NW-SE striking magnetic foliations (Fig. 1c). Magnetic foliations are dominantly subhorizontal and are parallel to bedding in the surrounding sediments (Fig. 1D), and the upper and lower contacts of subhorizontal dolerite sheets. Anomalous subvertical E-W and NW-SE striking magnetic foliations are associated with steps or broken bridges observed in the field and cross sections.

The mean bulk magnetic susceptibility of the dolerite samples is ~$1x10^{-2}$ SI units. This, together with high-temperature susceptibility measurements indicate that the AMS is carried by magnetite. Petrography indicates that this magnetite occurs as skeletal grains whose distribution and orientation is controlled by the petrofabric of the silicate rock forming minerals, plagioclase and pyroxene. These observations, and the lack of microstructural evidence for solid-state deformation, indicate that AMS is measuring a magmatic shape-preferred orientation and or distribution anisotropy that formed during emplacement and crystallization.

The AMS results are consistent with dominantly NW-SE magma flow within subhorizontal sheets. This is consistent with the NW-SE orientation of steps and broken bridges (e.g., Magee et al. 2019). We also infer that the polarity of sill propagation and magma flow was from SE to NW, based on the architecture of segmented sill sheet fronts observed in the field.

Our results indicate that the Jurassic dolerites of Tasmania represent a limited number of large, segmented sills that propagated laterally from SE to NW. This is inconsistent with a magma source immediate below Tasmania and implies lateral transport from some other location. However, the magma flow vector does not point back to the Ferrar dolerites in Antarctica, and therefore does not support the long-range Ferrar-Tasmania LIP hypothesis. Rather fabrics in the Tasmania dolerite are consistent with lateral flow perpendicular to the Gondwana margin with a source in the back-arc of the associated subduction zone.

Acknowledgements

We thank Andrew McNeill at the Department of Infrastructure, Energy and Resources, Mineral Resources Tasmania for logistical support and advice.

References

Burgess, S.D., et al. (2015), High-precision geochronology links the Ferrar large igneous province with early-Jurassic ocean anoxia and biotic crisis, *Earth and Planetary Science Letters*, 415, 90-99.

Choi, S.H., et al. 2019. Fossil subduction zone origin for magmas in the Ferrar Large Igneous Province, Antarctica, *Earth and Planetary Science Letters*, 506, 507-519.

Elliot, D.H. and Fleming, T.H. (2004), Occurrence and dispersal of magmas in the Jurassic Ferrar Large Igneous Province, Antarctica, *Gondwana Research*, 7, 223-237.

Faure, G. and Mensing, T.M. (2010), *The Transantarctic Mountains*, Springer Science.

Leaman, D. (1975), Form, mechanism, and control of dolerite intrusion near Hobart, Tasmania, *Australian Journal of Earth Sciences*, 22, 175-186.

Leat, P.T. (2008), On the long-distance transport of Ferrar magmas, *Geologic Society, London, Special Publications*, 302, 45-61.

Magee, C., et al. (2019), Structural signatures of igneous sheet intrusion mechanisms, Journal of Structural Geology, 125, 148-154.

Palmer, H.C. et al. (2007), Magnetic fabric studies of the Nipissing sill province, *Canadian Journal of Earth Science*, 44, 507-528.

Two case studies of peperites from Chile: Los Molles, V Región de Valparaíso, (~32°14′S) y Puerto Ingeniero Ibañez (~46°17'S), Región de Aysén

Gressier J.B.[1], Suarez M.[1] and Araño C.[1]

[1] *Earth Science School, Universidad Andres Bello, Santiago de Chile, Chile* – jean.b.gressier@gmail.com

Keywords: Peperite, Black shale, Chile.

Peperite is a textural term commonly used to describe clastic rocks that contain igneous and sedimentary components. These are formed by processes of magmatic fragmentation and mingling with unconsolidated, typically wet sediments. Several studies have described rocks with peperitic textures (e.g.: Scrope, 1827; Cas y Wright, 1978; De Goër, 2000; White et al., 2000; Skilling et al., 2002). Nevertheless, research has failed to englobe all the described characteristics into the term.

In this study we present two peperites. The first one, the Los Molles peperite, is our "model peperite". The second one, the Puerto Ibañez peperite, reach the limits of actual definitions of peperite.

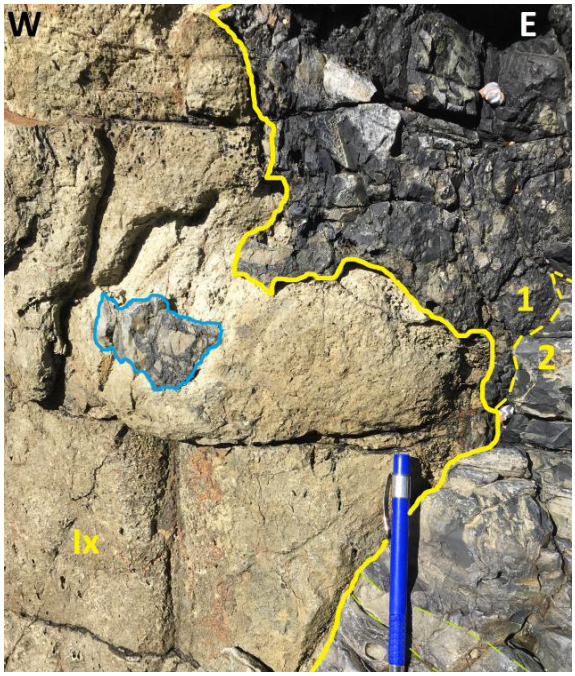

Fig. 1 – Contact (Yellow line) between the intrusive body (Ix) and the black shale (Lt), a host rock inclusion is observed (locked in blue) that presents various juvenile clasts of the associated magmatic body. 1- This outcrop sector presents juvenile clasts clastos juveniles immersed in the host rock, evidencing host sediment transport and fluidization, through host rock stratification destruction (So); 2- Original stratification, without juvenile clasts (Araño, 2018).

The Los Molles peperite born from the interaction between a hypabyssal dacitic magmatic body and black shales of the Triasic los Molles Formation (Cecioni y Westermann, 1968), characterized by marine and lake deposits, with some tuffic sandstone and acid lavas (Fig.1). The outcrop is located near Los Molles (~32°14′S), V Región de Valparaíso, Central Chile.

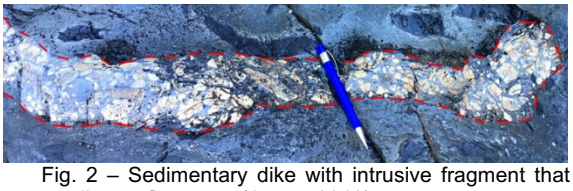

Fig. 2 – Sedimentary dike with intrusive fragment that present jigsaw-fit texture (Araño, 2018).

The Los Molles peperite meets the requirements both in the descriptive and genetic sense of the term peperite. Said outcrop, meets all characteristics and processes for peperitic rock formation, such as magma fragmentation and mix with host sediment, through fluidization of the no or poorly consolidated sediment (Fig.2).

Fig. 3 – Puerto Ibañez peperite top contact. Manuel Suarez serving as scale (Araño, 2018).

The Puerto Ibañez peperite is an outcrop composed of Cretaceous black shales that have been intruded by a hypabyssal dioritic magmatic body, which presents peperitic textures (Fig. 3, Araño, 2018). The shales belonging to the Katterfeld Formation (Valanginian-Hauterivian) are located

near Puerto Ingeniero Ibáñez (~46°17'S) Región de Aysén, Southern Chile.

Structures with a consolidated state prior the intrusion were found in the outcrop under study. Moreover, a radiometric dating was made in zircons of the intrusive body (Suárez et al., unpublished; Suárez and De la Cruz, unpublished). As a result, a difference of 50 Ma with the host rock was found, which would indicate the generation of peperitic textures in consolidated rock.

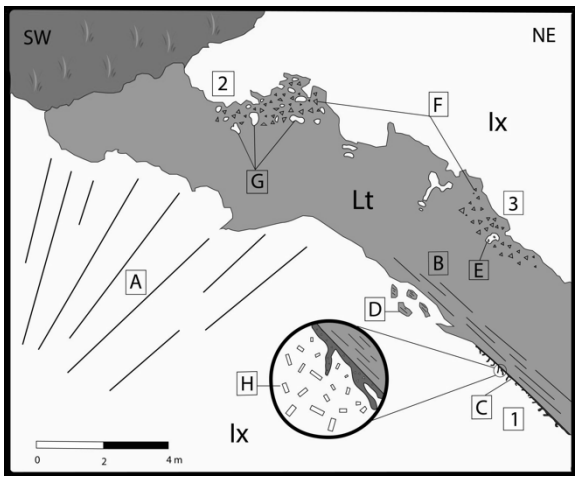

Fig. 4 – Puerto Ibañez peperite sketch. With: Lt: host rock; Ix: magmatic body; 1: lower contact; 2: top contact; 3: lateral contact. A: columnar disjunction; B: host rock tectonic foliation; C: brecciation of the magmatic body; D: immersed foliated black shale fragments in the intrusive; E: juvenile clast with black shale inclusions; F: Host rock brecciation; G: juvenile clasts immersed in the host rock; H: lower contact zoom, showing intrusive plagioclase crystals granulometric decrease. (Araño, 2018)

The mingling and magmatic fragmentation processes that form a peperite are evidenced in the outcrop by juvenile clasts immersed in the host rock (Fig.4). Furthermore, it is interpreted that the mixture of both components was promoted by hydromagmatic fluids transported during the emplacement of the intrusion. This intrusion generates a breccia in the host rock.

Based on the above, this work shows a limit of actual definitions of peperite. The Puerto Ibañez peperite meets the requirements in the descriptive sense of the term peperite, while it formed by a magmatic unit that has been fragmented in situ with a sedimentary unit, independently of its state of consolidation, evidencing a dynamic interaction between both components.

Acknowledgements

The authors are most grateful to Mrs. Kunik, owner of the Estancia La Pirámide, for her kind support to us during our field work. The work was funded by proyect FIC-Aysén 40000501 and the Universidad Andres Bello, Santiago, Chile.

References

Araño C. (2018), Estudio de rocas cretacicas aparentemente peperiticas en cercanias de Puerto Ingeniero Ibañez,(~46°17'S), Region de Aysen, Chile. Memoria de Titulo de la Universidad Andres Bello, Santiago, Chile.

Cas, R.A.F., Wright, J.V. (1987), Volcanic Successions, Modern and Ancient. edited by Allen and Udwin, London, pp. 528.

Cecioni, G., Westermann, G.E.G. (1968), The Triassic–Jurassic marine transition of coastal central Chile. *Pacific Geology*, 1, 41–75.

De Goër, A. (2000), Peperites from the Limagne trench (Auvergne, French Massif Central): A distinctive facies of phreatomagmatic pyroclastics. History of a semantic drift, in *Volcaniclastic Rocks From Magmas to Sediments*, pp. 91-110.

Scrope, G.P. (1827), Memoir on the Geology of Central France; Including the Volcanic Formations of Auvergne, the Velay and the Vivarais. *Longman, Rees, Orme, Brown and Green, London, pp. 79*.

Skilling, I.P., White, J.D.L., McPhie, J. (2002), Peperite: a review of magma-sediment mingling. *Journal of Volcanology and Geothermal Research*, 114, 1-17.

White, J.D.L., McPhie, J., Skilling, I.P. (2000), Peperite: a useful genetic term. *Bulletin of Volcanology*, 62, 65-66.

Architecture and morphology of mafic sills: Field observations from San Rafael Swell, Utah, US

Kjenes, Martin.[1,*], Chedburn, Lauren[2], Rotevatn, Atle[1], Schofield, Nick[2], and Eide, Christian H.[1].

[1] *Basin and Reservoir studies, Department of Geosciences, University of Bergen, Bergen, Norway - martin.kjenes@uib.no.*
[2] *Department of Geology and Petroleum Geology, University of Aberdeen, Aberdeen AB24 3UE, UK.*

Keywords: Sills, Flow bands, Magma transport.

Igneous intrusions, such as dykes, sills and laccoliths, are important components of volcanic plumbing systems in extensional tectonic settings, e.g. rifted margins and sedimentary basins (Hutton, 2009; Jerram and Bryan, 2018; Magee et al., 2016; Spacapan et al., 2016). In contrasts to dykes (i.e. vertical conduits), sills appear as layer parallel, tabular bodies of magma. The majority of sill mechanic models shows that sills are emplaced as continuous igneous sheets and propagates as hydraulic fractures. These models assume that the host rock behaves as a purely elastic medium, and only exhibits a single propagating point (Kavanagh et al., 2006; Galland et al., 2018). However, igneous bodies often prefer to propagate through mechanically weak formations, e.g. shale and mudstone, which may deform in an inelastic manner (Mudge, 1968; Scheibert et al., 2017; Wilson, et al., 2016). Based on previously conducted field observations and 3D seismic data, sills generally exhibit lobate (i.e finger-like) morphology when intruding in weaker, and in general, more unconsolidated host rocks (Eide et al., 2017; Schofield et al., 2012).

Even though sills have been studied for the last decades, questions regarding their architecture, flow conditions, inflation and relationship to sedimentary heterogeneity remains unanswered. This contribution presents a detailed study on excellent 3D outcrops in shallow (c. 3 km emplacement depth) mafic step-wise transgressive sills, emplaced at c. 3.7 to 4.6 Ma in San Rafael Swell, Utah.

Our results involve a vast range of data, ranging from large outcrop 3D models (>100m) to microscale (<1mm). Three different outcrops were chosen for further investigation due to variability in sill morphology, adjacent sedimentary formations, and spatial location. The following data was collected in the various outcrops: high—resolution images by UAV ('drone') (Fig. 1), sedimentary- and igneous-logging of host rock and intrusions, and 20 rock samples that will be used for petrological investigations. In addition, a more detailed study of certain features, such as magma bridges, steps, flow bands (Fig. 2), was carried out to understand how magma is transported within intrusions. Notably, flow bands were observed on the different localities, which exhibited a different mineralogy and grain size than the main intrusion (Fig. 2C).

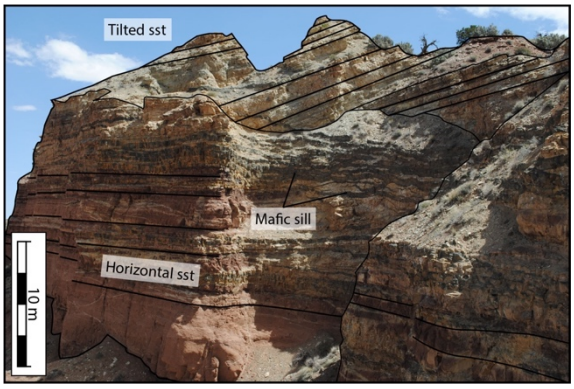

Fig. 1 – UAV photo from the Cedar Mountain outcrop, showing tilted layers of the Entrada sandstone (sst) related to adjacent intrusion.

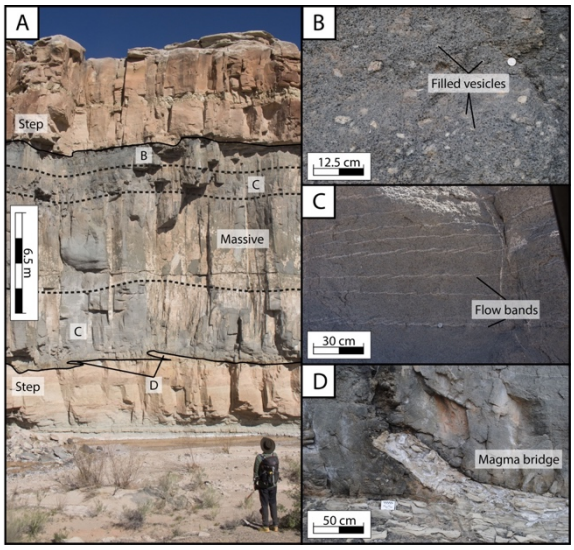

Fig. 2 – Photos from the Mussentuchit outcrop, showing an excellent 3D outcrop of a relative thick, massive sill. A) Overview figure of the sill, showing apparent layering. B) Upper part, which includes filled vesicles. C) Flow bands, which occurs at the bottom and at the top of the sill. D) Lower boundary between sill and Curtis Formation, which exhibits magma bridges.

The main aims of this study are to improve the understanding of sill emplacement mechanics and flow conditions. For example, modelling of sills can be further enhanced due to further understanding of processes behind flow bands by internal fracturing due to magmatic pulses or residual melt. These findings could also be implemented into studies on volcanic reservoirs, in terms of their post-intruding behavior. The three outcrops used in this study are excellent 3D outcrops that will shed light on how magma is transported in intrusions, and how it is affected by the sedimentary basin. The key outcrop, the Mussentuchit sill, is located in a meandering river channel, which results in a unique 3D outcrop to study sill architecture (Fig. 3).

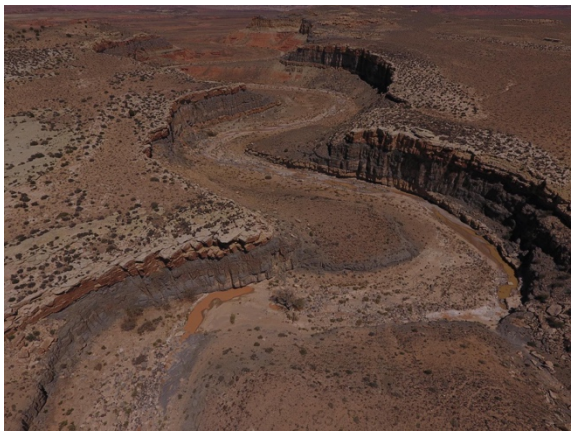

Fig. 3 – UAV photo of the Mussentuchit sill, displaying the extent of the river valley outcrop.

Acknowledgements

I would like to thank my supervisor Christian Haug Eide, and my co-supervisor Nick Schofield for all the help and discussions in the field. I would also like to thank them for constructive and insightful comments in the process of working on this project. This research project is supported through the PhD program at the University in Bergen. Lauren Chedburn is especially thanked for excellent collaboration in the field.

References

Eide, C. H., Schofield, N., Jerram, D. A., Howell, J. A., 2016, Basin-scale architecture of deeply emplaced sill complexes: Jameson Land, East Greenland, *Journal of Geological Society*, v. 174, p. 23-40.

Galland, O., et al. (2018), Storage and transport of magma in the layered crust-Formation of sills and related flat-lying intrusions, in *Volcanic and Igneous Plumbing Systems*, edited by S. Burchardt, pp. 111-136, Elsevier.

Hutton, D. J. P. G., 2009, Insights into magmatism in volcanic margins: bridge structures and a new mechanism of basic sill emplacement-Theron Mountains, Antarctica, *Petroleum Geoscience*, v. 15, no. 3, p. 269-278.

Jerram, D. A., Bryan, S. E., 2018, Plumbing systems of shallow level intrusive complexes, *Physical Geology of Shallow Magmatic Systems*, *Springer*, p. 39-60.

Kavanagh, J. L., Menand, T., Sparks, R. S. J., 2006, An experimental investigation of sill formation and propagation in layered elastic media, *Earth Planet*, Sci. Lett. 245, p. 799-813.

Magee, C., Muirhead, J. D., Karvelas, A., Holford, S. P., Jackson, C. A., Bastow, I. D., Schofield, N., Stevenson, C. T., McLean, C., and McCarthy, W. J. G., 2016, Lateral magma flow in mafic sill complexes, *Geosphere*, v. 12, no. 3, p. 809-841.

Mudge, M. R., 1968, Depth control of some concordant intrusions, *Geological Society of America Bulletin*, v. 79, p. 315-322.

Scheibert, J., Galland, O., Hafver, A., 2017, Inelastic deformation during sill and laccolith emplacement: insights from an analytic elasto-plastic model, *Journal of Geophysical Research: Solid Earth*, v. 122, p. 923-945.

Schofield, N., Stevenson, C., Reston, T., 2010, Magma fingers and host rock fluidization in the emplacement of sills, *Geology*, v. 38, p. 63-66.

Spacapan, J. B., O. Galland, H. A. Leanza, and S. Planke (2017), Igneous sill and finger emplacement mechanism in shale-dominated formations: a field study at Cuesta del Chihuido, Neuquén Basin, Argentina, *J. Geol. Soc. London*, *174*(3), p. 422-433.

Wilson, P. I.R., McCaffrey, K. J. W., Wilson, R. W., Jarvis, I., Holdsworth, R. E., 2016, Deformation structures associated with the Trachyte Mesa intrusion, Utah: implications for sill and laccolith emplacement mechanisms, *Journal of Structural Geology*, v. 89, p. 30-46.

Emplacement mechanisms of a dyke swarm across the Brittle-Ductile transition

Kjøll H.J.[1], Galland O.[2], Labrousse L.[3] and Andersen T. B.[1]

[1] *The Centre for Earth Evolution and Dynamics (CEED), University of Oslo, Oslo, Norway - h.j.kjoll@geo.uio.no*
[2] *Physics of Geological Processes, the NJORD Center, University of Oslo, Oslo, Norway*
[3] *Institut des Sciences de al Terre, Sorbonne Université, Paris, France*

Keywords: Dyke emplacement, brittle-ductile deformation, crustal thickening

Igneous dykes are the main magma transport pathways through the Earth's crust and, in volcanic rifts, they are considered to be the main mechanism to accommodate for tectonic extension. Their emplacement is controlled by a complex set of factors, such as crustal stress, crustal heterogeneities, topographic loading and magma viscosity (e.g. Spacapan et al., 2016; Kavanagh et al., 2018). Most models consider dykes as hydrofractures propagating as tensile cracks (mode I) in a brittle fashion with opening perpendicular to the least principal stress, implying that dykes emplaced in rifts are expected to be vertical and accommodate crustal extension. Because the rates for dyke emplacement are much higher than the tectonic strain rates, dyke emplacement is assumed to be a brittle process even in the ductile crust (e.g. Rivalta et al., 2015). A common assumption is that dyke orientation is controlled by tectonic stresses, such that dykes in rifts are expected to be vertical and perpendicular to extension.

In this presentation we report on detailed field observations of a spectacularly well-exposed dyke swarm to show that dykes were not systematically emplaced by purely brittle processes and that dyke orientation may differ from the dominant tectonic stress orientations. The dyke complex formed near the brittle-ductile transition at a magma-rich rifted margin during opening of the Iapetus Ocean. The magmatism was related to a large igneous province and the dyke swarm can be traced for more than 900 kilometers (Tegner et al., 2019; Kjøll et al., 2019). During the Silurian aged continent-continent collision of Baltica and Laurentia, the Iapetus margin was thrusted onto Baltica and is now exposed in the Scandinavian Caledonides in northern Sweden and Norway. Locally, the level of exposure is remarkable as retreating glaciers leave polished surfaces and glacial cirques exposed, allowing for continuous observations of large areas covering several kilometers.

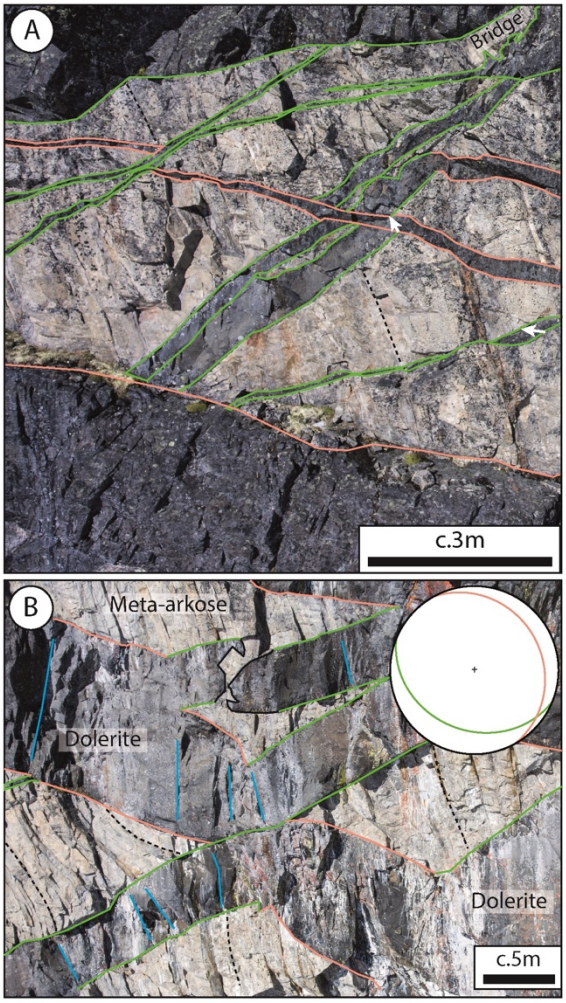

Fig. 1 – A) Complex cross-cutting relationships between the two orientations of dykes displayed. The central dyke displays a dramatic bend of c. 80°. Opening vectors are drawn as white arrows B) Two dykes with sharp and dramatic bends. Joints, orthogonal to the dyke margin can be observed in both dykes marked by blue lines. Black dashed lines indicate bedding in meta-arkose. Note partially broken bridge with angular edges.

Distinct dyke morphologies related to different emplacement mechanisms have been recognized: 1) Brittle dykes that exhibit straight contacts with the host rock, sharp tips, en-echelon segments with bridges exhibiting angular fragments (Fig. 1a and b); 2) Brittle-ductile dykes that exhibit undulating

contacts, rounded tips, ductile folding in the host rock and contemporaneous brittle and ductile features (Fig. 2a); 3) Ductile "dykes" that exhibit rounded shapes and mingling between the soft ductile host rock and the intruding mafic magma (Fig. 2b).

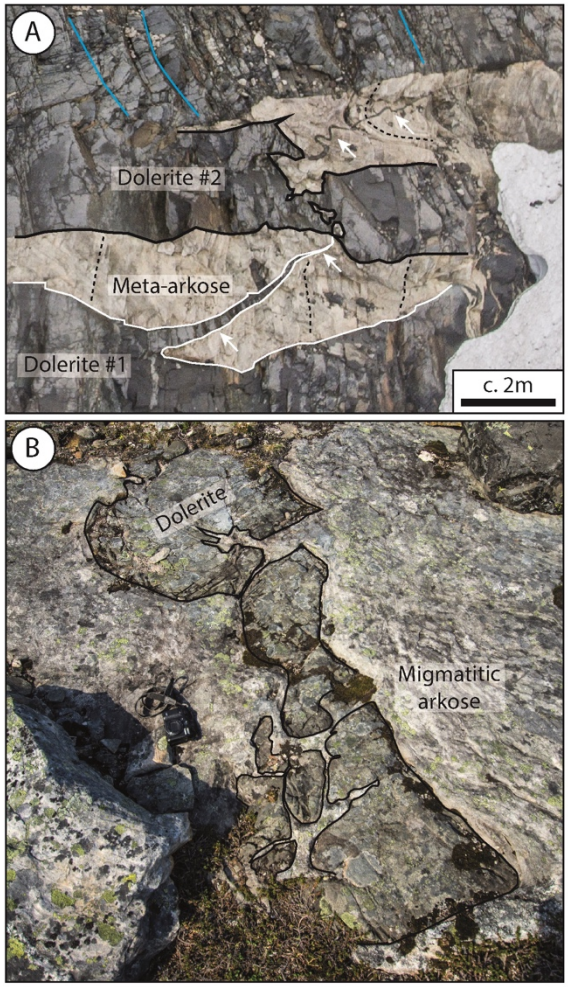

Fig. 2 – A) Shows the temporal evolution of the BDT as dolerite #1 shows a thin, tapered dyke offshoot which intruded meta-arkose, highlighted by white line and arrows. This thin offshoot is subsequently folded as dolerite #2 is emplaced. Black dashed line indicate bedding in the meta-arkose. Blue lines indicate preserved columnar jointing in a later dyke. B) Mafic magma which intruded a soft migmatitic arkosic sandstone formed tortuous contacts and complex lobes. Digital camera for scale.

The brittle dykes exhibit two distinct orientations separated by c. 30° that are mutually cross-cutting, suggesting that the dyke swam did not consist of only vertical sheets perpendicular to regional extension, as expected in rifts. We were able to use the well-exposed host rock layers as markers to perform a kinematic restoration to quantify the average strain accommodating the emplacement of the dyke complex: it accommodated for >100% extension, but counter-intuitively it also accommodated for 27% crustal thickening. We infer that the magma influx rate was higher than the tectonic stretching rate, implying that magma was emplaced forcefully, as supported by field observations of the host rock surrounding the mafic dykes. Finally, observations of typically "brittle" dykes that are subsequently being deformed by ductile mechanisms suggest that the fast emplacement of the dyke swarm triggered a rapid shallowing of the brittle-ductile transition. This would lead to a considerable weakening of the crust and perhaps help facilitate the continental break-up (Daniels et al., 2014; Kjøll et al., 2019). The interpretations of this study could potentially have large implications for surface topography and seismicity in active rifts and volcanic areas around the world.

Acknowledgements

HJK, L.L. and TBA acknowledges support from the Research Council of Norway (NFR) through its Centres of excellence funding scheme, to CEED, Project Number 223272. The field work and analyses conducted for this paper was funded by NFR Fri-Nat project number: 250327.

References

Daniels, K. A., Bastow, I., Keir, D., Sparks, R., and Menand, T., 2014, Thermal models of dyke intrusion during development of continent–ocean transition: *Earth and Planetary Science Letters*, v. 385, p. 145-153.

Kavanagh, J. L., 2018, Mechanisms of Magma Transport in the Upper Crust—Dyking, Volcanic and Igneous Plumbing Systems, Elsevier, p. 55-88

Kjøll, H. J., Andersen, T. B., Corfu, F., Labrousse, L., Tegner, C., Abdelmalak, M. M., and Planke, S., 2019, Timing of break-up and thermal evolution of a pre-Caledonian Neoproterozoic exhumed magma-rich rifted margin: *Tectonics*.

Rivalta, E., Taisne, B., Bunger, A. P., and Katz, R. F., 2015, A review of mechanical models of dike propagation: Schools of thought, results and future directions: *Tectonophysics*, v. 638, p. 1-42.

Spacapan, J. B., Galland, O., Leanza, H. A., and Planke, S., 2016, Control of strike-slip fault on dyke emplacement and morphology: *Journal of the Geological Society*, v. 173, no. 4, p. 573-576.

Tegner, C., Andersen, T. B., Kjøll, H. J., Brown, E. L., Hagen-Peter, G., Corfu, F., Planke, S., and Torsvik, T., 2019, A mantle Plume origin for the Scandinavian Dyke Complex: a "piercing point" for the 615 Ma plate reconstruction of Baltica?: *Geochemistry, Geophysics, Geosystems*, v. 20, no. 2, p. 1075-1094.

Magmatic fabrics related to different growth stages of the Cerro Bayo Cryptodome, Chachahuén volcano, Argentina

Tobias Mattsson[1], Steffi Burchardt[1], J. Octavio Palma[2], Olivier Galland[3], Bjarne S.G. Almqvist[1], Øyvind Hammer[4], Karen Mair[3], Yang Sun[1], Dougal A. Jerram[5,6]

[1] *Department of Earth Science, Uppsala University, Uppsala, Sweden* – tobias.mattsson@geo.uu.se

[2] *Y-TEC – CONICET, Av. Del Petroleo s/n - (Entre 129 y 143), Berisso, Buenos Aires, Argentina*

[3] *The Njord Centre, University of Oslo, Oslo, Norway*

[4] *The Natural History Museum, University of Oslo, Oslo, Norway*

[5] *CEED, University of Oslo, Oslo, Norway*

[6] *Dougal Earth Ltd., 31 Whitefields Crescent, Solihull, UK*

Keywords: cryptodome, magma flow, magmatic fabrics

Low aspect-ratio magmatic intrusions, such as crytptodomes, may cause destabilization of the volcanic edifice (e.g. Lipman et al., 1981; Voight et al., 1981). The stability of volcanic domes is especially dependent on the steepness of the dome flanks (e.g. Calder et al., 2002). In this study, we investigate the processes that governed the shape and affect the stability of a growing cryptodome.

The Cerro Bayo cryptodome was emplaced into the volcanic succession of the Chachahuén volcano, Argentina at about 6.7 ± 0.3 Ma (Pérez and Condat, 1996). Erosion has since its emplacement exposed the internal structure of the cryptodome. Cerro Bayo is about 1.3 km long, 1 km wide with >300 m of vertical exposure and yielding an estimated volume of ≥0.3 km^3. Cerro Bayo consists of a porphyritic trachyandesite with about 30 vol. % of plagioclase and amphibole phenocrysts in a crystalline groundmass. We did not observe any chilled zones within Cerro Bayo and therefore infer that it formed in a continuous or semi-continuous intrusive event.

Cerro Bayo has a concentric marginal structure consisting of a ≥120 m brecciated rim that transitions through a fractured zone to a largely coherent interior. An E-W oriented and fractured central ridge separates different domains within the interior of Cerro Bayo (cf. Fig. 1). These include the prominent southwestern and northern part of Cerro Bayo and the lower-elevation southeastern part.

To investigate the magma flow related to the emplacement of Cerro Bayo, we collected oriented samples for magmatic fabric analysis using anisotropy of magnetic susceptibility (AMS) and X-ray microtomography (μXCT). We also performed crystal-size distribution (CSD) analysis on the crystal cargo and microlites in Cerro Bayo to discern the crystallization history of the Cerro Bayo magma.

We found that the AMS fabric corresponds to the Shape-Preferred Orientation (SPO) of the magnetite crystals in Cerro Bayo, but also that the SPO of the amphibole phenocrysts is coaxial with the magnetite SPO. The AMS therefore both reflects the amphibole and oxide fabric and the magma flow in Cerro Bayo.

The magnetic fabric is generally contact-parallel within 100 m from the contact with the host rock. In a zone of prolate fabric in the western part of Cerro Bayo, the mineral lineation is sub-horizontal to shallow dipping at the low-lying terrain at the southern border zone of Cerro Bayo, but generally moderately dipping towards to the N-NW in the western central areas of Cerro Bayo (Fig. 1). The breccia zone displays several contact-parallel shear zones that surround meter long lenses of coherent rock (Fig. 2).

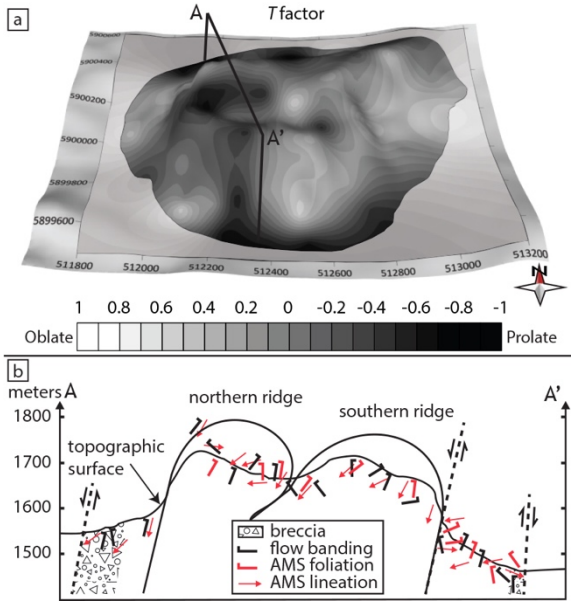

Fig. 1 – **a**) Ordinary kriging contour map of magnetic fabric shape draped onto a topographic surface of Cerro Bayo. **b**) Cross-section with magma flow indicators at a distance of ± 200 m from the cross-section.

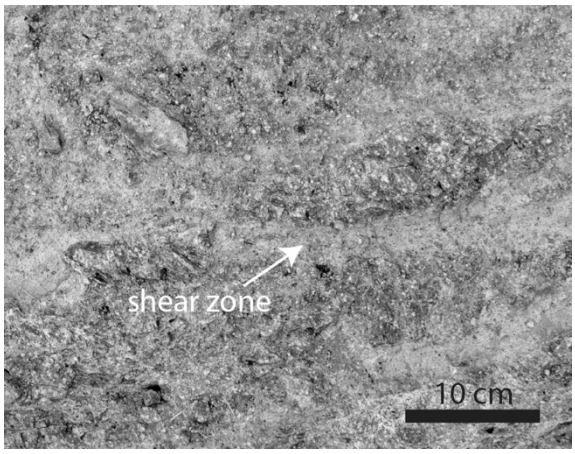

Fig. 2 – Shear zone in the western border breccia of Cerro Bayo.

The variations in fabric orientation correlate with the interior architecture of Cerro Bayo, which is why we interpret the fabric to have formed at different growth stages. We infer three stages of growth: (i) Initial inflation, which generated contact-parallel fabrics. (ii) Brecciation and fracturing of the rim of the intrusion caused by contact-parallel shear. (iii) In the final growth stage, a dominantly steeply to moderately inclined upward flow towards the S-SE from the western part of Cerro Bayo deformed and partly folded earlier emplaced magma. In Stage 3, the groundmass of the magma contained about 10 vol. % more crystals entering Cerro Bayo than the magma from the earlier growth stages. This indicates a relatively slower magma intrusion-rate into Cerro Bayo (cf. Riker et al., 2015), which could be related to a narrowing of the conduit towards the western part of the intrusion. The higher crystallinity likely affected the viscosity of the magma and made it more prone to spine-like growth of the intrusion (cf. Lejeune and Richet, 1995; Stevenson et al., 1996; Costa, 2005; Riker et al., 2015). Additionally, during Stage 3, the magma was forced to penetrate the solidified rim, which led to over-steepening of its southern flank.

Our results suggest that modification in magma flow from the conduit, combined with brecciation of the rim of the intrusion, caused the increased intrusion amplitude and partial over-steepening of the flank of the cryptodome.

Acknowledgements

The fieldwork was supported by the DIPS project (grant no. 240467) and the MIMES project (grant no. 244155) funded by the Norwegian Research Council awarded to O.G. O.P.'s position was funded by Y-TEC.

References

Calder, E. S., R. Luckett, R. S. J. Sparks, and B. Voight (2002), Mechanisms of lava dome instability and generation of rockfalls and pyroclastic flows at Soufrière Hills Volcano, Montserrat, *Geol. Soc. London, Mem.*, *21*(1), 173–190, doi:10.1144/GSL.MEM.2002.021.01.08.

Costa, A. (2005), Viscosity of high crystal content melts: Dependence on solid fraction, *Geophys. Res. Lett.*, *32*(22), L22308, doi:10.1029/2005GL024303.

Lejeune, A.-M., and P. Richet (1995), Rheology of crystal-bearing silicate melts: An experimental study at high viscosities, *J. Geophys. Res. Solid Earth*, *100*(B3), 4215–4229, doi:10.1029/94JB02985.

Lipman, P. W., J. G. Moore, and D. A. Swanson (1981), Bulging of the north flank before the May 18 eruption - geodetic data, in *The 1980 Eruptions of Mount Saint Helens, Washington. U.S. Geological Survey Professional Paper 1250*, edited by P. W. Lipman and D. R. Mullineaux, pp. 143–155, United States Government Printing Office, Washington, D. C.

Pérez, M. A., and P. Condat (1996), *Geología de La Sierra de Chachahuén, Area CNQ-23*, Buenos Aires, Argentina.

Riker, J. M., K. V. Cashman, A. C. Rust, and J. D. Blundy (2015), Experimental Constraints on Plagioclase Crystallization during H_2O- and H_2O–CO_2-Saturated Magma Decompression, *J. Petrol.*, *56*(10), 1967–1998, doi:10.1093/petrology/egv059.

Stevenson, R. J., D. B. Dingwell, S. L. Webb, and T. G. Sharp (1996), Viscosity of microlite-bearing rhyolitic obsidians: an experimental study, *Bull. Volcanol.*, *58*(4), 298–309, doi:10.1007/s004450050141.

Voight, B., H. Glicken, R. J. Janda, and P. M. Douglass (1981), Catastrophic rockslide avalanche of May 1980, in *The 1980 eruptions of Mount St. Helens, Washington. U.S. Geological Survey Professional Paper 1250*, edited by P. W. Lipman and D. R. Mullineaux, pp. 347–378, United States Government Printing Office, Washington, D. C.

Links between magmatic arc behavior and upper plate deformation in the Malargüe Andes

Mescua, J.F.[1,2], Sruoga, P.[3], Giambiagi, L.[1], Suriano, J.[1], Barrionuevo, M.[1] and Spagnotto, S.[4]

[1] *Instituto Argentino de Nivología, Glaciología y Ciencias Ambientales, CCT Mendoza, CONICET, Mendoza, Argentina* – jmescua@mendoza-conicet.gob.ar.
[2] *Facultad de Ciencias Exactas y Naturales, Universidad Nacional de Cuyo, Mendoza, Argentina.*
[3] *CONICET - SEGEMAR, Buenos Aires, Argentina*
[4] *CONICET - Universidad Nacional de San Luis, San Luis, Argentina.*

Keywords: volcanic arc, tectonics, Southern Central Andes.

The Neogene volcanic arc in the Malargüe fold-and-thrust belt (35ºS) has experienced an expansion towards the foreland since the late early Miocene and a retreat to its current position along the Argentina-Chile drainage divide in the Plio-Quaternary.

The expansion towards the foreland coincides roughly in time and space with the advance of contractional deformation and uplift (Mescua et al., 2014). However, a precise chronology of magmatic activity and its relationship with deformation/stress state in the upper plate has not been published .

In this presentation, we will review recent data on: (i) absolute dating of volcanic arc rocks using modern methods (U/Pb, Ar/Ar); (ii) recent geochemical analysis of volcanic arc rocks; and (iii) timing of deformation/uplift events obtained from fault-slip data and thermochronological studies.

Although the location of the volcanic front through time is usually interpreted as a proxy for the subduction angle (Folguera et al., x), we propose that the deformation in the upper plate has also an important role in the location of magmatic activity in oceanic-continental subduction systems, through (1) the stress state in the upper plate, (2) crustal thickness variations, and (3) the activity of faults that act as pathways for magma migration.

We document that, following the onset of contraction at ~20 Ma, in the westernmost sector of the belt, the arc expanded at ~18 Ma to the inner sector of the Argentinean Andes, and volcanism was never interrupted in this sector until the late Pleistocene when the arc focused in its present position along the drainage divide (Sruoga et al., 2008; 2009).

Until 13 Ma, this magmatism has geochemical characteristics transitional between island-arc and continental-arc setting (Sruoga et al. 2008, 2016). These volcanic rocks are deformed and folded. Since 13 Ma, volcanic rocks in the inner sector show predominant hypabyssal emplacements and steeper REE patterns, and are not deformed but only tilted in fault blocks.This period coincides with crustal thickening and migration of contraction to the external sector of the Malargüe fold-and-thrust belt.

The eastward advance of deformation and uplift was accompanied by arc expansion during the prolonged contractional period that produced the current orogenic front of the Malargüe fold-and-thrust belt in the late Miocene. Syn-contractional volcanics along the external sector of the belt span the 13-5 Ma period (Nullo et al., 2002: Horton et al., 2016)

The easternmost volcanic edifices with calk-alkaline geochemistry and arc signature were emplaced at 5 to 4 Ma, 200 km east of the current arc. During this same period, a well-established volcanic front seems to be developed at Risco Plateado, only 30 km east of the current arc. This volcanic front remained active until the early or Mid-Pleistocene (~ 1 Ma). Limited thermo- chronological data (U-Th/He on apatite) suggest out-of-sequence exhumation took place in the inner Malargüe fold-and-thrust belt at around 4 Ma (Bande et al., 2019), indicating that the Risco Plateado arc was coeval with active thrusting which may have channeled magma ascent. This period also records contraction and uplift in the easternmost Malargüe fold-and-thrust belt along the orogenic front (Silvestro et al., 2005).

The retreat of arc volcanism to its present position along the Argentina-Chile divide took place in the middle Pleistocene (after 1 Ma). This coincides with a change of the stress state in this region from a compressional regime (registered only in pre-Pliocene rocks) to a strike-slip one. Fault slip-data and reported focal mechanisms show dextral movement along N-S faults. These deep faults likely act as fluid pathways allowing a focused ascent of magma across the crust.

We conclude that the Neogene behavior of the arc shows an expansion coinciding with upper-plate contraction and crustal thickening. Between 16 and 5 Ma volcanism was distributed in a ~100 km-wide region, but a clear volcanic belt cannot be recognized. After 5 Ma, the arc was still wide, but a volcanic front with N-S trend developed along the Risco Plateado sector, coincident with the reactivation of thrusts in this area. After 1 Ma, the arc retreated to its current position favored by the development of N-S crustal strike-slip faults that act as magma pathways.

Acknowledgements

We acknowledge funding from Agencia Nacional de Promoción Científica y Técnica (project PICT2015-1181) and SEGEMAR.

References

Bande, A., A. Boll, F. Fuentes, B. Horton and D. Stockli (in press), Thermochronological constraints on the exhumation of the Malargüe fold-thrust belt, southern Central Andes, in *Opening and closure of the Neuquén Basin in the Southern Andes*, edited by D. Kietzmann and A. Folguera, Springer Earth System Science.

Litvak, V.D., M.G. Spagnuolo, A. Folguera, S. Poma, R.E. Jones and V.A. Ramos (2015), Late Cenozoic calc-alkaline volcanism over the Payenia shallow subduction zone, South-Central Andean back-arc (34° 30′–37° S), Argentina, *Journal of South American Earth Sciences*, *64*, 365-380.

Mescua, J.F., L.B. Giambiagi, A. Tassara, M. Giménez, and V.A. Ramos (2014), Influence of pre-Andean history over Cenozoic foreland deformation: Structural styles in the Malargüe fold-and-thrust belt at 35ºS, Andes of Argentina, *Geosphere*, *10*(3), 585-609.

Nullo, F.E., G.C. Stephens, J. Otamendi and P.E. Baldauf (2002), El volcanismo del Terciario superior del sur de Mendoza, *Revista de la Asociación Geológica Argentina, 57*(2), 119-132.

Silvestro, J., P. Kraemer, F. Achilli and W. Brinkworth (2005), Evolución de las cuencas sinorogénicas de la Cordillera Principal entre 35º-36º S, Malargüe, *Revista de la Asociación Geológica Argentina*, *60*(4):627-643.

Sruoga, P., Rubinstein, N.A., Etcheverría, M.P., Cegarra, M., Kay, S.M., Singer, B. y Lee, J., 2008. Estadío inicial del arco volcánico neógeno en la Cordillera Principal de Mendoza (35º). Revista de la Asociación Geológica Argentina, 63(3): 454-469.

Sruoga. P., M.P. Etcheverría, M. Cegarra, J.F. Mescua and S. Crosta (2016), Hoja Geológica 3569-13 Cerro Risco Plateado, Provincia de Mendoza. Escala 1:100000. Boletín 420, Instituto de Geología y Recursos Minerales, Servicio Geológico Minero Argentino, 170 p. Buenos Aires.

Top down or bottom up: identification and implications of invasive lavas versus shallow intrusions in sedimentary basins

John M. Millett[1,2], Dougal A. Jerram[3,4], Sverre Planke[1,4,5], Malcolm J. Hole[2], Natalia Famelli[6,7], David W. Jolley[2], Peter Ablard[8]

[1] *VBPR, Oslo, Norway - john.millett@vbpr.no*
[2] *Department of Geology and Petroleum Geology, University of Aberdeen, UK*
[3] *DougalEARTH Ltd., Solihull, UK*
[4] *CEED, University of Oslo, Norway*
[5] *The Arctic University of Norway, Tromsø, Norway*
[6] *Petrobras, Rio de Janeiro, Brazil*
[7] *Federal University of Rio Grande do Sul, Brazil*
[8] *Equinor, Aberdeen, UK*

Keywords: invasive lava flows, peperite, density loading

The subsurface transport and emplacement of magma in shallow sedimentary basin settings can include processes ranging from passive intrusion through peperite-style mingling to explosive near-surface interactions (Skilling et al., 2002; Wohletz, 2002; Galland et al., 2016). Where magma reaches the sediment surface, a diversity of emplacement styles ranging from effusive to explosive mechanisms in both the sub-aerial and sub-aqueous domains may occur. This results in the fundamental and standard division of sub-surface and surface related igneous domains each comprising ranges of associated volcanic facies.

In most instances this division is clear, however, in an increasing number of cases and especially for sub-surface investigations, the differentiation of shallow intrusions from erupted deposits is not always straight forward and the grounds for their separate definition may be challenged (Fig. 1). The implications of correct identification of intrusive compared to effusive domains may be significant in terms of understanding, for example in relation to stratigraphy, sub-surface fluid migration pathways, reservoir continuity, thermal influences on host rocks and climatic impacts. Therefore, any potential for incorrect identification of facies may have important geological and economic implications.

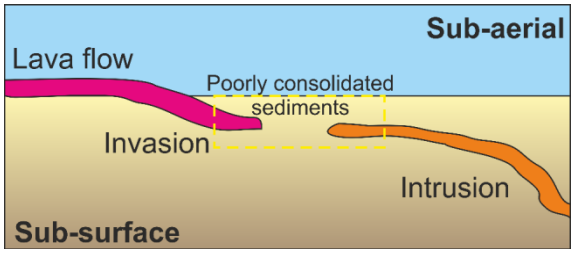

Fig. 1 - Simplified schematic highlighting the association of intrusions and invasive lava flows to the sub-surface and sub-aerial domains highlighting the region where they may coexist and may be easily confused.

The process of lava invasion, whereby lavas flowing across typically wet unconsolidated sediments begin to nose beneath the surface, in essence re-entering the sub-surface from which they have come, has been documented in several locations globally including the Columbia River Basalt Province, USA (Ebinghaus et al., 2014), St Cyrus, UK (Hole et al., 2013) and onshore Angola (Jerram et al., 2019) among others (Fig. 2).

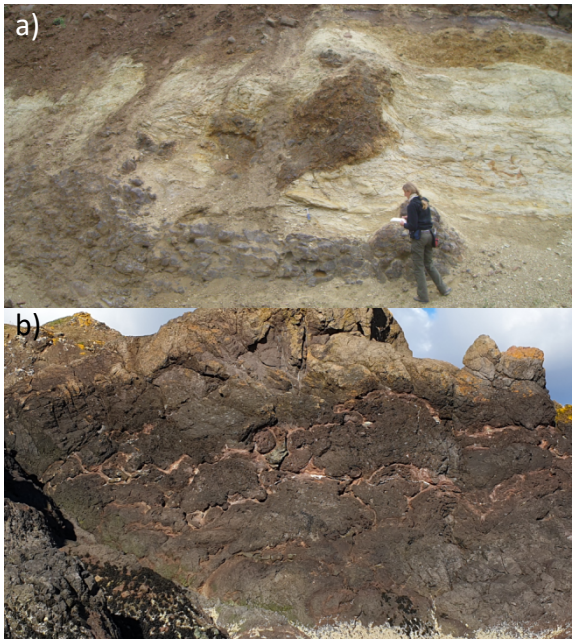

Fig. 2 – Field examples of interpreted invasive lava flows from a) Columbia River Basalt Province where an irregular intrusive body is interpreted to have propagated from the overlying lava flow into the underlying siliciclastic fluvial sediments, b) invasive pillow-like vesicular lobes intruding into pale red sediments of the Montrose Group, St Cyrus, UK.

This process relies on the density difference between liquid lava and unconsolidated sediment, and may be initiated by topographic variations,

dynamic mingling and sediment properties such as density, water saturation, grain size and porosity (e.g. Hole et al., 2013). A key requirement for an invasive lava, must be that the invasive portion of the flow is connected to a segment of the lava that was emplaced at the sediment surface, with the implied stratigraphic significance of this. If a magma body never reaches the surface, then it should not be termed an invasive flow and should instead be classified as a shallow intrusion regardless of vesicle content or flow structures etc. with the corollary critical point that it has no empirical stratigraphic implications.

Where field exposure is poor or in subsurface borehole settings (e.g. core data), differentiating invasive lava flows from shallow intrusions can be extremely challenging. With the increasing focus of exploration for hydrocarbons in sedimentary basins affected by volcanism, the number of examples of volcanism within sedimentary basins has increased with the result that cases where igneous units with internal structures dominated by typical lava flow features (e.g. asymmetrical vesicle and fracture distributions) but at the same time displaying clear evidence for invasive or peperitized flow tops is increasing (Fig. 3).

The maximum depth of lava flow invasion may be parameterized by calculating the depth of neutral buoyancy for a given magma-sediment setting, however, the maximum practical depth of invasion is likely to be significantly shallower than this and will be constrained by the rheological properties of the sediment and the nature of the magma sediment interactions. Improving the constraints on maximum potential invasion depths for invasive lavas in different settings and identifying features common to or exclusive to invasive flows compared to shallow intrusions is required in order to improve our understanding of the currently 'grey area' where both processes coexist. This will enable much needed error quantification for basin analyses and applications of stratigraphic correlation in such settings. In this contribution we use field and core-based examples to lay the groundwork for a revised classification of invasive lava flow characteristics with a focus on defining criteria for their sub-surface identification and implications.

Acknowledgements

UK NDR and Equinor are thanked for making the core images for the Rosebank field available.

References

Ebinghaus, A., Hartley, A.J., Jolley, D.W., Hole, M., Millett, J.M., 2014. Lava–sediment interaction and drainage-system development in a large igneous province: Columbia River Flood Basalt Province, Washington State, USA. Journal of Sedimentary Research 84 (11), 1041–1063.

Galland, O., Eoghan, H., van Wyk de Vries, Burchardt, S., 2016. Laboratory Modelling of Volcano Plumbing Systems: A Review. Advances in Volcanology, Springer. DOI: 10.1007/11157_2015_9

Hardman, J., Schofield, N., Jolley, D.W., Hartley, A.J., Holford, S., Watson, D., 2017. Controls on the distribution of volcanism and intra-basaltic sediments in the Cambo–Rosebank region, West of Shetland. Journal of the Geological Society, London. Online first, https://doi.org/10.1144/petgeo2017-061

Hole, M.J., Jolley, D.W., Hartley, A.J., Leleu, S., John, N., Ball, M., 2013. Lava–sediment interactions in an Old Red Sandstone basin, NE Scotland. Journal of the Geological Society, London, 170, 641–655.c

Jerram, D.A., I.R. Sharp, T.H. Torsvik, R. Poulsen, T. Watton, U. Freitag, A. Halton, S.C. Sherlock, J.A.S. Malley, A. Finley, J. Roberge, R. Swart, C. Puigdefabregas, C.H. Ferreira, V. Machado, 2018.Volcanic constraints on the unzipping of Africa from South America: Insights from new geochronological controls along the Angola margin, Tectonophysics, 760, 252–266.

Skilling, I.P., White, J.D.L., McPhie, J., 2002. Journal of Volcanology and Geothermal Research, 114, 1-17.

Wohletz, K., 2002. Water/magma interaction: some theory and experiments on peperite formation. Journal of Volcanology and Geothermal Research, 114, 19-35.

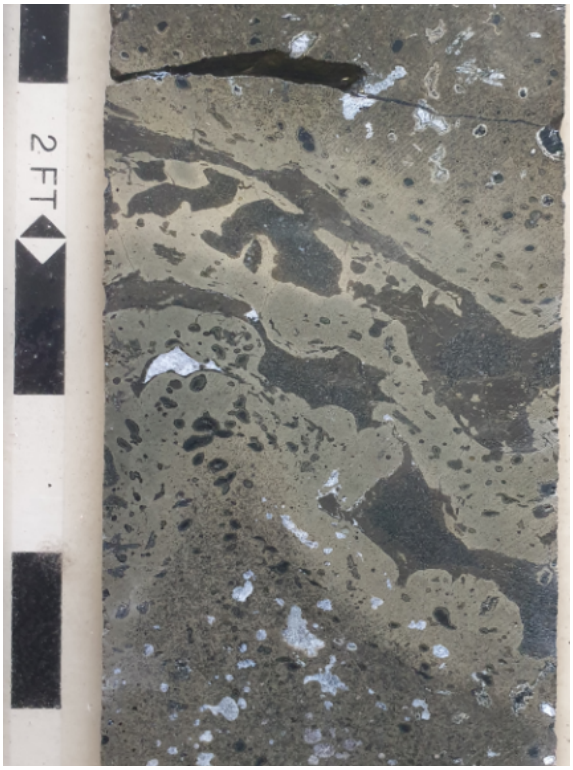

Fig. 3 – Core example of the upper contact of an igneous unit from the Rosebank field, UKCS (213/26-1), displaying an upper margin clearly mingled with overlying volcanic sediment. This unit comprises part of a volcanic sequence interpreted as lava flows (e.g. Hardman et al., 2017).

Structural framework of the tholeiitic and alkaline intrusive bodies on the onshore border of the Campos and Santos basins

Maria José Resende Oliveira[1], Renata da Silva Schmitt[2], Sérgio de Castro Valente[3], Vitor Savastano[4], Mário Neto Cavalcanti de Araújo[4] and Leonardo Campos Inocêncio[5]

[1] *PETROBRAS/LIBRA, Av. República do Chile 330, Torre Oeste, Rio de Janeiro, Brasil - m*joliveira@petrobras.com.br
[2] *Universidade Federal do Rio de Janeiro, Cidade Universitária, Rio de Janeiro, Brasil*
[3] *Universidade Federal Rural do Rio de Janeiro, BR 465, km 7, Seropédica, Brasil.*
[4] *PETROBRAS/CENPES, Av. Horácio de Macedo 950, Rio de Janeiro, Brasil*
[5] *Universidade do Vale dos Sinos, Brasil, Av. Unisinos 950, São Leopoldo, Brasil.*

Keywords: dykes, aerial images, Pontal do Atalaia.

Tholeiitic and alkaline mafic bodies crop out at the "Pontal do Atalaia", in Arraial do Cabo city, at the continental onshore border of Campos and Santos basins, SE Brazil. These igneous bodies form a complex brittle fabric cross cutting the Paleoproterozic granitic orthogneiss of the Região dos Lagos Complex, in the Cabo Frio Tectonic Domain (Schmitt et al. 2016).

The tholeiitic diabases belong to the Serra do Mar Dyke Swarm (Valente et al. 2007) that is correlated to the magmatic events of the Serra Geral, Cabiúnas and Camboriú formations. The latter two are considered the economic basement for the Campos and Santos basins (Winter et al. 2007; Moreira et al. 2007). These dykes occur as centimetric to metric bodies, in a N50E-S50W dominant trend, associated to the initial events of the Gondwana rupture. At the Cabo Frio region, 20 km north of the study area, Ar-Ar data indicated an age of 132 Ma (Early Cretaceous-Hauterivian) for the crystallization of amphibole and biotite (Carvas, 2017). According to Oreiro (2006), Ar-Ar ages (whole rock dating) for the Pontal do Atalaia tholeiitic dykes, varies between 58.1-62.7 Ma (Paleocene). Bennio et al. (2003) obtained 55 Ma (Eocene) for Ar-Ar dating on plagioclase at the same location. Here, we obtained zircon crystals from the tholeiitic dykes that will be analyzed with U-Pb method.

The alkaline rocks are composed of lamprophyres, syenites and trachytes and, more rarely, phonolites (Fig 1.). They occur predominantly as dykes, but also as sills, mainly the trachytes and stocks (syenites). Sometimes, breccias and cataclasites occur associated with them. The alkaline intrusive bodies intersect each other in several directions, indicating contemporaneity. However, they always cut the tholeiitic diabase dykes (Fig. 2). In the Cabo Frio region, K-Ar data indicate values of 72.4 Ma (Campanian) in alkaline feldspar and 50-54 Ma (Eocene) in biotite and whole rock for the alkaline intrusive rocks (Sonoki & Garda, 1988).

The dykes can be emplaced in ancient discontinuites of the country rocks, or cut them at a high angle. Reactivation of some discontinuities was observed, with multiple intrusions of tholeiitic and alkaline dykes parallel to Precambrian amphibolite bodies. NNW-SSE and ESE-WNW brittle structures are predominant in the Pontal do Atalaia area and evidence the tectonic inheritance from the orthogneisses fabric. The former is parallel to the ductile fabric of the orthogneisses. Oblique younger faults cut the alkaline dykes, indicating transtension.

High resolution (2cm / pixel) acquisition and processing of aerial images, obtained by an Unmanned Aerial Vehicle (UAV or drone), allowed detailed analysis of emplacement structural, such as intrusions in conjugate fractures, *én échelon* and relays arrays and broken dykes structures as bridges and horns. These data, associated with field observations help to establish the hierarchy, kinematics and tectonic settings of these intrusive bodies.

The integration of all data will contribute to better understanding the offshore geological evolution of the Campos and Santos basins, adjacent to this area, where the tholeiitic magmatism is related with the processes of the South Atlantic rifting and the intrusive alkaline rocks affect the pre- salt, intra-salt and post-salt sequences.

Fig. 1 – Phonolite dyke cutting at 90º the ductile foliation of the Paleoproterozoic orthogneisses. Alkali-feldspars phenocrystals are oriented parallel to the border of the dyke. Horizontal view.

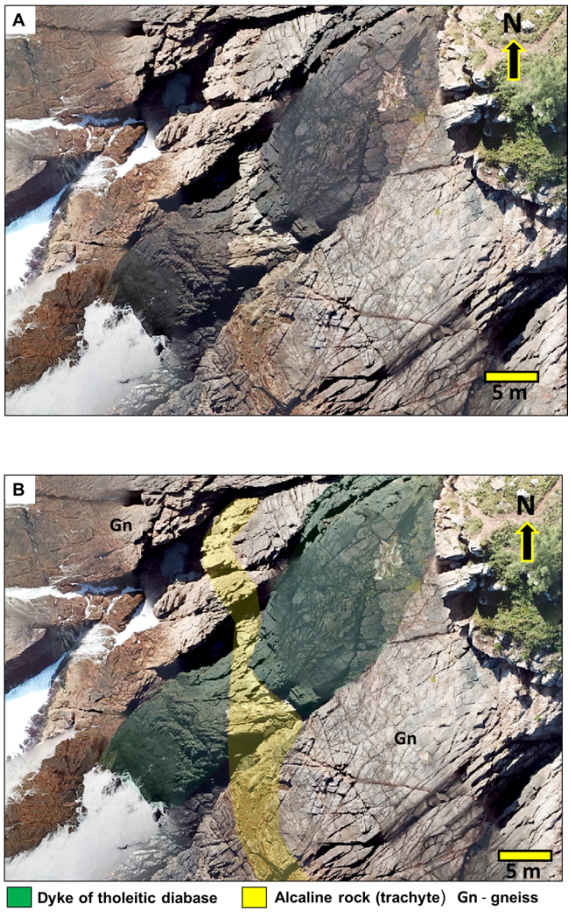

Fig. 2. Aerial image, after processing (A), the same image interpreted, showing the alkaline subvolcanic intrusive rock (trachyte) cutting the tholeiitic diabase dyke.

Acknowledgements

The authors thank Petrobras for supporting this work.

References

Bennio, L., Brotzu, P., D'Antonio, M., Feraud, G., Gomes, C. B., Marzoli, A. and Ruberti, E. (2003), The tholeiitic dyke swarm of the Arraial do Cabo peninsula (SE Brazil): 39 Ar/40 Ar ages, petrogenesis, and regional significance. *Journal of South American Earth Sciences*,**16(2):**163-176.

Carvas, K. Z. (2016), Diques mesozoicos subalcalinos de baixo titânio da Região dos Lagos (RJ): Geoquímica e geocronologia 40Ar/39Ar. Master Thesis, Instituto de Astronomia, Geofísica e Ciências Atmosféricas, Universidade de São Paulo, São Paulo, 129p.

Moreira, J. L. P., Madeira, C. V., Gil, J. A. and Machado, A. P. M. (2007), Bacia de Santos. *Boletim de Geociências da Petrobras*, Rio de Janeiro, **15**(2): p. 531-549.

Oreiro, S. G. (2006), Magmatismo e sedimentação em uma área na Plataforma Continental de Cabo Frio, Rio de Janeiro, Brasil, no intervalo Cretáceo Superior–Terciário. *Boletim de Geociências da Petrobras*, **14:** 95–112.

Sonoki, I. K. and Garda, G. M. (1988), Idades K-Ar de rochas alcalinas do Brasil Meridional e Paraguai Oriental: compilação e adaptação às novas constantes de decaimento. *Boletim IG-USP. Série Científica* **19:** 63-85.

Schmitt, R. S., Trouw, R. Van Schmus, W. R., Armstrong, R. and Natasha S. Gomes Stanton, N. S. G. (2016), The tectonic significance of the Cabo Frio Tectonic Domain in the SE Brazilian margin: a Paleoproterozoic through Cretaceous saga of a reworked continental margin. Brazilian Journal of Geology, **46**(1): 37-66.

Valente, S.C., Corval, A., Duarte, B.P., Ellam, R.B., Fallick, A.E. and Dutra, T. (2007), Tectonic boundaries, crustal weakness zones and plume-subcontinental lithospheric mantle interactions in the Serra do Mar Dyke Swarm, SE Brazil. *Revista Brasileira de Geociências,* **37**(1): 194 – 201.

Winter, W. R., Jahnert, R. J. and França, A. B. 2007. Bacia de Campos. *Boletim de Geociências da Petrobras*, Rio de Janeiro, **15**(2): 511-529.

Hydrothermal fluids in the Tromen Volcanic Complex, Patagonia, Argentina

Paola Orozco[1], Jimena Presa[2], Franco Tassi[3], Patricia Alvarado[1]

[1] *CONICET-CIGEOBIO (Centro de Investigaciones de Geósfera y la Biósfera). Universidad Nacional de San Juan. Meglioli 1160 sur- Rivadavia 5400 Prov. de San Juan Argentina* – paola.orozco@unsj-cuim.edu.ar
[2] *IIPG- Instituto de Investigaciones Paleobiológias y Geológicas. Universidad Nacional de Rio Negro. Av. J.A. Roca 1242, (8332) Gral. Roca, Río Negro, Argentina*
[3] *Dept. of Earth Sciences. University of Florence. Via La Pira 4, 50121. Florence, Italy*

Keywords: hydrothermal, Tromen, gases.

The study focuses on the geochemical and isotopic characteristic of thermal fluids in different zones within the Tromen volcanic complex, in Neuquén province between 36°30' S - 37°30' S and 69°40' W - 70°30' W. Geochemical samples were taken from springs, lagoons and bubbling pools.

The Tromen volcanic complex (TVC) is made up of several volcanic centers (Galland et al., 2007): Cerro Tromen, Cerro Negro del Tromen, Cerro Tillhue, Cerro Bayo and Cerro Wayle, surrounded to the east by large shield volcanoes (Eg. Auca Mahuida, Payun Matrun) with intraplate geochemical signatures (Llambías et al., 1982; Saal et al.,1993; Kay et al., 2006)

Tectonically, this sector constitutes one of the few examples of active backarc developed in extensional basins of the late Triassic to early Cretasic (Neuquén basin) (Zollner and Amos,1973; Ramos, 1977). The TVC is related to a normal subduction process (36°E) (Burd et al., 2013), of the Nazca plate under the Sudamerican plate after a state of horizontal subduction, indicated by the presence of arc and back arc in the last 25Myrs with a change in the geometry of the subduction zone recorded on the front of the arc during the late Cretaceous and late Miocene (Ramos and Folguera, 2005; Kay et al., 2006). The TVC is comprised between two fold and thrust belts (Folguera et al., 2008), Agrio fold and thrust belt to the west and Malargue fold and thrust belt to the east.

The complex is linked with a compressional setting (Kozlowski et al., 1996; Marques and Cobbold, 2006; Rossello, 2002; Galland et al., 2007; Messager et al., 2010) as well as other volcanic systems (eg. El reventador in Ecuador (Tibaldi, 2005).

For this study, major elements were analized, such as the cations (Na^+, K^+, Ca^{2+}, Mg^{2+}, Li^+, NH_4^+), anions (HCO_3^-, F^-, Cl^-, Br^-, NO_3^{2-}, SO_4^{2-}, PO_4^{3-}) and trace elements for waters as well as stable isotopes of $^{18}O/^{16}O$ and $^{2}H/^{1}H$ ratios in water (expressed as $\delta^{18}O$-H_2O and δD-H_2O ‰). Two bubbling pools data were analyzed for gases (CO_2, HCl, HF, SO_2, H_2S, S, N_2, CH_4, Ar, O_2, H_2, He, CO, $^{40}Ar/^{36}Ar$, $\delta^{13}C$, $\delta^{18}O$, δD, $\delta^{15}N_2$.). Geothermometers were taken from Giggenbach, (1988), Chiodini et al., (1995), D'Amore and Panichi, (1980) with temperatures ~200°C at depth. The magmatic materials were contaminated by the crust which can be observed due to low He (lower than 1 %He) in springs related with the Tomen fault.

It is noteworthy that the results of water gases and isotopes of this region are the first to be obtained, characterizing this sector of the Andean arc as a hydrothermal system of geothermal importance. Despite the distance between the Andean arc and the TVC, the magmatic activity continues, extending to the east. Moreover, the TVC is associated with the volcanic centers of Auca Mahuida, Domuyo, and Payenia system.

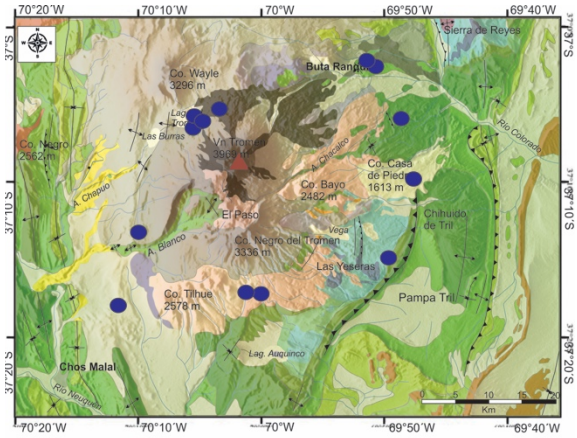

Fig. 1 – Geological map with the sample springs in the Tromen Volcanic Complex (modified from Galland et al., 2007 and Llambias et al., 2011).

Acknowledgements

The author is kindly grateful to Matias Portillo and Andrea Orozco for their help in the 2018-2019 campaign in Neuquén and also to Laboratory of Water and Gases- University of Florence, Italy.

Fig. 2 – Bubbling pool in Buta Ranquil location, on Tromen Volcanic Complex eastern flank.

References

Burd, A. I., Booker, J. R., Mackie, R., Favetto, A., & Pomposiello, M. C. (2014). Three-dimensional electrical conductivity in the mantle beneath the Payún Matrú Volcanic Field in the Andean backarc of Argentina near 36.5 S: Evidence for decapitation of a mantle plume by resurgent upper mantle shear during slab steepening. Geophysical Journal International, 198(2), 812-827.

Chiodini, G., Frondini, F., Marini, L., 1995. Theoretical geothermometers and PCO2 indicators for aqueous solutions coming from hydrothermal systems of medium-low temperature hosted in carbonate-evaporite rocks. Application to the thermal springs of the Etruscan Swell, Italy. Appl. Geochem. 10, 337–346.

D'Amore, F., Panichi, C., 1980. Evaluation of deep temperatures of hydrothermal systems by a new gas geothermometer. Geochim. Cosmochim. Acta 44 (3), 549–556.

Folguera, A., Bottesi, G., Zapata, T., & Ramos, V. A. (2008). Crustal collapse in the Andean backarc since 2 Ma: Tromen volcanic plateau, Southern Central Andes (36 40′–37 30′ S). Tectonophysics, 459(1-4), 140-160.

Galland, O., E. Hallot, P. R. Cobbold, G. Ruffet, and J. de Bremond d'Ars (2005), Volcanism in a compressional Andean setting: A structural and geochronological study of Tromen volcano (Neuquén province, Argentina). Tectonics 26, TC4010, 10.1029/2006TC002011.

Giggenbach, W.F., 1988. Geothermal solute equilibria. Derivation of Na–K–Mg–Ca geoindicators. Geochim. Cosmochim. Acta 52 (12), 2749–2765.

Kay, S.M., Burns, M., Copeland, P., 2006. Upper Cretaceous to Holocene magmatism and evidence for transient Miocene shallowing of the Andean subduction zone under the northern Neuquén Basin. In: Kay, S.M., Ramos, V.A. (Eds.), Evolution of an Andean Margin: A tectonic and magmatic view from the Andes to the Neuquén Basin (35–39°S): Geological Society of America, Special Paper, 407, pp. 19–60.

Kozlowski, E. E., C. E. Cruz, and C. A. Sylwan (1996), Geologı´a estructural de la zona de Chos Malal, Cuenca Neuquina, Argentina, paper presented at XIII Congreso Geolo´gico Argentino y III Congreso de Exploracio´n de Hidrocarburos, Buenos Aires.

Llambıas, E. J., Palacios, M., & Danderfer, J. C. (1982). Las erupciones holocenas del volcán Tromen (Provincia del Neuquén) y su significado en un perfil transversal EO a la latitud de 37 S. In Quinto Congreso Latinoamericano de Geologia, Buenos Aires (pp. 537-545).

Llambías, E. J., Leanza, H. A., Galland, O., Arregui, C., Carbone, O., Danieli, J. C., & Vallés, J. M. (2011). Agrupamiento volcánico Tromen-Tilhue. Geología y Recursos Naturales de la Provincia de Neuquén Leanza, H.; Arregui, C, 627-636.

Marques, F. O., and P. R. Cobbold (2006), Effects of topography on the curvature of fold-and-thrust belts during shortening of a 2-layer model of continental lithosphere, Tectonophysics, 415, 65 – 80.

Messager, G., Nivière B., Martinod, J., Lacan P. & Xavier, J.P. 2010.Geomorphic evidence for Plio-Quaternary compression in the Andean Foothills of the southern Neuquén Basin, Argentina. Tectonics, 29.

Ramos, V.A.,1977. In: Rolleri, E.O. (Ed.), Geología y Recursos Naturales de la Provincia del Neuquén, VII° Congreso Geológico Argentino. Actas, vol. I, pp. 9–24.

Ramos, V.A., Folguera, A., 2005. Tectonic evolution of the Andes of Neuquén: constraints derived from the magmatic arc and foreland deformation. In: Veiga, G., et al. (Ed.), The Neuquén Basin: a case study in sequence stratigraphy and basin dynamics: The Geological Society, Special Publication, 252, pp. 15–35.

Rossello, E.A., Cobbold, P.R., Diraison, M., Arnaud, N., 2002. Auca Mahuida (Neuquén Basin, Argentina): a Quaternary shield volcano on a hydrocarbon-producing substrate. 5th International Symposium on Andean Geodynamics (Toulouse), Extended Abstracts, pp. 549–552.

Saal, A., F. A. Frey, D. Delphino, and A. Bermudez (1993), Geochemical characteristics of alkalic basalts erupted behind Andean Volcanic Front (35°–37°S): Constraints on sources and processes in- volved in continental arc magmatism, Eos Trans.AGU, 74(43), Fall Meet. Suppl., 652.

Tibaldi, A. (2005). Volcanism in compressional tectonic settings: Is it possible?. Geophysical Research Letters, 32(6).

Zöllner, W. & Amos, A.J. 1973. Descripción geológica de la Hoja 32b, Chos Malal, provincia del Neuquén. Servicio Geológico Minero Argentino, Boletín 143: 91 págs., Buenos Aires.

Alkaline dykes of the Trindade Complex (Trindade Island, Brazil): field and petrographic aspects

Pasqualon N.G.[1], Lima E. F.[1], Brose G. C.[1], Luz F.R.[1], Rossetti L.M.M[1] and Rossetti, M.M.M.[2]

[1] *Department of Mineralogy and Petrology, Federal University of Rio Grande do Sul (UFRGS), Porto Alegre, Brazil - nati_pasqualon@yahoo.com.br*
[2] *Department of Geological Sciences, University of Canterbury, Christchurch, New Zealand.*

Keywords: Feeding systems, Melanephelinite, Lamprophyre.

Trindade Island is located at around 1.260 km from the Brazilian coast in the South Atlantic Ocean. The island is elongated along a NW-SE axis, with most of its structures indicating a NW direction of σ1 during its formation (Ferrari and Riccomini, 1999). Volcanic activity started at the mid-Pliocene, lasting until the Pleistocene (Cordani, 1970; Pires et al., 2016). The island is formed by lava flows, intrusions and pyroclastic rocks of strongly sodic alkaline, SiO_2 undersaturated nature, divided by Almeida (1961) into five geological units: Trindade Complex, Desejado Sequence, Morro Vermelho Formation, Valado Formation and Paredão Volcano (Fig. 1).

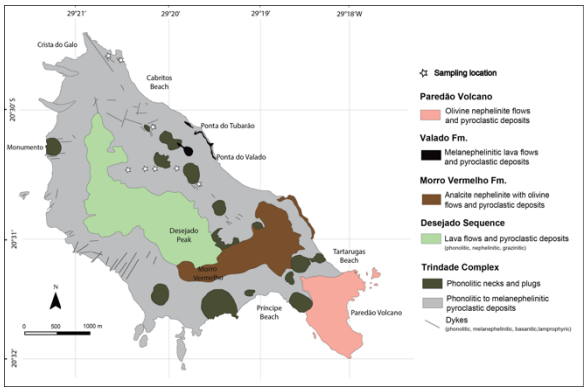

Fig. 1 – Geological map of Trindade Island modified from Almeida (1961) and Pasqualon et al. (2019) with sampling locations indicated by stars.

The Trindade Complex represents the oldest volcanic unit (3.9 Ma to 1.1 Ma - Cordani, 1970; Pires et al., 2016) and the basement of the island. This unit is composed of heterogeneous pyroclastic deposits (melanephelinites to phonolites), phonolitic subvolcanic intrusions, such as necks and plugs, and dykes of variable compositions, including olivine and clinopyroxene melanephelinites, monchiquites and analcime basanites (Marques et al., 1999).

This study aims to present preliminary results of the main field and petrographic aspects of the Trindade Complex dykes, in order to contribute to the understanding of the emplacement of these bodies and their petrogenetic history.

Nine dykes were selected for an initial detailed study. During fieldwork, some parameters such as geometry, sizes, structures and textures were described. Structural measurements were acquired using a compass. Petrographic analysis was carried out with conventional optical microscopy, using a petrographic microscope under transmitted light.

In general, the analyzed dykes intrude phonolitc necks or pyroclastic deposits of Trindade Complex. They present a tabular geometry, sharp contacts with the country rocks and thicknesses varying from 0.15 to 0.5 m. They are massive, at times with cooling joints perpendicular to their borders. The average orientation of the studied dykes is NW-SE trending with subvertical dips (Fig. 2).

Fig. 2 – Melanephelinitic dyke of approximately 0.5 m thick intruded in a phonolitic neck.

Petrographically, the dykes are hollo to hypocrystalline and porphyritic (10-20%) with a matrix that varies from microlithic/cryptocrystalline to fine-grained. Spherical and cylindrical vesicles may occur and these are partially filled by analcime and carbonates. Mafic enclaves (usually of pyroxene, hornblende and phlogopite) are common features.

The dykes were divided in 3 groups: phonolithic, melanephelinitic and lamprophiric. The phonolitic

dyke (n=1) is composed of phenocrysts and microphenocrysts of sanidine, zoned diopside, brown hornblende and, subordinately, of sodalite, titanite and apatite in a matrix with microliths of clinopyroxene, feldspathoid and titanomagnetite (Fig.3A).

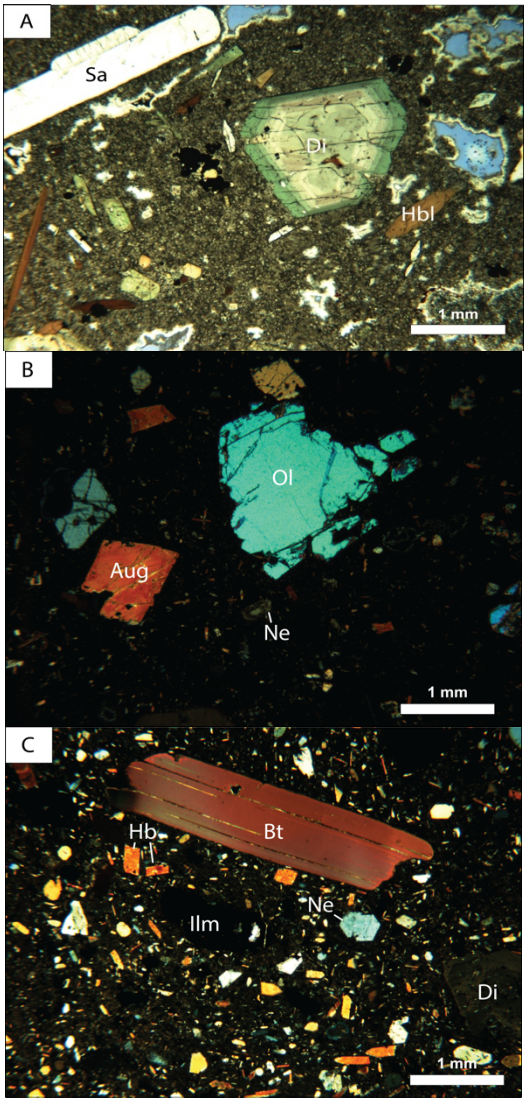

Fig. 3 – Photomicrographs of (A) phonolitic, (B) melanephelinitic and (C) lamprophyric dykes. Sa- Sanidine; Di – Diopside; Hbl – Hornblende; Ol- Olivine; Aug- Augite; Ne- Nepheline; Bt- Biotite; Ilm- Ilmenite. A) Plane- polarized light; B) and C) Cross-polarized light.

The melanephelinitic dykes (n=4) are composed of phenocrysts of olivine, augite/titano-augite, in a fine to microlithic matrix of nepheline, augite, titanomagnetite and, at times, phlogopite (Fig.3B). The lamprophyric dykes (n=4) presents a panidiomorphic texture and are composed of zoned diopside with exsolution lamellae and poikilitic texture, (hosting apatite and nepheline crystals), brow hornblende, biotite, nepheline and ilmenite in a microlithic matrix of clinopyroxene, nepheline, ilmenite, apatite and titanite (Fig. 3C).

The identification of three compositional groups in a few dyke samples from Trindade Complex suggests complex petrogenetic patterns for the feeding system of Trindade Island. The porphyritic texture indicates two distinct undercooling stages for the dykes and the presence of zoned clinopyroxene phenocrysts suggests a multistage crystallization. Mafic enclaves may suggest magma mingling or cumulate processes. Early ilmenite and titanite crystals indicate high Ti^{+4} activity in the early magmatic stages for the lamprophyric and phonolitic dykes. Euhedral biotite and amphibole in the lamprophyric dykes indicate a high volatile content.

This study will be complemented by geochemical, structural, geophysical and petrophysical analysis. Data interpretation and integration will contribute significantly to the discussion around the chemical and physical aspects of the Trindade plume and its activity during the formation of the island.

Acknowledgements

The authors acknowledge the financial support of the CNPq - Project CNPq-442812/2015-9 and the Graduate Program in Geosciences of UFRGS (PPGGEO), and Brazilian Navy (Marinha do Brasil) for all the logistical arrangements during field activities.

References

Almeida, F.F.M., 1961. Geologia e petrologia da Ilha daTrindade. 197f. Monografia XVIII, DGM/DNPM. Ministério das Minas e Energia, Rio de Janeiro.

Cordani, U.G., 1970. Idade do vulcanismo no oceano Atlântico Sul. Boletim IGA 1, 09–75.

Ferrari, A.L., Riccomini, C., 1999. Campo de esforços Plio-pleistocênico na Ilha da Trindade (Oceano Atlântico Sul, Brasil) e sua relação coma tectônica regional. Rev. Bras. Geosci. 29 (2), 195–202.

Marques, L.S., Ulbrich, M.N., Ruberti, E., Tassinari, C.G., 1999. Petrology, geochemistry and Sr–Nd isotopes of the Trindade and Martin Vaz volcanic rocks (southern Atlantic Ocean). J. Volcanol. Geotherm. Res. 93 (3), 191–216.

Pasqualon, N. G., Lima, E. F., Scherer, C.M.S., Rossetti, L. M. M., Luz, F. R. (2019). Lithofacies association and stratigraphy of the Paredão Volcano, Trindade Island, Brazil. Journal of Volcanology and Geothermal Research, 380, 48-63.

Pires, G.L.C., Bongiolo, E.M., Geraldes, M.C., Renac, C., Santos, A.C., Jourdan, F., Neumann, R., 2016. New 40Ar/39Ar ages and revised 40K/40Ar* data from nephelinitic–phonolitic volcanic successions of the Trindade Island (South Atlantic Ocean). J. Volcanol. Geotherm. Res. 327, 531–538.

Invasive lava flows or shallow sills: New observations from the Kajerkan quarry, NW Siberia

Sverre Planke[1], Alexander G. Polozov[2], John M. Millett[3], Dmitrii Zastrozhnov[3], Dwarika Maharjan[3], Dougal A. Jerram[4], Reidun Myklebust[5]

[1] *VBPR, Oslo, Norway; CEED, University of Oslo, Norway; The Arctic University of Norway, Tromsø* - planke@vbpr.no
[2] *IGEM-RAS, Moscow, Russia*
[3] *VBPR, Oslo, Norway*
[4] *DougalEARTH Ltd., Solihull, UK; CEED, University of Oslo, Norway*
[5] *TGS, Asker, Norway*

Keywords: Siberian Traps, invasive lava flows, shallow sills

Basaltic lava flows may bulldoze into poorly consolidated sediments, forming so-called invasive lava flows. Such invasive flows are sometimes mis-interpreted as extrusive lava emplaced at the paleo-surface, leading to incorrect stratigraphic and age relationships. Invasive lava flows are identified in numerous places worldwide, e.g. in the Columbia River Plateau Basalt Province, in central-east Greenland, onshore UK and offshore in the Faroe-Shetland basin (Millett et al., this volume). Modern invasive lava flows are also observed in snow-covered regions in the Kamchatka Peninsula (Edwards et al., 2014).

The initiation of the Siberian Traps magmatism occurred about 251 million years ago and is temporally associated with the global mass extinction at end-Permian times. We have conducted fieldwork in the Norilsk region in Siberia from 2006 to 2019 with recent focus on understanding the igneous facies and emplacement processes of the lowermost lava flows erupted directly on the end-Permian boggy surface (Jerram et al., 2016; Polozov et al., 2016). We have identified numerous locations of end-Permian boggy and shallow-water environments confirmed by hyaloclastite deposits, pillow basalts, and remnants of buried tree trunks within the basal part of the lowermost lava flow in the Norilsk area (Ivakinskaya Fm.). One of the specific features of the basal part of the Ivakinskaya Fm. is a type of hybrid rocks present around buried tree trunks where the basalt erupted directly onto organic-rich soil surfaces. In outcrop, these rocks are black and glassy, being present in small fissures or larger cracks in the aureoles around trees trunks. In the pillow basalts, formed at the basal part of lava flows erupted into shallow water, the black glassy rocks are less abundant, but sometimes present as black veins in altered grey pillow basalts.

Another typical setting of hybrid rocks is in shallow basaltic igneous intrusion emplacement into the coal-rich upper part of the Tunguska Group of late Permian age (Paderin et al. 2016; Svensen et al. 2018). These intrusions are present as tubular, sub-horizontal bodies of c 10 m thickness, and are well exposed a quarry south of the village of Kajerkan, northwest Siberia (Fig. 1). Three distinct igneous units have been mapped along the western quarry wall. The uppermost unit is interpreted as a lava flow based on the correlation to nearby flow fields and abundant vesicularity. The middle unit displays highly complex geometries (Figs. 1 to 3). Here, the coals have partly been assimilated by the intrusion, and have transform the magma to light-grey graphite-like breccia. We interpret these hybrid rocks to have formed during the interaction of lava and organic-rich sediments during the initial emplacement of magma onto, or into, the end-Permian organic-rich sedimentary sequences. Such eruptions may have

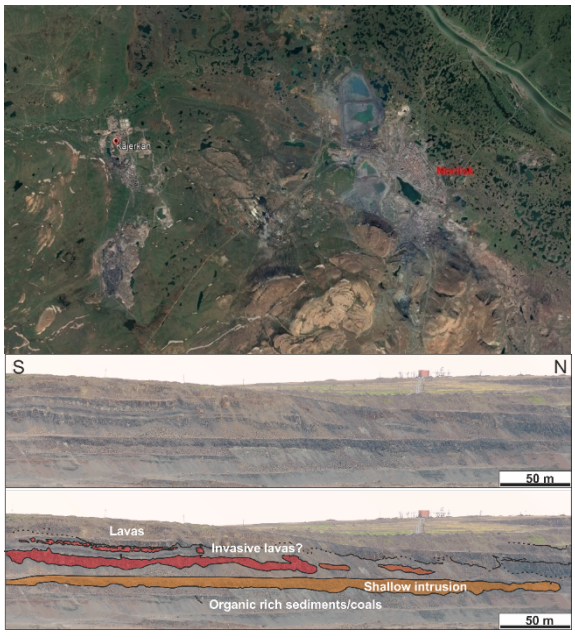

Fig. 1 – Location map showing the Kajerkan village and open pit quarry located about 15 km west of Norilsk, Siberia. The coal and sandstone quarry is located in the Late Carboniferous to Permian sediments of the Tunguska Group rocks just below the Siberian Traps lava flows. The western cliff of the quarry displays a sequence of basaltic rocks interlayered with sedimentary coal and sandstone beds. The igneous units are interpreted as a combination of lavas, invasive lava flows, and shallow sheet intrusions.

Fig. 2 – Field picture showing an interpreted invasive flow (dark brown) within coal-rich sediments (black) in a Kajerkan quarry wall. Note the strongly fractured igneous rocks with fine-grained quickly cooled horizontal and near-vertical contacts.

Fig. 3 – Field picture from the Kajerkan quarry showing a meter-wide igneous apophysis (dark brown) vertically extending into overlying coal-rich sediments (black), documenting the invasive character of the igneous unit.

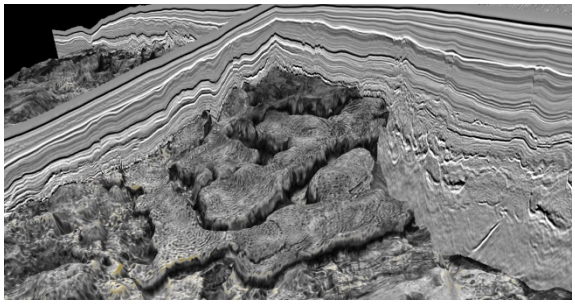

Fig. 4 – Interpreted invasive flow field in the northern Møre Basin offshore mid-Norway. The invasive lava flows display well-defined compression ridges stratigraphically located some 10's of meters below the Top Paleocene horizon. 3D seismic image of the top of the igneous rocks with RMS amplitudes (gray scale). The flows are approximately 1-3 km wide. Seismic data courtesy of TGS.

triggered massive degassing of sedimentary carbon during the end-Permian times.

Extensive new 3D seismic reflection data have recently been collected along the outer Møre Basin offshore Norway. We have interpreted Paleogene igneous sequences on these data using the methods of seismic volcanostratigraphy and igneous seismic geomorphology. Spectacular lobate igneous units are displayed in the Inner Flows region in the Modgunn Arch region in the northern Møre Basin (Fig. 4). Stratigraphically, these flows are located some 10's of meters below the Top Paleocene horizon. We interpret these units as a combination of invasive flows, where they can be imaged to have been fed from shallower horizons and as shallow intrusions where imaging reveals shallow transgression from depth at the foot of the palaeo-escarpment.

The consequences of magma emplacement into shallow soft sediment environments are important for understanding the temporal evolution of volcanism within sedimentary basins and for linking volcanism and climatic influences such as sill-induced thermogenic gas generation and outgassing. We interpret the Inner Flows as a combined invasive and intrusive complex. Our observations from offshore mid-Norway and onshore Siberia suggest that the process of shallow lava invasion may be more widespread than is generally accepted and that careful interpretation of seismic and field data may enable improved criteria for identification and mapping of these features.

Acknowledgements

We kindly thanks NorNickel for access to the Kajerkan quarry and TGS for access to seismic data.

References

Edwards BR, Belousov A., Belousova M, 2014. Propagation style controls lava-snow interactions. *Nature communication, 5, 5666.*

Millett JM, Jerram DA., Planke, S, Hole, MJ, and Famelli, N, 2019. Top down or bottom up: identification and implications of invasive lavas versus shallow intrusions in sedimentary basins. *Extended abstract, LASI6 conference, Malargüe, Argentina, 25-25.11.19.*

Paderin PG, Demenyuk AF, Nazarov DV, Chekanov VI, et al., 2016. State geological map of the Russian Federation. Scale 1: 1,000,000 (third generation). Series Norilsk. Sheet R-45 - Norilsk. Explanatory note. *St. Petersburg: VSEGEI Kartfabrika. 366 pp.*

Polozov AG, Svensen HH, Planke S, Grishina SN, Fristad KE, Jerram DA, 2016. The basalt pipes of the Tunguska Basin (Siberia, Russia): High temperature processes and volatile degassing into the end-Permian atmosphere. *PPP 441:51-64. j.palaeo.2015.06.035*

Jerram D.A., Svensen H.H., Planke S., Polozov A.G., Torsvik T.H., 2016. The onset of flood volcanism in the north-western part of the Siberian Traps: Explosive volcanism versus effusive lava flows. *PPP. 441:38-50. http://dx.doi.org/10.1016/j.palaeo.2015.04.022*

Svensen H.H., Frolov S., Akhmanov G.G., Polozov A.G., Jerram D.A., Shiganova O.V., Melnikov N.V., Iyer K., Planke S., 2018. Sills and gas generation in the Siberian Traps. *Phil. Trans. R. Soc. A 376: 20170080. http://dx.doi.org/10.1098/rsta.2017.0080*

Insights into the magmatic processes of shallow, silicic storage zone: Reyðarártindur Pluton, Iceland

Rhodes E.[1,2], Burchardt S.[1,2], Barker A.K.[1,2], Mattsson T.[1], Ronchin E.[1,2,3], Schmiedel T.[1,2] and Witcher T.[1,2]

[1] *Department of Earth Sciences, Uppsala University, Sweden* – emma.rhodes@geo.uu.se
[2] *Centre for Natural Hazards and Disaster Science, Sweden, www.cnds.se*
[3] *Department of Earth Sciences, Sapienza – University of Rome, Italy*

Keywords: Pluton, Iceland, felsic magma emplacement

Reyðarártindur is one of several felsic plutons exposed in Southeast Iceland, interpreted to be the shallow plumbing systems of late Neogene volcanic centres (Cargill et al., 1928; Furman et al., 1992; Padilla, 2015). These plutons are considered to preserve analogous plumbing systems to the central volcanoes active in Iceland today (Furman et al., 1992). Reyðarártindur is the oldest pluton in Southeast Iceland at 7.30 ± 0.06 Ma (Padilla, 2015), and has been conveniently incised by the Reyðará River, making it ideal for an in-depth study of the external and internal geometry of a shallow rift-zone magma plumbing system.

In order to analyse mechanisms of magma emplacement, we have conducted detailed structural mapping of the pluton and its basaltic host rock using drone-based photogrammetry. To complement this, we have also extensively sampled and analysed the geochemistry and petrology of the pluton interior. An outline of the pluton is shown in Figure 1, highlighting that the pluton is NNW-SSE trending, which is in contrast to the NE-SW regional dyke trend. A total thickness of 500 m and a calculated volume of 1.5 km^3 is exposed. While the pluton walls are steeply-dipping, the pluton roof is mostly flat. Deviations from the flat roof occur in the form of areas that are cut by steep dip-slip faults with displacements of up to 100 m. Roof faulting creates both structural highs (horsts) and lows (grabens, as well as a monoclinal structure) in the roof. Many of the faults are intruded by felsic dykes, some of them seem to have been the feeders of surface eruptions.

An estimated 95% of the pluton volume is rhyolitic in composition, with 73-76 wt.% SiO_2. Geochemically, the magma in the majority of the pluton is similar, but hand samples and thin sections show a large variety of textures. In the lower part of the exposure there is a zone of mingling and mixing between a matrix magma and several different types of silicic enclaves (Figure 1). The matrix magma is more mafic with an SiO_2 content of 68-73 wt.% and the enclaves vary in nature with no systematic shape, size or aspect ratio. There are at least two types of enclaves, and the predominant type is a coarse grained trachydacite with 64-69 wt.% SiO_2. These less evolved compositions are limited to a 1 km stretch of the riverbed in the centre of the pluton. Closer to the wall contacts (i.e. to the north and south of the mingling zone), the composition of the magma returns to that of the main magma body, as observed at higher elevations.

Our poster aims to summarise our results and present interpretations of the magmatic processes preserved in the Reyðarártindur pluton. Our preliminary results indicate that the pluton was emplaced by a combination of floor subsidence and roof doming, and that the pluton structure was modified during further magma intrusion into, and eruption from, the pluton.

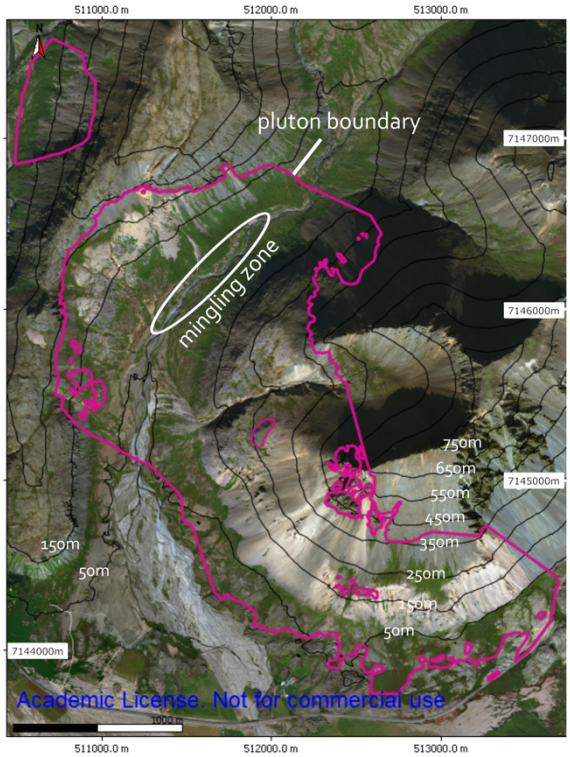

Fig. 1 – Map of the Reyðarártindur Pluton, South-East Iceland.

References

Cargill, H., Hawkes, L., and Ledeboen, J. (1928). The major intrustions of South-Eastern Iceland. Quarterly *Journal of the Geological Society of London 84*, 505–539.

Furman, T., Meyer, P. S., and Frey, F. (1992). Evolution of Icelandic central volcanoes: evidence from the Austurhorn intrusion, southeastern Iceland. *Bulletin of Volcanology. 55*, 45–62.

Padilla, A. (2015). Elemental and isotopic geochemistry of crystal-melt systems: Elucidating the construction and evolution of silicic magmas in the shallow crust, using examples from southeast Iceland and southwest USA [*PhD Dissertation: Vanderbilt University*].

Subsurface geometry and emplacement conditions of a giant dike system in the Elysium Volcanic Province, Mars

Rivas Dorado S.[1], Ruíz J.[2] and Romeo I.[3]

[1] *Departamento de Geodinámica, Estratigrafía, y Paleontología, Universidad Complutense de Madrid, Madrid, Spain* – samuelrivas@ucm.es

Keywords: Mars, dikes, aspect ratios

Dike emplacement at depth is a common mechanism used to explain some of the radial and concentric graben systems observed in the volcanic provinces of Mars (e.g., McKenzie and Nimmo, 1999; Plescia, 2003). Evidence for dike intrusion as the generating process includes the results of magma-ice interactions; i.e., massive water flows (Plescia, 2003), or a distinct dike-induced topography as observed in terrestrial dike intrusion episodes (Rubin and Pollard, 1988). We suggest that the surface geometry of grabens may be used as an additional tool to test if dike emplacement is the mechanism behind the formation of these grabens, and to make inferences about the host-rock and fluid pressures during emplacement.

The area of interest is located in the eastern flank of Elysium Mons and consists of a set 360 km-long NW-SE graben systems linked via en-echelon segments (Fig. 1). We mapped 29 individual structures and measured their maximum continuous lengths (*L,* between 1.9-156 km) and widths (*W*, between 0.13-3 km).

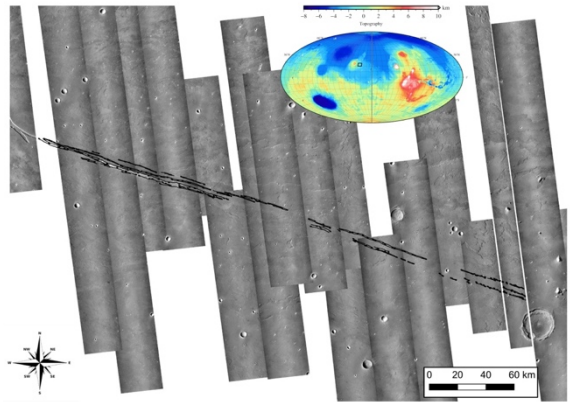

Fig. 1 – Location and general view of the studied graben system. A global topographic map of Mars is shown in the upper part of the image. A black square indicates the exact location of the graben complex.

We have used data from the MOLA instrument to construct 23 profiles orthogonal to the structures, in which area-balance calculations have been done for each observed graben. Fault dips of 60º and a sub-horizontal regional level have been assumed in each case. The position of fault escarpments has been defined through CTX images (30m/px res.). We calculated the boundary displacement and lost area below regional for each graben. Extension in the graben is assumed to be caused only by an intruding dike, and thus the boundary displacement is taken as a proxy for average dike width (D_w). Lost area below regional and boundary displacement were used to calculate the detachment depth, which is assumed to correspond to the top-dike depth (D_d).

However, not all the structures mapped in CTX images can be identified by MOLA, mainly because their widths lay below the instrument's resolution (average spacing between MOLA datapoints is 300 m). Consequently, dike widths cannot be calculated directly for all structures through area-balance, as described above. Instead, we have used the G_w-D_w relationships obtained from the area-balance exercise to extrapolate all the initial mapped graben widths (W) to dike widths (D_w). The dike widths obtained are between 9-356 m, which are consistent with previous estimates of the maximum widths for Martian dikes (Wilson and Parfitt, 1990) The calculated parameters were then used to make inferences about the properties of the host rock and of magmatic overpressures during emplacement.

The aspect ratio (*Width/Length*) and *Length* of a set of fluid-filled fractures are related via a power-law function in which the n exponent is near -0.5 (Olson, 2003). The W/L vs L relationship in the grabens mapped was consistent with this theory, and after transforming W to D_w., this relationship holds true. Graben lengths are assumed as dike lengths. Figure 2 shows the values obtained in this study, and a set of measurements for two studies in terrestrial dikes, all of which are consistent with the theory discussed previously.

The critical stress intensity factor (Kic), or simply the fracture toughness (Gudmundsson, 2009), of the host rock can be derived from the pre-exponential factor in the power functions mentioned above (Olson, 2003). Young Modulus values of 15-75 GPa,

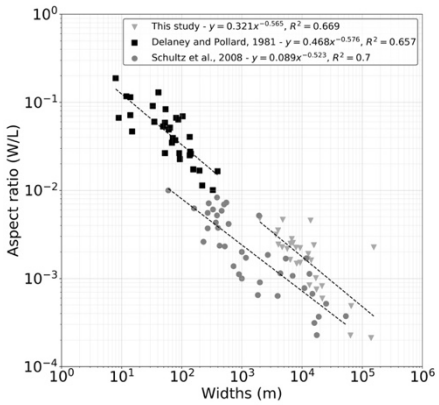

Fig. 2 – Aspect ratios vs lengths, and best-fit lines, for the inferred dikes in this study and two sets of terrestrial dikes. In both cases the exponential factor is close to -0.5.

which cover the range from altered to intact basalts, and Poisson Ratios of 0.2-0.3, were assumed. The stress factors obtained are between 3.1-15.5 GPa $m^{1/2}$. These values are similar albeit higher than those obtained by Schultz et al. (2008) in a set of basalt-hosted Ethiopian dikes, which were between 0.07-3.8 GPa m1/2. Finally, the excess pressure ΔPe (the difference between the fluid pressure and the lithostatic stress) under which fracturing occurred can be derived from K_i and the fracture's half-length a ($a = L/2$) via:

(1) $$\Delta P_e = \frac{K_i}{\sqrt{\pi a}}$$

The excess pressures ΔP_e obtained range between 6-276 MPa (Fig. 3). These values are within the same order of magnitude as modeled excess pressures in magmatic chambers in Tharsis calculated by Scott et al. (2002), which lay between 35-60 MPa. For comparison, stress factors and excess pressures were calculated also for all the terrestrial examples.

Dike widths estimated for the studied grabens yield aspect ratios consistent with fluid-filled cracks. On average, their widths are higher than terrestrial structures with the same lengths intruded in similar rocks. Oppositely, their calculated pressures are not very different from terrestrial overpressures in analogue host rocks (Fig. 3). This indicates that despite their larger size, the Martian dikes did not require significantly greater overpressures. This is likely caused by the shorter gravity on Mars (Wilson and Parffit, 1990), which imposes a much smaller lithostatic stress for the intrusions to overcome.

In conclusion, the Ki and ΔPe obtained are consistent with those from other authors calculated and Mars. Therefore, the method proposed here may be used to identify if dike emplacement is the process behind graben formation in other areas of Mars. It can also be used to make inferences about the properties of the brittle crust and driving magma pressures.

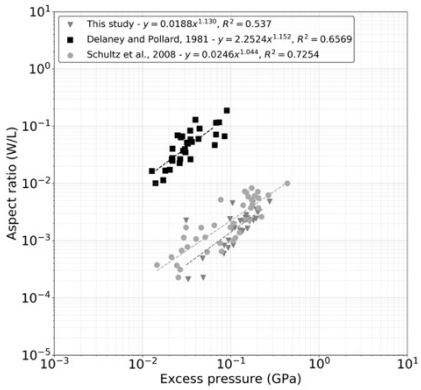

Fig. 3 – Maximum excess pressures for the Elysium dikes and the two terrestrial dike sets shown previously. Note that the calculated pressures for the Martian dikes are very similar to those of the basalt-intruded dikes in Ethiopia from Schultz et al., (2008).

Acknowledgements

This research has been supported by the projects AMARTE II (PR75/18-21613), funded by the research program Santander-UCM, and TECTOMARS (PGC2018-095340-B-100), funded by the Spanish Ministry of Science, Innovation and Universities.

References

Delaney, P.T., Pollard, D.D., 1981. Deformation of Host Rocks and Flow of Magma during Growth of Minette Dikes and Breccia-bearing Intrusions near Ship Rock, New Mexico, USGS Profesional Paper 1202.

Gudmundsson, A., (2011) Rock Fractures in Geological Processes. Cambridge University Press, Cambridge.

McKenzie, D., Nimmo, F. (1999), The generation of Martian floods by melting of ground ice above dykes, Nature, Vol. 397, pp. 231-233.

Olson, J.E. (2003), Sublinear scaling of fracture aperture versus length: An exception or the rule?, Journal of Geophysical Research, 108(10).

Plescia, J.B., (2003), Cerberus Fossae, Elysium, Mars: A source for lava and water. Icarus 164, 79–95.

Rubin, A.M., Pollard, D.D. (1988), Dike-induced faulting in Iceland and Afar, Geology 16, 413-417.

Schultz, R.A., Mège, D., Diot, H., 2008. Emplacement conditions of igneous dikes in Ethiopian Traps. J. Volcanol. Geotherm. Res. 178, 683–692. https://doi.org/10.1016/j.jvolgeores.2008.08.012

Scott, E.D., Wilson, L., Head, J.W.H. (2002), Emplacement of giant radial dikes in the northern Tharsis region of Mars, Journal of Geophysical Research, Vol. 107(E4).

Wilson, L.W., Parffit, E. A. (1990), Widths of dikes on Earth and Mars, Lunar and Planetary Institute.

Unroofing of Messinian shallow intrusions in Tuscany: mechanisms and timescales

Rocchi S.[1], Paoli G.[1], Vezzoni S.[1,2], Westerman D.S.[3] and Dini A.[2]

[1] *Dipartimento di Scienze della Terra, Università di Pisa, Pisa, Italy* – sergio.rocchi@unipi.it
[2] *Istituto di Geoscienze e Georisorse-CNR, Pisa, Italy*
[3] *Department of Earth and Environmental Science, Norwich University, Northfield, VT, USA*

Keywords: shallow pluton, magmatectonics, exhumation.

Exhumation of igneous intrusions usually takes several tens of Ma. However, in Tuscany, Messinian and early Pliocene intrusions have been exposed at the surface soon after their emplacement. The main four shallow-level plutons cropping out in Tuscany are Monte Capanne (7.0 Ma, Elba Island), Montecristo (7.0 Ma, Montecristo Island), Botro ai Marmi (5.4 Ma, Campiglia Marittima, mainland Tuscany) and Giglio (5.0 Ma, Giglio Island). Studying emplacement-unroofing histories is hampered at both Montecristo and Giglio plutons owing to poor country rock occurrences. On the other hand, Monte Capanne and Botro ai Marmi plutons have superb exposures of contacts against country rocks so that their emplacement-unroofing histories can be investigated in detail. Both plutons were quickly unroofed after their emplacement, yet by extremely different mechanism: brittle translation of the cover for Monte Capanne, ductile lateral extrusion of the overburden for Botro ai Marmi.

In western Elba Island, less than 1 Ma, a 2.7 km thick tectonostratigraphic section was inflated by the addition of a total of 2.4 km of intrusive laccolith layers (Rocchi et al., 2002) in a roughly circular region with a diameter of approximately 10 km. This intrusive complex thus built a domal structure with a slope of about 25° (Westerman et al., 2004). As pulses of Monte Capanne magma approached the base of the intrusive complex to add ~2.5 km more igneous rock (~110 km^3) underneath the laccolith intrusions (Rocchi et al., 2010), the slopes grew oversteepened. The system held in place throughout emplacement of the Monte Capanne pluton and long enough for a late-plutonic mafic dyke swarm to be injected throughout the whole vertical section (Dini et al., 2008). Ultimately, a tectonic discontinuity in the original tectonostratigraphic section failed triggering a catastrophic eastward tectonic-gravitational décollement that transported the top "half" of the intrusive complex about 8 km to the east on the Central Elba Fault (Fig. 1), over a <1.5 Ma period, with a rate of displacement in excess of 5–6 mm/a (Westerman et al., 2004).

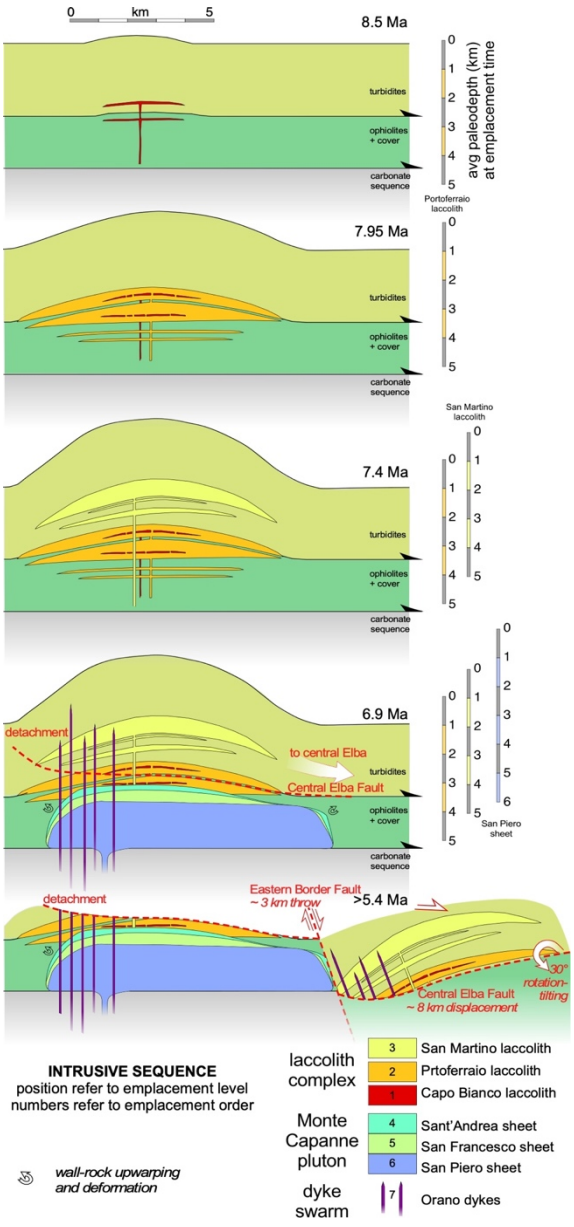

Fig. 1 – Rise and fall of the western Elba laccolith-pluton-dyke complex: a schematic summary, modified after Westerman et al. (2015).

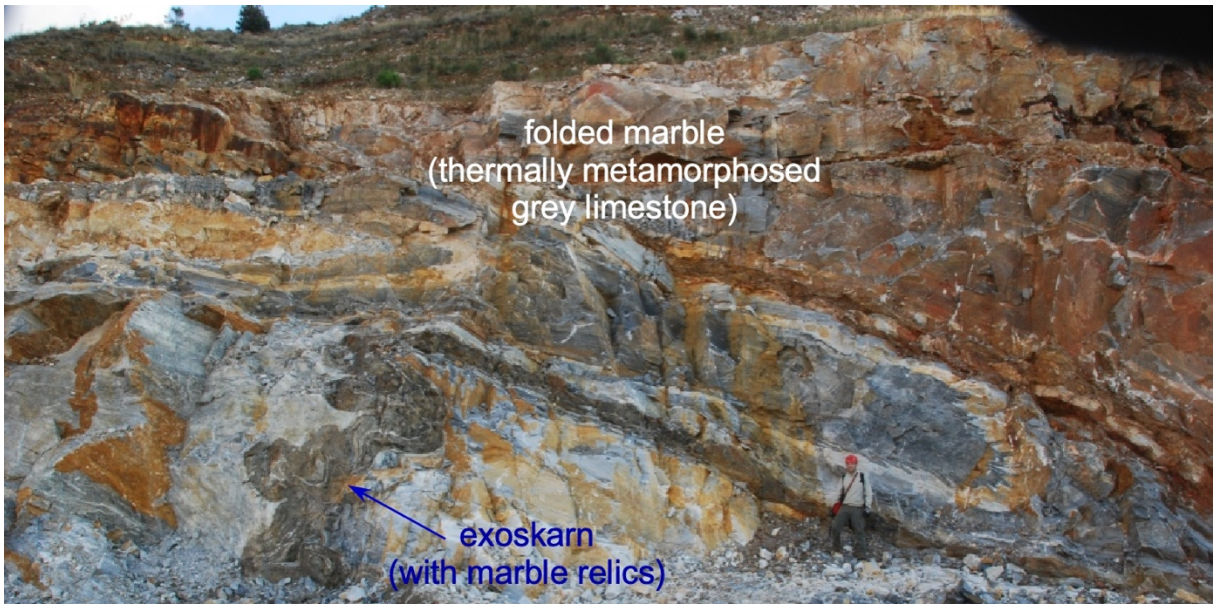

Fig. 2 – Ductile deformational structures at the contact of Botro ai Marmi pluton in the Campiglia Marittima area.

In the Campiglia Marittima area, detailed field mapping led to the reconstruction of local magmatic -deformation histories that overlap, chronologically and spatially, with regional extension (Vezzoni et al, 2017). A local deformation was triggered at the Miocene–Pliocene boundary by the intrusion of a monzogranitic pluton (~35 km^3) underneath a carbonate sedimentary sequence. The emplacement of the pluton produced a perturbation in the rheological behaviour of the carbonate host rocks, producing transient ductile conditions in the very shallow crust. The carbonate rocks were transformed to marble and thermally weakened to the point that they flowed laterally (Fig. 2), accumulating downslope of the pluton roof, mainly towards the east. As the thermal anomaly was decaying, the brittle–ductile boundary moved progressively back towards the pluton, and large tension gash-shaped volumes of fractured marble were generated, that were exploited by rising hydrothermal fluids to generate skarn bodies and ore shoots. Detailed geochronological investigations constrain to <180 ka the time span to achieve the lateral mass transfer.

In summary, Monte Capanne and Botro ai Marmi represent two prominent examples of quick unroofing of a shallow pluton. The first tells of a brittle history, governed mainly by gravitational instability, and has been reconstructed mainly by forensic-style evidence both for unroofing and timescales. The second is a ductile history, driven by heat and gravity, and is readable in spectacular structure exposures and precise isotopic dating of the unroofing timescale. Both examples show how magma-tectonics can generate large failure in the upper crust, triggering either hazardous mass movements or hydrothermal ore deposition.

Acknowledgements

This work has been carried out as part of the Ph.D projecte of SV and GP at the University of Pisa, with the support of the Project PRA_2016_33, P.I. SR.

References

Dini, A., Westerman, D.S., Innnocenti, F. and Rocchi, S., 2008. Magma emplacement in a transfer zone: the Miocene mafic Orano dyke swarm of Elba Island (Tuscany), in *Structure and Emplacement of High-Level Magmatic Systems,* edited by K. Thomson and N. Petford, Geol. Soc. London Sp. Publ. 302, pp. 131-148.

Rocchi, S., D.S. Westerman, A. Dini and F. Farina (2010), Intrusive sheets and sheeted intrusions at Elba Island (Italy), *Geosphere, 6*(3): 225-236.

Rocchi, S., D.S. Westerman, A. Dini, F. Innocenti and S. Tonarini (2002), Two-stage laccolith growth at Elba Island (Italy), *Geology*, *30*(11), 983-986.

Vezzoni, S., S. Rocchi and A. Dini (2018), Lateral extrusion of a thermally weakened pluton overburden (Campiglia Marittima, Tuscany). *International Journal of Earth Sciences, 107*, 1343-1355.

Westerman, D.S., A. Dini, F. Innocenti and S. Rocchi (2004), Rise and fall of a nested Christmas-tree laccolith complex, Elba Island, Italy, in *Physical Geology of High-Level Magmatic Systems,* edited by C. Breitkreuz and N. Petford, Geol. Soc. London Sp. Publ. 234, pp. 195-213.

Westerman, D.S., S. Rocchi, A. Dini, F. Farina and E. Roni (2015), Rise and Fall of a Multi-sheet Intrusive Complex, Elba Island, Italy, in *Physical Geology of Shallow Magmatic Systems - Dykes, Sills and Laccoliths,* edited by C. Breitkreutz and S. Rocchi, Springer, pp. 309-325.

Field observations and numerical models of a Pleistocene-Holocene feeder dike swarm associated with a fissure complex to the east of the San Pedro-Pellado complex, Southern Volcanic Zone, Chile

Javiera Ruz[1,2], John Browning[1,2,3], José Cembrano[1,2], and Pablo Iturrieta[1]

[1] *Departamento de Ingeniería Estructural y Geotécnica, Escuela de Ingeniería, Pontificia Universidad Católica de Chile, Santiago, Chile* – jnruz@uc.cl
[2] *Centro de Excelencia en Geotermia de los Andes (CEGA, FONDAP-CONICYT), Departamento de Geología, Universidad de Chile, Santiago, Chile.*
[3] *Departamento de Ingeniería Minería, Escuela de Ingeniería, Pontificia Universidad Católica de Chile, Santiago, Chile.*

Keywords: feeder dike swarm, Southern Volcanic Zone, regional tectonics.

Volcanic eruptions are usually fed by dikes which transport magma from a deeper crustal source to the surface. These sheet like intrusions are fractures that commonly form perpendicular to the least compressive stress (σ_3). It follows, that for vertical dikes to form, σ_3 must be horizontal (e.g. Gudmundsson, 2006). Thus, regional stress at convergent margins is apparently not favorable for the formation of vertical dikes. Nonetheless, deformation partitioning in oblique convergent margins, such as the Southern Volcanic Zone of Chile, allows for local transtension in the arc region, where σ_3 is commonly sub horizontal. In this setting, regional scale strike-slip faults (ie. Liquiñe – Ofqui fault zone) control the distribution and geometry of volcanoes and eruptive centers (e.g. Sielfeld et al., 2017). Therefore, understanding the mechanics of dikes and eruptive centers, along with their spatial distribution, would provide fundamental insights on the interplay between magma transport, crustal deformation and tectonic setting.

Here we present field observations of a dike swarm to the east of the San Pedro – Pellado complex, in the Southern Volcanic Zone of Chile. A systematic measurement of dike orientation (strike and dip), thickness and length was carried out. Where it was not possible to collect field data, dike strike, thickness and length were measured from satellite images (0.52 m resolution). These data were later used as input for mechanical FEM models and compared to previous fault and fracture measurements from the regional scale.

Detailed structural mapping in the *La Plata dike swarm* shows two populations of dikes, which were classified according to texture, attitude and thickness. The total length of the dike swarm was ~1100 m, but we also measured individual segments of the dikes which ranged in length between 4.30 to 55.15 m. The first (and oldest) population of dikes have a vesicular and porphyric hypo crystalline texture, with plagioclase crystals in an aphanitic magnetic black mass. These dikes range in thickness from 1.30 m to 5.60 m (mean thickness of 2.50 m) and strike dominantly NE (N20ºE – N75ºE). We interpret these initial dike injections to have fed a cinder cone, approximately 325 m in diameter, which is evident as a series of elevated lavas.

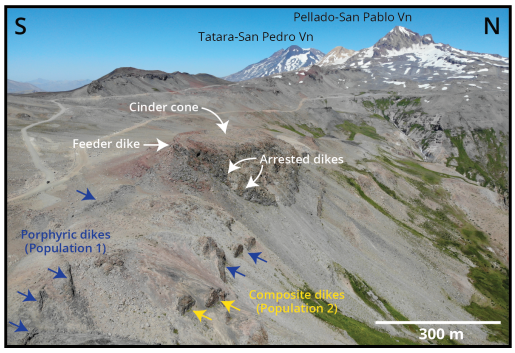

Fig. 1 – Aerial view of *La Plata feeder dike swarm* and the cinder cone. In the background, volcanoes Tatara-San Pedro and Pellado-San Pablo. Dikes indicated with a blue arrow correspond to the first (and oldest) population, while those indicated with a yellow arrow belong to the second (and youngest population) in the swarm.

The second (and youngest) population of dikes are composite, and tend to be thicker and lighter in color. The center has porphyric hypo-crystalline texture, with plagioclase and quartz. The margin (~ 0.5 m) has a phaneritic hypo-crystalline texture. These dikes have a slightly different orientation and strike dominantly ENE (N39ºE – N83ºE) and range in thickness between 3.05 m to 7.15 m (mean thickness of 4.70 m). The dike swarm intersects a scoria cone and we observe at least one feeder dike and two arrested dikes within the eastern segment of the cone. We also observe *flow like* and vesicular textures in the dikes, which we interpret as a transition from dikes to superficial lava flows, thus indicating that the dike swarm was most likely emplaced at very shallow depths. Moreover, cross-cutting relations indicate

that the composite dikes, correspond to a second diking event, but with a slightly different orientation.

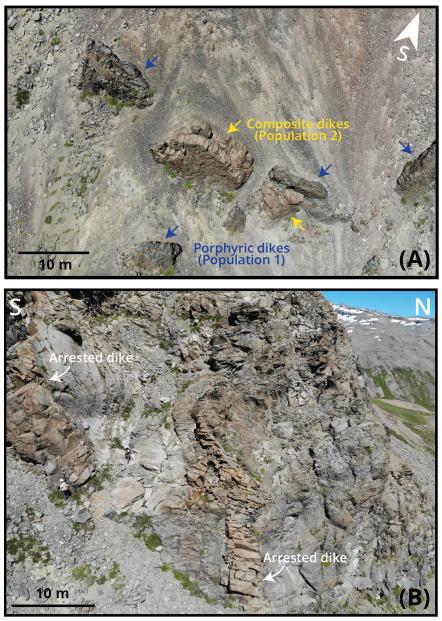

Fig. 2 – (A) Aerial plan view of two cross cutting dikes. Composite dike strikes ~N87ºE. It cuts a porphyric dike whose segments' strike N57ºE and N68ºE. Both population of dikes have a clastic edge that incorporates fragments of the host rock. (B) Section view of the eastern edge of the cinder cone, where two arrested dikes that strike N80ºE are observed.

To test the dike swarm's change in direction, we built a suite of 2D FEM mechanical models to solve the stress state within a simplified geometry representing the TSPP magmatic chamber. This is constrained by magnetotelluric and seismicity data around the TSPP, that show a high conductivity region in the upper crust and below the active volcanic complex (Reyes-Wagner et al., 2017), relating to a domain of partial melt. In our model, this is represented as a circular cavity embedded in an elastic medium, where normal-to-the-boundary traction is applied to simulate the internal magmatic pressure. Dikes were also modelled as elliptical cavities with an applied internal pressure. We performed sensitivity tests to determine the effect of a regional stress (regional compression and extension), internal pressure in the cavities and the material's elastic parameters on the output. We found that stress concentrators, such as those represented in our models, can shift the stress regime of the system. This shift in the orientation of the principal stresses (ie. from a vertical to a horizontal minimum stress) allows for the formation of vertical dikes. Future work in this model will aim to simulate the effect of an oblique convergence (ie. regional transpression).

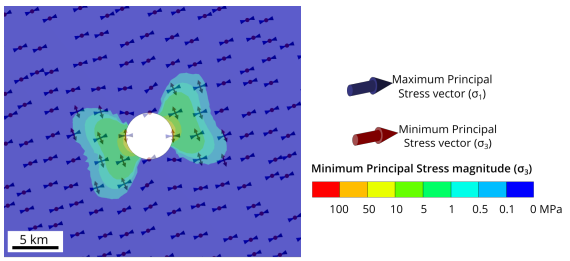

Fig. 3 – Example of a 2D FEM numerical model simulating an elastic medium (E=10 GPa) with a circular cavity (radius 2.5 km) with an applied internal pressure of 10 MPa. Compressive pressure of 10 MPa was also applied on the outside edges of the material. Principal stress rotation occurs close to the circular cavity.

Dike propagation orientation can be further enhanced by crustal discontinuities. This segment of the SVZ is characterized NE and NW dextral and sinistral faults, respectively, that are kinematically consistent with the prevailing Quaternary orogen-scale shortening. Moreover, to the west of the TSPP, the NS trending Melado Valley fault, is kinematically consistent with a 2012 6.0Mw earthquake with dextral displacement. Understanding the interplay between transverse, arc parallel faults and dike systems is therefore also relevant to assess in future work. Our results are important for understanding the emplacement of dikes associated with central volcanoes in the SVZ and can be applied to observations of dike emplacement elsewhere.

Acknowledgements

We are grateful to FONDAP-CONICYT project 15090013 (CEGA) and FONDECYT project 1141139.

References

Gudmundsson (2011). Deflection of dikes into sills at discontinuities and magma-chamber formation. Tectonophysics, 500, 50-64. 10.1016/jtecto.2009.10.015.

Reyes-Wagner et al (2017). Regional electrical structure of the Andean subduction zone in central Chile (35º – 36ºS) using magnetotellurics. Earth, Planets and Space. 69:142. 10.1186/s40623-017-0726-z.

Sielfeld et al (2017). Transtension driving volcano-edifice anatomy: Insights from Andean transverse-to-the-orogen tectonic domains. Quaternary International, 438, 33–49. 10.1016/j.quaint.2016.01.002.

Magma transport in the shallow crust – the dykes of the Chachahuén volcanic complex (Argentina)

Schmiedel T.[1,2], Burchardt S.[1,2], Guldstrand F.[3], Galland O.[3], Mattsson T.[1], Palma J. O.[4], Rhodes E.[1,2], Witcher T.[1,2], Almqvist B.[5]

[1] *MPT, Department of Earth Sciences, Uppsala University, Sweden* – tobias.schmiedel@geo.uu.se
[2] *Centre for Natural Hazards and Disaster Science, Sweden, www.cnds.se*
[3] *PGP-NJORD Centre, Department of Geosciences, University of Oslo, Norway*
[4] *Y-TEC – CONICET Av. Del Petroleo, Argentina*
[5] *Geophysics, Department of Earth Sciences, Uppsala University, Sweden*

Keywords: magma flow, dyke emplacement, magma rheology.

The recent eruptions of Kilauea on Hawaii 2018 and Bárðarbunga-Holuhraun on Iceland 2014/15 illustrated the abundance of magma transport in the shallow crust. In both examples, several kilometers of lateral magma transport were observed to take place in the form of a vertical sheet intrusion (dyke). Even though these two eruptions are prime examples of state-of-the-art volcano monitoring, observations of the scale and dynamics of subvolcanic features feeding eruptions are limited in active volcanic systems. Thus, very little is known about the lateral and vertical transport of magma and the physical mechanisms behind the propagation of dykes. Therefore, the investigation of ancient, eroded volcanic systems can increase our understanding of the physical mechanisms leading to magma transport in magmatic plumbing systems.

The field area for this ongoing study is the ancient Chachahuén volcanic complex located in the northern part of the Neuquén Basin, east of the southern volcanic zone (SVZ) of the Andes. The Chachahuén volcanic complex was dated to be of Miocene age (7.3-4.9 Ma, Kay et al., 2006, Peréz and Condat, 1996). Chachahuén began its activity with the extensive eruption of Matancilla basalts followed by several phases of effusive basaltic to explosive rhyolitic activity (Kay et al., 2006). A caldera collapse and the eruption of massive block and ash flows comprised the late stage activity (Kay et al., 2006). Erosion and quietened volcanic activity during the Quaternary, exposed the shallow part of the volcano's plumbing system, including two major vertical sheet intrusions: (1) the Great dyke (Figure 1) and (2) the Sosa dyke, which were formerly underlying the Chachahuén volcanic edifice (Burchardt et al., 2019).

The main objective of this ongoing study is to characterize the mechanisms of (lateral) magma transport within dykes to better understand the physical processes in otherwise inaccessible active volcanic systems. To achieve this objective, we investigate the effect of magma rheology (small-scale) on the outer shape and morphology of the dykes (large-scale). We apply a multiscale approach combining state-of-the-art techniques, i.e., drone/ ground-based photogrammetry, Fourier Transform Infrared Spectroscopy (FTIR), Electron Backscatter Diffraction (EBSD) and Anisotropy of magnetic susceptibility (AMS), with traditional geological methods, i.e., microstructural analysis and igneous petrology.

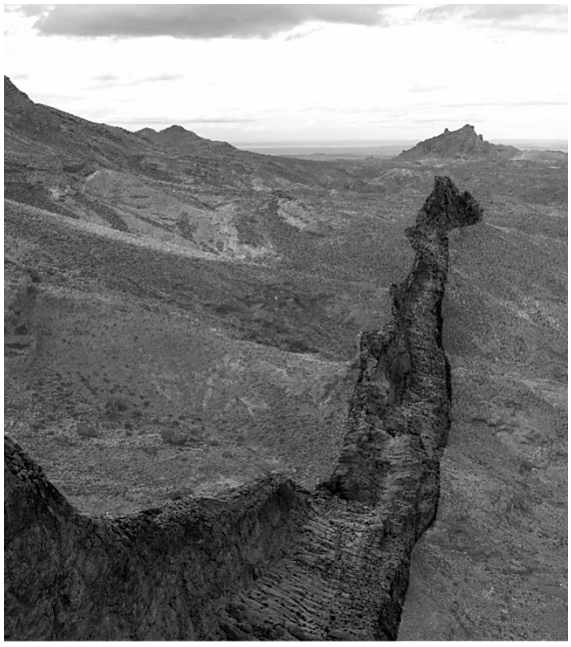

Fig. 1 – "The Great Dyke": A world-class outcrop of a subvolcanic sheet intrusion with the internal structure and outer morphology exposed in 3D (Thickness of the dyke c.15-25 m, exposed length 1.8 km).

Our first results using high-resolution 3D outcrop models, constructed from the collected photogrammetry data show a segmentation of the investigated dykes. Each of these dyke segments shows blunt ends (Figure 2). Two possible explanations can be used to explain these blunt ends: (1) highly viscous magma (Rocchi & Breitkreuz, 2018) or (2) a weak brittle host rock (e.g. Spacapan et al., 2017). To identify the dominantly controlling

mechanism(s), mapping of the host rocks and an examination of the internal structure of the dykes

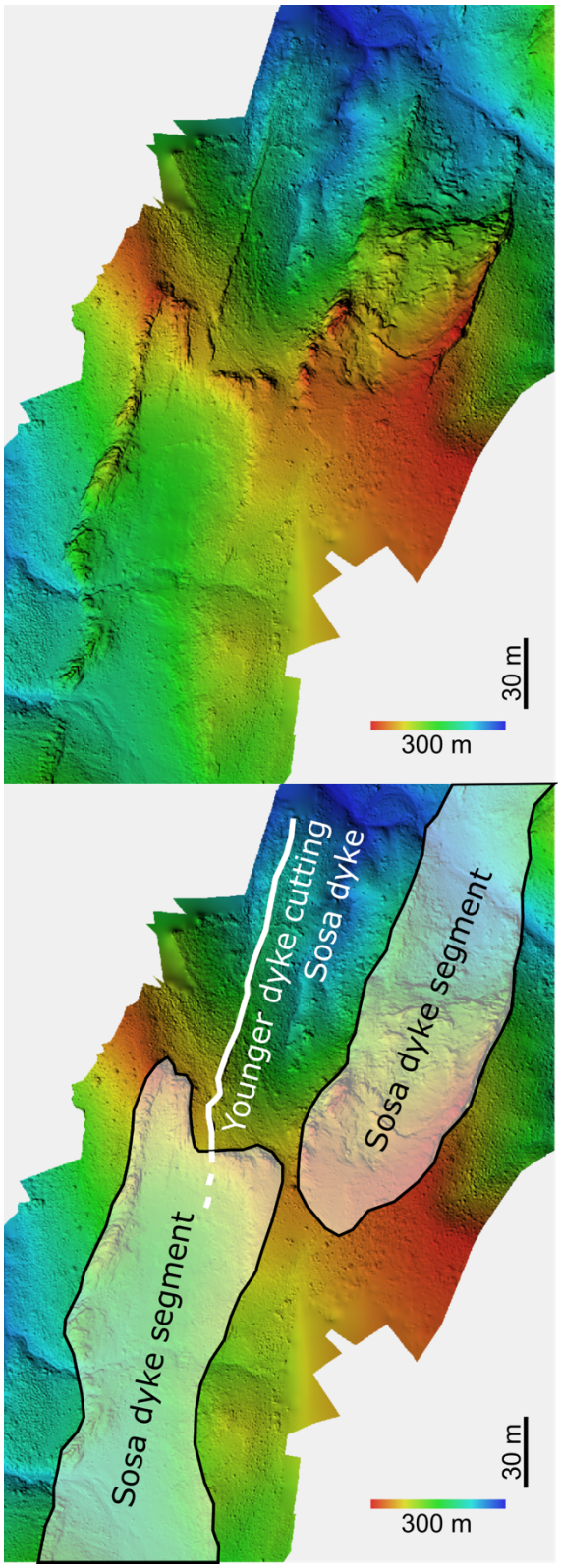

Fig. 2 – Digital Elevation Model (DEM) of the Sosa dyke: (top) uninterpreted raw data, (bottom) interpreted results, (Thickness of the dyke 20-50 m, exposed length 1.4 km)

are necessary. During field mapping, we observed that the dykes intruded into vastly different host rocks, ranging from welded block-and-ash flows to sandstone, to lavas. We therefore exclude the host rock as the primary control on dyke morphology.

At the moment thin sections for petrographic microstructural analysis and EBSD are being prepared, as well as cores for AMS analysis. The combined analysis of flow features (e.g., crystal alignment, crystal deformation) using these methods will allow for a characterization of the magma transport within the dykes. Moreover, the combination with FTIR, to determine the water content of the initial melt, will help to estimate the magma viscosity of the dykes during their emplacement.

Our poster aims to summarize the progress of investigation on the dykes of the Chachahuén volcanic complex. The new findings from this project will contribute to the general understanding on how the physical properties of the magma affect the shape of magma bodies and magma flow in the Earth's shallow crust.

Acknowledgements

This project is funded by the Knut and Alice Wallenberg Foundation through a Wallenberg Academy Fellow grant to SB. Thanks to The Royal Swedish Academy of Science (www.kva.se) for funding the participation of TS at the LASI6 conference.

References

Burchardt, S., T. Mattsson, J. O. Palma, O. Galland, B.Almquist, K. Mair, D. A. Jerram, Ø. Hammer and Y. Sun (2019), Progressive growth of the Cerro Bayo cryptodome, Chachahuén volcano, Argentina – implications for viscous magma emplacement, *JGR:Solid Earth*

Kay, S. M., O. Mancilla, and P. Copeland (2006), Evolution of the late Miocene Chachahuén volcanic complex at 37°S over a transient shallow subduction zone under the Neuquén Andes, in Special Paper 407: Evolution of an Andean Margin: A Tectonic and Magmatic View from the Andes to the Neuquén Basin (35°-39°S lat), edited by S. M. Kay and V. Ramos, pp. 215–246, Geological Society of America.

Pérez, M. A., and P. Condat (1996), Geología de La Sierra de Chachahuén, Area CNQ-23, Buenos Aires, Argentina.

Rocchi, S., & Breitkreuz, C. (2018). Physical Geology of Shallow-Level Magmatic Systems—An Introduction (pp. 1–10). DOI: 10.1007/11157_2017_32

Spacapan, J. B., O. Galland, H. A. Leanza, and S. Planke (2017), Igneous sill and finger emplacement mechanism in shale-dominated formations: a field study at Cuesta del Chihuido, Neuquén Basin, Argentina, *J. Geol. Soc. London*, *174*(3), 422-433.

An example of vesicle layering in laminar intrusive bodies from Neuquén basin

Serra-Varela, S.[1,2], González, S.N.[1,2], Martínez, M.[2], Urrutia[2], L. and Arregui, C.[2]

[1] *CONICET, Universidad Nacional de Río Negro. Instituto de Investigación en Paleobiología y Geología, Av. General Roca 1242 (R8332EXZ) - Rio Negro, Argentina.* ***ssvarela@unrn.edu.ar***
[2] *Universidad Nacional del Comahue – Facultad de Ingeniería, Departamento de Geología y Petróleo – Buenos Aires 1400 (Q8300) - Neuquen, Argentina.*

Keywords: vesicles; Neuquén basin; basic magmatism

The study area is north from Mt. La Bandera, in the Picún Leufú anticline which constitute a major structure in the Neuquen basin located south to the Huincul High. This structure strikes E-W from Mt. Picún Leufú to Los Molles where it turns NNE-SSW. Along this anticline the sedimentary rocks from the Cuyo, Lotena and Mendoza Groups crops out (Leanza et al. 1997; Ponce et al. 2014). These rocks host mafic sills and dykes and are also covered by volcanic lava flows. In the area there are at least three main magmatic units related to basic magmatism: 1) the Paleocene to middle Eocene Auca Pan Andesites which crops out south and west of the study area, mostly in the North Patagonian Andes region; 2) the Lohan Mahuida olivinic basalts (Basaltos I by Lambert 1956 in Leanza et al. 1997) and their possible intrusive equivalents from the Cerro Horqueta Formation, both considered upper Miocene; 3) Zapala and Santo Tomás olivinic basalts (Basalto II by Groeber 1929 in Leanza et al. 1997) possible Miocene to Plesitocene. The laminar intrusive bodies object of this contribution have not been assigned to any lithostratigraphic unit yet. In this contribution we are going to describe their main characteristics, evaluate their relationship with the host rocks and stablish a possible comparison with the known units previously mention.

The laminar intrusive bodies from Mt. La Bandera are hosted in different lithostratigraphic units as Molles (Cuyo Group), Quebrada del Sapo and Vaca Muerta (Mendoza Group). There are two main outcrops in an E-W strike-line separated by 5 km from each other. The width of the intrusives range between 1.5 to 4 mts and the outcrops extend for 2.5 km length. The bodies are sub-concordant with the stratigraphic sedimentary planes, dipping gently to the south (Fig. 1). The contacts with the country rocks are sharp and clear, no inclusions as enclaves or xenoliths were founded. There are no evidences of thermal effects over the country rocks in the contact with the igneous bodies.

The texture is lamprophyric (porphyritic where the phenocrysts are mafic), better defined (coarser) in the center than in the margins. The phenocrysts are biotite and they tend to form agglomerates of several crystals. The base is seriated, and its crystal size varies from fine to coarse from the margins to the center of the bodies respectively. It is composed of plagioclase, biotite and amphibole with magnetite as an accessory phase. As key characteristic, the bodies are intensely vesiculated and these vesicles are fill with zeolites (Fig. 2). The vesicles fill consists of radial fibers and occasionally shows a concentric mineral zonation.

Fig. 1 – General aspect of the Mt. La Bandera laminar Igneous bodies.

Regarding the structure of the bodies, an internal separation in layers can be observed (Fig. 2). A highly layered zone of tens of centimeters to few meters width can be individualized at the margins, in direct contact with the country rocks. In contrast, the center is coarse laminated or totally masive (as in not layered at all). There is a colour difference between light to medium grey in the center and dark to very dark grey margins. Both in the margins and in the center of the igneous body, the vesicles are elongated following the lamination. The vesicles in the center of the bodies are bigger than the ones in the margins and are less deformed. At the margins, the intense foliation is defined by the segregation of bands poor and rich in vesicles which are intensively stretched and elongated (Fig. 3). In both kinds of bands, the

elongated vesicles and the phenocrysts are oriented parallel to the contact surface with the country rock.

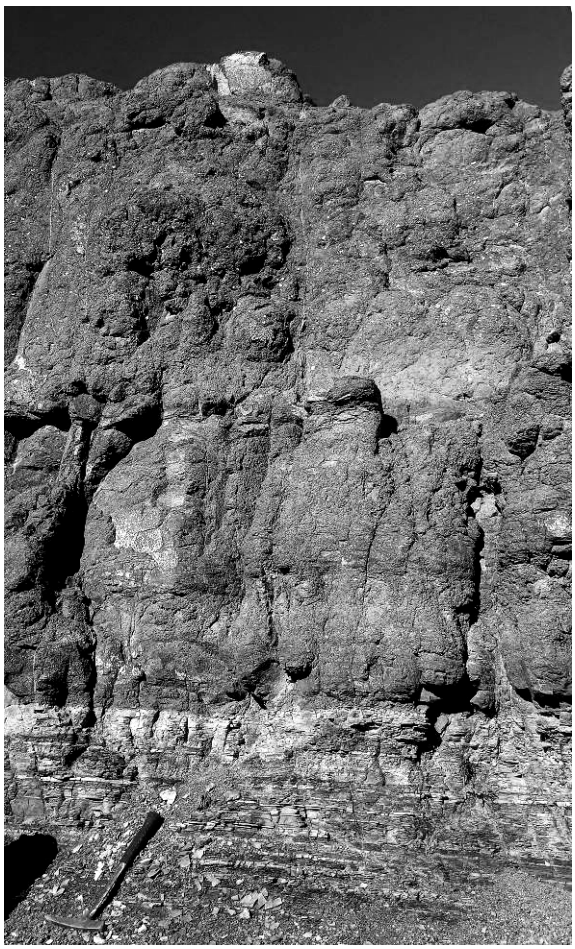

Fig. 2 – Close up to the igneous body and its contact with the country rock.

The homogeneous characteristic of igneous bodies in both trends of outcrops lead us to think that they belong to the same magmatic event. The contacts between the igneous bodies and its country rocks indicate a high rheological contrast between the magma and its country rocks at the time of the intrusion. Moreover, the absence of peperites in the country rocks and material flux from the host rock into the magmatic bodies indicate a dry condition for intrusion. The presence of vesicle shaped-preferred orientation is related to flow- related features in shallow level intrusions (Westerman et al., 2017). Moreover, vesicle layering has been mentioned by Toramaru et al., (1996) for igneous intrusions in shallow levels of the crust and involving low volumes of magma. The "thin in width" of the bodies described from Mt. La Bandera would probably represent a minor magma injection or are satellite apophysis of a major magmatic body that has not been founded yet. Based on its primary stratigraphic relations and its composition, the bodies described in this work could be compared to the Paleocene to middle Eocene Auca Pan magmatism.

Fig 3 – Highly stretched and elongated vesicles in the margin of the igneous body.

Acknowledgements

Works in the area are being carried out by a team from Universidad Nacional del Comahue in order to better understand the relation of these bodies with the country rocks, oil and gas generation and deformational events.

References

Leanza, H.A., Hugo, C.A., Herrero, J.C., Donnari, E. and Pucci, J.C. (1997), Hoja Geolólogica 3969 – III Picún Leufú. SEGEMAR, Boletin N°218 – 137 p.

Ponce, J.J., Montagna, A.O. and Carmona, N. (2014) *Geología de la cuenca Neuquina y sus sistemas petroleros: una mirada integradora desde los afloramientos al subsuelo*. 223 p. Fundación YPF-Universidad Nacional de Río Negro.

Toramaru, A., Ishiwatari, A., Matsuzawa, M., Nakamura N., Arai S. (1996) Vesicle layering in solidified intrusive magma bodies: a newly recognized type of igneous structure. *Bulletin of Volcanology 58*: 393.

Westerman D., Rocchi S., Breitkreuz C., Stevenson C., Wilson P. (2017) Structures Related to the Emplacement of Shallow-Level Intrusions. In: *Physical Geology of Shallow Magmatic Systems. Advances in Volcanology*. Edited by Breitkreuz C., Rocchi S. pp. 83-119. Springer

Studies of active volcanic plumbing systems: Lessons learned from recent magmatic activity in Iceland

Freysteinn Sigmundsson[1]

[1] *Nordic Volcanological Center, Institute of Earth Sciences, University of Iceland* – fs@hi.is

Keywords: magma movements, ground deformation, seismicity.

Studies of eroded volcano interiors at extinct volcanoes provide important information on magmatic processes in the past, but how can these be compared to ongoing magmatic processes at presently active volcanoes and monitoring of volcanic unrest? A variety of techniques can be applied to indirectly infer magma movements during unrest periods and eruptions, the most widely used techniques being studies of seismicity, ground deformation, volcanic gas release and temperature changes, as well as petrology and geochemistry. The subsurface of an active volcano is inherently difficult to image in detail, so a multidisciplinary approach is a key to improved understanding.

We compare the possibilities and limitations of available monitoring techniques, and lessons learned from studies of the most recent eruptions, unrest periods, and magma movements in Iceland (Sigmundsson et al., 2018). These include the Eyjafjallajökull 2010 summit and flank eruptions and previous unrest (Sigmundsson et al., 2010), Grímsvötn 2011 (Hreinsdóttir et al., 2014), Bárðarbunga-Holuhraun 2014-2015 (Sigmundsson et al., 2015). The preceding long-term unrest was different in each of these cases: (i) separate discrete basaltic sill intrusions, (ii) clear signs of continuous flow of magma towards shallow depth, (iii) elevated seismicity over years, with some increase and detected minor ground deformation in the last months prior to onset. The inferred main drivers of the eruptions are different: (i) Episodic injection of basaltic magma into more evolved magma during Eyjafjallajökull 2010 explosive eruption, driving pulses in activity and irregular mass eruption rate over six weeks, (ii) Relaxation of overpressure in a shallow magma body built up by previous magma inflow. Pressure relaxation over days, with superimposed pulses in activity due to conduit processes, leading to pulsating eruption plume at Grímsvötn 2011 for 7 days (iii) Magma buoyancy in a deep magma body driving magma upward and into a lateral dyke, with associated development of underpressure under weak caldera faults, triggering caldera collapse at Bárðarbunga. After onset of caldera collapse, piston-style subsidence driving flow out of magma body, resulting in a major lateral effusive eruption over a six-month long eruption.

Seismology is used to study both magma movements and the overall structure of volcanoes. Elevated seismicity in a crustal volume is often the first identified signal of volcanic unrest; a response to increases stress around a magma accumulation zone. A common paradigm is that earthquakes will track where magma moves in the subsurface, but experience in Iceland shows this is only partly true. For example, during the lateral dike propagation in 2014 at Bárðarbunga, only the bottom part of a near-vertical regional dike lighted up with earthquakes. Parts of inferred lateral dike path were also without seismicity. For the seismically active parts of dikes, relative earthquake relocation provides key information; sheet like features are very clear. Mapping localized magma bodies at depth through studies of seismic velocities and reflections have limited resolution in heterogenous volcanic crust, as there it is difficult to map localized low seismic velocities. However, seismology is well suited to map location of dense cumulate and intrusion complexes as linked with high seismic velocities.

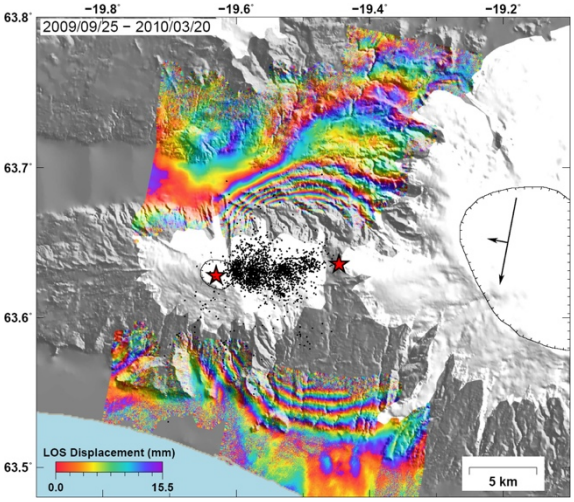

Fig. 1 – Interferogram formed by InSAR analysis showing signal due to magma intrusion at Eyjafjallajökull, Iceland, in 2010 (Sigmundsson et al., 2010). Each fringe = 15.5 mm.

Ground deformation on volcanos is mapped by multiple techniques, including GNSS (Global Navigation and Satellite System) geodesy and interferometric analysis of synthetic aperture radar images (InSAR). These reveal e.g. how surface may

uplift an expand in relation to intrusion. Observed deformation is typically modeled assuming localized magma source of simple geometry, located within host rock of uniform elastic properties. Under such assumptions, models are inferred for ground surface displacement in relation to pressure/volume change at depth. Uncertainties on model parameters can e.g. be derived by characterization of the posterior probability density functions of source model parameters using a Bayesian approach. Volume change of such deformation sources is typically best resolved parameter, as trade-off exists for lateral dimensions and thickness. Research has focused on the influence of different geometry of sources on the resulting surface deformation fields, but attention is now also on the contribution from variations in host rock properties and localized faulting for explaining details of surface deformation. Model errors are in general important to consider, although often not well addressed. The width of surface deformation field is often taken as an indicator of the depth of the magma source. However, if caldera faulting occurs as in Bárðarbunga 2014-2015, then the width of the deformation field is governed by the caldera width.

Petrology and geochemistry of eruptive products should be evaluated together with geophysical data. As an example, a detailed study has been conducted by Pankhurst et al. (2018) of processes leading the Eyjafjallajökull 2010 flank eruption. Large variation in composition of olivine crystal cores and chemical zonation around cores is observed. This has now been explained in terms of disequilibrium processes, that form systematic pattern at the population scale. A "Crystal Rain" model developed explains how single primitive melt produces crystals over a wide range in composition and generates systematic disequilibrium with variable chemical zonation, if magma stalls temporarily in sills.

The subsurface of a volcano may in reality be far from a typical cartoon sketch with one large magma reservoir with magma of uniform properties. The concept of a magma domain under a volcano (Fig. 2) may be more useful (Sigmundsson, 2016). When applying simplified geophysical model approaches to match multidisciplinary constraints on magma plumbing, one has to consider what part of a magma domain is active during a particular eruption. The magma domain in volcano roots may take various forms, and properties of the magma within it may vary significantly. It may include stratified magma sources or maybe a combination of more isolated magma packages (sills or other geometrical shapes). During an eruption only a small volume of the magma domain may be depressurized, suggesting limited connection between magma within a magma domain. Thus, co-eruptive ground deformation and geochemistry of eruptive products may only be used to resolve a subset of the magma domain imaged by seismic surveys or other techniques.

Direct observations from drilling into magma, as proposed at Krafla volcano within the Krafla Magma Testbed (KMT) initiative may be important next steps in advancing understanding of volcanoes.

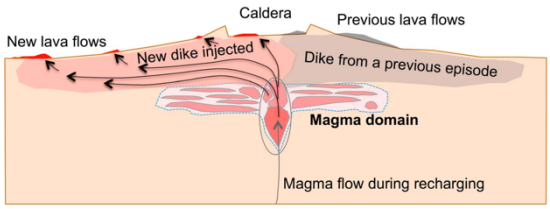

Fig. 2. A general schematic model of the uppermost volcano plumbing system. The crustal volume that hosts magma at a shallow level beneath a volcano can be referred to as a magma domain (light blue hatched outline). Its size and shape is highly variable from one volcano to another, as well as the amount of magma (reddish color) stored within the domain. It can hold magma of different composition, with varying amount of melts and crystals, and pockets with variable connectivity. Arrows indicate magma movements in a recent episode of recharging (thin arrow) and during a rift zone diking event and eruption (thick arrows) when a confined part of the magma domain deflated (oval outline).

Acknowledgements

Support from the University of Iceland Research Fund and the H2020 project EUROVOLC, funded by the European Commission (Grant 731070) is acknowledged.

References

Hreinsdóttir, S., F. Sigmundsson, M. J. Roberts, *et al*. (2014), Volcanic plume height correlated with magma pressure change at Grímsvötn Volcano, Iceland, *Nature Geoscience*, 7, 214-218.

Sigmundsson, F. *et al*. (2018), Magma Movements in Volcanic Plumbing Systems and their Associated Ground Deformation and Seismic Patterns, In *Volcanic and Igneous Plumbing Systems,* edited by S. Burchardt, 285-322, Elsevier.

Sigmundsson, F., + 36 others (2015), Segmented lateral dike growth in a rifting event at Bárðarbunga volcanic system, Iceland, *Nature*, 517, 191–195.

Sigmundsson, F., S. Hreinsdóttir, A. Hooper,, Th. Árnadóttir, R. Pedersen, M. J. Roberts, N. Óskarsson, A. Auriac, J. Decriem, P. Einarsson, H. Geirsson, M. Hensch, B. G. Ófeigsson, E. Sturkell, H. Sveinbjörnsson, K. Feigl (2010), Intrusion triggering of the 2010 Eyjafjallajökull explosive eruption, *Nature*, 468, 426-430, doi:10.1038/nature09558.

Sigmundsson, F. (2016), New insights into magma plumbing along rift systems from detailed observations of eruptive behavior at Axial volcano, *Geophys. Res. Lett*., 43, doi:10.1002/ 2016GL071884.

Pankhurst, M. J., D. J. Morgan, T. Thordarson, S. Loughlin (2018), Magmatic crystal records in time, space, and process, causatively linked with volcanic unrest, *Earth Planet. Science Letters*, 493, 231–241.

Drones, dykes and data analytics: discoveries from Volcán Taburiente (La Palma, Spain)

Sam Thiele[1], Alexander Cruden[1] and Steven Micklethwaite[1]

[1]*School of Earth, Atmosphere and Environment, Monash University*

Keywords: *dyke swarm, multiple-dyke, digital outcrop geology*

Sheet-intrusions are the most common means of magma transport in basaltic volcanoes, so knowledge of their propagation paths is critical for volcanic hazard analyses. Field-studies of exposed intrusions have provided significant insights into the processes that determine these propagation paths.

Recent advances in unmanned aerial vehicle (UAV) technology and modern photogrammetric techniques such as structure from motion have made it possible to capture and analyse exposed intrusions in unprecedented detail (Dering et al., 2019). Using these methods, we have captured digital outcrop models of the spectacularly exposed basaltic dyke-swarm that formed the plumbing system of Volcán Taburiente on La Palma (Canary Islands, Spain).

Ten million dyke orientation and thickness estimates have been extracted from 500 dykes (a total dyke-length of >50 km) using methods we have developed especially for this purpose (Thiele et al., 2017; 2019). These tools are freely available as part of the *Compass* plugin in the widely used and open-source point cloud analysis software CloudCompare. The measurements capture the orientation, thickness and associated uncertainty every 10 cm along ~60 % of the dyke margins and highlight a broadly radial dyke swarm with a focal point in the southern section of Caldera Taburiente.

We also take advantage of the near-continuous exposure (Fig. 1) to estimate the vertical and circumferential strain induced by the dyke swarm. These estimates highlight that, while the dykes are radial, N-S orientations are more frequent and probably gave Volcán Taburiente an elongate geometry. A simple Maxwell visco-elastic model can account for the observed strain without requiring a basal detachment or gravitational spreading. Significantly, this model can also replicate the observed dyke-aperture distribution.

Many of the dykes also contain internal chill margins and/or compositional variations, which suggest that they formed from two or more temporally separate dyking events. Chill margins of the internal dykes are ~1 cm thick and glassy, indicating that the exterior (older) dyke had cooled prior to subsequent intrusions (Fig. 2). The UAV mapping highlights younger intrusions that intersect and are reoriented along older ones by as much as 60˚; older dykes clearly provided preferenti-al propagation pathways (Fig. 3). This observation is counterintuitive, as dykes at this location crosscut weak and compliant phreatomagmatic tuff, scoria and matrix-rich volcanic breccia.

Fig. 1 – UAV image of a typical exposure along the eroded collapse scarp that defines Caldera Taburiente. Due to the dry climate and steep topography, these exposures are near continuous and allow the shallow volcanic plumbing system to be mapped in exquisite detail.

Multiple-dykes have previously been studied from a geochemical perspective to explore fractionation in magma chambers, but literature on the mechanics of their formation is lacking. It is commonly assumed that multiple-dykes form either because (1) the initial dyke did not have time to solidify completely before the subsequent magma injection, or (2) the solidified dyke (or its margin) is

weaker than the host rock it intrudes. Based on the previously described field-observations, geo-mechanical tests and numerical modelling we suggest that the multiple-dykes on La Palma were not formed by either of these mechanisms.

Instead, we propose that the multiple-dykes formed due to the mechanical contrast between solidified older dykes and the host-rock. Linear-elastic models show that the stiffness of the solidified dykes results in concentrated stress under volcanic and gravitational loading, and that within the dykes the principal compressive stress is rotated towards parallelism. Hence, we suggest that multiple-dykes form because subsequent intrusions tend to be deflected along the dyke contact (if the dyke has a weak margin) or within the dyke itself due to stress rotation.

Geomechanical tests also indicate that the dykes have anisotropic elastic, tensile strength and fracture toughness properties, which is probably due to a strong preferred orientation of plagioclase (flow foliation). This anisotropy will exaggerate the abovementioned stress rotation and encourages formation of margin-parallel joints during volcano inflation/deflation cycles, which in turn further enhance the anisotropy. Margin-parallel joints are observed in ~40% of dykes on La Palma and exhibit a wide variety of spacing and persistence. These will significantly reduce the dyke-parallel fracture toughness, and hence the energy required to form multiple dykes.

At large scale, solidified dyes form geomechanical discontinuities that give volcanic edifices a structural memory of past stress states. Deflection of dykes along these discontinuities cause subsequent intrusions to become misoriented with respect to external stresses and result in potentially unexpected propagation paths. The re-activation of older dykes also has implications for the organisation of magma plumbing systems by encouraging re-use of older vents and directing dykes along volcanic rift-zones or towards shallow magma reservoirs.

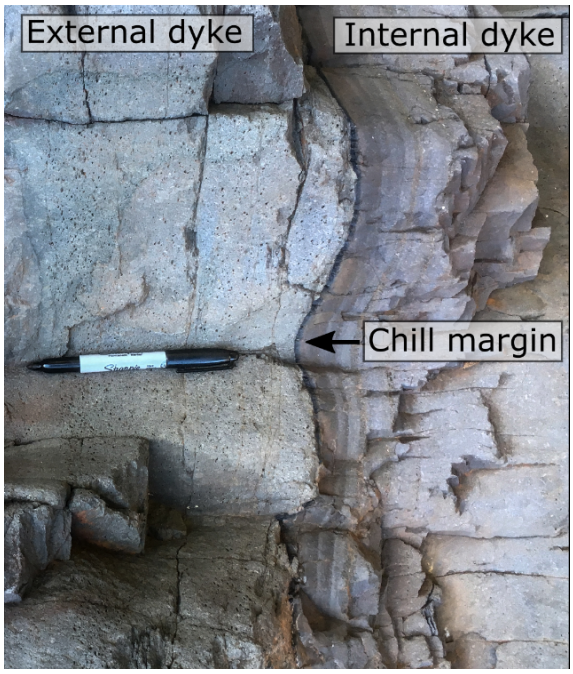

Fig. 2 – Glassy internal chill-margins showing that the internal dyke formed after the external one had cooled.

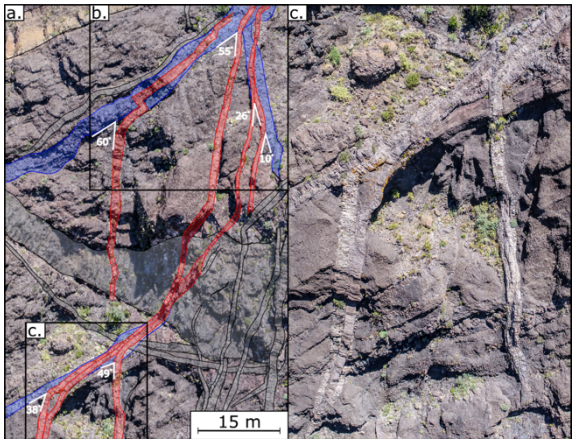

Fig. 3 – Interpreted digital outcrop model of a cliff-section showing older dykes capturing and re-orienting younger ones by as much as 60°.

Acknowledgements

The Authors would like to acknowledge and thank staff at Parque Nacional Caldera de Taburiente for their hospitality and support during fieldwork. STT was supported by a Westpac Future Leader scholarship and Australian Postgraduate Award.

References

Dering, G., Micklethwaite, S., Thiele, S. T., Vollgger, S. A., Cruden, A. R. Review of drones, photogrammetry and emerging sensor technology for the study of dykes: Best practises and future potential, *Journal of Volcanology and Geothermal Research, 373*, 148-166.

Thiele, S.T, Grose, L., Samsu, A., Micklethwaite, S., Vollgger, S. A., Cruden, A. R., Rapid, semi-automatic fracture and contact mapping for point clouds, images and geophysical data, *Solid Earth, 8*, 1241-1253.

Thiele, S.T., Grose, L., Tiangang, C., Cruden, A. R., Micklethwaite S., Extraction of high-resolution structural orientations from digital data: A Bayesian approach. *Journal of Structural Geology, 122*, 106-115.

The Taió plumbing system (Paraná-Etendeka igneous province, Southern Brazil)-Mapping, petrography and geochemistry

Waichel B.L.[1], Mouro L. D.[2], Vieira L. D.[3], Silva M. S.[2] and Muller C.[2]

[1] *Departamento de Geologia, Universidade de Santa Catarina, Florianópolis, Brasil* – breno@cfh.ufsc.br
[2] *Espepetro, Departamento de Geologia, Universidade de Santa Catarina, Florianópolis, Brasil*
[3] *Programa de Pós-Graduação em Ciência e Engenharia de Materiais, Universidade de Santa Catarina, Florianópolis, Brasil*

Keywords: plumbing system, sills, Paraná-Etendeka Province.

The plumbing systems of Large Igneous Provinces are an important portion of these huge magmatic and tectonic events. These systems not only permit the feeding of the overlying flood lavas but also can induce organic matter maturation, fluid migration and deform (folds and faults) sedimentary rocks of the basins. These systems can be well observed in large outcrops in Karoo Basin (South Africa) or in seismic data in basins from North Atlantic Igneous Province. In the well-known Paraná-Etendeka Province (PEP-Lower Cretaceous) many feeder systems, formed predominantly by isolated sill and dykes, which cut sedimentary rocks and basement in both side of the province (e.g. Ponta Grossa, Serra do Mar, Henties Bay-Outjo dyke swarms) occurs. However, a plumbing system formed by sills and dykes have never been identified. Then here we report the occurrence of the Taió plumbing system (TPS) in southern Brazil (Santa Catarina state, Fig. 1). The intrusive rocks of TPS are hosted by Paleozoic sedimentary rocks from Paraná basin (sandstones and carbonaceous shales), where a thermal effect can be observed along the contacts.

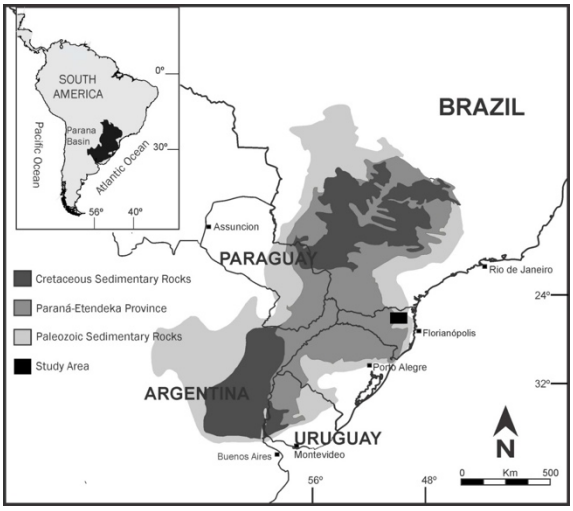

Figure 1 – Simplified geological map of Paraná Basin with study area.

In satellite images we observed 4 ring structures and a long NW lineament (Fig. 2). Field observation of very good outcrops show the occurrence of a thick sill at the top of the sequence, minor sills, a laccolith, a big dyke with NW orientation and some minor dykes (NE). A detailed geological mapping in area have shown the importance of intrusive rocks in the sequence, which represents 40% of the sequence (450m thick) and also show predominance of sills over dykes. The sills have thickness varying from 10 to 120 m, are mainly tabular layer-parallel sheets, but saucer-shaped and inclined sill also occurs. The major dyke of TPS is up to 80 m wide, 20 km long and has NW orientation. Lobe-like sills terminations have been identified and are evidence of magma propagation process between sedimentary layers. We have also observed chilled margins in all intrusive rocks, and a coarse dolerite occurrence in thick intrusions.

At the top of sequence crops out a sill (~100 thick) found in both sides of the valley (Fig. 3), forming a ring structure in map, like saucer-shape sills from Karoo (e.g. Golden Sill). Other two minor similar structures are observed in north portion of the area.

The samples are holocrystalline, with dark gray color, massive structure with fine to coarse granulometry and were classified as dolerites. The dolerites are composed mainly by plagioclase, clinopyroxenes, Fe-Ti oxides and minor orthopyroxene with intergranular and subophytic textures.

Petrography and whole-rock geochemistry were realized in 17 samples (table 1) and helped the understanding of the geometry of the plumbing system and give clues about the dynamics of the plumbing (dykes feeding sills or sills feeding dykes).

The rocks analyzed are basic and intermediate, subalkaline and tholeiitic, and classified as andesi-basalts and basalts, except for a differentiated sample of andesite. The geochemical data show that the intrusive rocks studied are of the high-TiO_2 (H-Ti) and low- TiO_2 (L-Ti) groups, with a predominance of the last one (Tab. 1). The basic to intermediate rocks of the A-Ti group correspond to the Paranapanema magma-type and the B-Ti group, to the Gramado magma-type.

High- TiO_2	Low- TiO_2
Sills ITC-2, ITC-8 , ITC-9, ITC-18, ITC-29, ITC-30	Sills ITC-3, ITC-10 , ITC-11
Dykes ITC 15, ITC-16	Dykes ITC-5, ITC-6 , ITC-7, ITC-24, ITC-26, ITC-28

Table 1- Geochemistry of sills and dykes of the TPS.

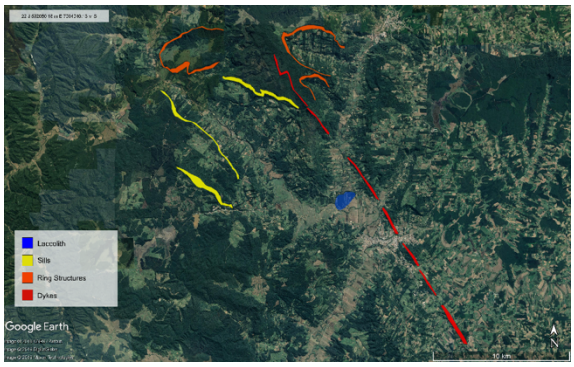

Figure 2 – Aerial image with ring structures, sills and a dyke.

Intrusions have been separated in high-TiO_2 and low- TiO_2, and in some areas is possible visualize the geometrical relation between sills and dykes. For example: the big high-TiO_2 NW dyke is segmented and in north portion is observed a connection with a high-TiO_2 minor sill. The dyke outcrop below and above of the sill level and is a good example of dyke feeding sill. This sill is small, ~10 m thick with lobate tips developed by advance of magma fingers, in this case we can infer the magma flow direction (to south) based in the geometry of the lobes.

A laccolith with thickness of ~15 m in the central portion and dome-like form is exposed in an old quarry (Fig. 2 and 4). The host rocks at the top of the laccolith was eroded and the intrusion is at the base of the exposed sequence of TPS (350 a.s.l.). The laccolith is near of the big NW dyke (Fig. 2) but contact relations between them is not observed in the field. Geochemical character of the intrusions rules out the connection between them, the laccolith is low-TiO_2 and the dyke is high-TiO_2. The probable feeder of the laccolith is a minor dyke (NE orientation, ITC 24) located at the north.

An interesting point in TPS is the fact that the laccolith is located at the base of the exposed sequence, where the uplift of the rock layers above is theoretically more difficult. The probable saucer-shape sill is located at the top of the sequence.

More field work and seismic data acquisitions are crucial to define the geometrical relations between intrusive rocks of TPS and to evaluate its effect in the sedimentary basin.

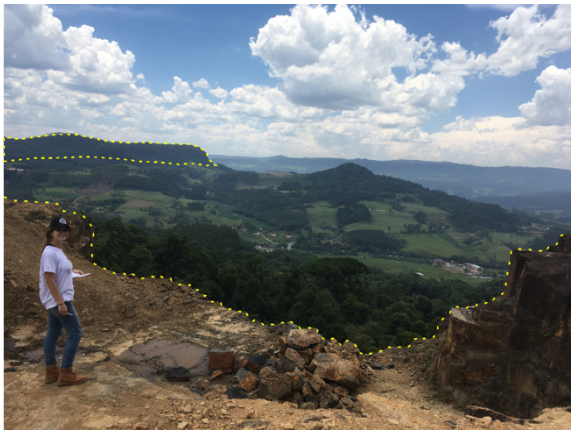

Figure 3 – Photograph of the thick sill, exposed in both sides of the valley.

Figure 4 – General view of old quarry in the laccolith.

Syn-magmatic fracturing in the Sandfell laccolith, East Iceland

Witcher T.[1], Burchardt S.[1], Heap M.[2], Mattsson T.[1] and Almqvist B.[1]

[1] *Department of Earth Sciences, Uppsala University, Sweden* – taylor.witcher@geo.uu.se
[2] *Ecole et Observatoire des Sciences de la Terre, University of Strasbourg, France*

Keywords: laccolith, magma, fracture.

The Sandfell laccolith is a Miocene rhyolitic intrusion exposed in eastern Iceland. Mattsson et al. (2018) performed the most recent study of its emplacement and discovered that over one third of the magma volume is intensely fractured in localized bands up to a meter thick, oriented more or less parallel to the contact with the wall-rock. This study focuses on the processes that produced these fracture bands and what effects they have on permeability evolution within the magma body, with the notion that our results could be applicable to modern active magma chambers. We hypothesize that the bands are records of multiple-stage fracturing related to laccolith growth. We present preliminary results on field observations and rock mechanical and physical property measurements correlated with hand-sample characterization of both the magmatic and the host rock types. The produced fracture network may provide pathways for degassing the magma, and/or fluid flow contributing to the development of a geothermal system. The results of this study will likely therefore be of economic interest to the geothermal industry.

In the field, the fracture bands exhibit a range of features, including tensile and shear fractures, as well as breccia in <1 m-thick bands that intersect, connect, and taper off. Permeability greatly varies between the first and last stage of the model, as was confirmed by tests on samples in the laboratory. Additionally, we tested both the magma and host rock for differences in thermal properties (thermal conductivity, thermal diffusivity, and specific heat capacity), permeability, porosity (vesicularity), and strength. We then measured the solidified magma's vesicularity, crystallinity, and permeability as a function of proximity to the fractures to see how the properties are affected.

Finally, we measured the thermal properties of an intact (unfractured) magma rock isolated from any fracture bands, then broke it and filled the cracks with a fluid of known properties, and tested it again to quantify any change.

Based on our preliminary results, we envisage a 3-stage model for the formation of the fracture bands. The first growth stage caused compression of the magma against the wall rock, and resulted in Mode I tensile fractures (Figure 1a). As more magma was injected, the margins of the laccolith sheared against the host rock to accommodate the extensional strain during emplacement and thus rotated the existing fractures as well as potentially opening new ones perpendicular to the contact (Figure 1b). Theoretically, this process repeated until complete brecciation of some zones where individual generations of fracture orientations are indistinguishable (Figure 1c).

Our upcoming work will focus on reproducing the fracturing process to better understand the dynamic processes that produced the fracture bands observed in the Sandfell laccolith. Moreover, we aim to quantify the effects fracture bands have for magma degassing and the transport of fluids in and around magmatic intrusions.

Acknowledgements

We thank Tobias Schmiedel for help with photogrammetry theory and software in the early stages of the project, as well as the Geological Survey of Sweden for access to their core-drilling facilities. This project is funded by the Knut and Alice Wallenberg Foundation through a Wallenberg Academy Fellow grant to SB.

Reference

Mattsson, T., Burchardt, S., Almqvist, B. S., Ronchin, E. (2018), Syn-emplacement fracturing in the Sandfell Laccolith, Eastern Iceland—implications for rhyolite intrusion growth and volcanic hazards, *Frontiers in Earth Science*, *6.* doi: 10.3389/feart.2018.00005

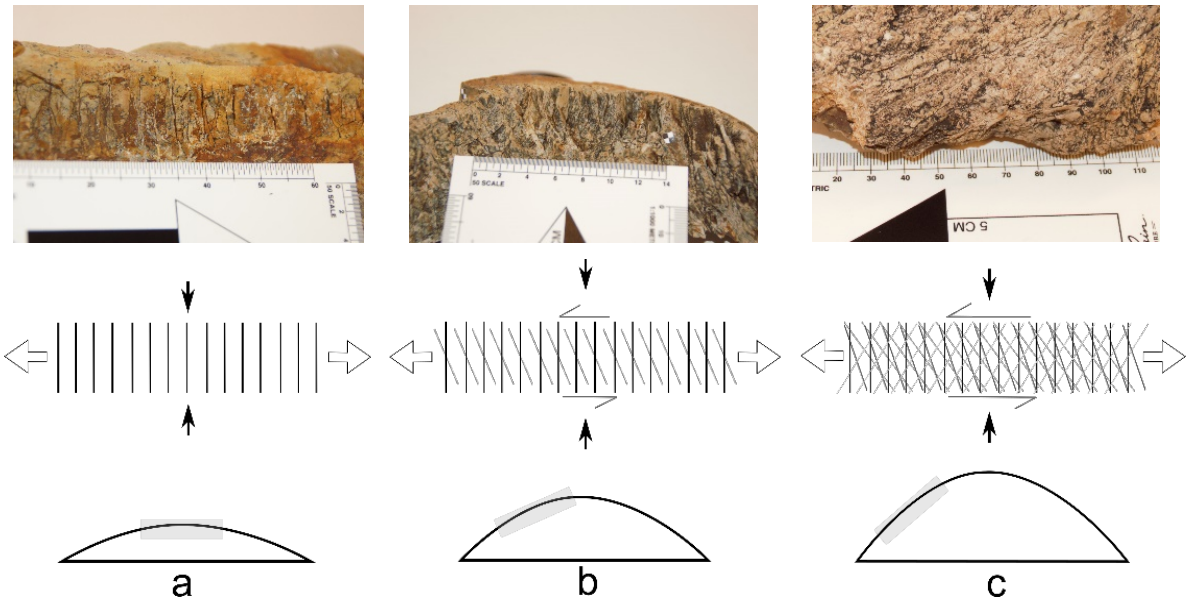

Fig. 1 – Model for fracture band development. Photos of hand samples representing their respective stages of laccolith growth at Sandfell, and a conceptual drawing of the mechanical response of the magma at the outer margin. Black arrows indicate greatest principal stress direction at the location marked by the grey box beneath, vertical and oblique lines between them represent fractures. White arrows point in the opening direction of least principal stress, lateral arrows indicate magnitude of shear. (a) The first stage produced Mode I fractures caused by compression of the magma against the host rock. (b) As the laccolith grew, the shear component reoriented preexisting fractures and the increased pressure opened new tensile fractures parallel to the direction of highest stress. (c) The shear component increased with steepening of magma dome shape, reoriented and perhaps reactivated older fractures, while compression continued to create new fractures until the separate generations were indistinguishable.

Session on Subsurface Imaging of Volcanic Plumbing Systems

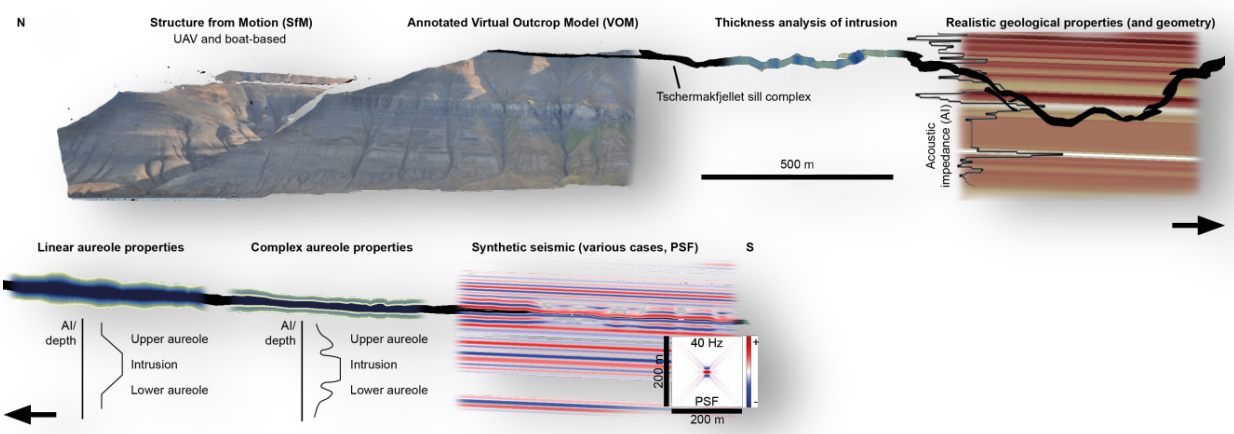

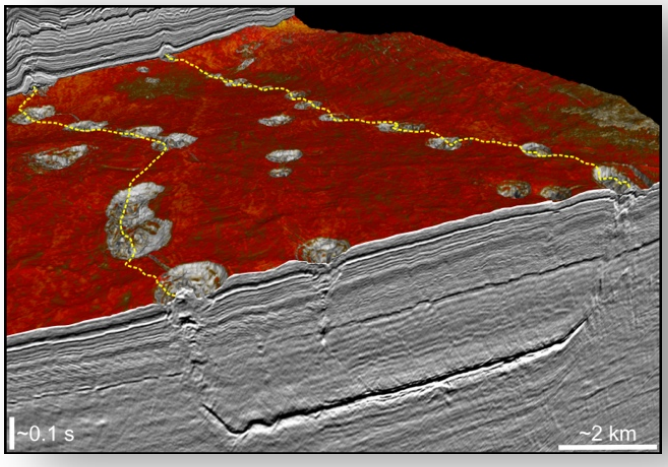

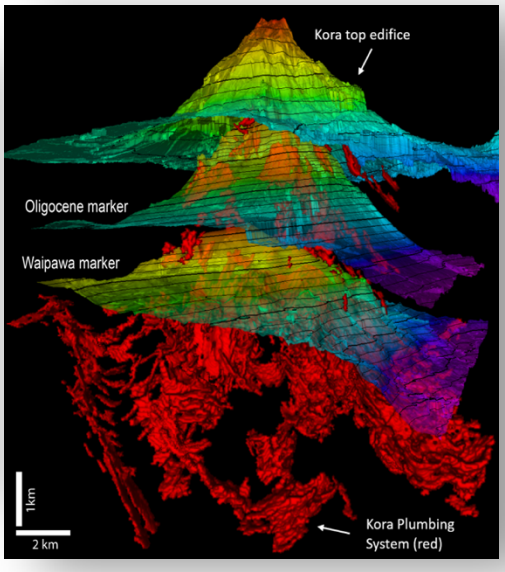

Contents

Seismic Reflection Imaging of Volcano Plumbing Systems in Sedimentary Basins

Alan Bischoff [1] and Andrew Nicol [1]

[1] *School of Earth and Environment, University of Canterbury, Christchurch, New Zealand* – alan.bischoff@canterbury.ac.nz

Keywords: seismic reflection volcanology, buried volcanoes, volcanic plumbing system

Ancient volcanic systems buried in sedimentary basins are common globally. Since the 1990's, an increasing availability of high-quality seismic reflection and borehole data acquired from magma-rich sedimentary basins have helped to improve our understanding of buried volcanic systems (e.g. Herzen 1995; Planke et al. 2000; Gallant et al. 2018). Seismic reflection interpretation provides a valuable opportunity to analyse in detail the processes that control the formation and evolution of buried volcanoes, including insights into edifice construction, and the geometry of the underlying plumbing system.

Despite significant advances have been made to recognize igneous rocks from seismic data, all remote-sensing techniques have limitations which places constraints on the resulting interpretations. Seismic imaging of magma-rich sedimentary basins is problematic manly because of the high impedance of igneous rocks, which tend to generate strong multiple reflections and lead to scattering of the seismic signal. The loss of seismic signal is particularly important beneath thick volcanic sequences due to their internal heterogeneities, and below volcanic edifices due to the presence of intrusive bodies that show a variety of shapes, inclinations, and associated deformation of the host strata (Fig. 1).

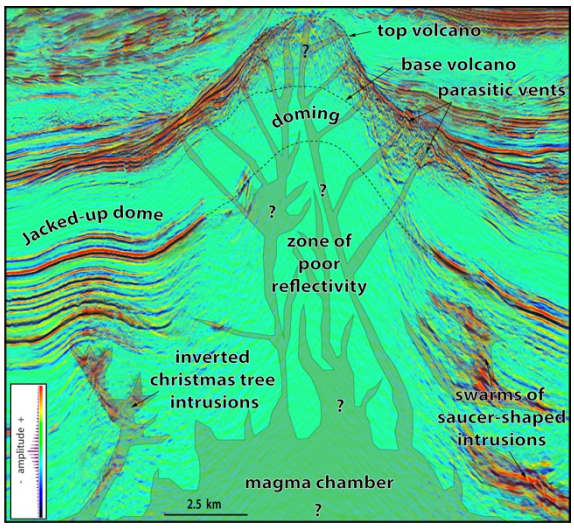

Fig. 1 – 2D seismic profile coupled with amplitude optical stacking showing part of the plumbing system of the Kora Volcano, Taranaki Basin. Modified from Bischoff et al. 2017.

The construction of a unified model that explain both volcanic morphology and the sub-volcanic plumbing system can help to overcome these limitations (Bischoff et al. 2017; 2019). In this work, we present examples of volcanoes buried in Zealandia sedimentary basins, contrasting the main characteristics of large polygenetic composite volcanoes and clusters of small-volume monogenetic volcanoes. We show the advantages and pitfalls of diverse seismic techniques, including conventional horizon picking, seismic attribute analyses, opacity rendering, optical stacking, and geobody extraction, demonstrating how modern 3D seismic visualization is revolutionizing interpretation of volcanoes buried in sedimentary basins (Fig. 2).

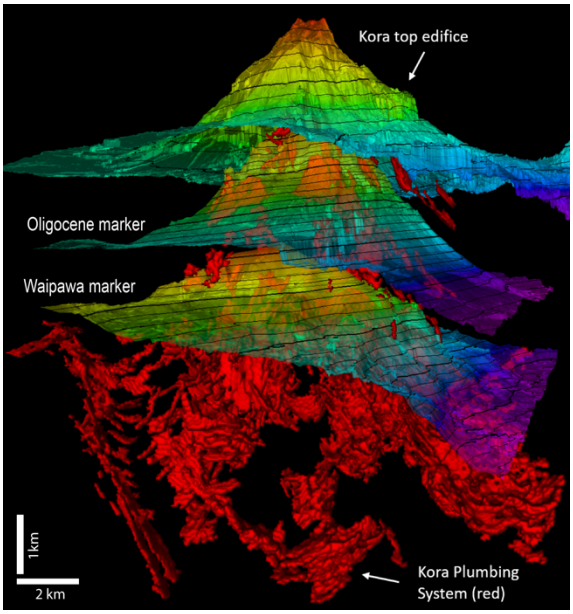

Fig. 2 – Conventional horizon picking of chronostratigraphic surfaces related with Kora Volcano (i.e. Waipawa, Oligocene and top edifice markers) coupled with geobody mapping and 3D visualization of its seismically detected plumbing system (red). Kora is an arc-related submarine stratovolcano currently buried by ca 1 km of sedimentary strata in the offshore Taranaki Basin, New Zealand. Intrusions preferentially were emplaced into Cretaceous-Paleocene grabens comprising terrestrial to marine organic-rich sedimentary strata. The location and geometry of the plumbing system was strongly controlled by pre-existing Cretaceous rift faults and contemporaneous Miocene rifting. The volume of intrusive rocks is estimated to be ca of 350 km^3, while the size of the volcanic edifice is around 80 km^3.

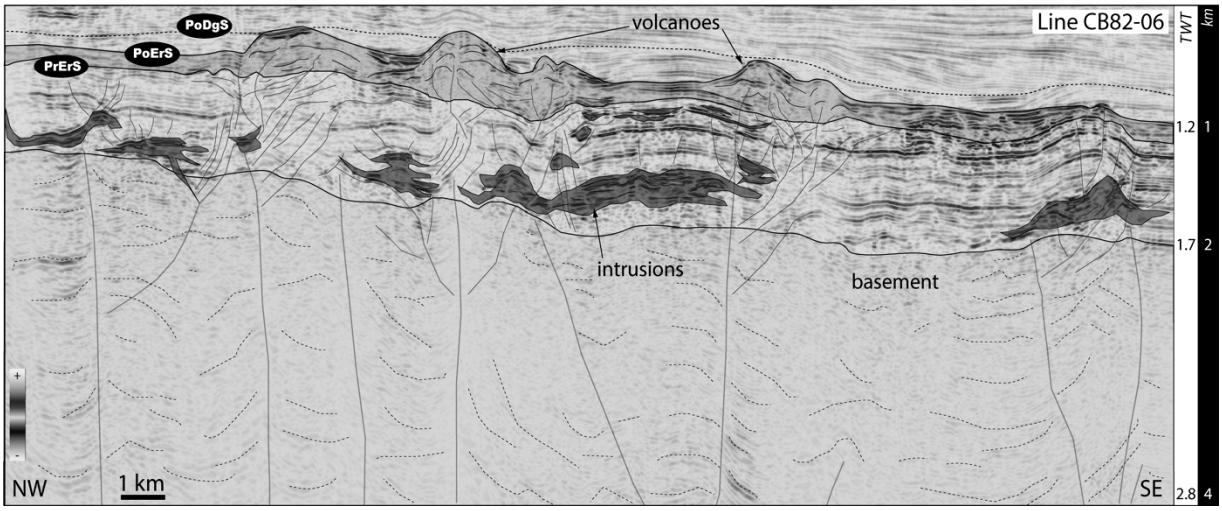

Fig. 3 – 2D dip section showing the shallow plumbing systems and some of the eruptive vents of the Maahunui Volcanic Field (MVF), a monogenetic intraplate volcanic field buried in the Canterbury Basin, New Zealand. Note the relationship between the location of intrusive bodies, overlying deformed host strata, and eruptive vents. Below the top of the basement horizon, seismic signal is scattered, and loss of reflectivity produce low quality seismic facies. However, it is still possible to approximately map the location of MVF magmatic conduits based on geometric aspect of internal fabric of the basement. Modified from Bischoff et al. 2019.

Our results indicate that in both polygenetic and monogenetic volcanoes, the lateral and vertical relationships between intrusive bodies vary systematically. Both plumbing systems typically cross-cut, emplace, and deform pre-magmatic sequences, showing similar geometries, sizes and spatial relationship to the relative eruptive centre.

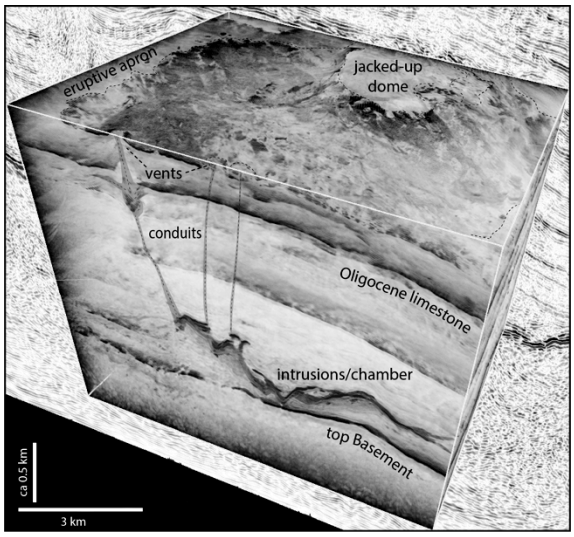

Fig. 4 – Amplitude opacity rendering seismic cube revealing a number of saucer-shaped sills emplaced into Paleocene sedimentary strata of the Canterbury Basin. Note the spatial relationship between the intrusive bodies and Miocene vents erupted at the paleo-sea-floor surface.

In detail, each volcanic system also display differences. Dikes and sills of polygenetic plumbing systems usually formed along, or branching from pre-existing fault structures, always converging towards a relatively stationary eruptive vent, and forming a large (>10 km^3) composite edifice (Fig. 1 and 2). By contrast, monogenetic plumbing systems typically disperse and emplace magma into large areas of the host basin, which at the surface, feeds clusters of small-volume (<1 km^3) volcanoes with morphologies comparable to maar-diatreme, spatter and tuff cones (Fig. 3 and 4).

Acknowledgements

We would like to thanks IHS Markit and Schlumberger for providing academic licence to use the Kingdom and Petrel software, and the MBIE of NZ for funding our research programme in buried volcanoes.

References

Bischoff AP, Nicol A, Beggs M (2017) Stratigraphy of architectural elements in a buried volcanic system and implications for hydrocarbon exploration: Interpretation, doi:10.1190/INT-2016-0201.1.

Bischoff AP, Nicol A, Barrier A, Wang H (2019) Paleogeography and Volcanic Morphology Reconstruction of a Buried Monogenetic Volcanic Field (Part 2). In press in the Bulletin of Volcanology.

Galland O, et al. (2018) Storage and transport of magma in the layered crust-Formation of sills and related float-lying intrusions, in *Volcanic and Igneous Plumbing Systems*, edited by S. Burchardt, pp. 111-136, Elsevier.

Herzer RH (1995) Seismic Stratigraphy of a Buried Volcanic Arc, Northland, New Zealand and Implications for Neogene Subduction. Marine and Petroleum Geology 12(5): 511–31. https://doi.org/10.1016/0264-8172(95)91506-K.

Planke S, Symonds PA, Alvestad E, Skogseid J 2000, Seismic Volcanostratigraphy of Large-Volume Basaltic Extrusive Complexes on Rifted Margins. Journal of Geophysical Research 105 (B8): 19335. doi:10.1029/1999JB900005.

Sill emplacement mechanisms and their relationship with the Pre-Salt stratigraphic framework of the Libra Area (Santos Basin, Brazil)

Leonardo Costa de Oliveira[1], Cristiano Camelo Rancan[2], Maria José Resende Oliveira[2]

[1] *Petróleo Brasileiro S.A., Av. Chile, 300, Rio de Janeiro, Brazil* – leogeo.oliveira@petrobras.com.br
[2] *Petróleo Brasileiro S.A., Av. Chile, 300, Rio de Janeiro*

Keywords: Sill, Santos Basin, Pre-Salt.

The stratigraphic framework of the Santos Basin was affected by important magmatic events along the Cretaceous and Eocene. In the Libra Area, which is the focus of this study, two groups of igneous rocks were recognized: Santonian/Campanian diabases with alkaline affinity, and basalts and tholeiitic diabases of Aptian age (Rancan et al., 2018). The characterization and delimitation of such magmatic events are of fundamental importance in the analysis of this basin, since they may have influenced both hydrocarbon migration and trapping processes, as well as the depositional and diagenetic evolution of the reservoirs due to the hydrothermal fluids originated in each one of these events.

However, the emplacement characterization of some sills in the Pre-Salt section is a challenging task, especially those near the interface between the base of salt and the top of reservoir, because of the impedance overlap of the basal anhydrite, the intrusive igneous and the carbonate reservoir (Penna et al., 2019). In this situation, the application of seismic attributes based on amplitude becomes unsatisfactory.

On the other hand, a series of recently published works have tried to overcome these difficulties through a new approach of seismic interpretation, involving the geometric characterization of diagnostic structures related to the igneous intrusions (*e.g.* Hansen, 2006), or by invoking laccolith models, especially when it considers the similar geomorphological and branching patterns of these rocks (*e.g.* Johnson & Pollard, 1973).

The difficulty of interpreting seismic sill features is further amplified mainly in exploratory areas where there are few wells drilled to calibrate the interpretation. In complex geological contexts, such as in saline domes or those related to igneous intrusions and magmatic extrusions of great extension, like the study area, the seismic velocities may vary a lot (laterally and vertically) and affect the horizons illumination below these structures. This fact is a limiting factor in the exploratory potential analysis process of a given basin, as well as the production of areas with significant oil reserves.

Here we propose a classification for the sills of the Libra Area highlighting the main seismic characteristics of each one of them and its relationship with the stratigraphic framework (Fig. 1).

The features assessed as possible igneous intrusions were identified according to the following criteria: (1) high amplitude positive reflectors, (2) discordant reflectors crossing one or more events and (3) reflectors with abrupt terminations.

The sills were classified into three types according to the geometry and stratigraphic level in which they were emplaced: Type 1 (in the pre-salt section), Type 2 (in the evaporitic section) and Type 3 (in the post-salt section). The Type 1 sills were in turn divided into five subclasses: Type 1a (open saucer-shaped sills near the base of salt), Type 1b (slightly planar transgressive sills), Type 1c (vent-related saucer-shaped sill), Type 1d (laccolith-like forced fold sill) and Type 1e (volcanic complex related sill).

In general, the type 1a sills have flat geometry and they are more difficult to map due to the mixture of the seismic signal response of the basal anhydrite, the carbonate rock and the sill itself. The identification of type 1a sills is important for the prediction of occurrence of igneous rocks near the interface of the base salt and the top of reservoir and also for building the production scenarios of the Libra area.

Type 1b sills are easier to recognize in conventional seismic mapping because they crosscut the reservoir rocks. However, this type of intrusion tends to form interconnected sill complexes and its recognition is fundamental in the reservoir flow modeling.

The Type 1c sills are typical saucer-shaped sills and are associated with the development of hydrothermal vents. The geometry varies according to the burial because the host-rock is usually pelitic. The escape of fluids is related closely to the tip of these sills. Vertical diffuse seismic features are observed, which may be related to the development of fumaroles in the bottom of the lake and would have controlled the sedimentary deposition pattern.

Type 1d sills have canopy-like geometry and result in forced folding of the overburden sediments.

The type 1e sills are associated with the development of volcanoes and large stratified volcanic flows. When the thickness of these features is above the seismic resolution, its geometry is

variable between planar transgressive and concordant layer sills. Type 1e intrusions have their sign added to the limestone of high velocity, which were verified by well data.

Type 2 sills tend to form larger areal bodies within the salt layer, which may be related to the low melting point of the soluble salts (*e.g.* carnalite and taquidrite), that would facilitate the expansion and emplacement of igneous rocks in the evaporitic section (Szatimari, oral information).

The Type 3 sills occur in the post-salt section, close to subaqueous volcanoes chrono-correlated to the Campaniano/Santoniano reflectors. This igneous rocks are narrower and easier to map than the sills types 1 and 2, because of the high impedance contrast with the predominantly siliciclastic envelope.

In general, the correct identification and positioning of the sills of types 2 and 3 were important for the refinement of the velocity model and focusing of reflectors below the salt.

According to Planke *et al.* (2005), the opening of the flanks of the saucer-shaped sills tends to be smaller in the shallower portions, near the paleosurfaces associated with them. This occurs due to the high compressibility of the hosted hydrated low energy facies. Closed features with a high degree of branching characterize the Type 1c, Type 1e and Type 3 sills.

In this way, the sills of types 1c and 1e may be associated with a magmatic event contemporaneous with the deposition of the pre-salt rocks, while those of type 3 would be related to the Campanian sedimentation. In other words they would be shallow intrusions in relation to a paleosurface synchronous to these magmatic events.

Although Type 1b sills have been mapped in the pre-salt section, not all of these are necessarily of this age. Because they are intrusive features, it is possible that some of them are younger than the pre-salt section.

Both types 1a and 1d sills are considerably younger than their hosted rocks. Thus, the sills of types 1a, 1d, 2 and 3 appear to have a clear genetic relationship associated with the post-Salt Campanian/Santonian magmatism widely known in the Santos basin.

Our results show a complex emplacement mechanism for the sills of the area of Libra, which would have affected the Santos Basin petroleum system at different moments of its evolution. This configuration reinforces the need for integrated vulcano-sedimentary studies for the correct understanding of the pre-salt limestones deposition.

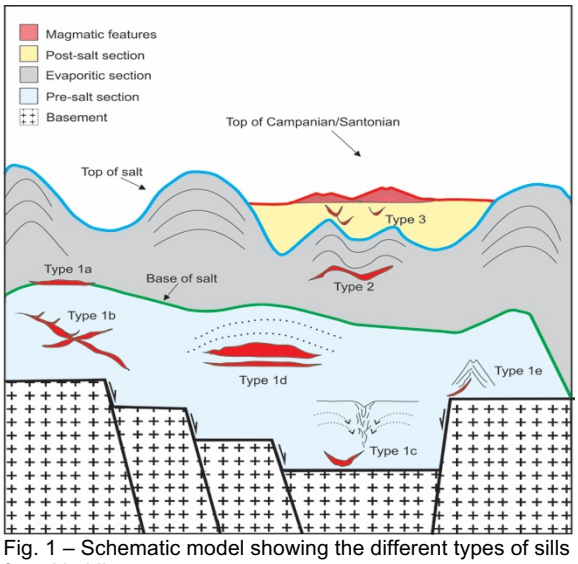

Fig. 1 – Schematic model showing the different types of sills found in Libra area.

Acknowledgements

The authors thank to Petrobras, Shell, Total, CNPC and CNOOC for releasing the data for publication. The first author thanks the geologist Peter Szatimari for helping in the interpretation of the intra-salt sills.

References

Hansen, D.M. (2006), The morphology of intrusion-related vent structures and their implications for constraining the timing of intrusive events along the NE Atlantic margin. *J. Geol. Soc*. 163 (5), pp. 789–800.

Johnson, A. M. and Pollard, D. D. (1973), Mechanics of growth of some laccolithic intrusions in the Hem-y Mountains, Utah, I. Field observations, Gilbert's model, physical properties and flow of the magma. *Tectonophysics* 18, pp. 261-309.

Penna, R., Araújo, S., Sansonowski, R., Oliveira, L., Rosseto, J., Geisslinger, A., and Matos, M. (2018). Igneous rock characterization through reprocessing, FWI imaging, and elastic inversion of a legacy seismic dataset in Brazilian Pre-Salt Province. *In: Society of Exploration* Geophysicists *Technical Program*. Expanded Abstracts 2018, pp. 3277-3281.

Planke, S., Rasmussen, T., Rey, S.S. and Myklebust, R., (2005), Seismic characteristics and distribution of volcanic intrusions and hydrothermal vent complexes in the Vøring and Møre basins. *In*: *Petroleum Geology Conference Series. Geological Society of London. Geological Society*, London, pp. 833–844.

Rancan C. C., et al. (2019), Rochas Ígneas do Bloco de Libra, Bacia de Santos. *In*: *Congresso Brasileiro de Geologia, 49*, Rio de Janeiro, p. 2012.

Sill emplacement in the Exmouth Plateau, NW Australia: The influence of host rock lithology and pre-existing structures on sill segmentation

Köpping J.[1], Cruden A.R.[1], Magee C.[2] and Nissanka Arachchige U.[1]

[1] *School of Earth, Atmosphere and Environment, Monash University, Melbourne, Australia – jonas.kopping@monash.edu*
[2] *Institute of Geophysics and Tectonics, School of Earth and Environment, University of Leeds, Leeds, LS2 9JT, UK*

Keywords: magma fingers, sill emplacement, 3D seismic reflection data.

Sheet intrusions (i.e., dykes and sills) do not always propagate as a continuous planar sheet. It is largely accepted that segments (i.e., magma fingers/lobes) can form at the outer margin of planar magmatic intrusions and they can act as linking elements within a large volcanic magma plumbing system. These geometries have been described using three-dimension (3D) seismic reflection data (e.g. Thomson and Hutton 2004), analogue and numerical models (e.g. Nissanka Arachchige *et al.* This Volume; Souche *et al.* 2019), and field-based observations (e.g. Galland *et al.* 2019). However, their 3D geometry, emplacement mechanisms, and associated host rock deformation are yet not fully understood. In this study, we use high-quality 3D seismic reflection data from the NW shelf of Australia to infer the emplacement mechanism of a fanning lobe network that includes elongated magma fingers. We demonstrate that the mechanical properties of host rock lithologies and pre-existing structures led to the formation of lobe-networks in the Exmouth Plateau. We further aim to present quantitative measurements of lobe geometries to allow for comparison between different seismic datasets and the results of analogue modelling.

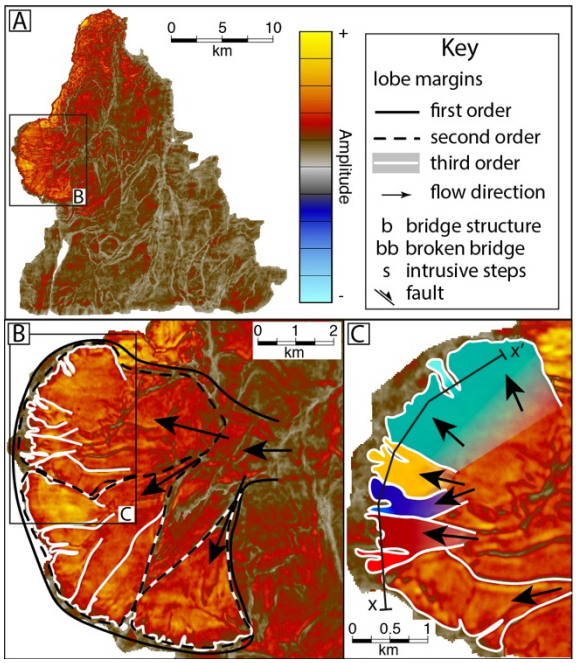

Fig. 1 – A) Absolut peak amplitude map of an inclined sheet intrusion in the Exmouth Plateau highlights a magma lobe network (B). Note that the highest peak amplitudes occur within the lobe network. Segment-segment contacts indicate the magma flow direction. C) Magma fingers emerge from third order lobes.

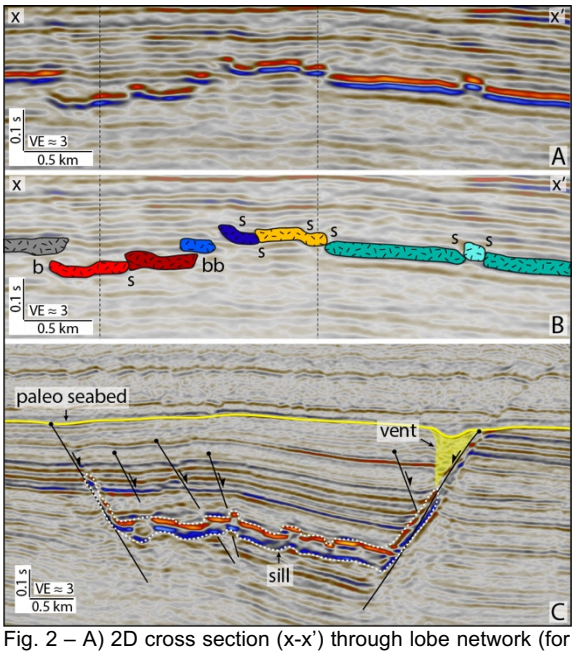

Fig. 2 – A) 2D cross section (x-x') through lobe network (for location of cross section see Fig. 1C). B) 2D cross section (Fig. 2A) with colour coded magma fingers/lobes (Fig. 1C) and possible intrusive structures and segment connectors indicated. C) 2D cross section of a sill intruding into a graben structure. The exploitation of pre-existing faults leads to the formation of inclined limbs and thus to an elongate saucer-shaped sill.

The Exmouth Plateau is a sub-section of the Northern Carnarvon Basin on the rifted margin of NW Australia. It is a thinned, subsided continental block formed in response to multiple episodes of extension during the Late Paleozoic and Mesozoic. Early Cretaceous rifting of Greater India from Australia triggered extensive mafic magmatism, which resulted in the emplacement of large sill complexes in fluvial sediments of Triassic age.

The Glencoe 3D seismic survey is located in the southern part of the Exmouth Plateau and images five sills with different morphologies. In this study, we focus on a large inclined sheet located in the south-western part of the Glencoe 3D survey (Fig. 1A). This sheet intrusion dips SSE and extends at least 30 km N-S and 27 km E-W. The complete geometry and size of the sill cannot be determined because the southern end is not covered by the seismic survey area. Sill segments and emerging magma fingers are observed at shallower levels (~ 3.5 - 3 s TWT) and form a fanning magma lobe network (Fig. 1B). Segments propagated on vertically offset horizons and form connectors (i.e., intrusive steps, broken bridges), indicating a brittle deformation regime. A magma flow pathway map based on segment-segment contacts highlights three different orders of lobes with magma fingers emerging from the outer margin of third order lobes (Fig. 1C). High amplitude reflectors only occur at shallow levels, especially in the area of the described lobe network and indicate a change in host rock lithology. We infer that this change in mechanical properties towards a softer host rock may have led to the formation of both the lobe network and magma fingers. Hydrothermal vents formed at the outer margins of the sill at shallow emplacement depths due to the expulsion of heated pore-fluids (Hansen 2006). This proves that pore-fluids, also essential for host rock fluidisation, were available in the host sediments during sill emplacement. We thus suggest viscous fingering (Schofield *et al.* 2010) as a potential emplacement mechanism for this sill.

Previous studies of 3D seismic reflection data have shown that pre-existing structures can strongly affect sill morphologies during magma emplacement (Magee *et al.* 2013). In the 3D Glencoe survey, we also observe two sills that intrude into a set of graben structures, leading to the formation of elongated channel-like intrusions. Here, bounding normal faults allow the sill to form an inclined limb resulting in an elongated saucer-shape. Where the sill is not bounded by a fault, two generations of sub-horizontal, fanning lobe networks are observed. The exploitation of extension-related normal faults appears to have promoted sill segmentation and developed an inconsistent stepping direction.

Our observations suggest that the formation of fanning lobe networks and emerging magma fingers in the Exmouth Plateau was affected by: (1) variations in host rock lithology, which potentially led to viscous fingering; and (2) by exploitation of pre-existing structures (i.e., normal faults). Detailed mapping of distinct lobe orders and a quantitative description of their geometries will allow for comparison of various datasets which will help to improve our understanding of magma finger formation.

Acknowledgements

Geoscience Australia is acknowledged for supplying the data used in this study. Down Under Geosolution is thanked for seismic interpretation software. Supported by ARC Discovery Grant DP190102422.

References

Galland, O., Spacapan, J.B., et al. (2019), Structure, emplacement mechanism and magma-flow significance of igneous fingers – Implications for sill emplacement in sedimentary basins, *Journal of Structural Geology*, *124*, 120–135.

Hansen, D.M. (2006), The morphology of intrusion-related vent structures and their implications for constraining the timing of intrusive events along the NE Atlantic margin, *Journal of the Geological Society, London*, *163*, 789–800.

Magee, C., Jackson, C.A.L. & Schofield, N. (2013), The influence of normal fault geometry on igneous sill emplacement and morphology, *Geology*, *41*, 407–410.

Nissanka Arachchige, U., Cruden, A.R., Weinberg, R.F. & Köpping, J. (This Volume), From Planar Intrusions to Finger-Like Channels: New insights from 3D Analogue Experiments, in: *LASI 6 - The Physical Geology of Subvolcanic Systems: Laccoliths, Sills and Dykes*.

Schofield, N.J., Stevenson, C. & Reston, T. (2010), Magma fingers and host rock fluidization in the emplacement of sills, *Geology*, *38*, 63–66.

Souche, A., Galland, O., Haug, Ø.T. & Dabrowski, M. (2019), Impact of host rock heterogeneity on failure around pressurized conduits: Implications for finger-shaped magmatic intrusions, *Tectonophysics*, *765*, 52–63.

Thomson, K. & Hutton, D. (2004), Geometry and growth of sill complexes: Insights using 3D seismic from the North Rockall Trough. *Bulletin of Volcanology*, *66*, 364–375.

Hydrothermal venting in sedimentary basins: similarities between ancient and modern (Møre Basin, Norway and Java, Indonesia)

Manton B.[1], Müller P.[2,3], Planke S.[1,2], Mazzini A.[2], Millett J.[1], Zastrozhnov D.[1], Schmid D.[4], Myklebust R.[5]

[1] *VBPR, Oslo, Norway* – ben@vbpr.no
[2] *Centre for Earth Evolution and Dynamics (CEED), Department of Geosciences, University of Oslo, Oslo, Norway*
[3] *GEOMAR Helmholtz Centre for Ocean Research, Kiel, Germany*
[4] *Physics of Geological Processes (PGP), Department of Geosciences, University of Oslo, Oslo, Norway*
[5] *TGS, Asker, Norway*

Keywords: Hydrothermal vent complexes, overpressure, fluid-flow

Igneous activity within sedimentary basins commonly triggers the release of hydrothermal fluids. These hydrothermal fluids are expelled at the seafloor or land-surface as hydrothermal vent complexes. We aim to compare two regions where there has been extensive research on hydrothermal vent complexes: offshore mid-Norway (e.g. Planke et al., 2005) and northeast Java, Indonesia (e.g. Mazzini, 2018).

Thousands of vent complexes formed offshore mid-Norway at the time of continental break-up in the earliest Eocene (c. 55.8 Ma). The gasses released by these vents are suggested to have contributed to a major increase in global temperatures known as the Paleocene-Eocene Thermal Maximum (PETM) (Svensen et al., 2004). Additionally, petroleum exploration may be impacted due to enhanced vertical migration through the complexes, which occur at reservoir levels (Cartwright et al., 2007).

In northeast Java, magma and hydrothermal fluids migrate from the Arjuno-Welirang volcanic complex to reach the carbon-rich NE Java sedimentary basin. The interaction between the hydrothermal fluids and the sedimentary rocks of this petroleum province is interpreted to have triggered fluid overpressures which led to the May 2006 dramatic Lusi eruption. Since then, Lusi has been relentlessly active expanding over a region of 7 km^2 submerging the surrounding town and forcing the relocation of 60,000 people. The hydrothermal origin of the overpressure is based on geochemical (e.g. Mazzini et al., 2018; Inguaggiato et al., 2018; Zaputlyaeva et al., 2019), mineral thermometry (Malvoisin et al., 2018) and geophysical (Fallahi et al., 2017) studies. Close to Lusi is located the older Porong paleo-vent system.

Seismic reflection data was used to compare hydrothermal vent complexes offshore mid-Norway with the hydrothermal vent complexes in northeast Java. Offshore Norway, a recently acquired 3D seismic cube in the northern Møre and southern Vøring basins covering 15,900 km^2 was interpreted. Both a conventionally processed and shallow high-resolution volume were used. The high-resolution data has a crossline spacing of 6.25 m, an inline spacing of 18.25 m and a dominant frequency range of 50-90 Hz. 15 stratigraphic levels have been mapped within the area as part of an integrated approach using seismic, gravity and magnetic data, from seafloor to Base Cretaceous. Horizons are tied with Norwegian Sea well data. For this study the focus has primarily been the Paleocene to the earliest Eocene sediments where the vents reach the paleo-seafloor. The seismic attributes: amplitude (reflection strength) and variance (spatial reflection variability) are found to be particularly useful for mapping vent locations.

In Java, vintage onshore 2D seismic data was used with a mean frequency of c. 20 Hz. Data was used from two wells (Banjarpanji-1 and Porong-1) for stratigraphy. 21 venting conduits were identified based on where the seismic data was disrupted vertically. The focus of this study are seismic lines across Lusi and Porong. However, at the time of seismic data acquisition, Lusi had yet to erupt.

Sills are identified as high amplitude hard reflections, with abrupt reflection terminations and transgressive geometries (Fig. 1). Hydrothermal vents are characterized by distinctive eye-shaped

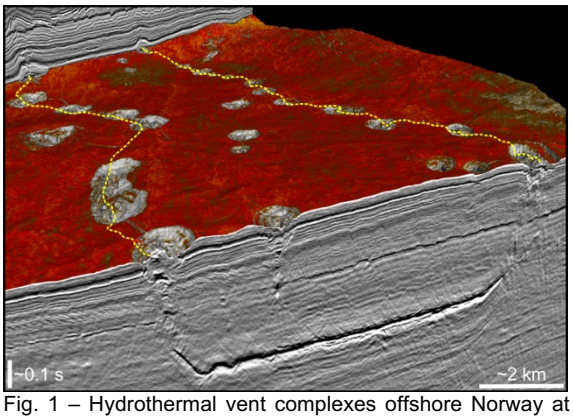

Fig. 1 – Hydrothermal vent complexes offshore Norway at Base Vent level. The hydrothermal vents appear as pale circular features in a blend of horizon amplitude and mean variance. The underlying sill is outlined in yellow. Most (but not all) hydrothermal vent complexes occur above the sill margin.

geometries in the upper part, consisting of craters or depressions with mound-like geometries above (Fig.

1). Offshore Norway the vents have clear connections to underlying sills via vertical conduits characterized by disrupted seismic reflections (Fig. 1). The close correlation between the vent locations and the underlying sills indicates their magmatic origin (Fig. 1). Deep imaging in the seismic data from Java is highly uncertain and rather geochemical and other geophysical data is used to interpret a magmatic connection.

Geometrically the hydrothermal vent complexes in Norway and Java are very similar. Both have approximately circular surface features. They both have inward dipping beds towards their central conduits (Fig. 2). The beds are interpreted to dip inwards due to the removal of fluid or rock volume at depth which is ejected at the surface during venting. Both also have bodies within their conduits (Fig. 2), suggesting complex plumbing systems and similar fluid migration processes.

Offshore Norway, within the seismic volume, many of the vents have features above them, including twenty four clustered amplitude anomalies, five singular soft-followed-by-hard

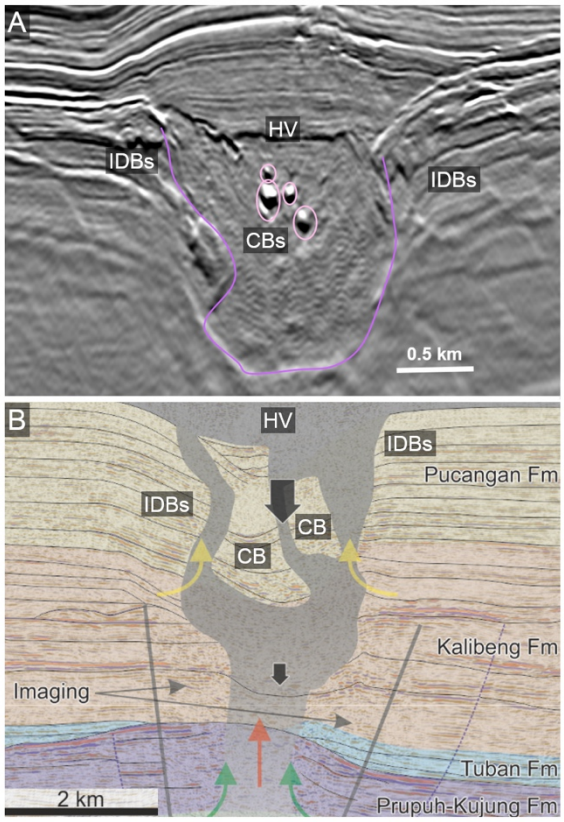

Fig. 2 – Comparison of hydrothermal vent complexes offshore Norway (A) and northeast Java (Porong) (B). In both cases hydrothermal vents (HV) occur above disrupted seismic data interpreted as conduits. Within the conduits are 'conduit bodies' (CBs). Around the conduits are inward dipping beds (IDBs).

amplitude anomalies and four mounds. The amplitude anomalies indicate the presence of localized migrated gas and the mounds indicate remobilized sediment, most likely caused by upward migrating fluids. The mounds are the shallowest of these features occurring at mid-Miocene level, indicating the vent complexes affected fluid flow tens of millions of years after forming in the earliest Eocene. The vent systems in Java are much younger, nonetheless, Lusi has shown prolonged fluid flow, indicating that the initial eruption has formed a long-lasting conduit for preferential fluid migration.

The similarities between hydrothermal vent complexes offshore Norway and in Java suggest they both formed in a similar way. In particular, that in both cases magmatic intrusions triggered upward migration of hydrothermal fluids creating circular conduits with surrounding inward dipping beds. In both cases these conduits act as pathways for long periods of fluid flow.

Acknowledgements

TGS and Lapindo Brantas are thanked for providing seismic and well data offshore Norway and Java respectively.

References

Cartwright, J., M. Huuse and A. Aplin (2007), Seal bypass systems, *AAPG Bulletin, 91, 1141-1166*.

Fallahi, M. J., A. Obermann, M. Lupi, K. Karyono and A. Mazzini (2017), The plumbing system feeding the Lusi eruption revealed by ambient noise tomography, *Journal of Geophysical Research, 122.*

Inguaggiato, S., A. Mazzini, F. Vita and A. Sciarra (2018), The Arjuno-Welirang volcanic complex and the connected Lusi system: Geochemical evidences, *Marine and Petroleum Geology, 90, 67-76.*

Malvoisin, B., A. Mazzini and S. A. Miller (2018), Deep hydrothermal activity driving the Lusi mud eruption, *Earth and Planetary Science Letters, 497, 42-49.*

Mazzini A. (2018), 10 years of Lusi eruption: Lessons learned from multidisciplinary studies (LUSI LAB), *Marine and Petroleum Geology, 90, 1-9*.

Mazzini A., F. Scholz, H. H. Svensen, C. Hensen and S. Hadi (2018), The geochemistry and origin of the hydrothermal water erupted at Lusi, Indonesia, *Marine and Petroleum Geology, 90, 52-66*.

Planke, S., T. Rasmussen, S. S. Rey and R. Myklebust (2005), Seismic characteristics and distribution of volcanic intrusions and hydrothermal vent complexes in the Vøring and Møre basins, *Geol. Soc., London, Petroleum Geology Conference series, 6, 833-844*.

Svensen, H., S. Planke, A. Malthe-Sørenssen, B. Jamtveit, R. Myklebust, T. Rasmussen-Eidem and S. S. Rey (2004), Release of methane from a volcanic basin as a mechanism for initial Eocene global warming, *Nature, 429, 542-5.*

Zaputlyaeva, A., A. Mazzini, A. Caracausi and A. Sciarra (2019), Mantle-derived fluids in the East Java sedimentary basin, Indonesia. *JGR: Solid Earth.*

Distribution and volume of Mesozoic intrusive rocks in the Parnaíba Basin constrained by well data

Diogo Michelon[1,2], Frederico Miranda[1], Egberto Pereira[2], Fernando Aragão[1,2], Sverre Planke[3]

[1] *Eneva S.A., Rio de Janeiro, Brazil* - diogo.michelon@eneva.com.br
[2] *Rio de Janeiro State University, Rio de Janeiro, Brazil*
[3] *VBPR, Oslo, Norway; CEED, University of Oslo, Norway; The Arctic University of Norway, Tromsø*

Keywords: magmatism, volume, Parnaiba Basin

The atypical igneous-sedimentary petroleum system of the Parnaíba Basin is linked to a complex network of Mesozoic dolerite sills and dykes that act as key factors for the existence of the hydrocarbon accumulations (Cunha *et al.*, 2012; Miranda *et al.*, 2018).

Thicknesses variation of the dolerite intrusions and their stratigraphic position in either the source rocks or the reservoir rocks are crucial for the efficiency of the petroleum system. Therefore, a better understanding of the magmatic emplacement processes and volumes, constrained by an accurate interpretation of these intrusive rocks, will help to improve the calibration of the geological models and reduce the exploratory uncertainties.

A common feature among the Paleozoic intracratonic basins in Brazil, such as Solimões, Amazonas, and Parnaíba basins located in the north and northeast of Brazil, are the sheet-like intrusive igneous bodies in the sedimentary sequences. Previous estimated volume of igneous rocks in these basins, based on wells and outcrops, is approximately 240,000 km³, mostly composed of dolerite sills (Wanderley Filho *et al.*, 2006).

Differently to the other intracratonic Paleozoic basins in Brazil, the Parnaíba Basin has the occurrence of two distinct large magmatic events:

- The first event is represented by the Mosquito Formation, dated as Triassic-Jurassic (200 - 160 Ma), is part of the Central Atlantic Magmatic Province (CAMP), (Marzoli *et al.* 1999) associated with the breakup of the Pangea, culminating in formation of the Atlantic equatorial ocean.
- The second event is represented by the Sardinha Formation, dated as Lower Cretaceous (130 - 120 Ma), associated to the opening of the South Atlantic Ocean (Fodor *et al.*, 1990; Marzoli *et al.*, 1999; Milani & Zalán, 1999).

Some authors have been trying to define the Mosquito and Sardinha formation boundaries using regional airborne magnetic data (Mocitaiba *et al.*, 2017) and geochronological dating of outcrop samples. As observed in Figure 1, the two magmatic events were separated into different provinces by these authors. Considering the limitations of the methods, the subsurface emplacement and occurrence of Mosquito and Sardinha formations, as well as the magma volume, could be underestimated. It is also worth to note that high-resolution geochronological data (e.g. U/Pb TIMS dating) is very sparse.

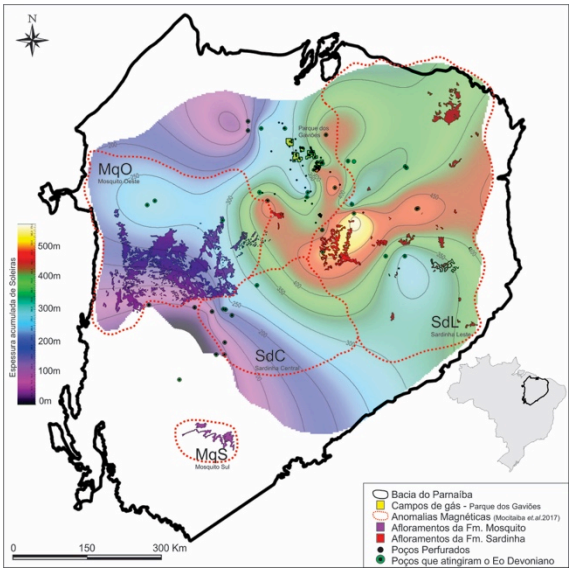

Fig. 1 – Parnaíba Basin dolerite thickness map with all drilled wells and defined features. Purple features represent the Mosquito Fm. outcrops in the west (MqO) and south (MqS). Red features represent the Sardinha Fm. outcrops in the east (SdL) and central (SdC). The dashed lines represent the limits of these formations considering the amplitude from analytic signal anomalies extracted from the airborne magnetic data and studied by Mocitaiba *et al.* (2017). The thicker part (yellow) is below the Sardinha Fm. outcrops and is confirmed by more than 500 m of dolerite sills in some wells. Thicknesses between 400 m to 500 m extends the magnetic domain outlines towards the central part of the basin, where gas fields are located.

The main exploratory gas activities are concentrated in the northern-central portion of the Parnaiba Basin where the gas field cluster is located (Figure 1). Drilled wells in this region, have confirmed the seismic interpretations and geological models that consider the presence of extended dolerite sills intrusions.

Through the integrated interpretation of igneous rocks on ca. 20,000 line km of 2D seismic data and in

170 wells it was possible to determine the continuity of the intrusions of the Mosquito and Sardinha formations in the different provinces (Figure 1). The two magmatic events are probably overlapping in the subsurface throughout the basin, including the northern-central portion that is not within the boundaries with magnetic anomalies (Figures 1 and 2).

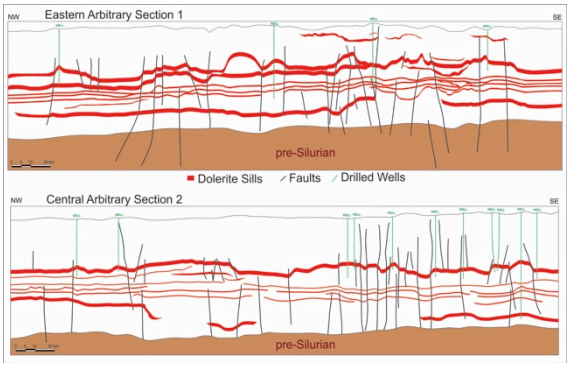

Fig. 2 – Igneous layers (red) interpreted on arbitrary seismic lines going from NW to SE. The upper section was extracted from the eastern part of the basin where many intrusive layers can be observed, including very shallow ones. The lower section was extracted from the central part of the basin across part of the gas production fields.

A thickness map of the dolerite sills was constructed based on the interpretation of the dolerite sills from all the 170 wells drilled in Parnaiba Basin, however only 40 of those reached the Lower Devonian sedimentary rocks and were input for the interpolation. The outline of the intruded basin area is constrained by seismic interpretation.

Based on the map interpretation on Figure 1, the larger dolerite thicknesses up to 500 m occurs in the central-eastern part of the basin overlapping the magnetic anomaly SdL (Sardinha East). The lower values are concentrated in the western part inside the MqO (Mosquito West) and SdC (Sardinha Central) domains. The map is showing intermediary thicknesses from 200 to 400 m outside the magnetic anomalies where it has many drilled wells. These mismatches could be caused by the sampling bias and accuracy of the different methods that is probably limiting the analyses to distinguish shallow and deep intrusive layers. Considering that the author (Mocitaiba et. Al. 2017) used the amplitude from analytic signal, the intermediary values of amplitude between Mqo and SdC over the gas fields region also represents dolerite sills anomalies although were not considered as igneous magnetic anomalies on that research.

All the results from different methodologies are good insights for the understanding of the geological complexity of the emplacement, however the integration of new data allowed to move forward and get different interpretation of the events.

Finally, the calculated volume of igneous rocks in the Parnaiba Basin sedimentary strata, based on the thickness map in Figure 1, is approximately 128,000 km^3. This magma volume estimation is just the first step in an ongoing study to improve the priority ranking of the potential prospects for the hydrocarbon accumulations in this atypical petroleum system. Since most of the wells have not reached the basement, we can affirm that the volume is underestimated. Meanwhile, we understand that this estimated volume is covering a great part of the basin with the available data and could be representative for future studies and magmatic events classification.

Acknowledgements

All the Authors kindly thanks Eneva for having authorized the submission of this abstract using the data and results, ANP and UERJ to support the research of this ongoing master's thesis.

References

da Cruz Cunha, P. R., Bianchini, A. R., Caldeira, J. L., & Martins, C. C. (2012). Parnaíba Basin–the awakening of a giant. *11th Simposio Bolivariano-Exploracion Petrolera en las Cuencas Subandinas.*

Fodor R. V., Sial A. N., Mukasa S. B., McKee E. H. (1990). Petrology, isotope characteristics, and K-Ar ages of the Maranhão, northern Brazil, Mesozoic basalt province. *Contributions to Mineralogy and Petrology*, 104(5):555-567.

Marzolli, A., Renne, P. R., Picirillo, E. M., Ernesto, M., Bellieni, G., Min, A. (1999). Extensive 200-Million-year-old continental flood basalts of the Central Atlantic Magmatic Province. *Science*, 284:616-618.

Milani, E. J. & Zalán, P. V. (1999). An outline of the geology and petroleum systems of the Paleozoic interior basins of South America. *Episodes*, 22, 199–205.

Miranda, F. S., Vettorazzi, A. L., da Cruz Cunha, P. R., Aragão, F. B., Michelon, D., Caldeira, J. L., Porsche. E., Martins, C., Ribeiro, R. B., Vilela, A. F., Corrêa, J. R., (2018). Atypical igneous-sedimentary petroleum systems of the Parnaíba Basin, Brazil: seismic, well logs and cores. *Geological Society, London, Special Publications*, 472, SP472-15.

Mocitaiba, L.S.R., de Castro, D.L. and de Oliveira, D.C., (2017). Cartografia geofísica regional do magmatismo mesozoico na Bacia do Parnaíba. *Geologia USP. Série Científica*, 17(2), pp.169-192.

Wanderley Filho, J.R., Travassos, W.A.S. and Alves, D.B., (2006). O diabásio nas bacias paleozoicas amazônicas-herói ou vilão. *Boletim de Geociências da Petrobrás*, 14(1), pp.177-184.

Santonian magmatism in Southern Santos Basin, Brazil: geophysical signature

Pinheiro Marcia[1], Gordon Andres, [2,3] and Stanton Natasha.[3]

[1] *Ecopetrol, Rio de Janeiro, Brazil, m2pinheiro@hotmail.com.*
[2] *AG-GEO Consulting, Rio de Janeiro, Brazil*
[3] *Universidade do Estado de Rio de Janeiro (UERJ), Rio de Janeiro, Brazil*

Keywords: *Santos Basin, Santonian magmatism, seismic.*

The Santos Basin, located on the Southeastern Brazilian margin (SEBM), is part of a continental rift system developed during the Early Cretaceous as a consequence of the breakup of Western Gondwana and subsequently evolving into a passive divergent margin (Fig.1).

On the SEBM, the onset of rifting and break up was associated with voluminous magmatism. Onshore the magmatic events comprise large tholeiitic flood basalts (Paraná LIPs), alkaline and tholeiitic dike swarms, and alkaline-carbonatitic dykes and plugs. Offshore, lava flows, dikes, sills, volcanic cones and SDRs have been recorded in seismic, magnetic and borehole data.

The regional compilation of published radiometric ages from onshore and offshore Meso-Cenozoic rocks indicate a long-term magmatic history ranging from 150 to 50 Ma. The stratigraphical record of Santos Basin is divided into basement, syn-rift, post-rift and drift supersequences with coeval magmatic pulses in Barresian/ Barremian, Aptian, Santonian/Campanian and Eocene times. Magmatism of Santonian age has been described offshore in Northern Santos Basin in seismic and well records, and in onshore dike swarms along the coast of Rio de Janeiro and São Paulo states (Moreira et al, 2005; Oreiro, 2006).

This study was conducted using a large 2D and 3D seismic dataset, exploration boreholes offshore, and magnetic data, as well as published radiometric dating and geochemical analysis of magmatic rocks. This contribution focus on the seismic characterization of magmatic intrusion and extrusions of Santonian age in the Southern Santos Basin (SSB).

The 3D seismic expression of the Santonian magmatism in the SSB, consist of volcanic cones, lava flows, magma conduits, sills and possible laccoliths. At least, 14 magmatic bodies have been identified, although they had not been drilled yet, the Santonian age has been assigned by correlation with neighbor wells with biostratigraphy data (Fig.1).

The distribution of magmatic bodies seems to be tectonically controlled by a NE-SW trending fault system (Figs. 1 and 2). In the analytic signal magnetic map of Fig. 1, there is a clear separation in the location of the magnetic sources. They are abundant at the east of the interpreted magnetic lineament (black and red dash line on Fig.1), and absent west of it. Magnetic sources, in the area of study, are interpreted to be related to magmatic products and the regional magnetic lineament of Fig.1 seems to be an important tectonic control in the regional distribution of magmatism.

Volcanic edifices

The volcanoes exhibit a rounded base in the order of 3 to 9 Km long and a range of heights from 170 to 250 TWT msec. (~320 to 475 m, assuming an average velocity of 3800 m/sec). In map view, the volcanic cones are aligned (blue arrows in Fig. 2), and in seismic section they display a close relationship with deep crustal faults (Figs. 3 and 4). Often, the volcanoes display an internal structure of stacking with a lateral-shift pattern of bright reflector, indicative of migration of the younger lavas during the eruption. Systematically, in all mapped volcanoes, the passage from the sedimentary host rock to the magmatic rocks correspond to a decrease in acoustic impedance. This observation can be supported by well SPS39 (Fig.1), drilled 120 Km northeast of the study area. Well SPS39 drilled 6 layers of tuffaceous rocks, summing up ~140 m thick, with an average sonic velocity and density values of 3800 m/sec and of 2.3 gr/cm^3. In this analog well, the volcaniclastic rocks are embedded in Santonian shales with average velocities of 4200 m/sec and densities of 2.45 gr/cm^3. This contrast in acoustic impedance supports the observed decrease in reflectivity. The volcanoes, in the area of study, are located beyond the Santonian shelf break (Fig.1), the eruptions are likely to be in a submarine environment and compositionally, hyaloclastic breccias are expected.

Magma intrusions and conduits

The good-quality of the 3D seismic reveal the presence of roots in the volcanic edifices with an inverted cone-shape and magma feeder conduits (Fig.3). These conduits (dikes?), crosscut the sedimentary section connecting the volcanoes base with old deep faults system (Fig.3).

Sill intrusions are abundant, mainly at the south west corner of the study area (Fig.2). These intrusions are characterized by high-amplitude reflections crosscutting the sedimentary section and commonly forming saucer-shaped geometries. The increase in the acoustic impedance may be indicative of dense magmatic rocks (diabases?). In seismic sections, some magmatic intrusions, interpreted as laccolith, display a biconvex shape, an increase in the acoustic impedance contrast, a concordant emplacement curving the overlying strata creating "drape" folds (Fig. 4).

The Santonian magmatism in SSB appears to be tectonically controlled by the reactivation of deep faults probably during the change of rotation poles between South American and African since 80 Ma ago.

References

Moreira, J.L.P., Esteves, C.A., Rodrigues, J.J.G., and C.S Vasconcelos (2005).Magmatism, sedimentation and stratigraphy of the northern region of Santos Basin, *Boletim de Geociências da Petrobras,* 14(1), 161-170.

Oreiro, S. G. (2006). Interpretação sismica dos eventos magmáticos pósaptianos no alto de Cabo Frio. sudeste do Brasil, gênese e relação com os lineamentos pré-sal, *Phd Thesis, Universidade do Estado do Rio de Janeiro*, p 160.

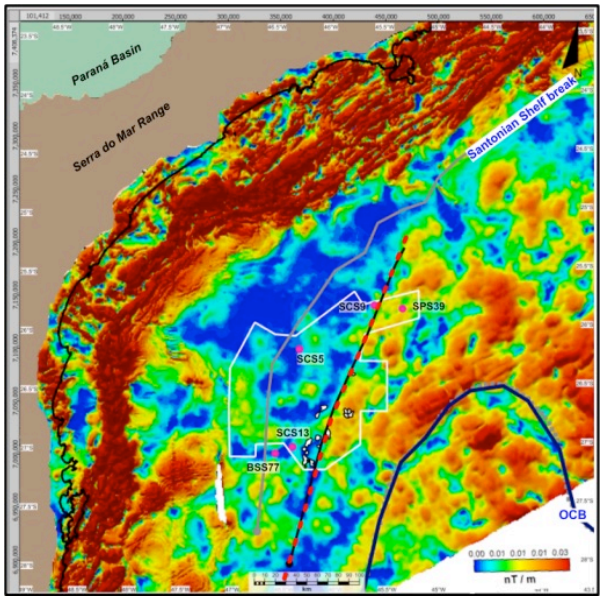

Fig. 1 – Analytic signal magnetic map of SBB. Displaying the location of 3D seismic (white line polygon); key wells (magenta dots); Santonian shelf-break (gray line), regional magnetic lineament (black line with red dash); Santonian magmatic bodies (white fill polygons), and Ocean-crust boundary (OCB-dark blue line).

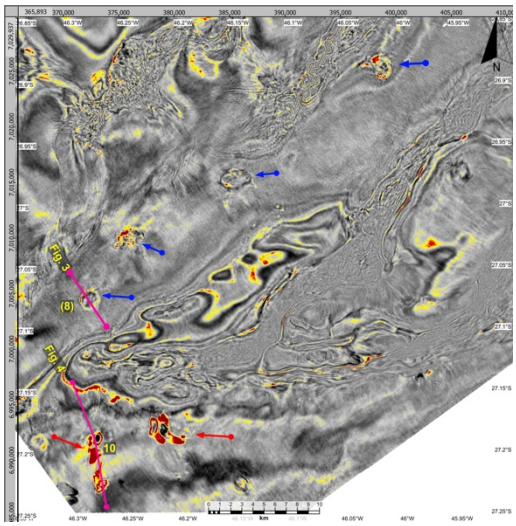

Fig. 2 – 3D seismic flatten time slice (420 msec. down from Top Maastrichtian) displaying the map view of volcanic edifices (blue arrows) and sill intrusions (red arrows).

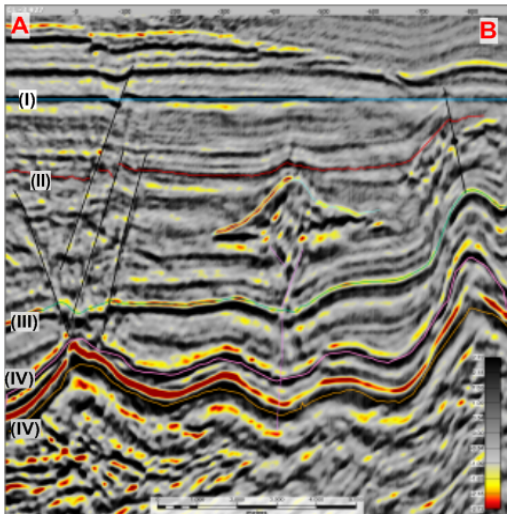

Fig. 3 – Example of volcanoes and magma feeder conduit (flatten at Top Maastrichtian). Dip view of volcanic cone (8). Horizon: (I)Top Maastrichtian, (II)Top Santonian, (III)Top Turonian, (IV)Top Salt, and (V) Base of Salt/Top Rift.

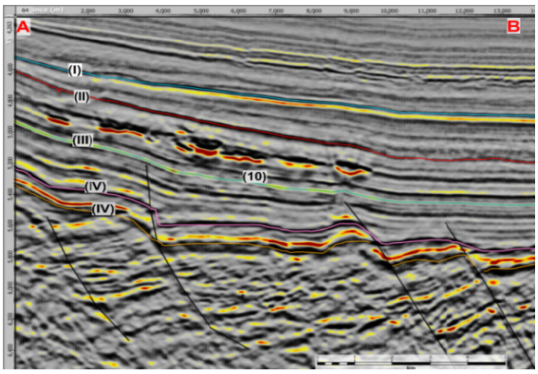

Fig. 4 – Seismic arbitrary line example across a series of sills units (e.g. sill unit 10). Line location in Fig. 2 and horizons reference / legend are the same as in Fig. 3.

From field observations to seismic modeling: The El Manzano Sill Complex (Argentina) as a showcase of the influence of igneous intrusions on petroleum systems

Rabbel O.[1], Galland O.[1] , Palma, O. [2], Spacapan, J.B. [2], Lecomte, I.[3], .and Mair K.[1]

[1] *The NJORD Centre, Department of Geoscience, University of Oslo, Oslo, Norway* – ole.rabbel@geo.uio.no
[2] *Y-TEC / YPF, La Plata, Argentina*
[3] *Department of Earth Science, University of Bergen, Bergen, Norway*

Keywords: Igneous intrusions, petroleum system, seismic modelling.

Igneous intrusions are present in many sedimentary basins with ongoing hydrocarbon production and exploration around the world. Such intrusions pose an important risk in hydrocarbon exploration, because they may affect all parts of a petroleum system, i.e. charge, migration, reservoir, trap, and seal (Senger et al 2017).

Prominent examples include the Neuquén Basin in Argentina, the Møre-Vøring Basins offshore Norway, Faroe-Shetland Basin in the North Atlantic, the Taranaki Basin in New Zealand as well as several basins onshore eastern China (see review by Senger et al. 2017). It is therefore crucial to properly quantify the volume, distribution and timing of igneous intrusions in prospective volcanic basins. A large part of our understanding of such intrusive complexes stems from geophysical studies, especially seismic interpretation studies. This is due to strong geophysical property contrasts with siliciclastic host rocks, which makes the detection of intrusions in seismic data relatively easy, as long as their thickness lies within the resolution limit of the available data (Planke et al 2015, Magee et al 2015).

In many cases, seismic interpretation is aided by field observations of igneous intrusions, commonly to draw an analogy to intrusion shapes that are observed in outcrops. Such studies may include seismic forward modeling to explore resolution and tuning effects based on simplified models (e.g., Planke et al 2015, Magee et al 2015), while recently real intrusion shapes from virtual outcrop models have been used to create more realistic seismic models (Eide et al 2018, Rabbel et al 2018).

However, two important aspects are often missing, or at least underrepresented, in the available literature: (1) acknowledging the range of possible geophysical properties of both intrusions and host rocks, and (2) integrating field-scale observations of the effects of intrusions on the petroleum systems with seismic-scale modeling studies. This is a challenging task, because it requires localities allowing such field observations (which are very rare), but also localities that provide seismic-scale outcrops. Field localities offering this kind of data integration could lead to a more holistic understanding of petroleum systems affected by igneous intrusions

Here, we present the El Manzano field locality (Figure 1a), which allows us to address the issues mentioned above. It includes an extremely well exposed, kilometer-scale sill complex emplaced in organic-rich shale, close to the Río Grande Valley in the northern Neuquén Basin, Argentina. The sill complex is a direct outcrop analogue to subsurface sills acting as oil reservoirs in the Río Grande valley oil fields, only some few kilometers east of El Manzano (Spacapan et al. 2018).

Preliminary results from detailed fieldwork direct evidence of the effects of intrusions on hydrocarbon maturation and migration. We observe measurable maturation aureoles around the intrusions, as well as abundant bitumen-filled fractures both within and around intrusions emplaced in the Agrio source rock. Some of these fractures take the form of dykes with thicknesses of several decimeters, and they locally seem to form injection structures associated with brecciation of adjacent rocks (Figure 2).

Additionally, we present the results of a seismic forward modeling study based on a modeling approach that integrates virtual outcrop models with well data to account properly for both realistic intrusion geometries and host rock property variations (Figure 1b). Our model results illustrate the strong effect that varying seismic properties of the host rock and sill intrusions can have on their seismic expression, e.g. when high-impedance sedimentary rocks (evaporates, carbonates) are involved, or sills are heavily fractured or altered. Depending on the resulting seismic property contrast, the reflections can be the “typical” high amplitude events, or show low to medium amplitude, well as complex interference patterns due to interactions between several intrusions and the host rock. This highlights that seismic forward modeling is only meaningful as a tool to aid seismic interpretation if (1) model properties are calibrated using relevant data, e.g. from local wells, and (2) both host rock and sill geometries

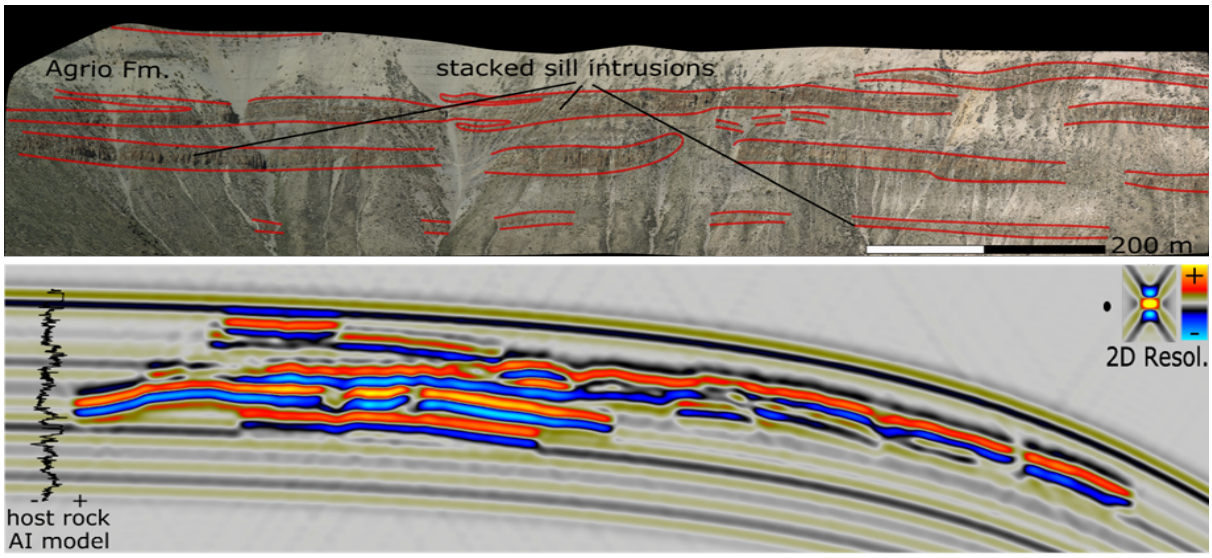

Fig. 1 – (a) Orthophoto of a part of the El Manzano sill complex with several sill intrusions and host rock intervals indicated. (b) Example of a seismic forward modelling result based on a host rock acoustic impedance model derived from well data and real sill geometries from El Manzano.

Fig. 2 – Dyke of solidified bitumen in El Manzano cross-cutting an andesitic sill (brown), and its baked shale host rock (grey). The stick next to the dyke is 1m long.

reflect the complexity that can be expected in the data.

With both detailed geological observations and seismic modeling data available from a single field location, the El Manzano locality can be considered a showcase for many aspects related to the presence of igneous intrusions in petroleum systems. Thus, El Manzano not only is of interest as a direct analogue for economically relevant oil fields in the Neuquén Basin, but also holds enormous educational potential for geoscientists working on related topics.

References

Eide, C.H., Schofield, N., Lecomte, I., Buckley, S.J., Howell, J.A., 2018, "Seismic interpretation of sill complexes in sedimentary basins: implications for the sub-sill imaging problem", *Journal of the Geological Society*, 175(2), p.193-209.

Magee, C., Maharaj, S.M., Wrona, T., and C. A.-L. Jackson, C.A.L., 2015. "Controls on the expression of igneous intrusions in seismic reflection data". *Geosphere* 11.4, p. 1024–1041

Planke, S., Svensen, H.H., Myklebust, R., Bannister, S., Manton, B., Lorenz, L., 2015, "Geophysics and remote sensing", *Advances in Volcanology*, Springer

Rabbel, O., Galland, O., Mair, K., Lecomte, I., Senger, K., Spacapan, J.B., Manceda, R., 2018, "From field analogues to realistic seismic modelling: a case study of an oil-producing andesitic sill complex in the Neuquén Basin, Argentina", *Journal of the Geological Society*, pp.jgs2017-116

Senger, K., Millett, J., Planke, S., Ogata, K., Eide, C.H., Festøy, M., Galland, O., Jerram, D.A., 2017, "Effects of igneous intrusions on the petroleum system: a review", *First Break*, 35(6), p.47-56.

Spacapan, J. B., Palma, J. O., Galland, O., Manceda, R., Rocha, E., D'Odorico, A., & Leanza, H. A. (2018). Thermal impact of igneous sill-complexes on organic-rich formations and implications for petroleum systems: A case study in the northern Neuquén Basin, Argentina. *Marine and Petroleum Geology*, *91*, 519-531.

Early Cretaceous igneous intrusions in Svalbard: seismic modelling as a link between boreholes, outcrops and seismic data

Senger K.[1], Betlem P.[1], Rabbel O.[2], Galland O.[2] and Lecomte I.[3]

[1] *Department of Arctic Geology, University Centre in Svalbard, Longyearbyen, Norway* – kim.senger@unis.no
[2] *Physics of Geological Processes, University of Oslo, Oslo, Norway*
[3] *Department of Earth Science, University of Bergen, Bergen, Norway*

Keywords: Spitsbergen, fluid flow, dolerite.

Igneous intrusions have a profound influence on subsurface fluid flow, with consequences for groundwater exploration, CO_2 sequestration and petroleum exploration (e.g., Senger et al., 2017). Quantifying the influence of igneous intrusions on fluid migration requires a solid understanding of the geometry of the igneous plumbing system. Fluid flow in and around intrusions is often related to the contact metamorphic aureoles, which are typically characterized using outcrop or borehole data. In this contribution, we investigate the effect that contact aureoles have on the seismic imaging of igneous intrusions.

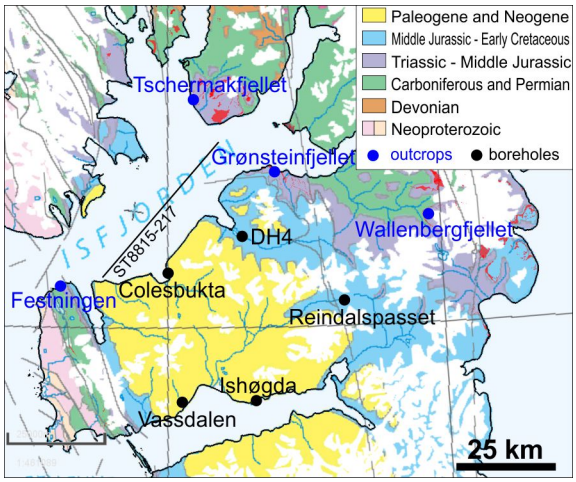

Fig. 1 – Geological map of the central Spitsbergen study area, locating key outcrops and the exploration boreholes that have penetrated igneous sills. The base map is provided by the Norwegian Polar Institute, and the igneous intrusions are highlighted in red.

In central Spitsbergen, field work, research drilling and 2D seismic interpretation has allowed identifying numerous sills and dykes in a reservoir-cap rock system targeted for CO_2 storage (Fig. 1; Senger et al., 2013). These intrusions, including one dyke cutting the reservoir-cap rock interface, are thought to create vertical baffles (i.e. dykes) but also intra-formational seals (i.e. sills) as encountered in several petroleum exploration boreholes in Svalbard. Even thin sills (2.2 m thick) generate significant contact metamorphic aureoles with reduced TOC, reduced porosity and enhanced fracturing. In Svalbard, the thorough documentation of contact metamorphic aureoles is presently missing from the petroleum exploration boreholes, even though at least five of the boreholes penetrate igneous intrusions (Senger et al., 2013). The Early Cretaceous predominantly basaltic intrusions exposed in Svalbard belong to the High Arctic Large Igneous Province and are relatively easily accessible in central Spitsbergen (Fig. 1).

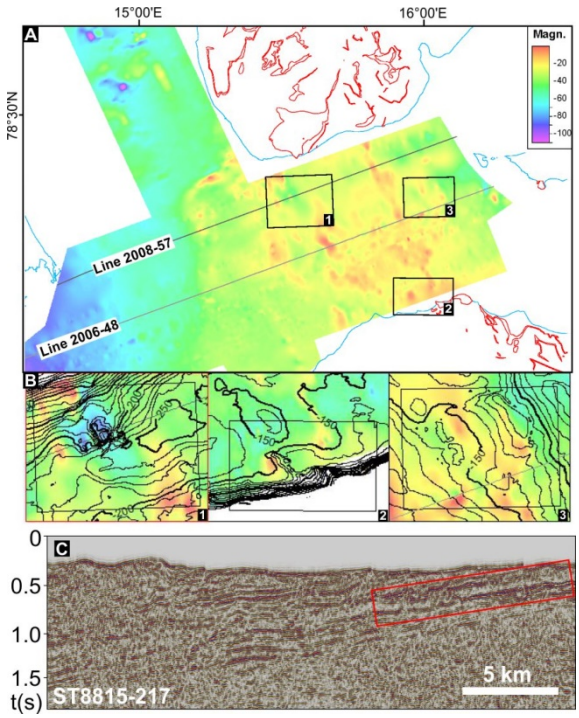

Fig. 2 – A) Ship-based magnetic data from the study area illustrating the connection between the onshore exposures on the northern and southern shores of Isfjorden. B) Zoom-in on magnetically anomalous features, including a possible hydrothermal vent complex (1), a feeder dyke system (2) and an igneous sill outcropping on the seafloor (3). Figure from Senger et al., (2013). C) Offshore 2D seismic line illustrating the overall stratigraphic dip and high-amplitude discontinuous reflectors interpreted as igneous intrusions, particularly prevalent in the area highlighted by the red rectangle. Refer to Fig. 1 for location.

In this contribution, we characterize the full range of igneous geometries exposed in central Spitsbergen,

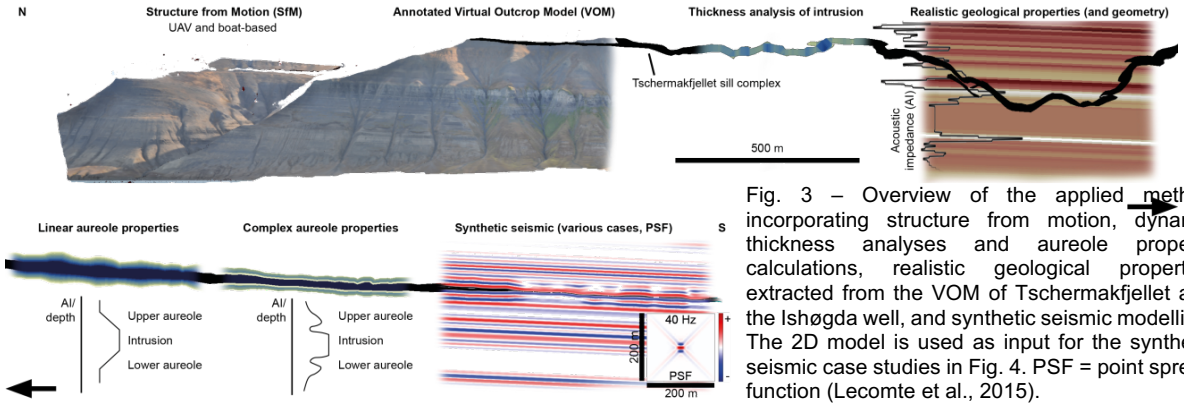

Fig. 3 – Overview of the applied method incorporating structure from motion, dynamic thickness analyses and aureole property calculations, realistic geological properties extracted from the VOM of Tschermakfjellet and the Ishøgda well, and synthetic seismic modelling. The 2D model is used as input for the synthetic seismic case studies in Fig. 4. PSF = point spread function (Lecomte et al., 2015).

utilizing virtual outcrop models (VOMs) and onshore-offshore 2D seismic data (Fig. 2). Secondly, we use well data to document the petrophysical signature of the intrusions, the associated contact metamorphic aureoles and the host rock, and implement our findings into outcrop-based seismic modelling (Fig. 3), building on the methodology presented by Rabbel et al. (2018). Implementing various contact metamorphic aureole scenarios sheds light on the impact of increasingly complex contact metamorphic aureoles on seismic imaging (Hagevold, 2019). Here we attempt to investigate how increasingly complex contact metamorphic aureoles, and highly cemented host rocks, may cause challenges for interpreters working on volcanic basins.

Fig. 2 illustrates the geophysical characterization of the intrusions through magnetic and seismic data. In addition, fieldwork and complementary acquisition of virtual outcrop models provides control on the wide range of intrusion geometries, including dykes, sills and transgressive sill segments Boreholes provide further constraints on the thickness and internal characteristics of the contact metamorphic aureoles (Fig. 3).

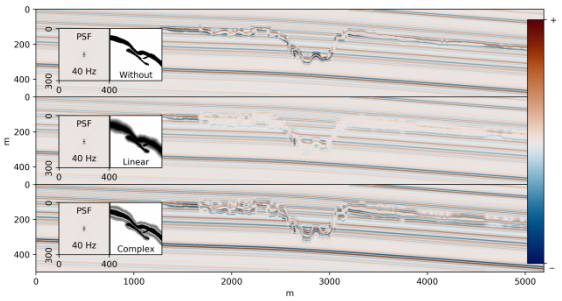

Fig. 4 – Comparison of the impact of different aureole types on seismic modelling (including host rock complexity). Insets indicate PSF (40 Hz) and aureole type. Featured aureole thicknesses are up to 200% of the sill thickness. Note the strong aureole-related non-visibility in the linear aureole scenario.

The highly cemented host rocks in Svalbard exhibit much higher velocities compared to normally compacted basins, thereby reducing the velocity contrast between the host rocks and the igneous intrusions. This is further reduced by the presence of contact metamorphic aureoles, which in linear transition (Fig. 3) cases give rise to a gradual change in properties (e.g., velocity) over the aureole's thickness (Fig. 4). More complex aureoles with enhanced fracture zones give rise to an acoustic impedance dip directly adjacent to the intrusion. In some cases, this improves the contrast to near aureole-less levels, depending on dominant frequency and local geometry and properties of both intrusion and host rock (Fig. 4).

Acknowledgements

This project has been partly funded by the University of the Arctic, the Research Centre for Arctic Petroleum Exploration and the University Centre in Svalbard. We sincerely appreciate an academic license of SeisRoX from NORSAR.

References

Hagevold, S., 2019, From outcrop to synthetic seismic: an integrated study of Botneheia, Central Spitsbergen. MSc thesis, University of Bergen.

Lecomte, I., Lubrano-Lavadera, P., Anell, I., Buckley, S. J., Schmid, D. W. & Heeremans, M. 2015: Ray-based seismic modeling of geologic models: Understanding and analyzing seismic images efficiently. Interpretation 3, SAC71-SAC89.

Rabbel, O., O. Galland, K. Mair, I. Lecomte, K. Senger, J. B. Spacapan, and R. Manceda, 2018, From field analogues to realistic seismic modelling: a case study of an oil-producing andesitic sill complex in the Neuquén Basin, Argentina: Journal of the Geological Society.

Senger, K., et al., 2013, Geometries of doleritic intrusions in central Spitsbergen, Svalbard: an integrated study of an onshore-offshore magmatic province with implications on CO2 sequestration: Norwegian Journal of Geology, 93, 143-166.

Senger, K., J. Millett, S. Planke, K. Ogata, C. Eide, M. Festøy, O. Galland, and D. Jerram, 2017, Effects of igneous intrusions on the petroleum system: a review: First Break, 35, no. June, 10.

Flat-topped uplifts bounded by peripheral faults associated with sill emplacement in the Tarim Basin, China

Zewei Yao[1,2], Guangyu He[1], Chun-Feng Li[2,3] , Chuanwan Dong[1], Xiaoli Zheng[4]

[1] *School of Earth Sciences, Zhejiang University, Hangzhou, China 310027*
[2] *Ocean College, Zhejiang University, Zhoushan, China 316021*
[3] *Laboratory of Marine Mineral Resources, Qingdao National Laboratory for Marine Science and Technology, Qingdao 266237, China*
[4] *Korla branch of BGP, CNPC, Korla 841000, China*

Keywords: Peripheral fault, Forced-folding, Saucer-shaped sills

Email address: zealway@zju.edu.cn (Zewe Yao)

Sill emplacement at shallow depth can cause overburden deformation and surface uplift. Understanding the detailed mechanism of overburden deformation is important because the uplifting process and deformation pattern (e.g. forced folding or ground deformation) are widely used to constrain the time and mechanism of sill emplacement (Schmiedel et al., 2017; Reeves et al., 2018). It is suggested that host rock uplifting above sill intrusions in sedimentary basins can be dominated by folding which has a dome shape or by faulting which has a flat top that is bounded by peripheral faults (Thomson, 2007). However, most of observed natural sills are associated with dome-shaped forced folds (Hansen and Cartwright, 2006).

In this paper, we, for the first time, present vivid examples of flat-topped, peripheral faults-bounded forced folds above saucer-shaped sills from the Tarim Basin, China (Fig. 1 and 2). The peripheral faults form at the terminations of inclined sheets or flat outer sills of saucer-shaped sills and their dip angles are distinctly larger than those of inclined sheets and flat outer sills. In plan view the peripheral faults which show a semicircular shape are coincide well with the edges of underlying saucer-shaped sills (Fig. 2). These observations indicate that these faults are induced by sill emplacement and formed accompanied with the flat-topped surface uplift. Thus, these faults are named by peripheral faults in this paper followed Johnson and Pollard (1973). The abstract can be submitted either as a .DOC or .RTF file. The .DOC format is preferred for abstracts including figures to keep the file size as low as possible.

It is interesting to note that the peripheral faults were preferentially formed in the shallower edges of a saucer-shaped sill. This phenomenon corroborates the results of analogous experiments of Galland (2012), in which steeper parts of the uplifted areas of the surface located the shallower parts of the underlying intrusion. The structural styles of the peripheral faults differ from a single outward-dipping reverse fault to an outward-dipping reverse fault linked to an inward-dipping normal fault (Fig. 3). Encouraged by the evolution of a caldera collapse with comparable fault styles (Acocella, 2007), fault pattern from the Fig. 3a to c may be the evolution path of a peripheral fault controlled by the growing thickness of the corresponding underlying sill.

In general, the peripheral faults and flat-topped uplift associated with sill emplacement discovered in the Tarim Basin have broad implications for both sill growth and the deformation of the host rock.

Acknowledgements

We would like to thank the SINOPEC Northwest Oilfield Com-pany for the permission to publish the seismic and borehole data used in this paper.

References

Acocella, V. (2007), Understanding caldera structure and development: An overview of analogue models compared to natural calderas. *Earth-Sci. Rev.* 85 (3-4), 125-160.

Galland, O. (2012), Experimental modelling of ground deformation associated with shallow magma intrusions. *Earth Planet. Sc. Lett.* 317-318, 145-156.

Hansen, D.M. and Cartwright, J. (2006) The three-dimensional geometry and growth of forced folds above saucer-shaped igneous sills. *J. Struct. Geol.* 28 (8), 1520–1535.

Johnson, A.M. and Pollard, D.D. (1973), Mechanics of growth of some laccolithic intrusions in the Henry mountains, Utah, I. *Tectonophysics.* 18 (3), 261-309.

Reeves, J., C. Magee and C. A. Jackson, (2018), Unravelling intrusion-induced forced fold kinematics and ground deformation using 3D seismic reflection data. *Volcanica.* 1 (1), 1-17.

Schmiedel, T., O. Galland, and C. Breitkreuz (2017), Dynamics of Sill and Laccolith Emplacement in the Brittle Crust: Role of Host Rock Strength and Deformation Mode. *Journal of Geophysical Research: Solid Earth*. 122 (11), 8860-8871.

Thomson, K. (2007), Determining magma flow in sills, dykes and laccoliths and their implications for sill emplacement mechanisms. *B. Volcanol.* 70 (2), 183-201.

Yao, Z., G. He, C. Li and C. Dong (2018), Sill geometry and emplacement controlled by a major disconformity in the Tarim Basin, China. *Earth Planet. Sc. Lett.* 501, 37-45.

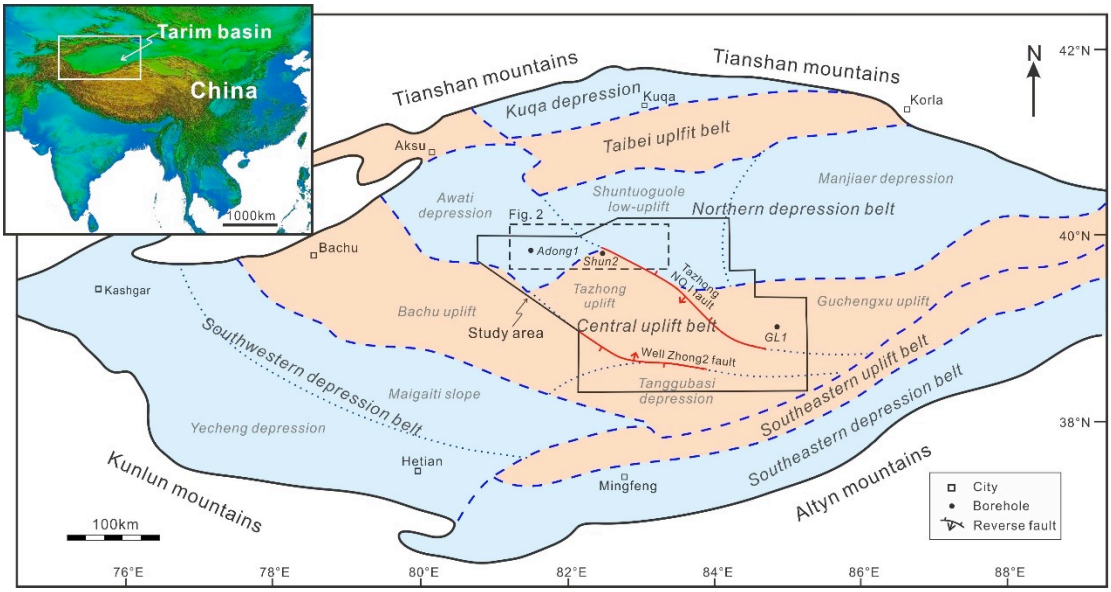

Fig. 1. Tectonic setting of the Tarim Basin (modified from Lin et al., 2012 and Yao et al., 2018). The inlet is the topographic image from Consultative Group on International Agricultural Research – Consortium for Spatial Information (CGIAR-CSI), showing the location of the basin.

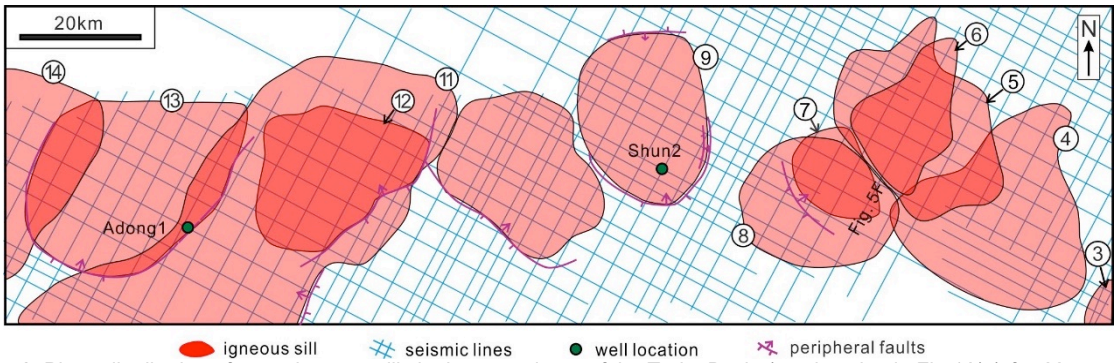

Fig. 2. Plane distribution of some igneous sills in the central part of the Tarim Basin (see location in Fig.1A) (after Yao et al. (2018)). Each sill is marked consecutively with a number in a circle.

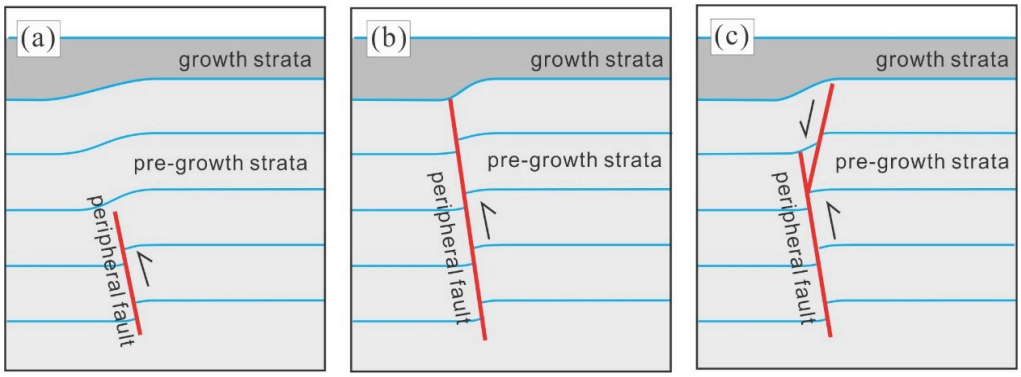

Fig. 3. Three different structural styles of peripheral faults. (a) The fault only cuts lower parts of the strata, but the deformation involves the entire part of the pre-growth strata. (b) The fault cut through the entire part of the pre-growth strata. (c) The peripheral fault is composed of a lower reverse fault and an upper normal fault.

Session on Modelling Volcanic Plumbing Systems

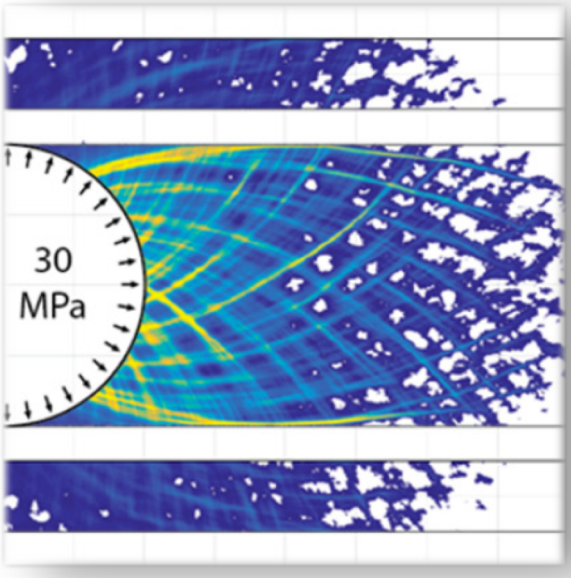

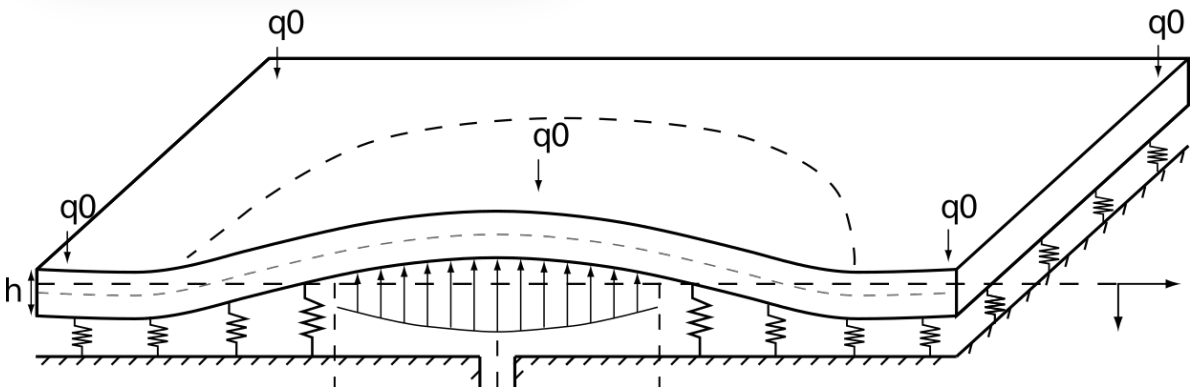

Contents

Volcano plumbing systems envisioned as complex dynamic networks

Annen C.[1], Nguyen-Huu T.[2, 3], Lesieur C.[2,4]

[1] *Univ. Grenoble Alpes, Univ. Savoie Mont Blanc, CNRS, IRD, IFSTTAR, ISTerre, 38000 Grenoble, France–* Catherine.annen@univ-savoie.fr
[2] *Institut Rhônalpin des systèmes complexes, IXXI-ENS-Lyon, 69007, Lyon, France*
[3] *Sorbonne Université, IRD, UMMISCO, F-93143, Bondy, France*
[4] *AMPERE, CNRS, Univ. Lyon, 69622, Lyon, France*

Keywords: Magmatic systems, complex networks, volcanic eruptions

Complex systems are widespread in nature. They are characterized by self-similarity, scale-invariance, and non-linearity. According to a series of observation that we detail below, volcanic plumbing systems are complex networks.

Self-similarity in volcanism and plutonism is spatial and temporal. Pelletier et al. (1990) showed that volcanic centers and plutons spatial distribution exhibits self-similar clustering and their analysis of a radiometric ages database shows temporal self-similar clustering.

Volcanic activity is characterized by cycles of high and low activity on the scale of ten thousand years. Within high activity periods, fluctuations are discernable on the scale of thousand years. Activity periods are marked by series of eruptions that last months or years and that are punctuated by explosions that last only minutes.

Multiple length and times scales are also observed on intrusions with batholiths being formed of plutons, plutons of magmatic units, and units of sills or dykes. Geochronology and heat transfer computation (Annen et al, 2015) indicates that for the granitic laccolith Torres del Paine (Chile) a few hundred thick units build by addition of metric or decametric sills over a few millennia and the entire laccolith was built over about 100,000 years (Fig. 1). If we assume that sills are emplaced over a few days or weeks, the relationship between sill/unit/laccolith thicknesses and the duration of their emplacement follows a power law typical of complex systems.

The complex character of magmatic systems is also recognizable in the relationship between the intensity or magnitude of volcanic eruptions and their return periods, which also follows a power law. Interestingly, this relationship seems to break for the largest eruptions. It suggests that a different mechanism controls the largest eruptions and the smaller ones (Deligne et al, 2010), although Papale (2018) attributes this apparent discrepancy to a statistical artefact and to the rarity of the large eruptions.

Networks are present at several scales in magmatism (Fig. 2): chains of silica in melts and crystal lattices in minerals, networks of crystals, melt, and gas channels in magma reservoirs, networks of veins, dyke and sills within magma bodies or intruding the country rock.

Fig. 1 – Torres del Paine laccolith (Chile) is formed of units that are themselves composed of sills. Picture in Annen et al (2015)

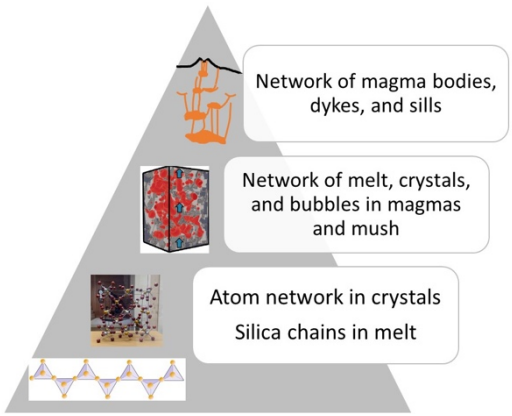

Fig. 2 – Networks at the different scales of magmatic systems from atomic scale to crustal scale. Pictures and cartoons from Parmigiani et al (2017), Earle open textbook https://opentextbc.ca/geology/, and Ji-Elle CC BY-SA 4.0, https://commons.wikimedia.org/w/index.php?curid=66340173

There is also a growing body of evidence that magma chambers and melt reservoirs form networks

that connect before or during eruptions. Beneath some active volcanoes, seismic and geodetic records point to a series of magma chambers or melt reservoirs at different levels in the crust (e.g. Elsworth et al, 2008, Dahren et al, 2012), in agreement with geochemical and petrological analysis of erupted products that indicate that magmas evolved at different pressure (e.g. de Silva and Gosnold, 2007). There are also evidence of magma reservoirs coexisting at the same level. Geochemical studies indicate that large caldera-forming eruptions drain several distinct magma pockets (Allan et al, 2012, Ellis and Wolff, 2012, Gualda and Ghiorso, 2013).

The network structure of magmatic systems is inherent in the model of transcrustal mush proposed by Cashman et al (2017) although a network of magma reservoirs does not necessarily require the presence of a transcrustal mush.

Envisioning magmatic systems as complex dynamic networks leads us to ask new sorts of questions. The plutonic/volcanic volume ratio is typically high (Crisp, 1984). Does this mean that volcanic eruptions correspond to an instability of the system? Are they the result of a form of cascading failures? Are volcanoes poorly connected peripheral nodes of the magma network? Are rare large caldera-forming ignimbrite eruptions (super-eruptions) related to magma stalling at one node of the network, with a giant magma chamber forming as a sort of major magma traffic jam, or, on the contrary, are super-eruptions the result of the destabilization and mobilization of a series of reservoirs, which get suddenly connected? In the first case, a large eruption would be linked to a reduced network connectivity, while in the second case it would be related to an increased network connectivity.

The behavior of a complex system can hardly be reduced or inferred from the properties of its constituents due to the emergence of new phenomenon at the global scale. Therefore, the information acquired on one or even several magma chambers is not sufficient to predict the evolution of the magmatic system as a whole. This means that our ability to forecast volcanic eruptions may remain limited until we progress in our knowledge of the behavior of magma chambers and conduits as a complex network. Therefore, a better understanding of the dynamics of the system might significantly increase the reliability of short term predictions.

Acknowledgements

C.A. received funding from the European Union's Horizon 2020 research and innovation program under the Marie Sklodowska-Curie grant agreement No. 794594

References

Allan, A. S. R., Wilson, C. J. N., Millet, M.-A., & Wysoczanski, R. J. (2012). The invisible hand: Tectonic triggering and modulation of a rhyolitic supereruption. Geology, 40(6), 563-566. https://doi.org/10.1130/g32969.1

Annen, C., Blundy, J. D., Leuthold, J., & Sparks, R. S. J. (2015). Construction and evolution of igneous bodies: Towards an integrated perspective of crustal magmatism. Lithos, 230, 206-221.

Cashman, K. V., Sparks, R. S. J., & Blundy, J. D. (2017). Vertically extensive and unstable magmatic systems: A unified view of igneous processes. SCIENCE, 355(6331).

Crisp, J. A. (1984). Rates of magma emplacement and volcanic output. Journal of Volcanology and Geothermal Research, 20, 177-211.

Dahren, B., Troll, V., Andersson, U., Chadwick, J., Gardner, M., Jaxybulatov, K., & Koulakov, I. (2012). Magma plumbing beneath Anak Krakatau volcano, Indonesia: evidence for multiple magma storage regions. Contributions to Mineralogy and Petrology, 163(4), 631-651.

Deligne, N. I., Coles, S. G., & Sparks, R. S. J. (2010). Recurrence rates of large explosive volcanic eruptions. Journal of Geophysical Research, 115(B6). https://doi.org/10.1029/2009JB006554

de Silva, S. L., & Gosnold, W. D. (2007). Episodic construction of batholiths: Insights from the spatiotemporal development of an ignimbrite flare-up. Journal of Volcanology and Geothermal Research, 167(1-4), 320-335.

Ellis, B. S., & Wolff, J. A. (2012). Complex storage of rhyolite in the central Snake River Plain. Journal of Volcanology and Geothermal Research, 211-212(0), 1-11.

Elsworth, D., Mattioli, G., Taron, J., Voight, B., & Herd, R. (2008). Implications of magma transfer between multiple reservoirs on eruption cycling. Science, 322(5899), 246-248.

Gualda, G. R., & Ghiorso, M. (2013). The Bishop Tuff giant magma body: an alternative to the Standard Model. Contributions to Mineralogy and Petrology, 166(3), 755-775. Papale, P. (2018). Global time-size distribution of volcanic eruptions on Earth. Scientific Reports, 8(1), 6838.

Parmigiani, A., Degruyter, W., Leclaire, S., Huber, C., & Bachmann, O. (2017). The mechanics of shallow magma reservoir outgassing. Geochemistry Geophysics Geosystems, 18(8), 2887-2905.

Pelletier, J.D., 1999. Statistical self-similarity of magmatism and volcanism. Journal of Geophysical Research-Solid Earth 104, 15425–15438.

Laboratory modeling of coeval brittle and ductile deformation during magma emplacement into viscoelastic rocks

Bertelsen H.S.[1], **Galland O.**[1], Rogers B. D.[1], Dumazer G.[2] and Abbana Benanni A.[3]

[1]*Physics of Geological Processes (PGP), The NJORD Centre, Dept of Geosciences UiO, Oslo, Norway,* – olivier.galland@geo.uio.no
[2]*PoreLab, the NJORD Center, Physics Department, University of Oslo, Norway*
[3]*Ecole Normale Supérieure de Lyon, France*

Keywords: Laboratory Modelling, Magma emplacement, Viscoelastic host, Polariscopy.

The mechanics of magma transport and emplacement in the Earth's crust generally corresponds to the flow of a viscous fluid into a solid, which deforms to accommodate the incoming volume of magma. Depending on magma viscosity and host rock rheology, the magma/host mechanical systems can exhibit distinct and/or mixed physical behaviours, which lead to (1) intrusions of significantly diverse shapes (*e.g.* sheets to "blobs") and (2) contrasting deformation patterns in the host.

Currently, models of magma emplacement mainly account for end-member mechanical behaviours of crustal rocks. (1) A popular model for the emplacement of high-viscosity magma in the lower ductile crust addresses the host rock as a viscous fluid. In these models, the magma intrusions are considered as *diapirs*. (2) Models accounting for the emplacement of thick, so-called "punched laccoliths" in the brittle crust address the host rock as a Coulomb brittle (plastic) material. In these models, magma intrusions are emplaced by *pushing* their host rock, which is displaced along fault planes. (3) Most models of emplacement of igneous sheet intrusions (*i.e.*, dykes, sills, cone sheets, thin laccoliths) in the brittle crust address the host rock as an elastic solid. In these models, magma intrusions are addressed as idealised *tensile hydraulic fractures*, the thickening of which is accommodated by elastic bending of the host rock.

However, the Earth's crust is neither purely viscous, plastic, nor elastic, but, as stated, visco-elasto-plastic. Therefore, even if purely viscous diapiric rise, plastic faulting, or elastic hydraulic fracturing may happen, most intrusions are likely to be accommodated by hybrid viscous, plastic and elastic deformations of the host.

Here we present a series of 2D experiments where a viscous fluid (oil) was injected into a host matrix (laponite gel)(Fig. 1), the visco-elasto-plastic rheology of which is varied from dominantly viscous to dominantly elastic (Bertelsen et al, 2018). We performed a parameter study to test the effect of the rheology of the host matrix on the emplacement of model magma. The main results of our studies are the following.

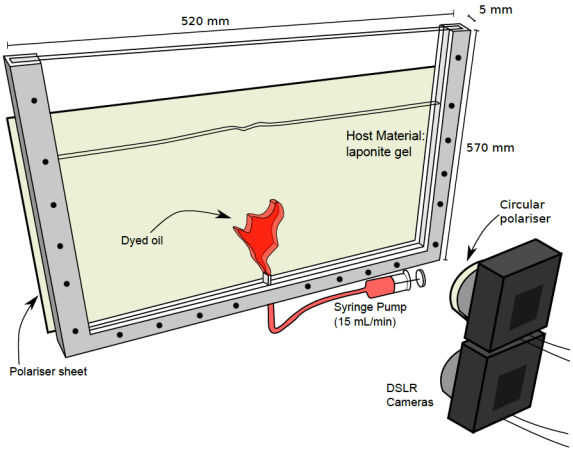

Fig. 1 - Drawing of the experimental setup. A Hele-Shaw cell filled with a viscoelastic laponite gel is intruded by dyed olive oil. The cell is backlit with a diffused white light source. Intrusion flow rate is controlled with a syringe pump. The cell stands between a polariser sheet and a circular polariser mounted on the camera lense: strain-induced birefringence in the gel, as well as the gel/oil interface, is captured by the camera because the polarisers are crossed.

- Our experiments reproduce a broad diversity of intrusion shapes, ranging from diapirs, viscoelastic fingers, hydraulic fractures, and complex, angular intrusions (Fig. 2).
- The oil intrusion in the elastic gel is a thin conduit with a sharp tip, like magmatic dykes, whereas the oil intrusion in the viscous gel is rounded, like diapirs.
- The laponite gels in our experiments exhibit coeval viscous, elastic and plastic deformation patterns to accommodate the intruding oil. In addition, we observe coeval tensile and shear brittle failure accommodating the propagation of the oil.
- Our experiments reproduce several magma emplacement mechanisms in the same experimental apparatus.
- Qualitatively, laponite gels appear to be relevant crustal rock analogues. Significant additional effort is required to constrain their mechanical properties, in order to discuss their physical similarity to natural rocks.

- Finally, we our experiments show that revealing magma emplacement necessitates analysing both the shape of intrusions and the deformation mechanisms in the host rock.

Overall, our exploratory experiments show that it is essential to account for the visco-elasto-plastic rheology of the Earth's crust to fully understand magma emplacement processes. Overall, our models suggest that emplacement mechanisms accounting for end member rheologies of the host rock may be uncommon in nature, as supported by field and geophysical observations. Our models imply fundamental new thinking of our physical approach of magma emplacement models.

Acknowledgements

This study was supported by the Faculty of Mathematics and Natural Sciences at the University of Oslo through doctoral fellowship grants to H.S. Bertelsen and B.D. Rogers.

References

Bertelsen, H.S., Rogers, B.D., Galland, O., Dumazer, G., Abbana Bennani, A., 2018. Laboratory modelling of coeval brittle and ductile deformation during magma emplacement into viscoelastic rocks. Frontiers in Earth Science 6, https://doi.org/10.3389/feart.2018.00199.

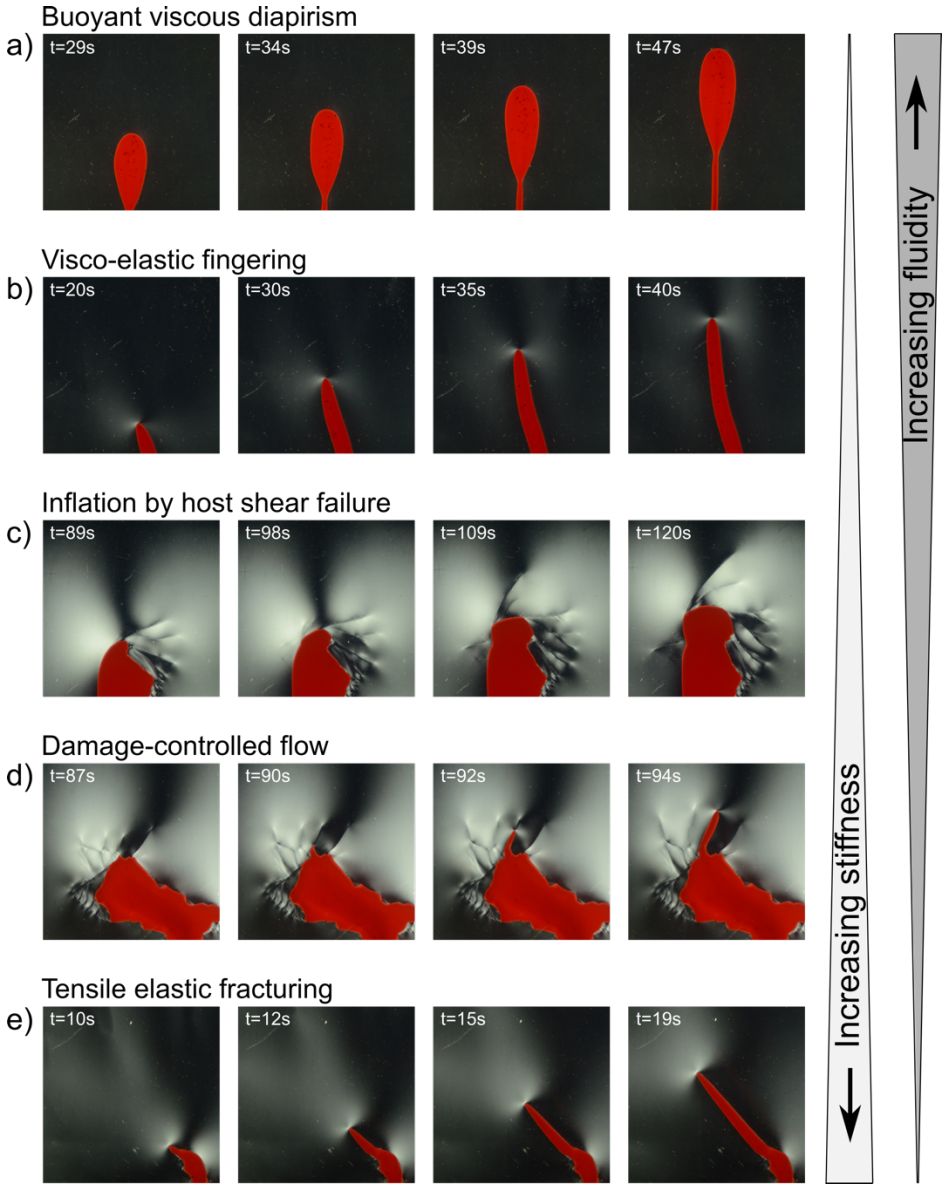

Figure 2. Time series of polarized photographs illustrating characteristic mechanisms of oil emplacement, for downward increasing gel stiffness and upward increasing of gel fluidity (Bertelsen et al., 2018). a) Viscous diapirism in Experiment E1. b) Viscoelastic fingering in Experiment E2. c) Intrusion inflation by shear failure of the host in Experiment E6. d) Intrusion of sheet intrusion along damage/ fault produced during earlier steps of oil intrusions in Experiment E7. e) Hydraulic fracturing of sheet intrusion in Experiment E7 .

Strain Patterns of Viscous Dyke Propagation in a Cohesive Crust, Visualized and Quantified from Quasi-2D Laboratory Experiments

Guldstrand F.[1], Bertelsen H.S.[1], Souche A.[1], Galland O.[1], and Zanella A.[2]

[1]*Physics of Geological Processes (PGP), The NJORD Centre, Dept of Geosciences UiO, Oslo, Norway,* – f.b.b.guldstrand@geo.uio.no
[2]*L.P.G., CNRS UMR 6112, Université du Maine, Avenue Olivier Messiaen, 72085 Le Mans Cedex 9, France*

Keywords: Laboratory Modelling, Sheet Intrusions, Deformation.

The emplacement of magmatic intrusions in the shallow crust is a fundamental process in generating new crust. This process provides the main mechanism of magma transport ultimately feeding volcanic eruptions. In the brittle crust, intrusions dominantly exhibit sheet shapes, either vertical (dykes) or horizontal (sills). Common models of sheet intrusions assume linear elastic deformation of a strong host, low viscosity magma, and tensile propagation (Rivalta et al., 2015; Kavanagh et al. 2018). However, sheet intrusions also readily occur where magma is viscous and host rock is weak, such as in sedimentary basins and at felsic volcanoes. Here, emplacement can be accommodated by plastic deformation and shear failure of the host (Pollard, 1973 Spacapan et al., 2017). Intrusions of high viscosity magma may also form finger-shaped intrusions and, in the case of extreme viscosities, cryptodomes (Spacapan et al., 2017, Tobita et al, 2001). How the emplacement of viscous sheet intrusions transitions into finger-shaped intrusions is currently poorly understood (Fig. 1).

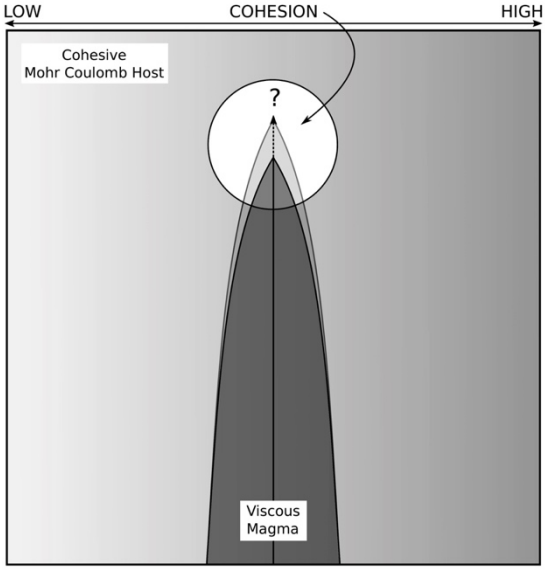

Fig. 2 - Our experiments aim to address how the cohesion of a host rock failing according to a Mohr Coulomb criterion may affect the propagation and emplacement of a viscous intrusion.

Field observations show that sharp tipped intrusions may be one end-member of sheet intrusion emplacement that appear to have propagated through tensile opening (Pollard, 1973). However, seismicity monitored during dyke intrusion events (Agustsdottir et al. 2016) and numerical models (Souche et al. 2019) provide evidence that the Coulomb properties of the Earth's brittle crust, and the associated shear failure, play an important role during sheet intrusion emplacement. Laboratory models studying the surface deformation associated with intrusions into Mohr Coulomb materials show drastically differing surface deformation patterns from that of currently used models of vertical sheet intrusions (Guldstrand et al. 2017). Yet, further investigation into how intrusions propagate in Mohr Coulomb materials is required.

In this study, we present quantitative laboratory modeling of a viscous golden syrup intruding into fine-grained cohesive flour of varying cohesion in a thick 2D Hele-Shaw cell (Fig. 2).

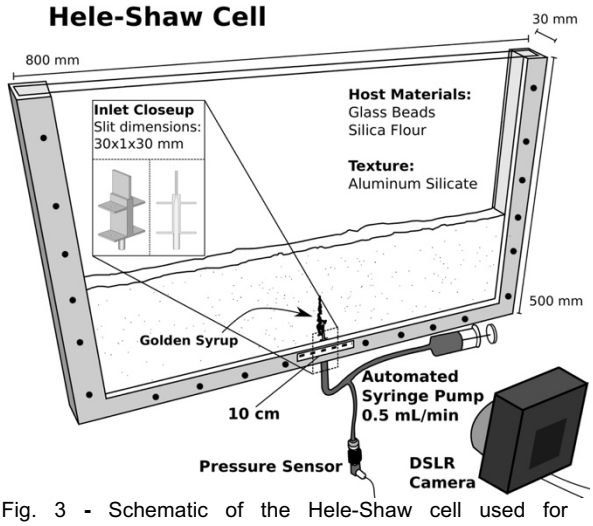

Fig. 3 - Schematic of the Hele-Shaw cell used for experiments.

The model setup uses compacted mixes of cohesive silica flour and glass beads. Mixing these two fine-grained powders allows us to tune and test the effect of cohesion. Golden syrup is injected at a constant flowrate of 0.5 ml/min. Pressure of the syrup is monitored and cameras take photographs each 120/180 s, depending on the experiment. The images

are corrected for lens distortion before applying a digital image correlation algorithm, available through the open source structure-from-motion software MicMac. This allows us to map the small displacements accommodating the emplacement of the syrup (Fig. 3).

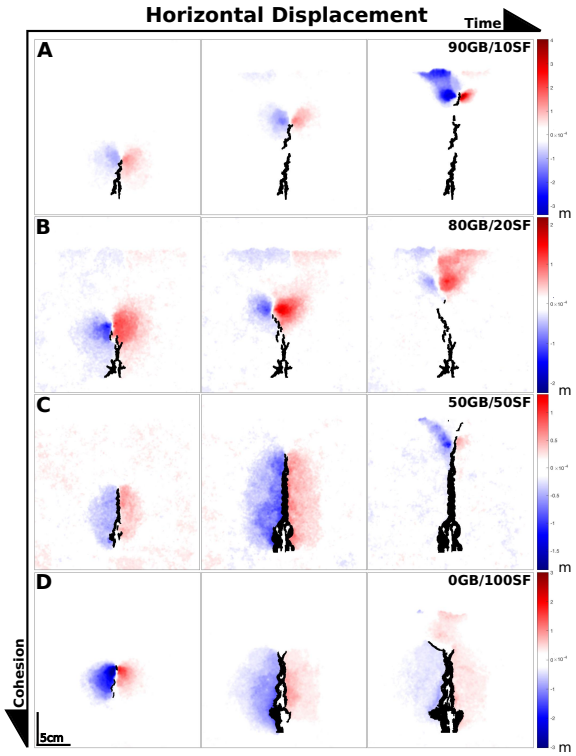

Fig. 3 – The rows show intrusions (black) into mixes of 90/10 (A), 80/20 (B), 50/50 (C) and 0/100 (D). Columns show experiment photos at an initial, intermediate and late time step. A and B shows that deformation, during propagation, is mainly concentrated to and beyond the intrusion tip. C and D show the entire fracture being active and displacing during vertical propagation. Once critical failure of the overburden occurred, pathways were created for the fluid to utilize for the final ascent and any opening of the intrusion ceased.

We present 8 experiments, of which 4 are repeats. For each experiment we present the final intrusion shapes and analyze the incremental internal host deformation throughout the experiment. Our results show that different intrusion shapes form depending on host cohesion, with lower cohesion hosts leading to finger shaped intrusions and higher cohesion hosts leading to sheet intrusions (Fig. 3).

Our experiments demonstrate the different emplacement mechanisms associated with these two intrusion types. In low cohesion experiments, finger shaped intrusions concentrate horizontal deformation to the tip of the intrusion while simultaneously producing significant uplift of the overburden. In high cohesion hosts, sheet intrusions form with deformation and dilation occurring over the entire fracture. The uplift above these intrusions is significantly smaller than in low cohesion experiments. However, both intrusions produce uplift and shear bands extending from the intrusion tip. Pressure readings from the experiments also provide further evidence of the differing emplacement dynamics. We conclude that the cohesion of Mohr Coulomb materials has a governing control on the emplacement mechanics and shapes of viscous magmatic intrusions and the resulting deformation.

Acknowledgements

Guldstrand and Souche's position was funded by the DIPS project (grant no. 240467, Norwegian Research Council). The authors thank T Schmiedel & M Moura for performing contact angle measurements of the Golden Syrup. R Mourgues is acknowledged for assisting in a guest researcher visit in Le Mans.

References

Ágústsdóttir, T., Woods, J., Greenfield, T., Green, R. G., White, R. S., Winder, T., ... & Soosalu, H. (2016). Strike-slip faulting during the 2014 Bárðarbunga - Holuhraun dike intrusion, central Iceland. *Geophysical Research Letters*, *43*(4), 1495-1503.

Guldstrand, F., Burchardt, S., Hallot, E., & Galland, O. (2017). Dynamics of surface deformation induced by dikes and cone sheets in a cohesive Coulomb brittle crust. *Journal of Geophysical Research: Solid Earth*, *122*(10), 8511-8524.

Kavanagh, J. L., Burns, A. J., Hazim, S. H., Wood, E. P., Martin, S. A., Hignett, S., & Dennis, D. J. (2018). Challenging dyke ascent models using novel laboratory experiments: implications for reinterpreting evidence of magma ascent and volcanism. *Journal of Volcanology and Geothermal Research*, *354*, 87-101.

Pollard, D. D. (1973). Derivation and evaluation of a mechanical model for sheet intrusions. *Tectonophysics* 19(3): 233-269.

Rivalta, E., Taisne, B., Bunger, A. P., & Katz, R. F. (2015). A review of mechanical models of dike propagation: Schools of thought, results and future directions. *Tectonophysics*, *638*, 1-42.

Souche, A., Galland, O., Haug, Ø. T., & Dabrowski, M. (2019). Impact of host rock heterogeneity on failure around pressurized conduits: Implications for finger-shaped magmatic intrusions. *Tectonophysics*.

Spacapan, J. B., Galland, O., Leanza, H. A., & Planke, S. (2016). Igneous sill and finger emplacement mechanism in shale-dominated formations: a field study at Cuesta del Chihuido, Neuquén Basin, Argentina. *Journal of the Geological Society*, *174*(3), 422-433.

Tobita, M., Murakami, M., Nakagawa, H., Yarai, H., Fujiwara, S., & Rosen, P. A. (2001). 3-D surface deformation of the 2000 Usu eruption measured by matching of SAR images. *Geophysical Research Letters*, *28*(22), 4291-4294.

Shear versus tensile failure mechanisms induced by sill intrusions – Implications for emplacement of conical and saucer-shaped intrusions

Haug Ø. T.[1], Galland O.[1], Souloumiac P.[2], Souche A.[1], Guldstrand F.[1], Schmiedel T.[1] and Maillot B.[2]

[1] *PGP, the Njord Center, Department of Geosciences, University of Oslo, Norway* – olivier.galland@geo.uio.no
[2] *Géosciences et Environnement Cergy (GEC), Université de Cergy-Pointoise, France*

Keywords: shear failure, limit analysis modelling, plasticity.

Voluminous igneous intrusions and sand injectite complexes have been documented in many sedimentary basins worldwide. Their emplacement is a result of overpressurized fluids (magma or fluidized sediments) that forcefully create room for themselves by deforming their brittle host rock. These overall concordant intrusions also exhibit other shapes like cones, saucer shapes, transgressive sheets, and laccoliths (e.g., Galland et al., 2018).

Numerous field observations document the occurrence of complex deformation and damage patterns associated with the emplacement of igneous intrusions and sand injectites in sedimentary basins. At small, intrusion tip scale, significant brittle shear and/or ductile shear has been documented to accommodate the propagation of intrusion tips (e.g. Galland et al., 2018, and references therein). At larger, intrusion scale, some authors argue that shear failure controls, at least partly, the emplacement of magma or fluidized sediments into conical intrusions, saucer-shaped intrusions, or laccoliths.

These observations are evidence that inelastic deformation of the host rock plays an important role in accommodating the emplacement of intrusions. However, most models of sill emplacement only consider elastic deformation of the host rock, while the plastic component is assumed to be negligible. Nevertheless, Scheibert et al. (2017) show that adding a small component of plastic deformation at the tips of the intrusions can significantly modify their emplacement dynamics. In addition, Haug et al. (2017) show that the emplacement of saucer-shaped intrusion's inclined sheets are likely governed by shear failure of the sill overburden. The models of Scheibert et al. (2017) and Haug et al. (2017) therefore suggest that the elastic assumption of the established models of sill and laccolith emplacement is too simplistic, and this may explain why these models cannot reproduce the natural diversity of intrusion shapes.

To date, our current understanding of how inelastic deformation governs intrusion emplacement is very limited. Consequently, it is not clear whether tensile fracturing or inelastic shear deformation of brittle host rock is the dominant mechanism accommodating intrusion emplacement.

Here we use a rigid plasticity approach, through limit analysis modeling, to study the conditions required for inelastic deformation of sill overburdens (Figure 1; Haug et al., 2018). Each simulation calculates (1) the mechanical conditions leading to failure of the sill's overburden and (2) the expected distribution of plastic failure. All simulations produced a localized band of plastic deformation nucleating upward from the tip of the sill (Figure 2). We perform a large parameter study to derive an empirical law of the conditions for shear failure of sill overburdens.

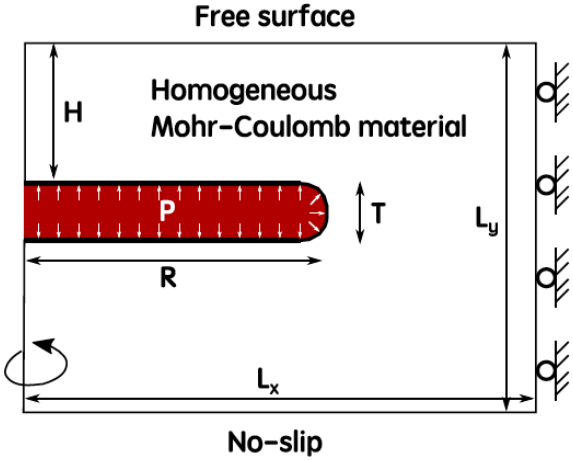

Fig. 1 – Sketch of model setup. The system considered consists of an elongated cavity exerting a homogeneous pressure within a homogeneous and isotropic Mohr-Coulomb material. The system is in an axisymmetric setting with a free surface at the top, free slip on the right, and no slip at the bottom boundary. From Haug et al. (2018).

Our study shows that

1. The damage patterns exhibit three distinct geometries depending on the model parameters: Case (1) relatively straight damage zones from sill tips to the surface (Figure 2, top), Case (2) curved damage zones from the sill tip to the surface (Figure 2, center and bottom), and Case (3) short damage zones, also rooted at the sill tips but restricted below a certain depth, above which damage is distributed.

2. Straight damage of Case (1) occurs when R/H < 1, that is, when sill's radius is smaller than the sill's depth. Such failure mechanism is expected to occur

when the magma overpressure is high and/or if the overburden is weak. This straight morphology strongly resembles V-shaped or cone sheet intrusions (Figure 2, top).

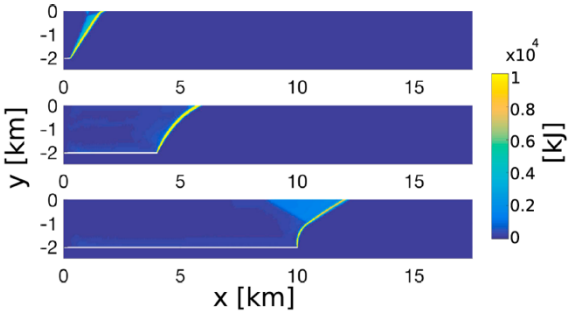

Fig. 2 – Cross-section maps of damage distribution from three models with varying values of R/H (see parameter definition in Fig. 1). (top) R/H = 0.05, (middle) R/H = 2, (bottom) R/H = 5. The other parameters are kept constant (C/(ρgH) = 0.2, ϕ = 30◦). The horizontal white lines locate the considered sill. The color scale represents the energy dissipated by damage (in kJ), which shows a localization from the tip of the sill toward the surface.

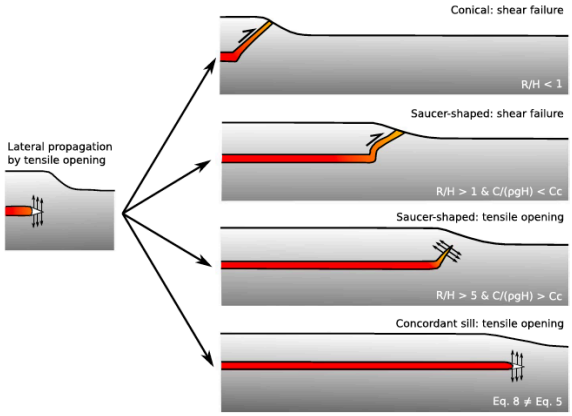

Fig. 3 – Illustration of proposed scenarios for cone sheet and saucer-shaped sill formation. Once a sill is formed, it propagates laterally by tensile opening at its tip. At a certain radius, shear failure of the overburden that becomes favored over tensile opening at the tip created a damage zone similar. The magma predominantly follows the weakness created by the damage. From Haug et al. (2018).

3. Curved damage of Case (2) strongly resembles saucer-shaped intrusion's inclined sheets. Our models show that this failure mechanism is favorable in most geological conditions. Conversely, the damage of Case (3) occurs only for shallow sills emplaced in high-cohesion rocks.

4. The straight damage of Case (1) and the curved damage of Case (2) dominantly accommodate shear failure, whereas the damage of Case (3) dominantly accommodates tensile failure.

5. These damage patterns mimic typical intrusion morphologies (cone sheets, inclined sheets), suggesting that damage associated with shear failure is a first-order mechanical precursor for magma emplacement in the brittle crust.

6. The overpressure required to trigger shear failure follows predictable trends for variable R/H, C/(ρgH) and ϕ, which we describe in the form of an empirical scaling law (Haug et al., 2018). This scaling law provides accurate predictions when compared to geological data.

7. We integrate our shear failure model with an established tensile hydrofracture propagation model, and we mapped the mechanical conditions that are favorable for shear failure or tensile failure. This analysis suggests that sills initially propagate laterally by tensile opening at the sill tip, until reaching a critical value of R/H and triggering failure of the overburden, which controls the subsequent emplacement of the magma (Figure 3).

8. This integration provides, for the first time, the physical conditions for the formation of V-shaped intrusions, saucer-shaped intrusions, and large concordant sills (Figure 3).

Our study shows that the brittle Coulomb properties of the Earth's crust can play a major role during magma emplacement and propagation.

Acknowledgements

Haug and Schmiedel's positions are funded by the Faculty of Mathematics and Natural Sciences at the University of Oslo. Souche and Guldstrand's positions are funded by the Research Council of Norway through the DIPS project (grant 240467).

References

Galland, O., et al., 2018. Storage and transport of magma in the layered crust-Formation of sills and related flat-lying intrusions. *In*: Burchardt, S. (ed.) *Volcanic and Igneous Plumbing Systems*. Elsevier, 111-136.

Haug, Ø.T., O. Galland, P. Souloumiac, A. Souche, F. Guldstrand & T. Schmiedel, 2017. Inelastic damage as a mechanical precursor for the emplacement of saucer-shaped intrusions. *Geology*, 45, 1099-1102.

Haug, Ø.T., O. Galland, P. Souloumiac, A. Souche, F. Guldstrand, T. Schmiedel & B. Maillot, 2018. Shear versus tensile failure mechanisms induced by sill intrusions - Implications for emplacement of conical and saucer-shaped intrusions. *Journal of Geophysical Research: Solid Earth*, 123, 3430-3449.

Scheibert, J., O. Galland & A. Hafver, 2017. Inelastic deformation during sill and laccolith emplacement: insights from an analytic elasto-plastic model. *Journal of Geophysical Research: Solid Earth*, 122, 923-945.

Laboratory modelling of sill and dyke emplacement

Kavanagh J.L.[1], Martin S.[1], Urbani, S., Williams K.[1], Donadio A.[2], Wood E.[1], Zavada P.[3] and Dennis D.J.C.[4]

[1] *School of Environmental Sciences, University of Liverpool, Liverpool, UK* – Janine.kavanagh@liverpool.ac.uk
[2] *School of Physical Sciences, University of Liverpool, Liverpool, UK*
[3] *Institute of Geophysics, Academy of Sciences of Czech Republic, Prague, Czech Republic*
[4] *School of Engineering, University of Liverpool, Liverpool, UK*

Keywords: magma, experiments, intrusions.

A fundamental aspect of volcanism is the nature of the underlying plumbing system, which is responsible for storing and transporting magma through the lithosphere to potentially feed volcanic eruptions. Key plumbing system structures are dykes and sills and by improving our understanding of how they form we will be better able to interpret the evidence of current magma flow and how it occurred in the past (e.g. Martin et al. 2019).

All methods to study the dynamics of magma intrusion involve interpretation of indirect measurements; from studying static exposed fossil magma intrusions in the field, to measuring the gradual surface deformation or subsurface seismicity created as magma moves through the subsurface. Scaled laboratory experiments offer the opportunity to link these indirect measurements with their dynamic origins. In this contribution we will present results from some new experiments which explore the coupled dynamics of magma flow and host-rock deformation.

Laboratory model volcanic plumbing systems

The broad aims of laboratory models (sometimes called analogue models) are not to reproduce their natural counterpart but instead to explore the parameter space, identify geometric, kinematic or dynamic regimes, and test hypotheses derived from e.g. field evidence. Scaled analogue models of dykes and sills have been carried out since the 1950's. The choice of rock analogue material depends on the underlying model being explored, and ranges from elastic deformation (using e.g. transparent gelatine solids) or a cohesive granular material (e.g. compacted silica flour).

Gelatine experiments: the effect of fluid rheology

Relatively few experiments have focused on the role of magma rheology on dyke and sill propagation. End-member rheologies are Newtonian (e.g. water) or non-Newtonian yield-strength fluids (e.g. plaster-of-Paris). Magma comprises variable proportions of bubbles, crystals and melt and may have a non-Newtonian shear-thinning rheology.

To prepare the gelatine experiments, Forty-litres of gelatine are poured into clear-Perspex tank and refrigerated for several hours at 5°C. Layered experiments require a 2-stage preparation, with the lower layer completely solidifying before the upper layer is emplaced. The mechanical properties of the bonded interface between the gelatine layers is controlled by the temperature of the solid lower layer and the liquid upper layer, with a low temperature lower layer (5°C) and low temperature upper layer (21°C, which is approximately the gel temperature) producing a weak interface. No initial stress-field is imposed in the experiment. When the gelatine layers have solidified, the magma analogue is injected through the base of the tank using a peristaltic pump and a tapered injector (Fig. 1).

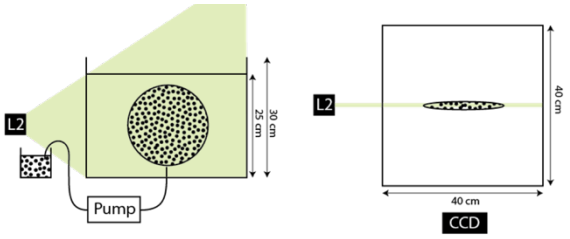

Fig. 1 – Side (left) and top (right) sketch view of the gelatine experiment setup with passive-tracer particles in the injecting fluid (Kavanagh et al. 2018).

The injected fluid rheology was varied and the results recorded using tracer particles, polarised light and surface monitoring. Post-processing of the data using digital image correlation and particle image velocimetry reveals variations in flow velocity and the development of a fluid jet which meanders and becomes unstable during ascent (Fig. 2).

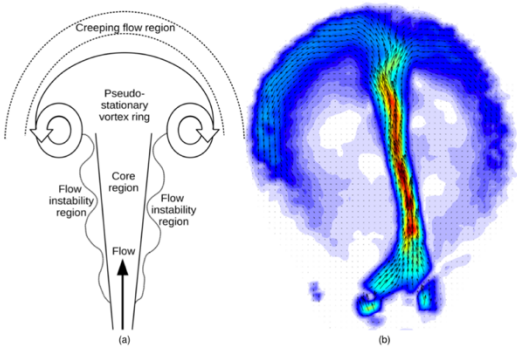

Fig. 2 – Diagram (left) depicting key fluid dynamic structures identified using PIV (right) on the growing Newtonian fluid - filled experimental dyke.

Flour experiments: magnetic flow indicators

Multi-coloured plaster of Paris (a Bingham fluid and the magma analogue) seeded with magnetite particles was loaded sequentially or annularly into a piston (Fig. 3), and this was injected through a central port in the base of a 1.2 x 1.2 x 0.5 m box filled with fine grained wheat flour (a cohesive granular material and the crust analogue). This created an experimental plumbing systems which once solidified were excavated and photographed so the external morphology could be characterised in 3D.

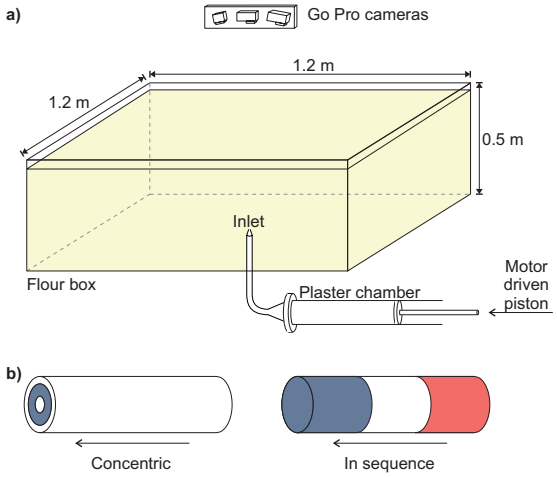

Fig. 3 – a) Diagram of flour box and injection system, and b) the two different colouring schemes used in the plaster chamber.

Cup structures, sheet-like dykes and tube-like conduits were identified (Fig. 4), which were covered in surface crenulations and lineations. When annular colouring was used, the internal structures were characterised by slicing the intrusions into thin sheets. When sequential colouring was used, the external colour of the intrusion indicated different parts of the system had been active at different times.

Closely-spaced sampling across the length, breadth and thickness of the intrusion slices permitted the detailed three-dimensional mapping of magnetic fabrics using anisotropy of magnetic susceptibility. The observed fabrics indicate that a series of complex processes occurred during emplacement, which are preserved by the orientation of magnetic particles and are therefore a potential direct analogy to magnetic fabrics rocked in fossil dykes and sills (Martin et al. 2019).

Conclusions

Overall the analogue experiment results demonstrate how both the magma rheology and host-rock deformation mode needs to be considered when interpreting field-based observations of magma intrusion. They provide measurements of dynamic processes which can be compared with their natural counterparts to infer the nature of magma intrusion in the crust.

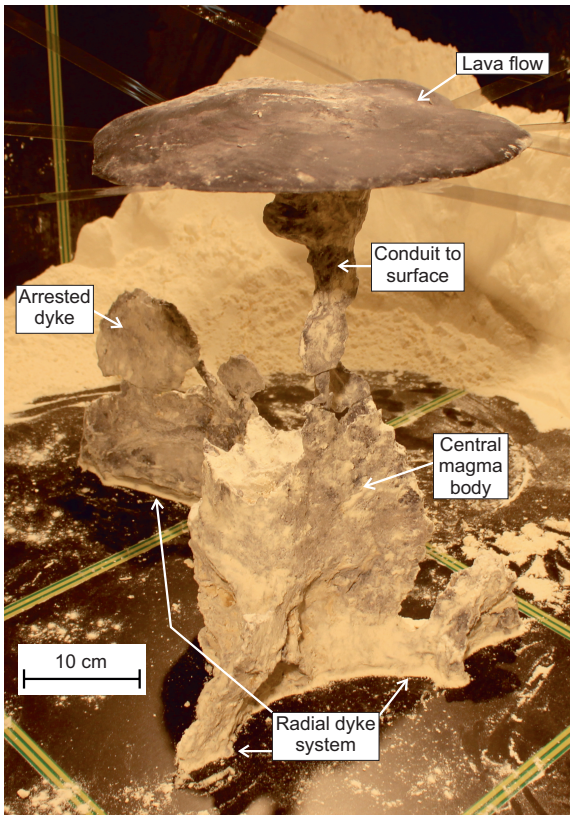

Fig. 4 – Annotated photograph of an excavated plaster experimental intrusion with key structures indicated.

Acknowledgements

The authors wish to thank the organisers of LASI 6 and sponsors for their support which has made this conference contribution possible.

References

Kavanagh, J. L., Burns, A. J., Hazim, S. H., Wood, E. P., Martin, S. A., Hignett, S., & Dennis, D. J. (2018). Challenging dyke ascent models using novel laboratory experiments: implications for reinterpreting evidence of magma ascent and volcanism. *Journal of Volcanology and Geothermal Research*, *354*, 87-101.

Martin, S. A., Kavanagh, J. L., Biggin, A. J., & Utley, J. E. (2019). The origin and evolution of magnetic fabrics in mafic sills. *Frontiers in Earth Science*, *7*, 64.

From Planar Intrusions to Finger-Like Channels: New insights from 3D Analogue Experiments

Nissanka Arachchige U.[1], Cruden A.[1], Weinberg R.[1] and Köpping J.[1]

[1] *School of Earth, Atmosphere and Environment, Monash University, Melbourne, Australia* – (uchitha.nissankaarachchige@monash.edu)

Keywords: Sills, fingers and lobes, magma channels.

The geometries of planar igneous intrusions such as dykes, sills and inclined sheets have often been used to delineate emplacement mechanisms, magma flow pathways, and melt source locations in crustal magma plumbing systems. It is known that dykes and sills do not always propagate with uniform margins but instead break down into finger-like and/or lobate segments. The morphology and propagation mechanism of these segments and how they connect are still debated and mostly explained by brittle-elastic instabilities (Nicholson and Pollard, 1985), where tensile brittle fracture leads to the formation of segment connectors such as steps and broken bridges.

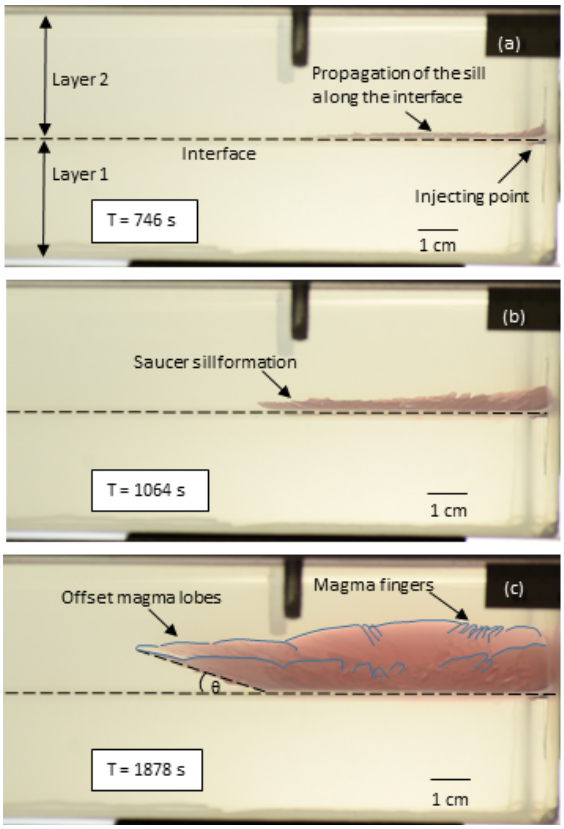

Fig. 1 – *Side view: (a) Propagation of a sill along the interface, (b) saucer sill formation. (c) Offset lobes and fingers formed at the host rock-magma margin. θ is the dip of the inclined sheet.*

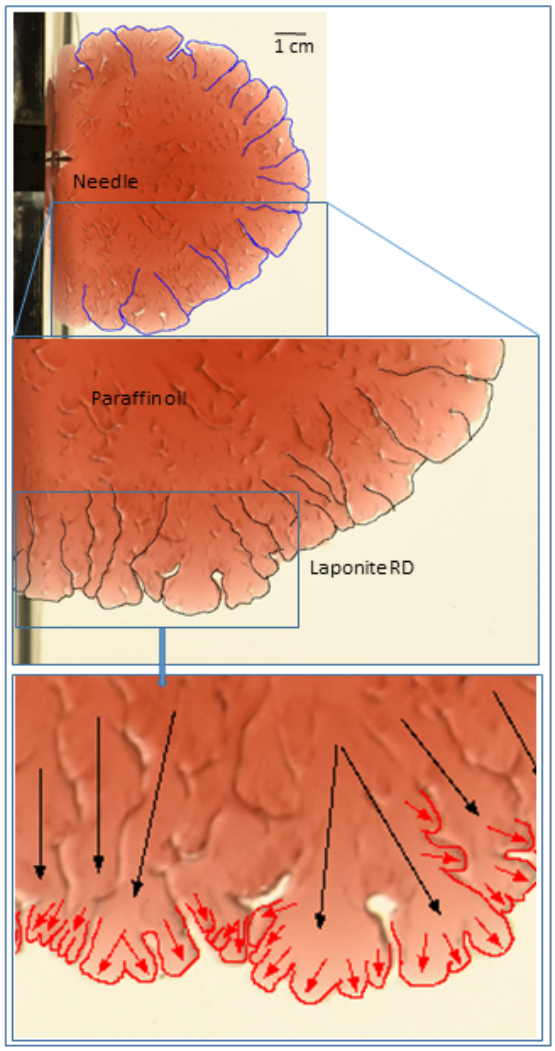

Fig. 2 – *Overhead view: Formation and propagation of lobes and magma fingers and associate magma pathways. Paraffin oil (red) is injected from the left through a needle into transparent Laponite RD. Sill expands radially and breaks into lobes and fingers. Lobe segments show distinct primary (blue) and secondary margins (black) and final magma directions (black and red arrows).*

However, non-brittle emplacement mechanisms such as ductile flow processes and heat-induced fluidization (Schofield et al. 2012; Magee et al. 2016) also show the development of such segments. Recent

studies have also suggested that magma cooling and solidification can contribute to formation of segments (Chanceaux and Menand 2014, 2016).

Here we present an isothermal experimental approach to model segmented sill margins and to analyze their propagation mechanisms. Paraffin oil (magma analogue) is injected horizontally via a peristaltic pump into horizontal interfaces between layers of Laponite RD gels (host rock analogue) with varying visco-elastic-plastic properties (Ruzicka and Zaccarelli 2011; Kaushal and Joshi 2014) at constant flux. Propagation of the resulting sill is monitored photographically in plane and plane-polarised light, taking advantage of the photo elastic properties of Laponite. Rheological measurements show that Laponite RD gel is in the elasticity dominated, linear visco-elastic (LVE) domain when strain amplitudes are < 3.17 %. Its Young's modulus and shear strength increase with increasing concentration and time (aging), with plastic failure occurring at strain values in between 15.2% and 20.2%.

Result of the experiments indicate that the structure and propagation of the model sills are largely controlled by the rheology of the host rock analogue, whereby ascending bulbous and saucer shaped sills form when Laponite RD has either low or high elastic stiffness, respectively. The experiments reveal that fluid-driven cracks initially propagate along the horizontal interface between Laponite layers as an inner flat sill. They then transition into an inclined sheet to define an overall saucer shaped intrusion morphology. Saucer shaped sills (Fig. 1) form in the experiments when the inner sill diameter to overburden thickness ratio is > (1.3 - 1.5). The dip of the inclined sheets varies from 11.5° to 35.5° and this angle is shallower when the inclined sheet forms and becomes steeper as it approaches the surface of the experiments.

In experiments using stiff Laponite RD analogue host rocks, segmented fingers and lobes develop at the leading edge of both inner sills and inclined sheets (Fig. 2). These structures re-merge by forming steps and broken bridge structures that are parallel to the local propagation direction of the analogue sill. Long and narrow finger-like channels develop mostly in primary lobes parallel to the long axis direction of the sill and saucer intrusion. Passive markers within these channels show that magma flows faster in channelized regions compared to both the surrounding regions and at the propagating crack tip.

Scaling arguments and pressure measurements reveal that when the fluid-filled crack initiates, elastic stress dominates over viscous and toughness stresses. In our experiments, sill propagation and formation of saucer intrusions occur during a change from an elastic to a toughness-dominated regime. We suggest that the geometries, host rock deformation and propagation of sill segments observed here are closely related to elastic instabilities. Our results are consistent with previous field and experimental observations on the formation of sheet intrusion segments and provide new insights on how offset lobate segments and magma fingers emerge from initially planar fractures in layered viscoelastic host rocks. Future experimental work will focus on cooling and solidification of analogue magmas in order to quantify how crystallization influences the formation of magma fingers and channels, and to compare the propagation of sill segment propagation with isothermal experiments.

Acknowledgement

Supported by ARC Discovery Grant DP190102422.

References

Chanceaux, L., Menand, T., (2016). The effects of solidification on sill propagation dynamics and morphology. Earth and Planetary Science Letters 442, 39–50.

Chanceaux, L., Menand, T., (2014). Solidification effects on sill formation: An experimental approach. Earth and Planetary Science Letters 403, 79–88.

Kaushal, M., Joshi, Y.M., (2014). Linear viscoelasticity of soft glassy materials. Soft Matter 10, 1891–1894.

Magee, C., Muirhead, J.D., Karvelas, A., Holford, S.P., Jackson, C.A.L., Bastow, I.D., Schofield, N., Stevenson, C.T.E., Mclean, C., Mccarthy, W., Shtukert, O., (2016). Lateral magma flow in mafic sill complexes: Geosphere, v. 12, 809–841.

Nicholson, R., Pollard, D.D., (1985). Dilation and linkage of echelon cracks. Journal of Structural Geology 7, 583–590.

Pollard, D.D., Segall, P., Delaney, P.T., (1982). Formation and interpretation of dilatant echelon cracks. Geological Society of America Bulletin 93, 1291–1303.

Ruzicka, B., Zaccarelli, E., (2011). A fresh look at the Laponite phase diagram. Soft Matter 7, 1268–1286.

Schofield, N.J., Brown, D.J., Magee, C., Stevenson, C.T., (2012). Sill morphology and comparison of brittle and non-brittle emplacement mechanisms. Journal of the Geological Society 169, 127–141.

Magma-induced deformation of the Earth's upper crust in nature and in laboratory experiments scanned by X-ray Computed Tomography

Poppe S.[1], Holohan E.P.[2], Galland O.[3] and Kervyn M.[1]

[1] *Department of Geography, Vrije Universiteit Brussel, Brussels, Belgium* – sam.poppe@vub.be & sam35poppe@gmail.com
[2] *UCD School of Earth Sciences, University College of Dublin, Dublin, Ireland*
[3] *Physics of Geological Processes, University of Oslo, Oslo, Norway*

Keywords: intrusion, analog modeling, Digital Volume Correlation.

Understanding the propagation and geometry of magmatic intrusions and the related surface displacement is critical for hazard and risk assessment at volcanoes. Magma ascends through the Earth's crust towards its final subsurface position, or eventually towards its eruption site at the surface. Magma intrusions propagate and grow by deforming their crustal host rocks and by displacing the Earth's surface. Because directly observing this process is impossible, accurate volcanic eruption forecasts depend on indirect geophysical monitoring of seismicity and surface deformation (e.g. Sigmundsson et al. 2018).

The lack of direct observations makes the interpretation of geophysical monitoring data a challenge, and results in heavily debated questions such as: What are the physical mechanisms that control magma-induced deformation? How do magma intrusions grow to their final geometries? How can surface deformation patterns be interpreted in terms of the intrusive processes in the subsurface?

To offer a new perspective on these questions, this presentation summarizes the observations and conclusions from the recently completed doctoral dissertation of the first author. This work compares observations from exposed volcanic plumbing systems and geophysical records of recent intrusions with novel 4D laboratory experiments.

First, magma-host rock interactions were investigated at a small-scale outcrop in the Oslo Rift System, Norway (Figure 1). We infer from structural and geochemical analyses that the propagation of mafic dyklets there was controlled by regional, pre-existing structural weaknesses in the host rock and thermo-chemical interactions between the sedimentary host rock and the magma (Poppe et al., in prep. (A)). Thermal contact metamorphism produced a secondary fluid, comprising a pore-fluid-magma mixture, that likely propagated along and ahead of the magma body. The magma propagated by opening-mode fracturing and bending of the host rock. At locations in e.g. Australia, Argentina, on the contrary, mixed-mode or shear-mode fracturing has been inferred (e.g. Dering et al. 2019; Spacapan et al. 2017).

Fig. 1 – Two overlapping dyklet tips intruded into sedimentary host rock on Hovedøya Island, Oslo Rift, Norway. Note the tapering geometry of the magma-filled fractures as well as the shear displacement along pre-existing fractures in the central, competent limestone layer (from Poppe et al., in prep. a). The ruler scales 30 cm.

Second, a novel 4D laboratory modeling approach was developed to overcome limitations of past laboratory models regarding (1) mechanically relevant rheology of model rock materials, and (2) imaging subsurface magma-induced deformation. As for (1), a set of detailed material tests showed that dry sand-plaster mixtures display more complex mechanical behavior than hitherto appreciated, and that these mixtures are suitable as analogues for the Earth's upper crust (Poppe et al., in prep.(B)). As for (2), 3D displacement and strain fields within sand-plaster host material, induced by analogue golden syrup intrusions, were quantified in laboratory models over time by using medical wide beam X-ray Computed Tomography (CT) and Digital Volume Correlation (DVC).

The obtained displacement and strain fields show that analogue intrusions propagate by mixed-mode deformation of their sand-plaster host material (Figure 2).

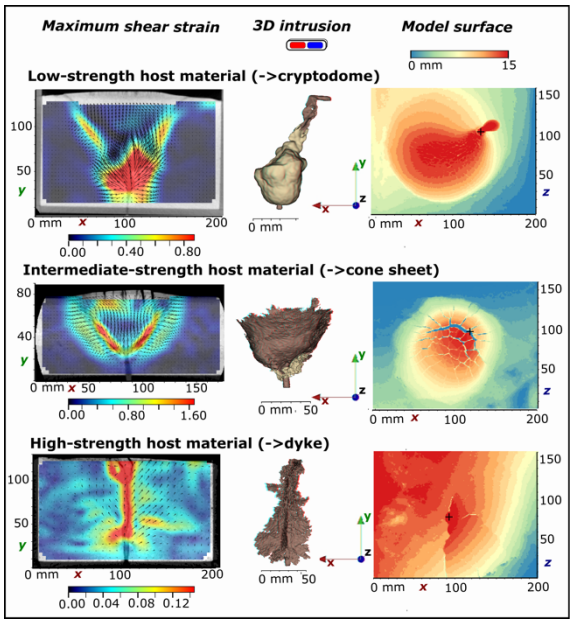

Fig. 2 – Cumulative maximum shear strains in the central vertical X-Y cross-section through the model domain, final 3D rendering of the analogue intrusion, and final model surface topography, extracted from the reconstructed imagery of laboratory models of golden syrup intrusion in sand-plaster host material, by using medical X-ray Computed Tomography (adapted from Poppe et al., 2019).

The dominance of the fracturing mode is largely controlled by the host rock rheology, among other physical parameters, and leads to a spectrum of intrusion geometries as observed in nature. In low- to medium-strength host material, shear-mode fracturing dominates and thick cryptodomes or cup shapes form. In medium- to high-strength host material, opening-mode fracturing dominates and thin cone sheets, inclined sheets and dykes form (Figure 2; Poppe et al., 2019).

Finally, we extracted surface displacements from the reconstructed CT imagery by using dedicated Matlab codes. Unlike previous models assuming linear elastic rheology and tensile fracturing, our models of golden syrup dykes and steeply inclined sheet intrusions induce dome- or bulges-and-through-shaped uplift of the model surface without net subsidence. Comparable surface displacement patterns were observed during recent sheet intrusion events. Our results suggest that mixed-mode magma-induced fracturing may occur in the weak, highly fractured upper portion of some volcanoes and may affect surface displacement patterns. Consequently, we propose that geodetic inversion models for such settings should incorporate more complex non-elastic behavior.

Acknowledgements

S. Poppe was financed through an FWO-Flanders Ph.D. aspirant fellowship (2014-2019) and Vocatio grant (2014). He is a Fulbright and Belgian-American-Educational-Foundation fellow since November 2019. This work was carried out at VUB, Belgium, in collaboration with N. Buls, G. Van Gompel, B. Keelson (UZ Brussel, Belgium), J. Brancart, P. Claeys, A. Delcamp, S. Goderis, P. Tournigand, N. de Winter (VUB, Belgium), M. Rosenau (GFZ Potsdam, Germany), R. Mourgues (U Maine, France), D. Hollis, A. Nila (LaVision UK Ltd.), and benefited from discussions with P. Boulvais, S. Burchardt, P. Grosse, J. Kavanagh, M. Poland, the PGP group at Oslo University and many others.

References

Dering, G.M., S. Micklethwaite, A.R. Cruden, S.J. Barnes, and M.L. Fiorentini (2019), Evidence for Dyke-Parallel Shear during Syn-Intrusion Fracturing, *Earth Planet. Sci. Lett.,* 507, 119–30.

Poppe, S., E.P. Holohan, O. Galland, N. Buls, G. Van Gompel, B. Keelson, P. Tournigand, D. Hollis, A. Nila, and M. Kervyn (2019), An Inside Perspective on Magma Intrusion: Quantifying 3D Displacement and Strain in Laboratory Experiments by Dynamic X-Ray Computed Tomography, *Frontiers in Earth Science,* 7, 62.

Poppe, S., O. Galland, N. de Winter, S. Goderis, P. Claeys, V. Debaille, M. Kervyn (A), Structural and geochemical interations between magmatic dyklets, chill margins, calcite veins and sedimentary host rocks : the case of Hovedoya Island, Oslo Fjord, Norway, *in preparation.*

Poppe, S., E.P. Holohan, M. Rosenau, O. Galland, A. Delcamp, M. Kervyn (B), Mechanical properties of analog quartz sand and gypsum powder (plaster) mixtures : implications for laboratory models of the Earth's upper crust, *in preparation.*

Sigmundsson, F., M. Parks, R. Pedersen, K. Jónsdóttir, B.G. Ófeigsson, R. Grapenthin, S. Dumont, et al. (2018), Magma Movements in Volcanic Plumbing Systems and Their Associated Ground Deformation and Seismic Patterns, in *Volcanic and Igneous Plumbing Systems*, edited by S. Burchardt, pp. 285–322, Elsevier.

Spacapan, J. B., O. Galland, H. A. Leanza, and S. Planke (2017), Igneous sill and finger emplacement mechanism in shale-dominated formations: a field study at Cuesta del Chihuido, Neuquén Basin, Argentina, *J. Geol. Soc. London*, *174*(3), 422-433.

Coulomb failure of Earth's brittle crust controls growth, emplacement and shapes of igneous sills, saucer-shaped sills and laccoliths

Schmiedel T.[1,2,3], Galland O.[1], Haug Ø. T.[1], Dumazer G.[4] and Breitkreuz C.[5]

[1] *PGP-NJORD Centre, Department of Geosciences, University of Oslo, Norway*
[2] *MPT, Department of Earth Sciences, Uppsala University, Sweden* – tobias.schmiedel@geo.uu.se
[3] *Centre for Natural Hazards and Disaster Science, Sweden, www.cnds.se*
[4] *PoreLab-NJORD Centre, Department of Physics, University of Oslo, Norway*
[5] *Geological institute, Technical University Bergakademie Freiberg, Germany*

Keywords: magma emplacement, laboratory models, limit analysis.

Tabular, igneous intrusions are fundamental elements of volcanic and igneous plumbing systems in the Earth's brittle crust. They accommodate the bulk of the magma transport and storage in the Earth's brittle crust. Tabular intrusions exhibit a broad variety of shapes, ranging from thin sheet intrusions (sills, saucer-shaped sills, cone sheets), to more massive intrusions (domed and punched laccoliths, stocks). Such a diversity of intrusion shapes reflects different emplacement mechanisms caused by contrasting host rock and magma rheologies. Most current models of tabular intrusion emplacement assume that the host rock behaves purely elastically, whereas numerous field observations show that shear failure plays a major role.

Here we will report the results of Schmiedel et al. (2019), we investigate the effects of the host rock's Coulomb properties on magma emplacement by integrating (1) laboratory models using dry Coulomb granular model hosts of variable strength (cohesion) and (2) limit analysis numerical models (Figure 1). Our results show that both, sheet and massive tabular intrusions initiate as a sill, which triggers shear failure of its overburden along an inclined zone of shear damage at a critical sill radius, which depends on the emplacement depth and the overburden's cohesion. Two scenarios are then possible (Figure 1, bottom): (1) if the cohesion of the overburden is significant, opening of a planar fracture along the precursory weakened shear damage zones to accommodate magma flow, leads to the formation of inclined sheets, or (2) if the cohesion of the overburden is negligible, the sill inflates and lifts up the overburden, which is dissected by several faults that control the growth of a massive intrusion. Finally, we derive a theoretical scaling (Figure 1, Theoretical model) that predicts the thickness-to-radius aspect ratios of the laboratory sheet intrusions. This theoretical prediction shows how sheet intrusion morphologies are controlled by a mechanical equilibrium between the flowing viscous magma and Coulomb shear failure of the overburden. Our study suggests that the emplacement of sheet and massive tabular intrusions are parts of the same mechanical regime, in which the Coulomb behaviour of the Earth's brittle crust plays an essential role.

Acknowledgements

Thanks to The Royal Swedish Academy of Science (www.kva.se) for funding the participation of T. Schmiedel at the LASI6 conference.

References

Delpino, D., Bermúdez, A., Vitulli, N., & Loscerbo, C. (2014). Sistema de Petróleo no convencional relacionado con lacolitos Eocenos de intraplaca. In Área altiplanicie del Payún, cuenca Neuquina, paper presented at IX Congreso de Exploración y Desarrollo de Hidrocarburos (pp.223–242). Instituto Argentino del Petróleo y el Gas: Mendoza.

Galland, O., Planke, S., Neumann, E.-R., Malthe-Sørenssen, A., 2009. Experimental modelling of shallow magma emplacement: application to saucer-shaped intrusions. *Earth Planet. Sci. Lett. 277*, 373–383. DOI: 10.1016/j.epsl .2008.11.003.

Haug, ØT., Galland, O., Souloumiac, P., Souche, A., Guldstrand, F., Schmiedel, T., 2017. Inelastic damage as a mechanical precursor for the emplacement of saucer-shaped intrusions. *Geology 45*, 1099–1102. DOI: 10.1130/G39361.1.

Haug, Ø. T., O. Galland, P. Souloumiac, A. Souche, F. Guldstrand, T. Schmiedel, and B. Maillot (2018), Shear versus tensile failure mechanisms induced by sill intrusions -- Implications for emplacement of conical and saucer-shaped intrusions, *Journal of Geophysical Research: Solid Earth*, *123*, 3430-3449. DOI: 10.1002/2017JB015196

Schmiedel, T., O. Galland, Ø. T. Haug, G. Dumazer, and C. Breitkreuz (2019), Coulomb failure of Earth's brittle crust controls growth, emplacement and shapes of igneous sills, saucer-shaped sills and laccoliths, *Earth Planet. Sci. Lett.*, *510*, 161-172. DOI: 10.1016/j.epsl.2019.01.011

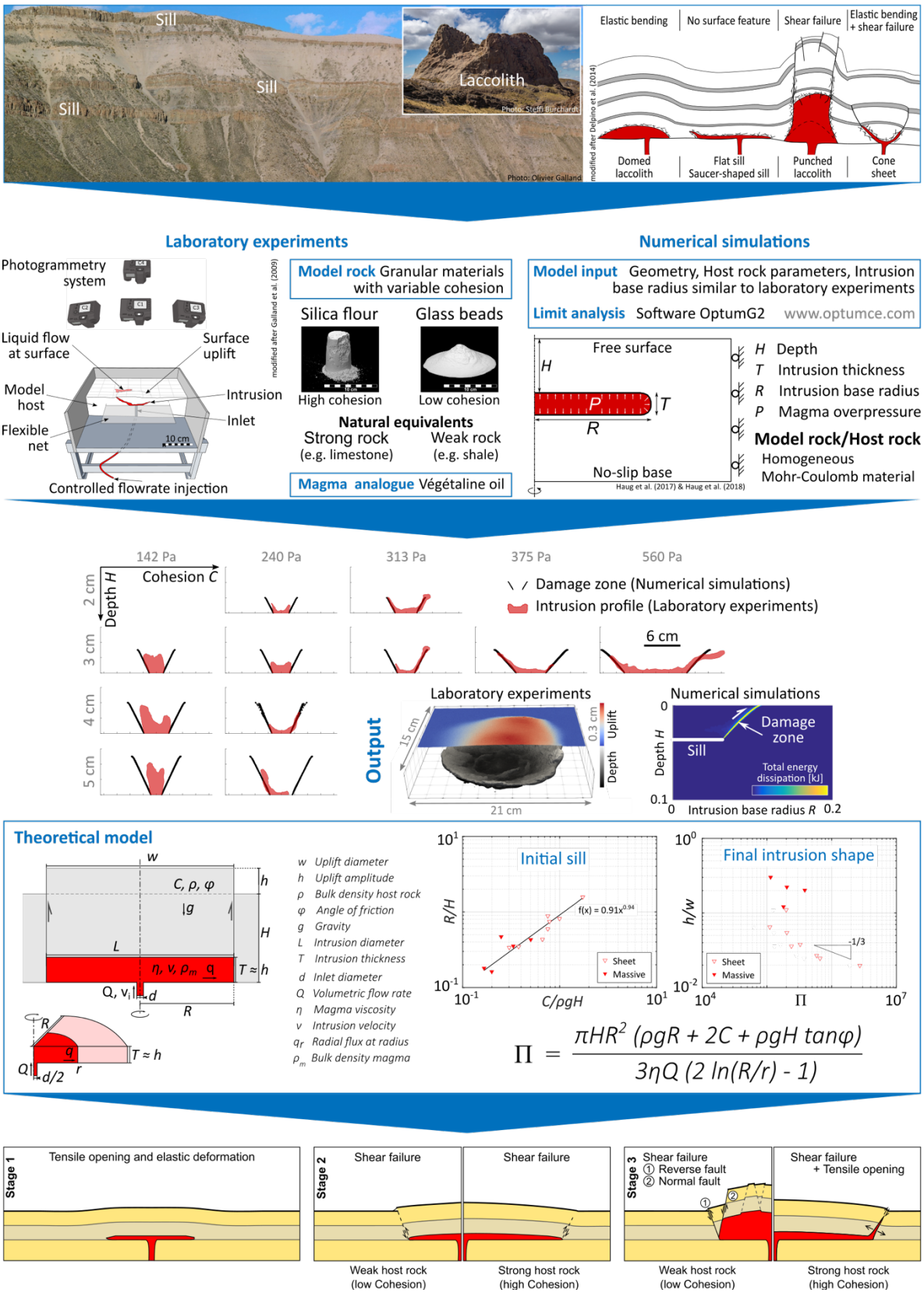

Fig. 1 – Graphical representation of “Coulomb failure of Earth’s brittle crust controls growth, emplacement and shapes of igneous sills, saucer-shaped sills and laccoliths” (Schmiedel et al., 2019).

Numerical modelling towards fast melt transport in magmatic continental crust via dykes

Herbert Wallner and Harro Schmeling

Institut für Geowissenschaften, Goethe-University, Frankfurt a.M., Germany – wallner@geophysik.uni-frankfurt.de

Keywords: Numerical Modelling, Magmatism, Extraction.

Melting and melt ascent in the continental crust is an important process contributing to its structural and compositional evolution. Even the physical understanding is poor. Numerical modelling is a way to study and improve the knowledge of magmatic systems, their various aspects and processes involved.

We developed a thermo-mechanical-compositional two-phase flow formulation based on the conservation equations of mass, momentum, energy, and composition for melt and solid, including compaction of the solid matrix, melting, melt segregation, melt ascent and freezing. We apply non-linear visco-plastic rheology using power law parameters of quartzite or granite and plasticity derived from Byerlee's Law. For melting and freezing a simplified binary melting model is utilized. Meta-greywacke serves as the initial rock type for solidus and liquidus definition. Their chemical composition, i.e. for us the enrichment or depletion in SiO_2 of the advected silicic melt and solid, is tracked. Melt mobility depends on the viscosity of the melt in combination with permeability of the partially molten rock; they essentially determine the retention number. Numerical approximation is done with our code FDCON based on Finite Differences with markers in an Eulerian formulation in 2D.

Plutonism and additionally second phase segregation, for instance by accumulating melt beneath the solidus of the stiff upper crust, can be modelled by this physics, see Fig. 1 and Schmeling et al. 2019. However, observations show additional fast melt transport mechanisms acting on a short time scale. These symptomatically cannot be handled numerically by the same approach due to the big difference of time-step length of several orders.

A widely used practice is the extraction of melt and its intrusion in a given emplacement level or extrusion to the surface. Our approach uses a parametrization of three critical limits where vertically connected partially melted zones serve as source region of extraction. The source regions undergo compaction, inducing under-pressure and attracting ambient melt. In a higher, colder crustal level the emplaced melt dilatates the matrix, and usually freezes immediately; heating and an increase of enrichment occurs. Such approaches locally violate mass and momentum equations more or less, and, more importantly, magma is redistributed at ad-hoc positions. Argumentation for intrusion levels are low constraint and do not follow the idea of self-consistency.

The most obvious fast magma transport mechanism through the subsolidus region is dyking. Aim of our DFG-research project "Modelling melt ascent through the asthenosphere-lithosphere-continental crust system: Linking melt-matrix-two-phase flow with dyke propagation" is coding the combination of two-phase flow physics and consistently draining the melt from the top of the partially molten regions, emplace the fast transported magma volumes and feed them back complying conservation laws. For the slow two-phase flow system "dyking" is time-independent, happening within a time step. From the perspective of dykes the surrounding stress field is static. Fig. 2 shows a conceptual sketch.

Spatially, single dykes are not resolved in the spacing of the matrix-melt system. The melt to be extracted at a node may serve several dykes or a swarm. Accordingly, for the feedback, melt volumes of stagnated dykes, mostly sills must be integrated and distributed suitable to nodes.

In our approach "dyking" can be subdivided in generation (1), propagation (2), and stagnation (3) of a dyke. 1) For the nucleation and formation of a self-propagating dyke the combination of several conditions, like a) position near the melt front, b) enough melt supply, c) stress concentration above rock toughness must be fulfilled. 2) In a preliminary simple approach the propagation of a dyke in an subsolidus elastic medium exposed to regional stresses is controlled by the minimum principle stress direction. A more advanced approximation, where the crack orientation at the dyke tip is given by the maximum total energy release (strain and gravitational), will be implemented. The numerical code is based on the Boundary Element Method for fluid filled fractures. For crack opening, thus, propagation, a specific fracture energy threshold must be exceeded. 3) The criterion for stagnation of a dyke in the 1st approach is simply dipping downward; in the better 2nd approach the dyke will stop when energy release is below the threshold.

The model layout intents to allow fundamental study of magmatism in a thick crust. Therefore, we apply a 50 km high square 2D box with reflective

vertical sides; it is assumed to dip into the lower crust where a bottom heat flux serves for energy to generate melt. A scenario of a continental crust above an uprising mantle plume approaching the crust, probably underplating it, serves as background idea. Increasing the heat flux from below, held for 1 Ma and subside afterwards, thus, a heat puls, shifts temperature above solidus. Partial melting starts and increases for some time. An additional temperature perturbation localizes the process in the centre of the symmetric model. Typical phases of the evolution are doming, upward segregation, formation of a melt band, localization of melt in the band, upward arching of instabilities, ascending fingers and freezing. The behaviour pattern varies with controlling parameters and boundary conditions. Extraction above a threshold or dyking modifies the evolution and resulting structures. A selected model of extraction and emplacement is presented and opposed to first results of models with dyking.

References

Schmeling, H., G. Marquart, R. Weinberg, H. Wallner (2019), Modelling melting and melt segregation by two-phase flow: new insights into the dynamics of magmatic systems in the continental crust, *Geophysical Journal International, 217(1),* 422-450.

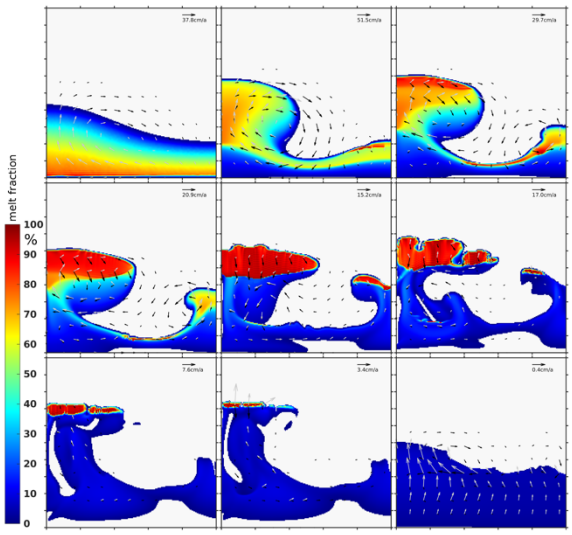

Fig. 1 – Time steps of melt percentage for a typical model with melt segregation, full compaction, 85 mW m^{-2} nominal surface heat flux, and a retention number of 3. Matrix and fluid velocities are indicated by black and grey arrows, respectively.

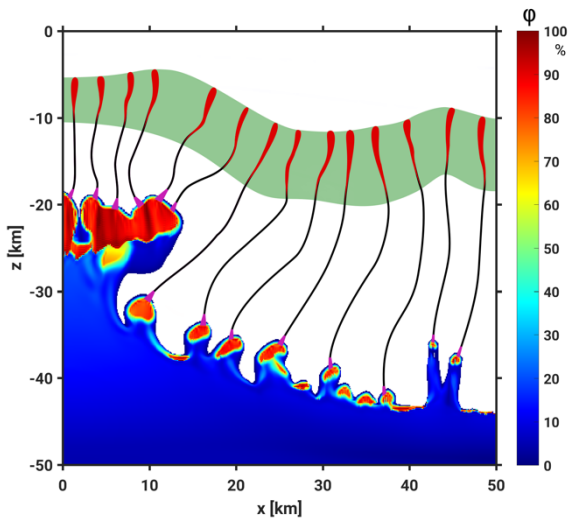

Fig. 2 – Sketch of proposed modelling approach. Melt fraction of an exemplary two-phase flow model of a magmatic crust is shown. High melt accumulations serve as source regions for dykes, which follow imaginary paths upward until they stagnate. Features of the green emplacement zone will be fed back into the two-phase flow crustal model.

Magma ascent and emplacement below impact craters on the Moon

Damian Walwer [1], Chloé Michaut [1],Virginie Pinel [2], Mokhtar Adda-Bedia [3]

[1] *Geology laboratory, ENS Lyon, Lyon, France* – damian.walwer@ens-lyon.fr
[2] *Institut des Sciences de la Terre, University of Savoie Mont Blanc, Grenoble, France*
[3] *Physics Laboratory, ENS Lyon, Lyon, France*

Keywords: Intrusion, Crater, Moon.

Floor fractured craters are a class of crater on the Moon that presents deformed uplifted and fractured floors (see figure 1). Those peculiar morphological characteristics are caused by the endogenous modifications of the crater floor by underlying magmatic intrusions in the forms of shallow sills and laccoliths. However, the lunar crust shows a very low density making the magma negatively buoyant and preventing it from rising toward the surface. Here we provide two independent observations that show that the driving mechanism that counterbalances the negative buoyancy of the magma in the lunar crust and allows its emplacement near the surface is provided by a modification of the stress field caused by the crater cavity that unloads the underlying elastic medium. The first observation is the total uplift of the crater floor that provides estimates of the intrusion thickness when it reaches the weight that compensates for the driving pressure responsible for magma ascent if the additional magma pressure caused by the elastic deformation of the overburden is negligible. The second observation is the total length of fractures covering the crater floor that, as stated by Griffith theorem of brittle fracture, reflects the stress modifications caused by laccoliths emplacement and thickening. Those two observations are correlated. We show that to fully explain the driving pressure responsible for magma emplacement as estimated from these two observations one needs to take into account two antagonistic effects that crater unloading has on a vertical dyke emanating from the mantle/crust boundary (fig. 2). On the one hand, crater unloading decreases the stresses exerted by the surrounding medium on the vertical fissure filled with magma favoring tensile opening of the dyke and further vertical ascent of magma. On the other hand, it also decreases the magma pressure at its source.

Acknowledgements

This work has been realised thanks to the financial support of the IDEXLyon Project of the University of Lyon and the Region Auvergne Rhône-Alpes.

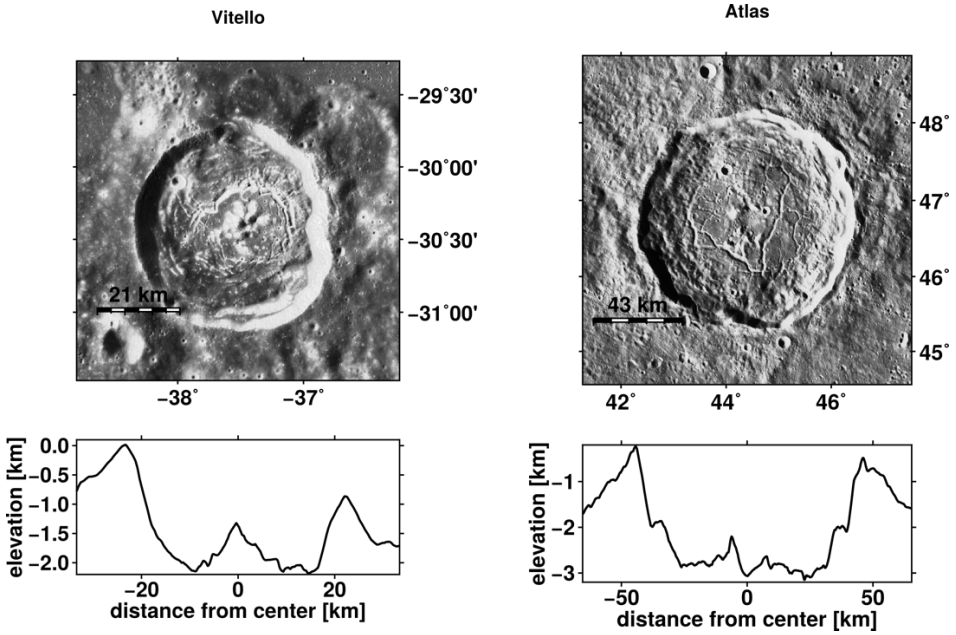

Fig. 1 - Examples of two floor fractured craters on the Moon. The maps show images of the fractured floors of Vitello and Atlas. While Vitello display a circular fracture, Atlas shows less symmetry in its fractures pattern. The graphs below the maps display East/West topographic cross-sections for the two craters that reveal their uplifted floor.

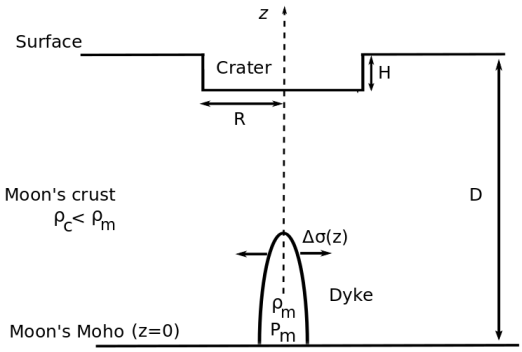

Fig. 2 - Schematic representation of the components of the model that allow to compute the driving pressure leading to magma emplacement below impact craters. A vertical dyke emanating from the Moon's Moho inside which magma pressure is P_m and magma density ρ_m is subjected to tensile stress $\Delta\sigma$ caused by the crater cavity of radius R and depth H.

Geometries of magmatic intrusions in anisotropic rocks

Zanella A.[1], Garreau T.[2]

[1] *Géosciences Le Mans, UMR 6112 CNRS, Le Mans Université, Le Mans, France* – alain.zanella@univ-lemans.fr
[2] *Géosciences Le Mans, Le Mans Université, Le Mans, France*

Keywords: *anisotropy,* fracturing, magmatic intrusions.

On Earth, sedimentary basins represent a preferential area for interactions between deep and surficial geological processes. Magmatic intrusions are very common in sedimentary basins. In the Neuquén Basin, Argentina, magmatic intrusions are especially well known in anisotropic mudstones that could be potential source rocks for petroleum such as the Vaca Muerta Formation. Because of the potential thermal effect on the organic matter (Rodriguez et al., 2007, 2009; Witte et al. 2012; Spacapan et al. 2019), the geometries of magmatic bodies are very useful to understand. Nevertheless, these geometries are often difficult to predict because of the very complex mechanical properties of anisotropic sediments.

To investigate the effects of the anisotropy on the geometry of magmatic intrusions, we performed experimental models in a hele-shaw cell. The size of the cell is of 70x40x3 centimeters and an injector (with a pump system) is used at the bottom (20 cm deep) to intrude a fluid into the model. In our model, a glucose syrup represents the magma and we used a mixture of granular materials to represent a variable degree of anisotropy in the model. Thus, we used: 1) sand to represent an isotropic granular material, 2) pure grains of micas to represent a high anisotropic degree and 3) a mixture of sand and micas to be able to have an intermediate degree of anisotropy. All our materials are mixed with gelatin to introduce cohesion between the grains.

In the experiments with a pure isotropic material (1), the geometry of the intrusions was in 'V', developing 2 shear zones due to the injection of the syrup as well as the bulge of the surface of the model. In the experiments with a pure anisotropic material (3), we formed horizontal fractures filled by the syrup. The propagation of the fractures followed the anisotropy and was located few centimeters above the injector. As for the previous experiment set, we obtained a bulge at the surface. In the last set of experiments, we used the mixture (2). The geometries of the developed intrusions were more random, showing a competition between vertical and horizontal growth of the filled fractures (Fig. 1). Thus, several levels of horizontal fractures are linked together by vertical fractures.

In our experiments, we demonstrate that the anisotropy has a great impact on the geometry of fluid injections as in the case of viscous fluid such as magmas. We infer that the anisotropy seems to be one of the most important mechanical parameters involved to understand the geometry of fractures in rocks.

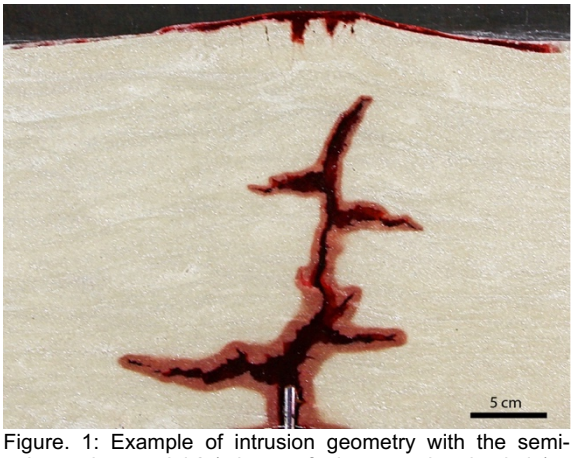

Figure. 1: Example of intrusion geometry with the semi-anisotropic material 2 (mixture of micas, sand and gelatin).

References

Abdelmalak, M. M., Mourgues, R., Galland, O., and Bureau, D., 2012. Fracture mode analysis and related surface deformation during dyke intrusion: Results from 2D experimental modelling, Earth Planet. Sci. Lett., 359-360, 93–105, doi: 10.1016/j.epsl.2012.10.008.

Galland, O., Burchardt, S., Hallot, E., Mourgues, R., and Bulois, C., 2014. Dynamics of dikes versus cone sheets in volcanic systems, J. Geophys. Res. Solid Earth, 119, 6178–6192, doi: 10.1002/2014JB011059.

Mourgues, R., Bureau, D., Bodet, L., Gay, A., & Gressier, J. B., 2012. Formation of conical fractures in sedimentary basins: Experiments involving pore fluids and implications for sandstone intrusion mechanisms. Earth and Planetary Science Letters, 313, 67-78.

Rodriguez, F., Villar, J.H., Baudino, R., 2007. Hydrocarbon Generation, Migration, and Accumulation Related to Igneous Intrusions: an Atypical Petroleum System from the Neuquén Basin of Argentina. SPE Paper 107926-PP, p. 4.

Rodriguez Monreal, F., Villar, H.J., Baudino, R., Delpino, D., Zencich, S., 2009. Modeling an atypical petroleum system: a case study of hydrocarbon generation, migration and accumulation related to igneous

intrusions in the Neuquén Basin, Argentina. Mar. Petroleum Geol. 26, 590-605, doi: http://dx.doi.org/10.1016/j.marpetgeo.2009.01.005.

Spacapan, J. B., D´Odorico, A., Palma, O., Galland, O., Senger, K., Ruiz, R., ... & Leanza, H. A., 2019. Low resistivity zones at contacts of igneous intrusions emplaced in organic-rich formations and their implications on fluid flow and petroleum systems: A case study in the northern Neuquén Basin, Argentina. Basin Research, doi: 10.1111/bre.12363.

Witte, J., Bonora, M., Carbone, C., Oncken, O., 2012. Fracture evolution in oil-producing sills of the Rio Grande Valley, northern Neuquén Basin, Argentina. Am. Assoc. Petroleum Geologists Bull. 96 (7), 1253-1277, doi: 10.1306/10181110152.

Session on Contact Metamorphism and Associated Mineralization

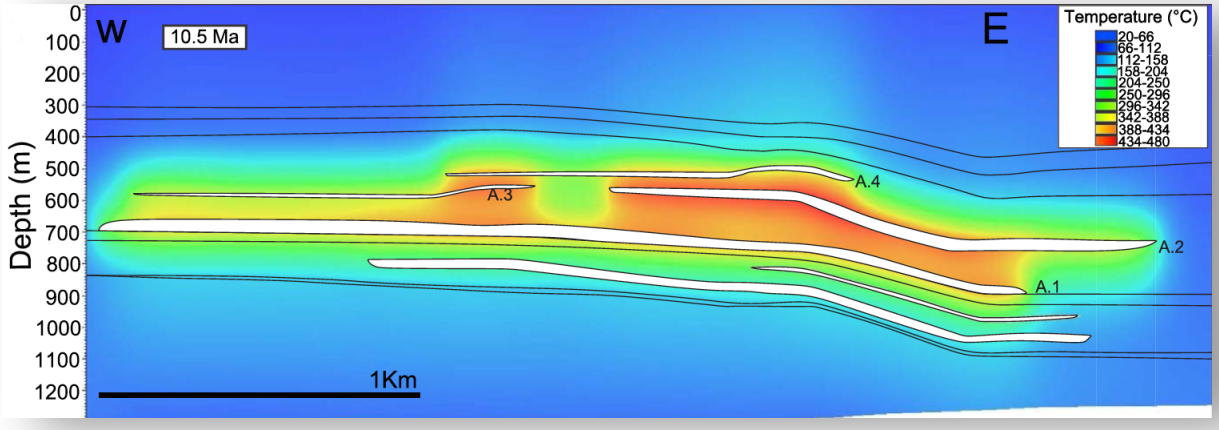

Contents

Magma fingers, chonoliths and Ni–Cu–PGE sulfide ore deposits

Cruden, A.[1], Barnes, S.[2], Magee, C.[3], **Köpping J.[1]**, Nissanka Arachchige U.[1], and Fiorentini, M.[4]

[1] *School of Earth, Atmosphere & Environment, Monash University, Melbourne, Australia* – sandy.cruden@monash.edu
[2] *CSIRO Mineral Resources Flagship, Perth, Australia*
[3] *Institute of Geophysics and Tectonics, School of Earth and Environment, University of Leeds, Leeds, UK*
[5]*School of Earth Science, University of Western Australia, Perth, Australia*

Keywords: magmatic Ni-Cu-PGE sulfides, chonoliths, .

Intrusion-hosted Ni–Cu–PGE magmatic sulfide deposits accumulate within crustal-scale magma plumbing systems that transport mantle-derived mafic and ultramafic magmas from mantle sources to the surface. Magmatic sulfide mineralization within such systems occurs in a variety of traps that form due to a combination of structural and fluid-mechanical processes. Ore-hosting structures include tubular chonoliths (e.g., Nebo-Babel and Limoiera), ribbon-shaped sills (e.g., Noril'sk and Nkomati/Uitkomst), funnel-shaped jogs within conduits (e.g., Voisey's Bay Ovoid), elongate funnel-shaped flares within dyke-like intrusions (Eagle, Tamarack) and blade-shaped dykes (e.g., Expo-Ungava) (Barnes et al., 2016). Considerable research has been focused on the links between lithospheric architecture and Ni–Cu–PGE mineralization and the geochemical origins of sulfide mineralization. Far less work has addressed the physical processes involved in the transport of the host magmas, how high-flux channels develop, and where sulfide liquids separate and accumulate to form ore deposits.

Pipe-like chonolith intrusions (Fig. 1A) are economically highly important with 58 of the 61 known examples in the world hosting Ni–Cu–PGE mineralization, 26 of which are producing mines (Beresford and Hronsky 2014). A major challenge for mineral explorers is that high-value mineralized pipes are exceedingly rare, making up <0.01% by volume of the magma plumbing systems in which they occur (Barnes et al. 2016). In other words, Ni–Cu–PGE deposits have a much smaller "footprint" compared to other base metal deposits. Narrowing down the search space for Ni–Cu–PGE mineralization is further compounded by the fact that very little research has been carried out on the form, structure and emplacement of pipe-like intrusions. This is partly due to their rarity and also because their economic significance has only recently been realized by the mineral exploration community (Beresford and Hronsky 2014).

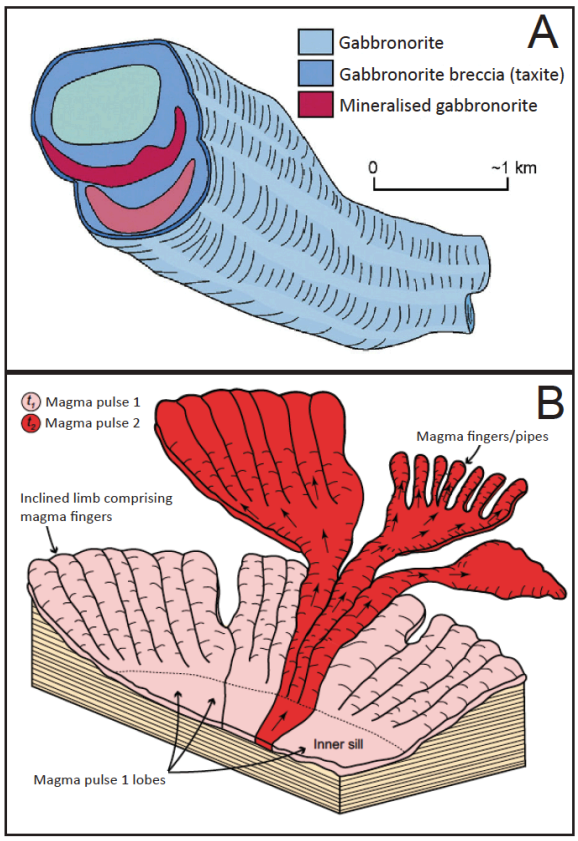

Fig. 1 – A) Pipe-like magma conduit (chonolith) defined by drilling, Nebo-Babel deposit, WA (Seat et al., 2007). Note this sketch has been flipped upside down to reflect the likely original, pre-deformation geometry of the intrusion and its mineralization. B) Conceptual sketch of a sill system based on 3D seismic data and field observations. Sill margins break down into fingers, which can further evolve into high-flux magma channels (Magee et al., 2016).

The magma plumbing systems that host Ni–Cu–PGE sulfide mineralization can be many thousands of kilometers wide. They transport enormous volumes of magma from the mantle through the crust via interconnected networks of sub-vertical and sub-horizontal dykes and sills. Their stair-stepping architecture can be focused above the mantle source or become laterally displaced from it over 100s to 1000s of kilometers (Magee et al. 2016).

Based on constraints from field observations, 3D seismic surveys and bore hole drilling data, we

discuss the form and emplacement mechanisms of pipe-, tube- and ribbon-shaped chonoliths. Using existing theory and preliminary laboratory experiments, we hypothesize that chonoliths form by the viscous or elastic destabilization of propagating dykes and sills and coeval or subsequent amplification (elongation and widening) by the development of solidification instabilities and or thermo-mechanical erosion. Such emergence is often strongly controlled by pre-existing country rock structure. We also suggest that chonoliths form linking conduits in crustal-scale sill systems, which explains the association between Ni–Cu–PGE sulfide deposition and high magma fluxes. A process-based understanding of chonolith development within magma plumbing systems should aid in the development of new exploration strategies for intrusion-hosted Ni–Cu–PGE sulfide deposits.

Acknowledgements

Supported by Australian Research Council Discovery Grant DP190102422

References

Barnes, S.J., Cruden. A.R., Arnt, N., and Saumur. B-M. (2016), The mineral system approach applied to magmatic Ni−Cu−PGE sulfide deposits, *Ore Geology Reviews*, 76 296-316.

Beresford, S., and Hronsky, J. (2014), The chonolith Ni–Cu model: expanding the footprint of Ni-Cu deposits, Abstract, 12th International Platinum Symposium, Institute of Geology and Geochemistry, UB RAS, 2014, p. 23.

Magee, C., Muirhead, J.D., et al., (2016), Lateral magma flow in sill-complexes, *Geosphere*, 12, 1-33.

Seat, Z, et al., (2007), Architecture and emplacement of the Nebo–Babel gabbronorite-hosted magmatic Ni–Cu–PGE sulfide deposit, West Musgrave, Western Australia, *Mineralium Deposita*, 42, DOI 10.1007/ s00126-007-0123-9.

Complex metamorphic and metasomatic processes and products: preliminary mineralogical assemblages from Irati Fm and Serra Geral intrusions (Stavias Quarry, Rio Claro SP, Brazil)

Gaspar JC.[1,2], Mettraux M.[1], Neumann R.[3], Homewood P.[1], Dias-Brito D.[1] and Arai M.[1]

[1] *UNESPetro, Instituto de Geosciências Exatas, Universidade Estadual "Julio de Mesquita Filho", Rio Claro SP, Brasil*
[2] *josecarlosgaspar@gmail.com*
[3] *CETEM Av. Pedro Calmon, 900 - Cidade Universitária 21941-908 - Rio de Janeiro RJ, Brasil*

Keywords: metasomatism, metamorphism, Irati.

The interaction of Serra Geral magmas with the Assistência Member of Irati Formation, Paraná Basin, has been subject of a detailed research program as pointed out by Mettraux et al. (this Conference, ANP Project 20435-4). In the Stavias Quarry, Rio Claro SP, a >70m diabase intrusion is overlain by a thin heterolithic cover comprising about 3m of carbonates and black shales that are typical of the Assistência Member. A detailed investigation by µ-XRF, XRD, and SEM showed that thermal metamorphism was the first event occurring in the country rock followed by complex metasomatic processes. The large igneous body was clearly the source of heat for the contact metamorphism and for the fluids (at least in part) having caused hydrothermal alteration of the metamorphic assemblage. Samples were collected at the contact with the diabase and within the first 50cm from the contact in order to investigate the more intense metamorphism and metasomatic alteration that affected the country rocks, mostly the carbonate layers. Initial results, essentially the mineral parageneses due to both metamorphic and metasomatic processes are presented here.

Contact metamorphic assemblages include diopside and grossular, widespread as main constituents, with subordinate amounts of tremolite and wollastonite (as patches). The full mineral assemblages are difficult to determine due to late alteration superimposed on these minerals. This well-known assemblage is typical in aureoles of calc-silicate rocks surrounding igneous intrusions. Common decarbonation and dehydration reactions resulted in mineral assemblages with very low carbonate abundance and minerals with little or no water in their structures.

The most conspicuous hydrothermal minerals are apophyllite and pectolite; apophyllite occurs as anhedral, equant to sub-equant crystals (usually 10 to 200µm) and usually forms patches, while pectolite crystals form fibrous aggregates (usually 5 to 300µm) usually associated with apophyllite but locally making almost monomineralic rock portions. Analcime is commonly associated with both apophyllite and pectolite. These minerals show that Na, K and F were present in the fluids. A calcic plagioclase is commonly associated with the analcime as well as other metasomatic minerals.

The stable clinopyroxene under the metasomatic conditions seems to be aegirine, which occurs as very fine euhedral to subhedral (around 10µm) crystals, often associated with pectolite (Fig 1).

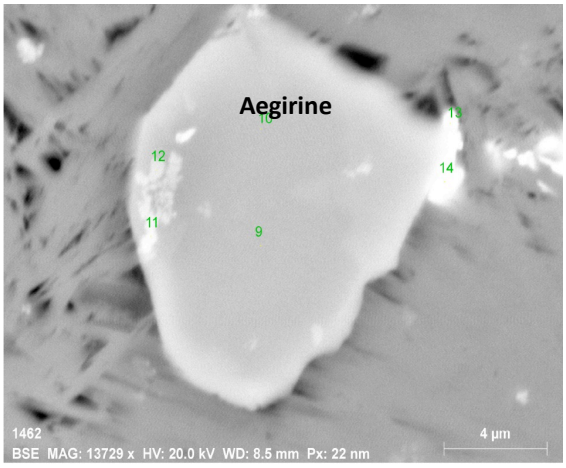

Fig. 1 – Aegirine crystal in a matrix of fibrous pectolite. Very light gray colors correspond to barite crystals.

A large part of metamorphic diopside, however, presents an aegirine-rich border with variable thickness indicating exposure to the metasomatic fluids. Aegirine-rich diopside may also form isolated veins while augite may occur as solitary crystals in association with other metasomatic minerals. This indicates both variable fluid compositions and changing physicochemical conditions in the alteration system. The small aegirine crystals and the aegirine-rich borders indicate that Na and Fe^{3+} were both abundant in the fluids.

Metamorphic grossular occurs as subhedral round crystals, which may be fully replaced by prehnite as a consequence of metasomatic reactions (Fig. 2). On the other hand, grossular may form aggregates composed of anhedral crystals, or may form veins intimately associated with metasomatic minerals, showing that grossular may be both metamorphic and metasomatic in origin (Fig. 3).

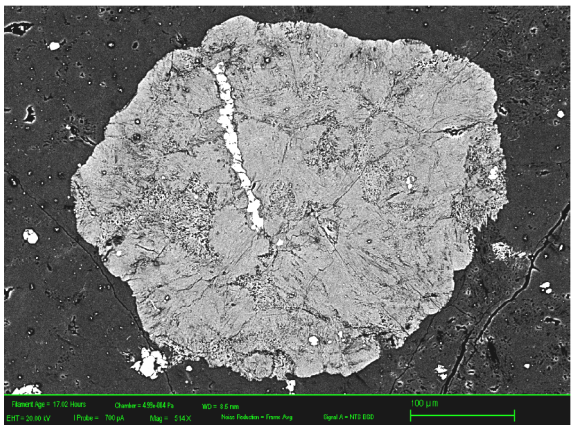

Fig. 2 – Pseudomorph of grossular composed of prehnite in a groundmass of apophyllite. Light gray vein inside the pseudomorph is diopside.

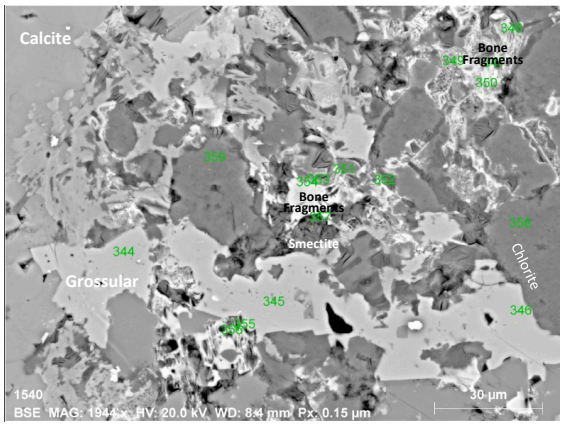

Fig. 3 – Grossular intimately associated with metasomatic minerals indicating its late stage origin. Smectite is possibly montmorillonite.

Calcite is the only carbonate associated with the metasomatic assemblages. A calcic amphibole may also be found. Chlorite (Mg-rich) and a smectite (probably montmorillonite) may be abundant in some rock portions. Smectite appears to be the last mineral to be formed by the metasomatic reactions.

Aggregates composed of euhedral magnetite and interstitial Sr-rich apatite may also be found. Sr-apatite may sometimes present higher content of Sr in borders and patches suggesting later stages reactions (Fig. 4).

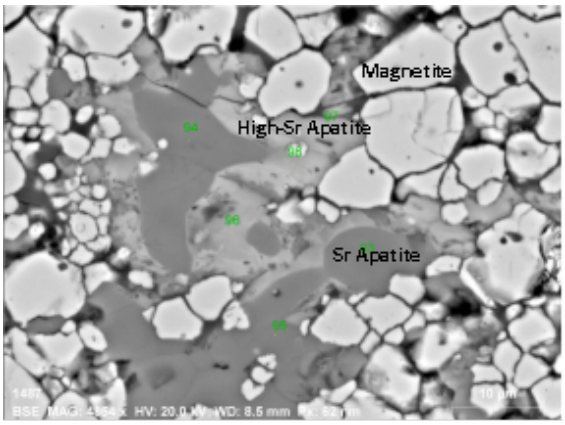

Fig. 4 – Magnetite and Sr-rich apatite aggregate. Lighter gray areas in apatite contain more than 20 wt% SrO while darker areas contain around 8 wt%.

Pyrite also forms aggregates, which seems to be in contradiction with the presence of the oxidizing fluids that have reacted with the metamorphic diopside, causing its Fe^{3+} borders and the crystallization of the magnetite aggregates. Reactions with ilmenite (probably detrital) formed titanite and baotite. Perovskite is also present. Barite occurs in trace amounts.

Clearly the metasomatic process either was a long-lasting system with continuous changes in its chemical composition and physicochemical conditions or was a multi-staged sequence of reactions due to different fluid injections.

Acknowledgements

H.Brito, R.Rohn, I.Anderson, D.Biotto, C.Lacerda, J. da Silva, JM. Cazonatto and R.Goya are thanked for technical support, discussions and suggestions. This project is funded by ANP Project 20435-4, Libra Group, through Fundunesp.

References

Mettraux, et al., (2019) Hydrothermal and other metamorphic aureole processes: initial results from outcrop and mineralogical data from the Irati Fm and Serra Geral intrusions (Rio Claro SP, Brazil). Lasi6 Conference.

Sill driven fluid circulation and hydrothermal venting in sedimentary basins

Karthik Iyer[1], Dani Schmid[1,2], Sverre Planke[3,4], Frederico Miranda[5], Fernando Aragão[5], Dougal Jerram[6,4], John Millet[3]

[1] *GeoModelling Solutions GmbH, Zurich, Switzerland*
[2] *PGP, University of Oslo, Norway*
[3] *VBPR, Oslo, Norway*
[4] *CEED, University of Oslo, Norway*
[5] *Eneva, Rio de Janeiro, Brazil*
[6] *DougalEARTH, Solihull, UK*

Keywords: *hydrothermal vent complexes, numerical models, Parnaiba*

Hydrothermal vent complexes are intimately linked to igneous sheet intrusions in sedimentary basins where they form conduits for the release of fluids and gases generated in metamorphic aureoles during thermogenic heating of organic content and formation water naturally present in sedimentary rocks (e.g. Planke et al. (2005)). Examples of this association have been observed globally and are linked to catastrophic climate change in the geological past (e.g. Heimdal et al. (2018), Svensen et al. (2018)). We use numerical models to show that two general styles of flow patterns develop around cooling intrusions which alter the thermal history of the basin and transport produced gases out of the subsurface (Iyer et al., 2013; Iyer et al., 2017). The first is associated with relatively high permeability systems where vigorous hydrothermal circulation is set up resulting in multiple plumes forming in the vicinity of the sill (Figure 1). The positions of these plumes depends on the sill geometry and results from fluid focusing at sill tips and topographical highs. Degassing in these systems is controlled by sediment permeability and occurs over a timescale ranging from tens to hundreds of thousands of years.

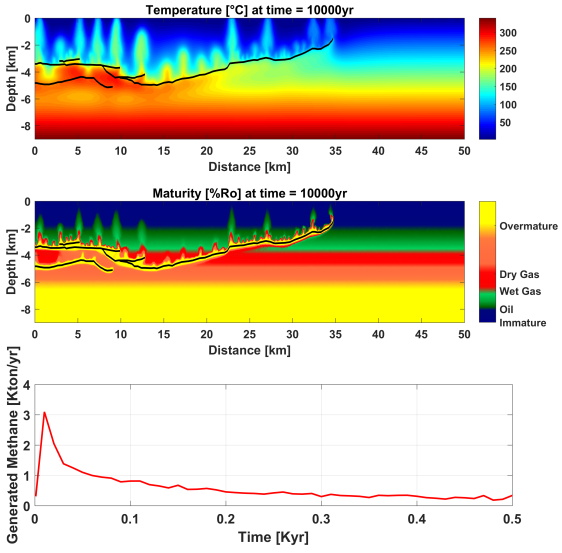

Fig. 1 Temperature and maturity of the high permeability reference simulation after 10,000 years. The rate of methane generation increases drastically as the sediment directly adjacent to the sill is initially heated up. The rate then decreases as the thermal aureole gradually widens and hydrothermal plumes are formed.

The second style, on the other hand, forms explosive vents in low permeability systems and is controlled by overpressure generation and fracture formation in the sill aureole as enormous quantities of gas are generated around the sill. In such cases, fluid focusing coupled with overpressure migration towards the sill tips results in rapid vent formation after only few tens of years. Overpressure migration occurs in self-propagating waves before dissipating at the surface. The size of the vent depends on the region of overpressure accessed by the sill tip and results in the formation of fewer large vents than in high permeability, plume systems.

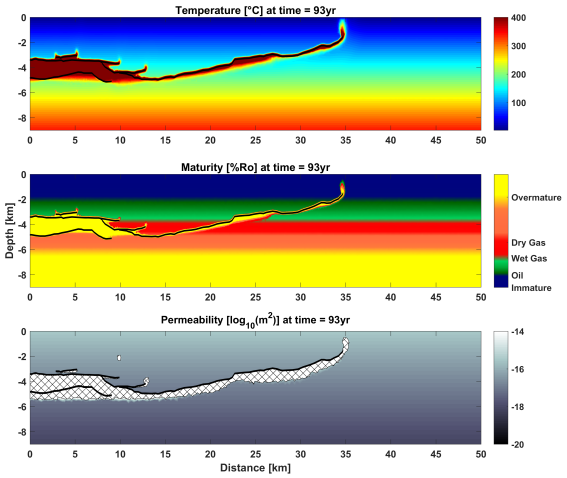

Fig. 2 Temperature, maturity and permeability in the low permeability simulation with fracture formation after 80 years. A single large vent structure is rapidly formed above the main sill tip due to sustained overpressure. Overpressure is produced around sills where large volumes of gas are generated by thermal cracking of organic matter in the host sediments. Overpressure generated below the sill cannot dissipate upwards through the sill and, therefore, migrates along the sill until the tip is reached. This migration happens in waves due to the cycle of overpressure generation,

fracture formation, pressure reduction and fluid flow. The mechanism, therefore, self-generates fluid pathways until the overpressure wave reaches the surface and leaves the system. This process restarts once enough overpressure is built up again due to kerogen breakdown resulting in the observed waves.

The generation and rate of degassing from such systems is compared to that associated with warming during the Paleocene-Eocene Thermal Maximum (PETM) by upscaling the results to the Vøring and Møre Basins which are a part of the North Atlantic Igneous Province (NAIP). We find that the rate of degassing in high permeability systems couple with the estimated vent structures in these Basin cannot adequately explain the negative carbon isotope excursion (CIE) associated with the PETM when the organofacies of the sediment is accounted for. However, explosive vent formation and violent degassing in low permeability systems occurs relatively quickly and may explain the negative CIE providing that other regions in the NAIP with significantly better source rock properties are also affected.

Igneous intrusions also significantly impact the petroleum systems of the basin in which they are formed (Muirhead et al. (2018); Spacapan et al. (2018)). They can be either detrimental to such systems by over-maturing or cracking already in-place hydrocarbons or, on the other hand, generate hydrocarbons at shallow levels where source rocks are immature. They can either act as seals for hydrocarbon reservoirs (e.g. Parnaíba Basin, Brazil) or also as reservoirs for liberated hydrocarbons (e.g. Neuquén Basin, Argentina). Here, we will present new results on the impact of sill intrusion on the existing petroleum system in the Parnaiba Basin in Brazil. The numerical model is based on a published cross-section (de Miranda et al., 2018) across a drilled region where dolerite sill complexes are responsible for triggering source rock maturity, creating four-way closures and sealing gas accumulations in the sedimentary strata (Figure 3).

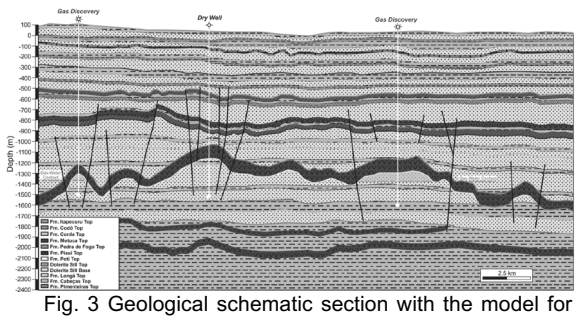

Fig. 3 Geological schematic section with the model for the major trapping mechanism for commercial gas accumulations in the Parnaíba Basin, Brazil (modified from Miranda et al., 2018).

Acknowledgements

We thank Eneva for supporting this work.

References

de Miranda, F. S., Vettorazzi, A. L., da Cruz Cunha, P. R., Aragão, F. B., Michelon, D., Caldeira, J. L., Porsche, E., Martins, C., Ribeiro, R. B., and Vilela, A. F., 2018, Atypical igneous-sedimentary petroleum systems of the Parnaíba Basin, Brazil: seismic, well logs and cores: Geological Society, London, Special Publications, v. 472, no. 1, p. 341-360.

Heimdal, T. H., Svensen, H. H., Ramezani, J., Iyer, K., Pereira, E., Rodrigues, R., Jones, M. T., and Callegaro, S., 2018, Large-scale sill emplacement in Brazil as a trigger for the end-Triassic crisis: Scientific Reports, v. 8, no. 1, p. 141.

Iyer, K., Rüpke, L., and Galerne, C. Y., 2013, Modeling fluid flow in sedimentary basins with sill intrusions: Implications for hydrothermal venting and climate change: Geochemistry, Geophysics, Geosystems, v. 14, no. 12, p. 5244-5262.

Iyer, K., Schmid, D. W., Planke, S., and Millett, J., 2017, Modelling hydrothermal venting in volcanic sedimentary basins: Impact on hydrocarbon maturation and paleoclimate: Earth and Planetary Science Letters, v. 467, p. 30-42.

Muirhead, D. K., Duffy, M., Schofield, N., Mark, N., and Rowe, M. D., 2018, Making oil from magma: Geological Society, London, Special Publications, v. 484.

Planke, S., Rasmussen, T., Rey, S. S., and Myklebust, R., 2005, Seismic characteristics and distribution of volcanic intrusions and hydrothermal vent complexes in the Vøring and Møre basins, *in* Doré, A. G., and Vining, B. A., eds., Petroleum Geology: North-western Europe and global perspectives - Proceedings of the 6th Petroleum Geology Conference.: London, Geological Society.

Spacapan, J. B., Palma, J. O., Galland, O., Manceda, R., Rocha, E., D'Odorico, A., and Leanza, H. A., 2018, Thermal impact of igneous sill-complexes on organic-rich formations and implications for petroleum systems: A case study in the northern Neuquén Basin, Argentina: Marine and Petroleum Geology, v. 91, p. 519-531.

Svensen, H. H., Frolov, S., Akhmanov, G. G., Polozov, A. G., Jerram, D. A., Shiganova, O. V., Melnikov, N. V., Iyer, K., and Planke, S., 2018, Sills and gas generation in the Siberian Traps: Philosophical Transactions of the Royal Society A: Mathematical, Physical and Engineering Sciences, v. 376, no. 2130.

Metamorphism of pre-salt limestones produced by Santonian-Campanian alkaline sills in the Libra Block, Santos Basin

Ren Kangxu[1], Oliveira M. J. R.[2], Zhao Junfeng[1], Zhao Jian[1], Oliveira L. C.[2], Rancan C. C.[2], Carmo I. O.[3] and Deng Qicai[4]

[1] *CNODC Brasil, Praia de Botafogo, 228, Sala 1001, Ala A, Botafogo, Rio de Janeiro, Brasil* – email: renkangxu@163.com
[2] *PETROBRAS/Libra, Av. República do Chile, 330, 26ºAndar, Torre Oeste, Rio de Janeiro, Brasil*
[3] *PETROBRAS/Cenpes, Av. Horácio de Macedo, 950, Quadra 7,Coroa Central, sala 9005A, Rio de Janeiro, Brasil*
[4] *CNOOC Brasil, Rua Lauro Müller, 116, Botafogo, Rio de Janeiro, Brasil*

Keywords: Sill, pre-salt limestone, metamorphism

The igneous rocks in the Libra Block of Santos Basin, southeastern Brazil are relatively common, including events from Valanginian-Hauterivian, Aptian, Santonian-Campanian and Eocene (Moreira et al., 2007). They occur in pre-salt, intra-salt and post-salt layers (Rancan et al. 2018). The emplacement of both extrusive and intrusive igneous rocks, may create barriers within the carbonate sedimentary successions (De Luca et al. 2015). This paper focuses on the impact of intrusive igneous rocks on the associated limestone host rocks.

Sills are the most extensive type of occurrence for the pre-salt intrusive igneous rocks in many boreholes from Libra Block. In the northwest structure (Mero Field) they are predominant in the Barra Velha Fm., and secondarily in the Itapema Fm. Thicknesses of these sills vary greatly, usually with less than one meter to dozens of meters. The rock types include alkaline diabase, alkaline gabbro and lamprophyre (Rancan et al., 2018; Marins et al., 2016, 2017). $^{40}Ar/^{39}Ar$ testing dating show dominant activities during Santonian-Campanian with a range of 83.3 ± 0.7 Ma to 72.4 ± 4.9 Ma (Rancan et al. 2018).

Due to the high temperature of the alkaline magma intruding the carbonate layers, baking of the host rocks is developed unavoidably. Typically, this thermal contact baking will form an aureole parallel to the intrusion. In the Libra Block, both intrusions and the host limestone were sampled by drill cores and sidewall cores (SWC). This support the better understanding the phenomenon of baking aureoles in limestone reservoirs.

Based on macroscopic and microscopic analysis of the samples, it is observed that the most significant phenomenon of limestone in the contact bake zone is the apparent fading, that is, the rock change from the original gray or dark gray to white and grayish white. Color variations include uniformity and non-uniformity. The latter is more common, such as spotted, decentralized, banded, and so on. The minerals in the limestone aureole undergo recrystallization and the grain size increasing. In addition, the porosity of the reservoir has also changed significantly. This change in limestone is called marbleization, which is a very important factor for reservoir prediction (Fig. 1).

According to a comprehensive study of logging data and core and SWC data, very thin intrusive rocks (less than 1 m) have no obvious effect on the host limestone. Aureole in this case is difficult to discern on the logging curves. Continuous core data indicates that this effect is only a few centimeters deep. It is speculated that this is related to the fact that the thin layer intrusive rocks carry less heat and cool faster. By studying this relationship in wells, it appears that the thicker the intrusion, the thicker the aureole formed by baking in host limestone. It shows that the thickness of aureole and the intrusion have a close correlation, in a non-linear binary relationship (Fig. 2).

Thin section identification (Fig. 3a) and NMR (Nuclear Magnetic Resonance) data support the thermal baking has a negative effect on limestone reservoir development. The average porosity is about 6.20%~13.60% for non-baked limestone reservoir, while the average porosity of carbonate rocks in contact thermal metamorphic aureole is about 0.23%~4.42% (Fig. 3b). The main reason for the decrease in porosity after metamorphism is that the high degree recrystallization and high degree of cementation (Fig. 3a), the particle becomes more regular and tighter arrangement, and the original reservoir space is occupied in this process.

The thickness of the intrusive rock in pre-salt layer of Libra is generally in order of tens of meters. The aureoles formed in host limestone rock by direct baking due to these intrusions are also less than twenty meters in thickness. Although intrusive rocks and their baking effects are risk factors for reservoir development, they mainly develop in the shape of sill at the top of the BVE Fm. and distribute in local areas. For the quality reservoirs often have hundreds of meters in thickness, the impact exerted by the intrusive rocks is predicated to be relatively low.

Marbleization of aureole above intrusion in A well

Marbleization of aureole below intrusion in A well

Dark gray limestone of non-aureole and white marble of aureole above intrusion in B well

Fig. 1 – Marbelization of the intrusion aureole in pre-salt limestone in the Libra Area, Santos Basin.

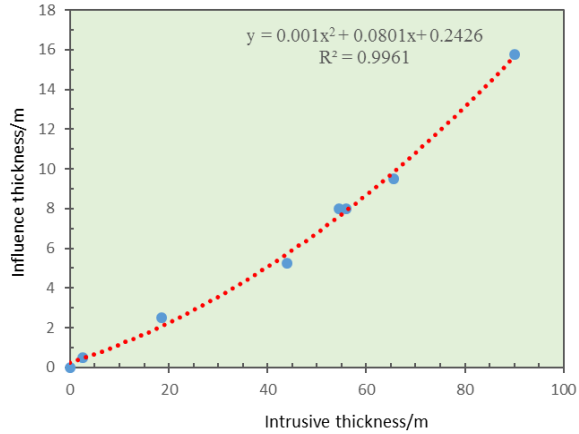

Fig. 2 – Relationship between the thickness of the aureoles and intrusions in Libra.

Acknowledgements

The authors would like to extend gratitudes to PPSA, Petrobras S.A., and partners (Shell, Total, CNOOC and CNPC), for permission to publish this paper, and the professionals from E&P, CENPES and the reviewers for the collaboration.

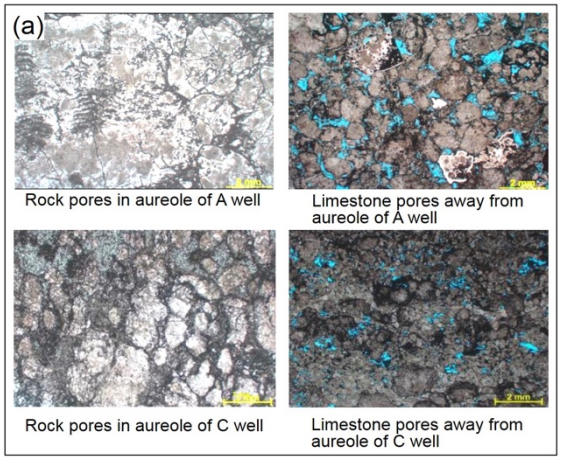

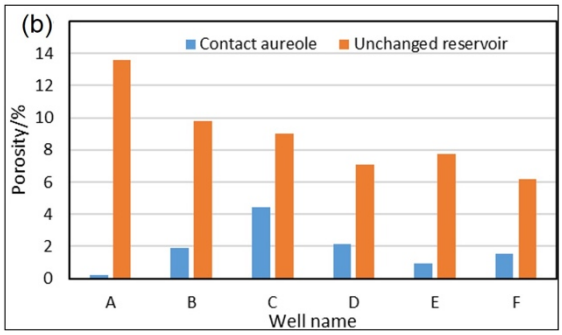

Fig. 3 – Pore and porosity of affected and unaffected limestone by intrusionr. (a) – thin sections show pore characteristics in aureole and away from aureole in A and C well; (b) – porosity in the aureole and away from the aureole.

References

De Luca P. H. V., Carballo J., Cerdà M. E., et al., (2015), What is the Role of Volcanic Rocks in the Brazilian Pre-salt? DOI: 10.3997/2214-4609.201412890, *77th EAGE Conference & Exhibition 2015* — IFEMA Madrid, Spain.

Marins G., (2016), Petrography of Sidewall Core Samples of Igneous rocks from the 3-RJS-740 Well-Santos Basin, *Petrobras Internal Report*,16P.

Marins G., Zucchetti M., (2017), Petrography of Sidewall and Well Core Samples of Igneous rocks from the 3-RJS-741 Well, Santos Basin, *Petrobras Internal Report*,36P.

Moreira et al. (2007), Bacia de Santos, *Boletim de Geociências da Petrobras,15*(2), pp. 531-549.

Rancan C. C., et al. (2018), Rochas Ígneas do Bloco de Libra, Bacia de Santos. In: *Congresso Brasileiro de Geologia, 49*, Rio de Janeiro, p. 2012

Hydrothermal and other metamorphic aureole processes: initial results from outcrop and mineralogical data from the Irati Fm and Serra Geral intrusions (Rio Claro SP, Brazil)

Mettraux M.[1, 2], Gaspar JL.[1], Neumann R.[3], Homewood P.[1], Arai M.[1], Dias-Brito D.[1]
[1] *UNESPetro, Instituto de Geosciências Exatas, Universidade Estadual "Julio de Mesquita Filho", Rio Claro SP, Brasil*
[2] *moho1959@yahoo.fr*
[3] *CETEM Av. Pedro Calmon, 900 - Cidade Universitária 21941-908 - Rio de Janeiro RJ, Brasil*

Keywords: hydrothermal, aureole, Irati.

Thermal metamorphism of the Permian Assistência Mb (Irati Fm) from sill margins and aureoles has been intensively studied on outcrop and from boreholes along the eastern margin of the Paraná basin, particularly from aspects of organic geochemistry and clay mineralogy (Santos Neto 1993; Araújo et al. 2000; Anjos & Guimarães 2008; Santos et al. 2009; Cioccari 2018). However, observations of host rock mineral parageneses and their relationships with the diabase sills suggests a strong overprint by hydrothermal and possibly other processes on the initial thermal effects.

Fig. 1 – Diabase sills and apophysis intruding the Assistência Mb, Irati Fm, Partecal quarry. The lift truck is parked about 1m above the top of the major intrusive body.

Progressive extraction from quarries close to Rio Claro (SP) has exposed both the Irati Fm host rock, as well as both thicker (>70m) and thinner (0.5m to 3m) tabular igneous intrusions. Intrusions similar to those exposed near Rio Claro SP have been described in the Jacu structure, about 150km to the SSW. Seismic surveys over this structure show large igneous bodies (several km's broad) lying below, within and above the Irati Fm. Costa et al. (2016) have interpreted these intrusions (from their geometry on seismic) to be layer-parallel, saucer shaped, climbing and fault-block types (Planke et al. 2005).

Quarry faces at the Partecal quarry (Assistência SP, Fig. 1) provide fresh, accessible sections allowing detailed sampling of the Irati Fm Assistência Mb sediments. The sampled section extends above the main >70m intrusion, across a 1m thick subsidiary sill and a 2m thick apophysis (both lying parallel to and several meters above the top of the main body) to the overlying Corumbataí Fm. This section, together with several samples spaced laterally, provided the material for this study.

Petrography was carried out by optical microscope on stained thin sections (normal and extra large size). Cathodoluminescence was made on the same thin sections, as well as chemical element analyses by micro XRF and SEM-EDS. Fragments of thin section billets and picked grains were ground and analyzed by XRD/Rietveld method for bulk mineralogy and specific mineral determinations.

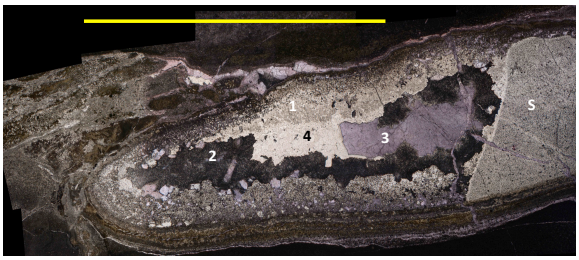

Fig. 2 – Early diagenetic silica nodule (partially preserved on far right: S) was partially dissolved by hydrothermal fluids. Scale bar = 1cm. Phases precipitated in the cavity (left side) include1: silica around the cavity; 2: saddle dolomite; 3: Fe-calcite; 4: megaquartz.

Mineralization of the host rock aureole is found in the form of nodules, as cavity fillings, as fracture fills and in places as pervasive replacement of primary sediment (e.g. finely laminated silty marls)

or of diagenetic features (e.g. chert nodules). Aureole minerals comprise diopside, talc, tremolite, chlorite, albite, apophyllite, biotite, lizardite, smectite, apatite, quartz, calcite, saddle dolomite, hexagonal pyrite, magnetite, srebrodolskite and REE minerals or incorporation of REE as trace elements in more common minerals.

Numerous cavities were formed by dissolution of diagenetic silica (an early process presumably linked to the intrusion) then to be progressively filled by paragenetic sequences comprising for instance microquartz, calcites (Mg, Fe, Mn), saddle dolomite, calcite, megaquartz (in that order, Fig. 2).

Some fractures, recording layer-parallel extension, document cementation during brittle to ductile deformation and fracture opening (Hooker et al. 2012; Laubach et al. 2018). The stretching of the Irati Fm host rock is not uniform, but affects thin layers or beds that form layer-parallel shear zones at different distances from the intrusion, even as far as the overlying Corumbataí Fm (about 15m above the main intrusive body). The deformation, however, was caused most probably by the mechanical effect of the main intrusion. Cementation of these fractures comprises uncommon minerals such as srebrodolskite together with magnetite. Organic matter in this section has been thermally altered, perhaps providing a link between the mineralization process involved here and pyrometamorphism (Grapes 2006).

The heterogeneity of the host rock also exerts a strong control on the distribution of aureole minerals at the bedding scale (in this case with a very low Kv/Kh resulting from the 5cm to 10cm heterolithic layering of carbonates and high-TOC marls). At the bed scale, aureole minerals vary over mm and cm distances from marl-carbonate bedding surfaces to the interior of carbonate beds.

The paragenetic sequences and spatial distribution of aureole minerals in cavities, nodules and fractures, as well as the diffuse occurrence of minerals in the host rock, show more effects from hydrothermal and fluid convection or other processes than from simple conductive or radiative heating.

The respective roles of heat and fluids from the main, thicker intrusion compared to the thinner sill and apophysis are still under evaluation. The evidence from the distribution, the composition and the paragenesis of aureole minerals in the Partecal quarry indicates the major role played by hydrothermal and possibly other processes triggered by the Serra Geral intrusions, rather than just a simple thermally driven contact metamorphism.

Acknowledgements

H.Brito, R.Rohn, I.Anderson, R.Goya, D.Biotto, C.Lacerda, J. da Silva, and JM. Cazonatto are thanked for technical support, discussions and suggestions. This project is funded by ANP: 20435-4, from the Libra Group through Fundunesp.

References

Anjos, C.W.D. & Guimarães, E.M. 2008, Metamorfismo de contato nas rochas da Formação Irati (Permiano), norte da Bacia do Paraná. Revista Brasileira de Geosciências, 38(4) 629-641.

Araújo, L.M., Trigüis J.A., Cerqueira, J.R., Freitas, C.S. 2000, The Atypical Permian Petroleum System of the Paraná Basin, Brazil. In: Mello M.R. & Kats B.J. (eds) Petroleum system of South Atlantic Margins. AAPG Memoir 73. 377-402.

Cioccari, G.M. 2018, Interpretação geoquímica e modelagem térmica na geração atípica de hidrocarbonetos – um exemplo na Formação Irati, Bacia do Paraná. Porto Alegre: Universidade Federal do Rio Grande do Sul, Instituto de Geociências PhD. 1-197.

Costa, D.F.B., Santos, W.H., Bergamaschi, S. & Pereira, E. 2016, Analysis of the geometry of diabase sills of the Serra Geral magmatism, by 2D seismic interpretation, in Guareí region, São Paulo, Paraná Brazilian Journal of Geology, 46(4): 605−615.

Grapes, R.H., 2006. Pyrometamorphism. Springer Berlin Heidelberg New York. ISBN-10: 3-540-29453-8. 1-275.

Hooker, J.N., Gomez, L.A., Laubach, S.E., Gale, J.F.W., Marrett, R., 2012. Effects of diagenesis (cement precipitation) during fracture opening on fracture aperture size scaling in carbonate rocks. In: Garland, J., Neilson, J.E., Laubach, S.E., Whidden, K.J. (Eds.), Advances in Carbonate Exploration and Reservoir Analysis. 370. Special Publication Geological Society, London, pp. 187-206.

Laubach, S.E., Lamarche, J., Gauthier, B.D.M., Dunne, W.M. & Sanderson, D.J. 2018, Spatial arrangement of faults and opening mode fractures. Journal of Structural Geology 108. 2-15.

Planke S., Rasmussen T., Rey S.S., Myklebust R. 2005. Seismic characteristics and distribution of volcanic intrusions and hydrothermal vent complexes in the Vøring and Møre basins. In: Doré A.G. & Vining B.A. (eds.). Petroleum geology: North-West Europe and global perspectives. Proceedings of the 6th Petroleum Geology Conference, London, 833-844.

Santos, R.V., Dantas, E.L., Oliveira, C.G., Alvarenga, C.J.S., Anjos,C.W.D., Guimarães, E.M., & Oliveira, F.B. 2009, Geochemical and thermal effects of a basic sill on black shales and limestones of the Permian Irati Formation. Journal of South American Earth Sciences, 28(1): 14–24.

Santos-Neto, E.V. 1993. Caracterização geoquímica e paleoambiente deposicional da sequência carbonato-pelítica superior da Formação Irati no Estado de São Paulo, Bacia do Paraná. Dissertação de Mestrado, Instituto de Geociências, Universidade Federal do Rio de Janeiro, Rio de Janeiro, 123 p.

When mining saves the day: Studying emplacement processes of subvolcanic bodies in poorly outcropping volcanic terrains

Páez, G.N.[1], Permuy Vidal C.[1] and De Martino F.[1]

[1] *CONICET and Instituto de Recursos Minerales (INREMI), Facultad de Ciencias Naturales y Museo, Universidad Nacional de La Plata. La Plata, Argentina* – gerardo.paez.unlp@gmail.com

Keywords: Sill, Cryptodome, Epithermal.

Poorly outcropping volcanic terranes pose a challenging task when studying volcanic and subvolcanic processes. This is especially true for two of the most economically relevant volcanic provinces of South America: the Paleocene Belt in Northern Chile (Fig. 1a; Espinoza et al., 2011) and the Deseado Massif in the Southern Argentinean Patagonia (Fig. 1b; Guido, 2004).

These two regions are characterized by numerous mines producing precious metals (Au and Ag) from epithermal deposits genetically related to the evolution of complex volcanic events: the Paleocene Chile-Alemania Fm. in the Paleocene Belt (Espinoza et al., 2011), and the Jurassic Bahía Laura Volcanic Complex in the Deseado Massif (Guido, 2004). In both regions, the close relationship between volcanism and epithermal mineralization makes understanding volcanic processes a priority in order to focus exploration efforts.

In this abstract we summarize two examples of how access to mining infrastructure and information (open-pits, underground labors and drill holes) can provide invaluable information for studying intrusion mechanisms of subvolcanic bodies in poorly outcropping regions.

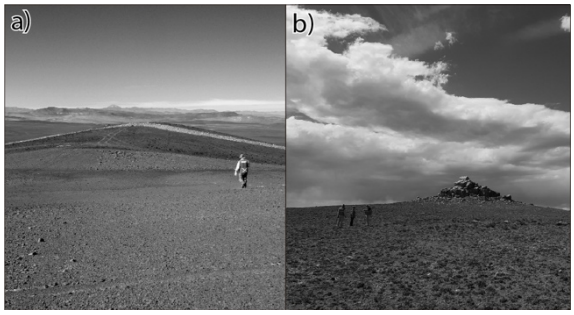

Fig. 1 – a) Typical outcrops in the Paleocene Belt in the Atacama Desert, northern Chile. b) Outcrops in the eastern Deseado Massif in the southern Argentinean Patagonia.

El Guanaco mine is one of the youngest gold deposits formed during the evolution of the Paleocene Belt of norther Chile (~45 Ma; Páez et al., 2018). The mine is located about 180 km to the SW of the city of Antofagasta and produces gold and minor silver from a structurally controlled high-sulfidation epithermal deposit (Páez et al., 2018).

The local geology includes well stratified pyroclastic deposits including lithic-rich lapilli-tuffs, lapilli-tuffs and several meter-thick surge deposits that show accretionary lapilli, impact sags and soft-sediment deformation. This sequence is intruded by dacitic cryptodomes, basaltic sills and small andesitic porphyries.

Outcrops around the mine are poor (Fig. 1a) so we took advantage of the 300 m deep Dumbo Open pit and RC drillhole information to reconstruct the facies model of the basaltic sills. Two sills were identified in concordance within the pyroclastic sequence, these bodies follow first order discontinuities within the pyroclastic sequence and were named Lower Basaltic Sill (15–20m thick) and Upper Basaltic Sill (7–10m thick). RC drillings surrounding the open pits show that these bodies converge to the east into a single intrusion up 50 m in thickness, and to the west they get progressively thinner until they completely disappear.

The coherent facies of these bodies may form both sheet-like and lobe-like bodies, ranging from 2 to 10 m in thickness (Fig. 2), that in all cases are enclosed within a brecciated selvage made mostly of closely packed peperites and dispersed peperites. Most facies show gradational contacts (Fig. 2), however some coherent lobes can also intrude into the breccias. The Upper Basaltic Sill shows a symmetric distribution of the breccia facies around a coherent core, whereas the Lower Basaltic Sill shows an asymmetric distribution of the breccia facies.

The second example, the Don Nicolas mine, is one of the oldest epithermal deposits of the Deseado Massif (~168 Ma, De Martino et al., 2017). The mine is located 220 km south of the city of Comodoro Rivadavia and produces silver and gold from a low-sulfidation epithermal deposit composed of a series of veins and stockworks (De Martino et al., 2017).

The local geology includes welded crystal-rich ignimbrites overlaid by an extensive rhyodacite dome complex and later intruded by andesitc bodies and rhyolitic dikes (De Martino et al., 2017). Within the dome complex, some bodies intrude into the pyroclastic sequence forming cryptodomes, when this occurs the preferred host rock are a series of stratified surge deposits showing carbonized wood, accretionary lapilli and impact sags.

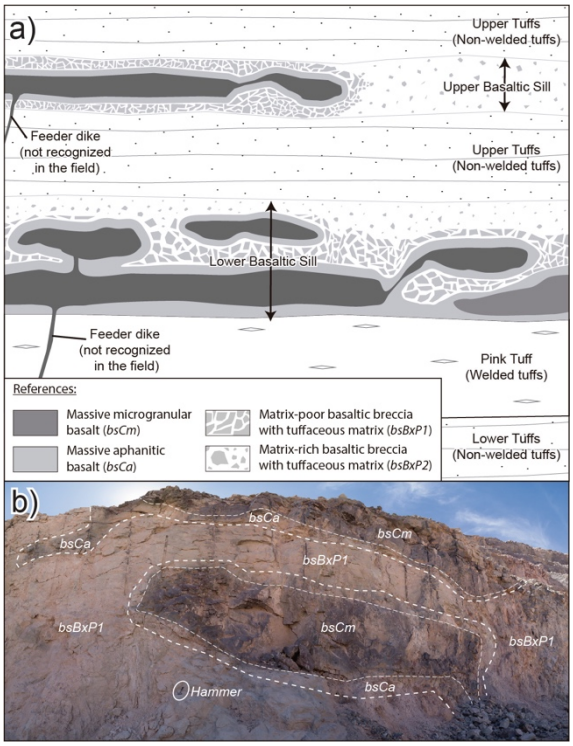

Fig. 2 – a) Facies model for the El Guanaco Mine Basaltic Sills (not to scale). b) Rock face at the Dumbo Open-Pit.

As in the previous example, outcrops around this body are poor (Fig. 1b) so we study the 70 m deep Armadillo Open pit and a selected number of diamond drill holes to reconstruct the facies model of one of these cryptodomes. The studied case is a large, irregular body with a thickness exceeding 80m (Fig. 3). Internally, is composed of a flow-banded coherent core surrounded by a thick envelope of breccias including three facies in a concentric array: intrusive hyaloclastites in the interior, followed by closely packed peperites, and then dispersed peperites toward the outer portions of the breccia envelope (Fig. 3). In all cases contacts between facies and with the host rocks are gradational.

The presence of widespread peperites in both examples evidence intrusion into soft and poorly consolidated pyroclastic rocks saturated in water. The relatively simple internal structure of the Don Nicolas mine cryptodome, combined with the gradational facies contacts, and the presence of upward forced strata atop of the intrusion, suggests that this body may have formed from a single intrusive pulse, involving the steady injection of magma in a more or less continuous episode. A slightly more complex inflation history is interpreted for the basaltic sills at El Guanaco Mine, where the presence of both gradational and intrusive contacts among the coherent facies (e.g. lobes) and the peperitic domains suggests multiple injections and/or an episodic magma supply, thus leading to a more complex facies arrangement.

Both described examples show how the presence of mining labors an infrastructure are invaluable for gaining access to quality outcrops in regions characterized by poor outcrops.

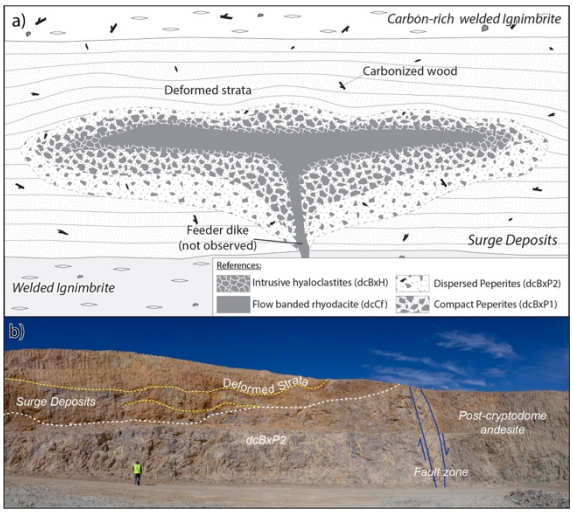

Fig. 3 – a) Facies model for the Don Nicolas mine cryptodome (not to scale). b) Rock face at the Armadillo Open-Pit.

Acknowledgements

We want to thank thanks Stabro Kasaneva (Austral Gold) and Silvio Franco (Minera Don Nicolás) alongside the geological staff of both mines for their support, acces and productive discussions.

References

Espinoza, F.; Matthews, S.; Cornejo, P.; Venegas, C. (2011). Carta Catalina, Región de Antofagasta. Servicio Nacional de Geología y Minería, Carta Geológica de Chile. *Serie Geología Básica 129*: 63 p. Santiago, Chile.

Páez, G.N., Permuy Vidal, C., Galina, M., López, L., Jovic, S.M., Guido, D.M. (2018). Intrusive hyaloclastite and peperitic breccias associated to sill and cryptodome emplacement on an Early Paleocene polymagmatic compound cone-dome volcanic complex from El Guanaco mine, Northern Chile. *J. Volcanol. Geotherm. Res.* 354, 153–170.

Guido, D. (2004). Subdivisión litofacial e interpretación del volcanismo jurásico (Grupo Bahía Laura) en el este del Macizo del Deseado, provincia de Santa Cruz. *Rev. la Asoc. Geológica Argentina* 59, 727–742.

De Martino, F.J., Echeveste, H.J., Jovic, S.M., Tessone, M. (2017). Estratigrafía volcánica bimodal de los Proyectos Martinetas y Microondas, Sector Oriental del Macizo del Deseado, Santa Cruz, Argentina. XX Congreso Geológico Argentino ST-9: 34-38. San Miguel de Tucumán, Tucumán. Argentina.

Controls on porphyry style mineralization in continental arc settings

Rubinstein N.[1]

[1] *IGeBA, Department of Geology, University of Buenos Aires, Buenos Aires, Argentina* – narubinstein@gmail.com

Keywords: tectonic setting, magmatic signature, structural arrangement

Porphyry Cu systems consist of large volumes of rocks (10−>100 km^3) affected by hydrothermal alteration centered on Cu-bearing porphyry stocks with ages ranging from the Archean to the Cenozoic (e.g., Seedorff et al., 2005). The deeper parts of porphyry Cu systems also may host Cu, Au, and Zn skarns whereas their shallower parts may contain high- and intermediate-sulfidation epithermal Au ± Ag ± Cu mineralizations. These deposits currently represent the world's largest source of Cu, typically with average grades of 0.5 to 1.5% Cu, <0.01 to 0.04% Mo, and up to 1.5 g/t Au and with chalcopyrite and bornite as the main Cu-bearing minerals (Sillitoe, 2010).

Porphyry deposits occur in subduction-related scenarios (magmatic-arc, flat-slab and post-collision settings). At contractional settings, these deposits emplaced during declining orogenic conditions following arc-transverse structural corridors, in areas with high surface uplift (Tosdal and Richards, 2001; Billa et al., 2004; Sillitoe and Perelló, 2005; Sillitoe, 2010; Japas et al., 2013; among others). Moreover, they tend to occur in orogen-parallel belts developed during defined metallogenic epochs with durations of 10 to 20 m.y (Fig. 1).

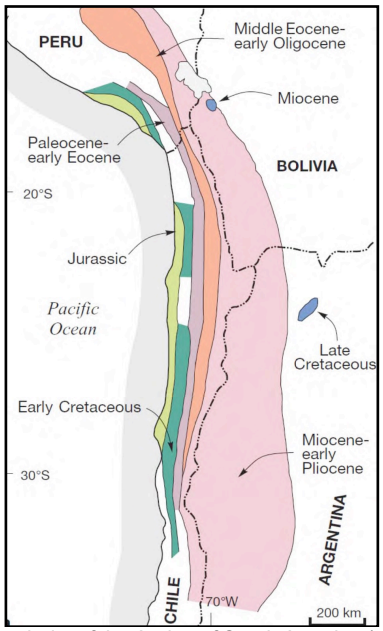

Fig. 1- Copper belts of the Andes of South America (modified from Sillito and Perelló, 2005).

The formation of porphyry-type mineralization depends on several factors which include magmatic and hydrothermal processes. The simplified genetic model assumes the exsolution of magmatic fluids from a cooling magma, the partitioning and subsequent transport of metals in the fluid, effective fluid focussing, cooling, and reaction with wall rocks to precipitate the metals in a confined area. If these processes operate effectively, an economic porphyry deposit can form (Richards, 2011). The action of the hydrothermal fluids produces alteration-mineralisation patterns on the surrounding rocks depending on the character of the fluids, wall rock and intrusive compositions, and permeability. These patterns display a broad-scale zoning that comprises, centrally from the bottom upward, potassic (biotite-K-feldspar), chlorite-sericite (chlorite-sericite-hematite), sericitic (quartz-sericite), advanced argillic (quartz-alunite-pyrophyllite-dickite-kaolinite) and propylitic (chlorite-epidote-albite-carbonate) alteration (Fig. 1) with the alteration progressively younger upward.

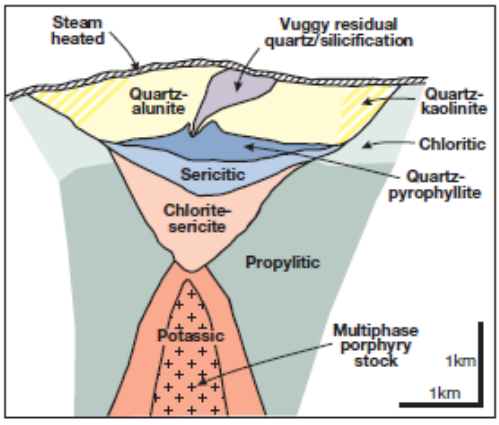

Fig. 2 - Generalized alteration-mineralization zoning pattern sketch for a porphyry Cu system (Sillitoe, 2010).

The character of the magmas is a first-order control on porphyry systems formation. Fertile magmas are characteristically calc-alkaline, hydrous and oxidant. Hydrous magmas can effectively transport and concentrate metals whereas the high oxidation state inhibit the early crystallization of sulfides preventing their partitioning into the aqueous phase (Cline and Bodnar 1991; Richards 2005,

among others). Moreover, porphyry systems are closely linked to magmatism with adakitic signature, particularly in the Andes (e.g. Bissig et al, 2003; Chiaradia et al., 2012; Carrasquero et al, 2017 among others). It is widely accepted that these deposits result from an initial melting in the metasomatized mantle wedge yielding oxidized and sulfur-rich mafic magmas and a secondary melting by injection of dykes and sills in the MASH zone of the lower crust, yielding a crustal and mantle-derived magma, with a high content of volatiles and metals (Richards, 2011).

Furthermore, structural arrangements are key for the porphyry deposits emplacement and evolution at regional and local scale. At regional scale active intra-arc fault systems determine the location and geometry of porphyry Cu systems (Sillitoe and Perelló, 2005). Moreover, intersections between arc-parallel structures and continent scale deep transverse fault zones are particularly important for porphyry Cu formation with the latter facilitating the ascent of small magma bulks precursor of porphyry Cu systems (Richards, 2000). At deposit scale fractures resulting from the local deformation regime and affecting the mineralizing intrusions are crucial since they act as a plumbing system not only allowing fluids to separate (boiling) and escape from the magma but also focusing them to a depositional site. At this scale the fracturing pattern is also conditioned by the rheology of the host rock which depends not only on the lithology and thermal conditions (Barton, 2007) but also on the alteration style. Fractures linked to intrusion processes (syn- and post-emplacement) to a lesser extent also contribute to the hydrothermal plumbing system. Magma emplacement causes substantial damage to the rock of the country at a local level because it is overpressured (e.g., Galland and Scheibert, 2013). Besides, thermal contraction at the margins of the intrusion leads to post-emplacement fracturing (Senger et al., 2015). Therefore, the structural analysis performed at different scales allows to build a conceptual model for fluid flow in porphyry system (e.g. Japas et al., 2013).

Ultimately, porphyry copper deposits result from the complex interactions and feedbacks of many processes at different scales Therefore, to build a robust genetic model for a specific deposit, all the processes involved in its genesis must be considered.

References

Barton, N. (2007), Thermal over-closure of joints and rock masses and implications for HLW repositories, in: Proceedings of 11th ISRM Congress, 109-116.

Billa, M., D. Cassard, A.L.W. Lips, V. Bouchot, B. Tourlière, G. Stein, and L. Guillou-Frottier (2004), Predicting gold-rich epithermal and porphyry systems in the Central Andes with a continental-scale metallogenic GIS. *Ore Geology. Reviews*,. 25, 39–67.

Bissig, T., A. Clark, and A. Von Quadt (2003), Petrogenetic and metallogenetic responses to Miocene slab flattening: new constraints from the El Indio-Pascua Au-Ag-Cu belt, Chile/Argentina. *Mineralium Deposita*, 38, 844-862.

Carrasquero, S.I., N.A. Rubinstein, A.L.R. Gómez, M. Chiaradia, D. Fontignie and V.A. Valencia (2017), New insights into petrogenesis of Miocene magmatism associated with porphyry copper deposits of the Andean Pampean flat slab, Argentina, *Geoscience Frontiers,* 9 (5), 1565-1576.

Chiaradia, M., , A. Ulianov, K. Kouzmanov and B. Beate (2012), Why large porphyry Cu deposits like high Sr/Y magmas? *Scientific Reports*, 2.

Cline, J.S., and R. J. Bodnar (1991). Can economic porphyry copper mineralization be generated by a typical calcalkaline melt? *Journal of Geophysical Research*, 96, 8113-8126.

Galland, O.and J. Scheibert (2013). Analytical model of surface uplift above axisymmetric flat-lying magma intrusions: implications for sill emplacement and geodesy. *Journal of. Volcanology and Geothermal Research*, 253, 114–130.

Japas, M.S., N.A.Rubinstein and L.E. Kleiman (2013), Strain fabric analysis applied to hydrothermal ore deposits emplaced during changing geodynamical conditions (Infiernillo and Las Picazas, San Rafael Massif, Argentina). *Ore Geology Reviews*, 53, 357–372.

Richards, J.P. (2000), Lineaments revisited: Society of *Economic Geologists Newsletter,* 42, 14−20.

Richards, J.P. (2005), Cumulative factors in the generation of giant calc-alkaline porphyry Cu deposits, in: *Super porphyry copper and gold deposits: A global perspective*, edited by Porter, T.M. pp. 7−25, PGC Publishing.

Richards, J.P. (2011), Magmatic to hydrothermal metal flux in convergent and collided margins. *Ore Geology Review*s, 40, 1–26.

Seedorff, E., J. Dilles, J Proffett, M. Einaudi, L. Zurcher, W.J.A. Stavast, D. A. Johnson and M. D. Barton (2005), Porphyry Deposits: Characteristics and origin of hypogene features. *Economic Geology, 100th Anniversary volume*, 251-298.

Senger , K., S.J. Buckley, L. Chevallier, A. Fagereng, O. Galland , T.H. Kurz, K. Ogata, S. Planke, and J. Tveranger (2015), Fracturing of doleritic intrusions and associated contact zones: Implications for fluid flow in volcanic basins, *Journal of African Earth Sciences* ,102,70–85.

Sillitoe, R. H. (2010), Porphyry Copper Systems. *Economic Geology*,105, 3-41.

Sillitoe, R. H. and J. Perelló (2005), Andean Copper Province: Tectonomagmatic Settings, Deposit Types, Metallogeny, Exploration, and Discovery. *Economic Geology, 100th Anniversary volume*, 845-890.

Tosdal, R.M. and J.P. Richards (2001). Magmatic and structural controls on the development of porphyry Cu±Mo±Au deposits, in: *Structural Controls on Ore Deposits, Reviews in Economic Geology 14*, edited by J.P. Richards and R.M.Tosdal, pp. 157–181.

Mesozoic Subvolcanic mafic system of Uruguay: a new perspective for mineral exploration

Scaglia F.[1] and Muzio R.[2]

[1] *Programa de Desarrollo de las Ciencias Básicas, Universidad de la República, Montevideo, Uruguay* – scagliageo@gmail.com
[2] *Instituto de Ciencias Geológicas, Iguá 4225, Montevideo, Uruguay*

Keywords: mafic, Mesozoic, Uruguay.

The Paraná Magmatic Province (PMP) is located in central South America and represents one of the largest igneous provinces in the world, related to rift processes and the southern Atlantic ocean opening (Peate, 1997).

The volcanic sequence is mainly represented by tholeiitic basalt lava flows, known as Serra Geral Formation in Brazil; Arapey Formation in Uruguay; Alto Paraná Formation in Paraguay; and Posadas Formation in Argentina; and minor rhyolites and rhyodacites in the upper portion. Also, remnants of this volcanism can be found in Namibia and Angola (Melfi et al., 1988).

In Uruguay, the PMP comprises, the basaltic/ andesite lava flows which extends almost over 40.000 km2 in the northwest part of the country (Arapey Formation; Bossi, 1966) and also related mafic intrusions (named as Cuaró Formation, Preciozzi et al., 1985). The mafic intrusions are both dykes and sills very well exposed and preserved in the central and northeast region.

The most significant dyke swarms occur in San Gregorio de Polanco and Melo localities, where the dykes trend NW-SE. The thickness of these dykes usually varies from 1m to 40m while the length falls between 2 and 50 km (Scaglia, 2010). On the other hand, there are several sills spread in the northeast region, some with up to 1.200km2. Geochemically, these intrusions of tholeiitic nature, low Ti (less than 2%), low incompatible elements content (Gramado magma-type), with evidence of multipulse events, and influenced by AFC processes (Scaglia, 2013; Muzio et al., 2017).

These dykes and sills cut out Paleozoic sedimentary rocks (Figure 1); a) in the central part, with significant presence of dykes, they cross cut Devonian rocks including organic rich shales, and, b) in the northeastern region, dykes and sills intrude into Carboniferous-Permian sedimentary rocks, also with restricted organic rich strata (Scaglia, 2013). This interaction magma-sediment is being studied looking for possible for potentially organic matter maturation processes.

Usually, the sills are porphyritic to glomeroporphyritic and have the following mineral assemblage: plagioclase (An35e50), clinopyroxene (augite), olivine ± opaque minerals (Muzio et al., 2012). Meanwhile, the dykes are dominantly glomeroporphyritic and are fine-grained to aphyric near the contacts. Phenocrysts include plagioclase (An55) and clinopyroxene (augite and occasionally, augite-pigeonite), with or without relicts of olivine (iddingsitized; celadonite is also present) and opaque minerals (titaniferous magnetite; Scaglia, 2010; Muzio et al., 2013).

Nowadays there is an increasing interest in the knowledge of the Uruguayan intrusive bodies is carry by oil and gas companies and mining companies. As a result of intense mapping work and petrological studies in these subvolcanic bodies, including description of a deel borehole, some aspects to be considered related to mineral exploration are presented.

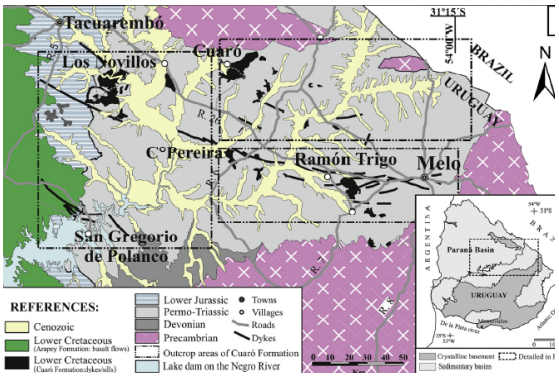

Fig. 1 – Map of Uruguay, with the main exposed areas of subvolcanic mafic systems (Muzio et al., 2017).

1) The San Gregorio de Polanco dyke swarm has potential for mineral exploration, at deeper levels. The content of titaniferous magnetite in some rock samples reach up to 15%.

2)The Cuaró Sill (Figure 2), was drilling in 2014, but it was recently described and we found an interesting hydrothermal altered intercept from 4 to 9 meters depth, with presence quartz veinlets bearing pyrite and galena; and from 6 to 9meters depth a pervasive phyllic alteration was observed (sericite, chlorite, quartz, carbonates and sulphides). This borehole with (62m final depth), cut microgabbroic rocks. Also whole rock geochemical data from

outcrops were analyzed for the following incompatible elements (Sc, Ti, V, Cr, Mn, Fe, Co, Ni, Cu y Zn) but they show only low contents; specially for Cr (0,016-0,054%), Ni (30-716ppm), Cu (102-140ppm), Co (48-75ppm) and V (282-345ppm); indicating an important role of fractionation of olivine, pyroxene and magnetite mineral phases.

3)A new dyle recently found and correspondent to the Melo dyke swarm, presents a rhythmic layered texture, composed by alternation of dark mafic aphanitic bands with lighter fine grain bands (Figure 3). Petrographic and geochemical characterization is yet being carried out.

All these featues as well as the evidence found during the last five years, show that the Mesozoic magmatic activity in Uruguay (southern portion of PMP), was not a closed system, and the new data such thickness of bodies, hydrothermal fluids - mineralisation, differentiation magmatic processes and multipulse signatures, are essentials to understand and expand the knowledge looking forward mineral exploration.

Fig. 2 – Panoramic view of typical sill geomorphology, Uruguay.

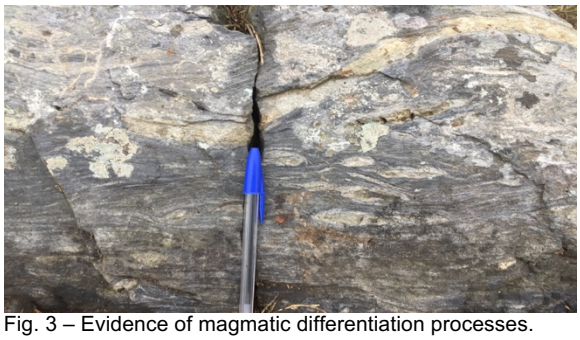

Fig. 3 – Evidence of magmatic differentiation processes.

Acknowledgements

F.S kindly thank to the ANII (Agencia Nacional de Investigación e Innovación- Uruguay) for the financial support for his PhD scholarship.

References

Bossi, J. (1966). Geología del Uruguay. Departamento de *Publicaciones de la Universidad de la República*, Montevideo, pp. 460.

Melfi, A.J., Piccirillo, E.M., Nardy, A.J.R., 1988. Geological and magmatic aspects of the Paraná Basin - an introduction. In: Piccirillo, E.M., Melfi, A.J. (Eds.), *The Mesozoic Flood Volcanism of the Paraná Basin: Petrogenetic and Geophysical Aspects. Instituto Astronómico e Geofísico*, Sao Paulo, pp. 1-14.

Muzio, R., Scaglia, F., Masquelin, H., 2012. Petrochemistry of mesozoic mafic intrusions related to the Paraná magmatic province, Uruguay. *Int. Geol. Rev*. 54, 844-860 nº7.

Muzio, R., Scaglia, F., Masquelin, H., 2013. Titaniferous magnetite and barite from the San Gregorio de Polanco dike swarm, Paraná Magmatic Province, Uruguay. *Earth Sci. Res*. J. 17 (2), 151-158.

Muzio, R.; Peel, E.; Porta, N. & Scaglia. F. (2017). Mesozoic dykes and sills from Uruguay: Sr - Nd isotope and trace element geochemistry. *Journal of South American Earth Sciences*, 77 p. 92-107.

Peate, D.W., 1997. The Paran_a magmatic province. In: Mahoney, J.J., Coffin, M.F. (Eds.), *Large Igneous Provinces: Continental, Oceanic and Planetary Flood Volcanism, Geophysical Monograph*, vol. 100, pp. 217-245.

Preciozzi, F; Spoturno, J; Heinzen, W. & Rossi, P. (1985). Memoria explicativa de la Carta Geológica del Uruguay aescala 1:500.000. *DINAMIGE-MIEM*.Montevideo, 2 figuras, 1 mapa, 72 pp.

Scaglia, F. (2010). Estudio petrológico de los diques básicos Mesozoicos en la región de San Gregorio de Polanco, Uruguay. *Tesis de grado de la Licenciatura en Geología*, Universidad de la República, Montevideo, 138 pp.

Scaglia, F. (2013). Estudio petrogenético del Sill de Cuaró, Departamento de Tacuarembó, Uruguay. *Tesis de Maestría, PEDECIBA* (área Geociencias), Universidad de la República, Montevideo, 172 p.

Session on Petroleum Implications of Volcanic Plumbing Systems

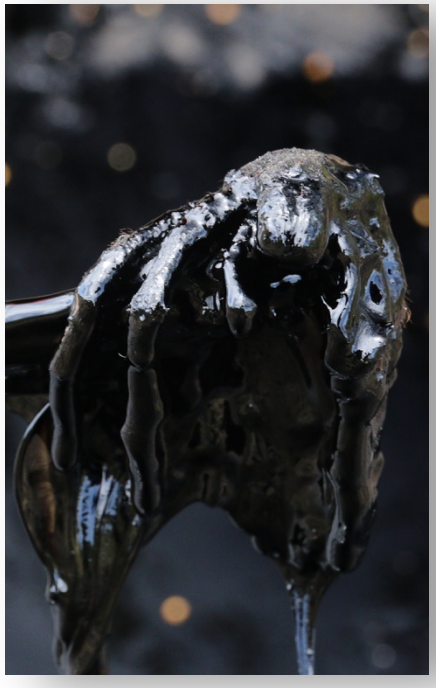

Contents

Influence of Cerro Bayo igneous intrusions in the development of an Unconventional shale type field in the Vaca Muerta Formation (Neuquén basin, Argentina)

Alvarez, Pablo[1], Licitra, Diego Tomás[2], Ruderman, Guillermo[3], Bidondo Juan Carlos[3] and D'Angiola Marta[4]

[1] *YPF S.A.*– pablo.alvarez@ypf.com
[2] *YPF S.A. Calle Talero 360, Neuquén, Argentina*
[3] *YPF S.A. Octógono, Rincón de los Sauces, Argentina*
[4] *Weatherford Arg. company, Buenos Aires, Argentina*

Keywords: Vaca Muerta, Intrusive, prediction.

Cerro Bayo volcanic complex is located in the north of Neuquén province (figure 1). It was emplaced 6.7 Ma ago (Perez and Condat 1996) and which main body is andesitic-basaltic to andesitic. From an oil perspective, it was historically studied due to the presence of nearby conventional fields (limestones and sandstones) mostly developed by vertical wells.

Currently the area is revitalized by the interest in Vaca Muerta Formation (Weaver 1931). The study of this igneous complex became relevant due to its impact on the drilling, fracturing and production stages of the organic marlstones of VM.

Previous studies in the area (González and Aragón 2000) described this volcanic complex as a Christmas-tree laccolith. It is composed by a central body from which many sheets like intrusions or concordant (sills) depart. In its superior part some verticals (dikes) are present.

With the arrival of 3D seismic in the area (year 2002, figure 2), it is possible to map these intrusions along its extension and see patterns that could affect Vaca Muerta field development.

It can be seen how these bodies commence from the volcanic cone and grow radially. The emplacement can be either concordant or cutting thru stratification. These can be due to difference in rock densities o high mechanical contrast (Palma et al and reference cited there). Also, could be an indication of local variations of stress regime acting in the area. The former emplacement can be an indication of inverse regime and the latter either normal or strike-slip. (Hubbert 1956).

The stress regime controls the development of hydraulic fractures. This affects directly the stimulated rock volume (SRV, Fisher et al. 2004) and later production. Hence, understanding igneous emplacement could be use as proxy for hydraulic fracture propagation behavior.

Another important point is that igneous bodies act as hydraulic barriers for the growth of hydraulic fractures, impacting negatively on the expected SRV (Vallejo et al. 2014)

In these contribution, different emplacement types will be shown. Also, the ways these bodies were map and consider when assigning risk for different areas of the field. Finally, how these bodies were handle during drilling stage of wells and its future stimulation.

Also, the use of electric logs as predictive tools will be described (figure 3), both the ones run in pilot vertical wells use the define landing points and logging while drilling (LWD) tools use to take real time decision in conjunction with mud logging.

Fig. 1 – Location map with seismic cross section of figure 2 and leasing block limits

Acknowledgements

The authors would like to thank YPF S.A. management for permission to publish this work

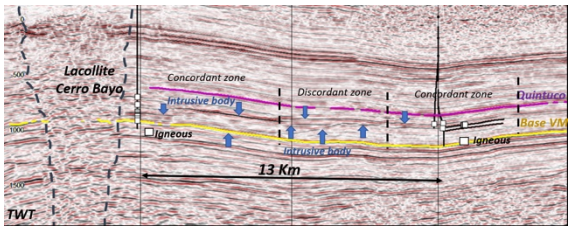

Fig. 2 – Cross section West-East-North, showing the finger type sills from the mean source to the horizontal wells locations in Vaca Muerta

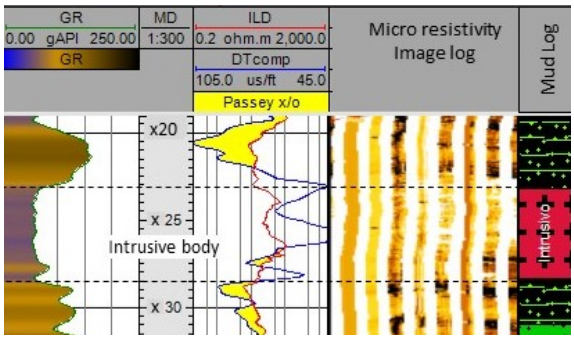

References

Fischer, M.K., Heinze, J.R., Harris, C.D., Davidson B.M., Wright, C.A. and Dunn, K.P. (2004), Optimizing horizontal completions in the Barnett shale with microseismic fractur mapping. *SPE 09951-MS, presented at the SPE Annual Technical Conference and Exhibition held in Houson, Texas U.S.A., 26-29 september 2004 , 11 p.*

González, P.D., and Aragon, E. (2000), El cerro Bayo de la sierra Negra, Neuquén: ejemplo de un lacolito tipo Arbol de Navidad. *Revista de la Asociación Geológic Argenitna, 55 (4): 363-377.*

Hubbert, M.K. and Willis, D.G. (1957), Mechanics of Hydraulic Fracturing. Society of Petroleum Engineers, *AIME, pp.153-163*

Palma, O. Burchardt, S., Galland. O., Mair, K. and Leanza, H.A. (2017), Evidencias de deformación frágil druante el emplazamiento de un lacolito: el caso del cerro Bayo de Chachahuén, sur de Mendoza, Argentina. *XX Congreo Geológico Argentina, 7-11 de agosto de 2017, San Miguel de Tucumán.*

Perez M.A and Condat, P. (1996), Geología de la Sierra de Chachahuén, Área CNQ-23. *Geólogos Asociados S.A., reporte interno YPF (inédito) 82p, Buenos Aires.*

Vallejo, M.D., Lombardo, E., Crespo, P. and Cuervo, S., (2018), Identificación y caracterización de intrusivos ígneos en la formación Vaca muerta y su impacto en el diseño de una campaña de exploración. Caso de estudio: El Trapial, cuenca Neuquina. Argentina, *10° Congreso de Exploración y Desarrollo de Hidrocarburos. Simposio de Recurso No Convencionales, pp. 557-570.*

Weaver, C. (1931), Paleontology of the Jurassic and Cretaceous of West Central Argentina. *Memoir, University of Washington 1, 469 p, Seattle.*

Intrusion-Related Source Rock Maturation in the Parnaíba Basin, Brazil, and Implications for the Petroleum System

Fernando Aragão[1,2], Frederico Miranda[1], Lilian Souza[1], René Rodrigues[2], Sverre Planke[3]

[1] *Eneva, Rio de Janeiro, Brasil* – fernando.aragao@eneva.com.br
[2] *Paleontology and Stratigraphy Department, Rio de Janeiro State University, Brasil*
[3] *VBPR, Oslo, Norway; CEED, University of Oslo, Norway; The Arctic University of Norway, Tromsø*

Keywords: Petroleum systems, sills, Pimenteiras Formation, Parnaíba Basin

The Parnaíba Basin is located in the northeast of Brazil and corresponds to the second largest onshore gas production in the country. The recent exploratory success is due to the understanding of the atypical igneous-sedimentary petroleum system in which extensive dolerite sills are responsible for triggering source rock maturation, creating traps, and sealing the gas accumulations (Magoon & Dow, 1994; Rodrigues, 1995; Miranda et al., 2018).

The best characterized source rock intervals in the basin are within the Devonian Pimenteiras Fm. It contains four specific source rock intervals, defined as source A, B, C, and D (Figure 1) with good potential for hydrocarbon generation and extensive regional distribution (Rodrigues, 1995).

Considering that overburden was not enough to guarantee the thermal maturity for the Pimenteiras Fm. (Rodrigues, 1995; Miranda et al., 2014), the emplacement of the dolerite intrusions into the source rock intervals played an important role on the maturation and generation of the 1 Tcf of gas discovered in the basin since 2010 (Cunha et al., 2012; Miranda et al., 2018).

For this study were used preexisting data and rock samples collected from thirteen wells located in the central portion of the basin and analyzed using geochemical techniques of total organic carbon, rock-eval pyrolysis, stable carbon isotopes, and vitrinite reflectance to characterize the source rock. Additionally, well logs and 2D seismic data were used to aid in the interpretation of the implications of the dolerite sill complexes on the Pimenteiras Fm. maturation.

The results obtained from the geochemical analyses showed that the four wide-spread source rock intervals have a good quality. Total organic carbon (TOC) contents varies from 0.5 to 7%. It is worth to mention that these values represent the residual TOC after the thermal effect of the intrusions, therefore original TOC values would likely be higher. Well-based isopach maps calculated for each source rock interval showed that thicknesses can vary from 2 to approximately 37 meters. The source rock interval C is considered to be the best interval, with largest thicknesses and very good TOC contents, reaching up to a maximum of 5%.

Even with only a few vitrinite reflectance analyses, the maturity results indicate a trend of increasing thermal maturation towards the central portion of the basin, where the main gas fields are located.

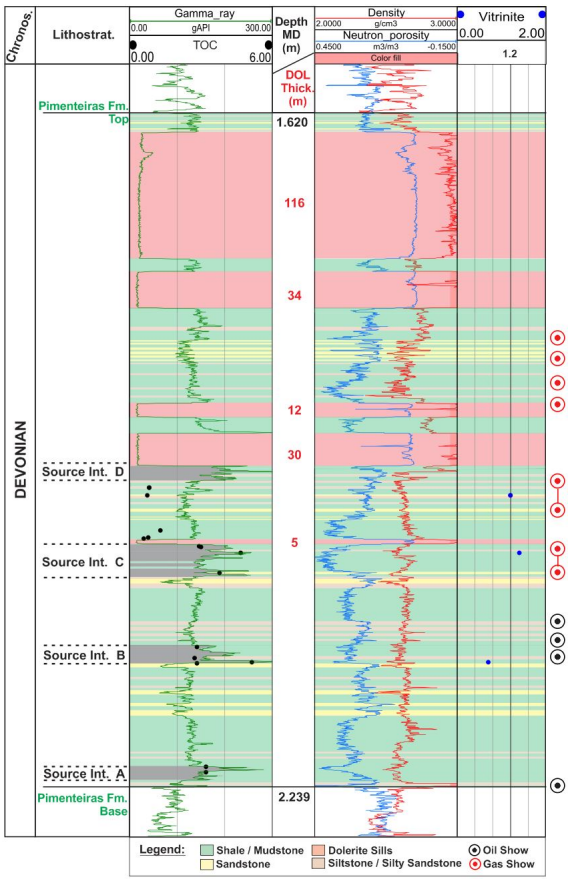

Fig. 1 – Composite log of the Pimenteiras Fm. with the source rock intervals A, B, C, and D (gray color), total organic carbon (TOC), and vitrinite reflectance (%Ro). The thermal maturity of the source rock intervals is related to the proximity to the intrusions. Ro values of 1,2% close to the dolerites is associated with gas shows. Further away from the sills the source rock intervals have a lower maturity, Ro of 0,7%, and is associated with oil shows in cuttings and sidewall cores.

Through the integrated correlation of maturity profiles, descriptions of sidewall cores, and wireline log interpretation from wells located along a NW-SE regional section, it could be observed that the number of sills, their thicknesses, and their depth of emplacement are crucial factors controlling the generation efficiency and the type of hydrocarbon generated.

In the area of the gas fields the sidewall cores collected in the organic-rich intervals (Figure 2) showed a greater concentration of pyrite-filled fractures and open fractures interpreted as the result of overpressure caused by kerogen transformation and expulsion related to the generation process, also known as "beef fractures" (Cobbold, 2013; Al Duhailan *et al.*, 2015).

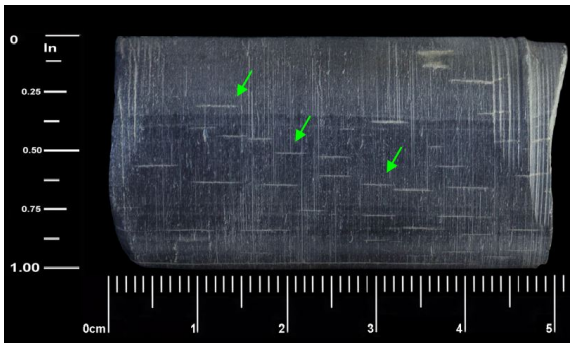

Fig. 2 – Sidewall core collected in the organic-rich source rock interval C of the Pimenteiras Fm. Highlighted in green arrows are the beef fractures interpreted as the result of overpressure caused by kerogen transformation and gas expulsion.

The resistivity logs, integrated with rock sample descriptions, were used to evaluate the extent of the thermally affected zones around the sills. It was observed an intense recrystallization, cementation, and concentration of pyrite either in laminations and disseminated in the matrix occurs in these zones, corresponding directly to anomalously low resistivities observed in the logs (Figure 3). The interpretation indicates that the thickness of the thermally affected zones above and below the sill is approximately equivalent to the thickness of the sill itself.

In summary, the aim of this master's project is to contribute to the understanding of the elements that are involved in the hydrocarbon generation process in the atypical petroleum system of the Parnaíba Basin. The new data, results, and discussions will be helpful to improve the exploratory success, define petroleum provinces and serve as analogues for less explored volcanic petroleum basins.

Acknowledgements

The authors would like to thank Eneva and the Brazilian National Petroleum Agency for supporting the industry and fortifying the interaction with the universities.

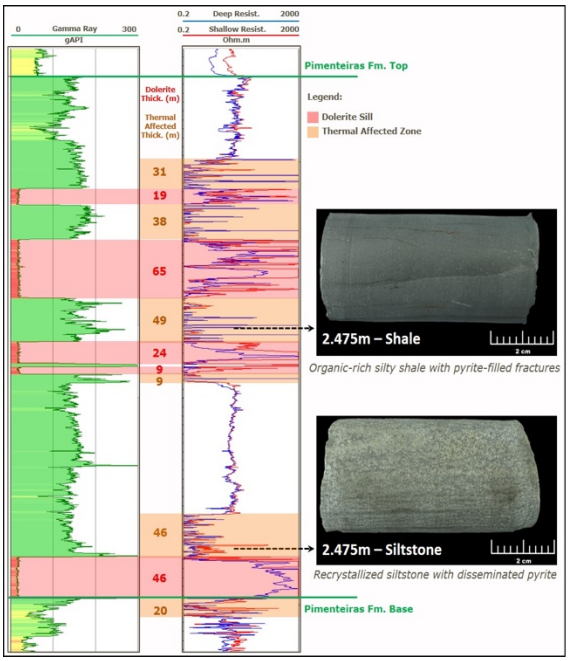

Fig. 3 – Composite log (Gamma Ray and Resistivity) with the thermally affected zones, dolerite sills, and the sidewall cores plotted. The samples show intense recrystallization, pyrite-filled fractures and concentration of pyrite in laminations and disseminated in the matrix, which it is associated with the anomalously low resistivities zones being interpreted as the thermally effect zones.

References

Al Duhailan, M. *et al.* (2015), Analyzing "Beef" Fractures: genesis and relationship with organic-rich shale facies: Proceedings of the 3rd Unconventional Resources Technology Conference.

Cobbold, P.R. *et al.* (2013), Bedding-parallel fibrous veins (beef and cone-in-cone): Worldwide occurrence and possible significance in terms of fluid overpressure, hydrocarbon generation and mineralization. *Marine and Petroleum Geology 43*, 1-20.

Cunha, P. R. C. *et al.* (2012), Parnaíba Basin – the awakening of a giant. *11th Simpósio Bolivariano – Exploracion Petrolera en las cuencas subandinas; Session Nuevas Fronteras I*, Cartagena das Indias, Colômbia. ACGGP.

Magoon, L.B. and Dow, W.G. (1994), The petroleum system. In: The Petroleum System-from Source to Trap. AAPG, Memoirs, 60. AAPG, Tulsa, 3–24.

Miranda, F. S., et al. (2018), Atypical igneous-sedimentary petroleum systems of the Parnaíba Basin, Brazil: seismic, well logs and cores: *Geological Society, London, Special Publications*, v. 472, no. 1, p. 341-360.

Rodrigues, R. A (1995), Geoquímica Orgânica da Bacia do Parnaíba. *Tese de Doutorado*. 225p. IG- UFRGS, Porto Alegre.

Structural and magmatic controls in reservoirs of the Mulichinco Formation in the Auca Mahuida Volcano field, Neuquén Province, Argentina

Chiacchiera S.[1], Ribas S.[2] and Orts D.[1 3]

[1] *Universidad Nacional de Río Negro, General Roca, Argentina* – s.chiacchiera@unrn.edu.ar
[2] YPF S.A., Eduardo Talero 360, Neuquén, Argentina
[3] CONICET - Instituto de investigación en Paleobiología y Geología, Av. Gral. Julio A. Roca 1242, General Roca, Argentina

Keywords: Auca Mahuida, magmatism, Petroleum system

The Auca Mahuida volcano, developed northeast of the Neuquén basin (37º45'S and 68º56'W), is a product of the volcanism that constitutes the volcanic province of Payenia. It was formed between 1.87 y 0.88 My (Rossello et al. 2002) and it is isolated from the Andean zone, about 100 km east of the current deformation front. Also, the volcano is located on the edge of a NNW-SSE Precuyan depocenter (Upper Triassic - Lower Jurassic). The development of the Agrio fold and thrust belt and the eastward progression of the deformation produced subsidence by tectonic load and the inversion of the depocenters in this area. Both, the load related subsidence and the tectonic inversion structures worked as a control for the volcanism of Auca Mahuida (Cristallini et al. 2014). The rise of magma occurred through sedimentary rocks that form a complex petroleum system in the Neuquén basin.

This work analyzes a 9 km^2 area located northeast to the main crater (Fig. 1) within the oilfield called "Volcán Auca Mahuida", in concession to YPF S.A. The study area has nine wells that have been directionally drilled from existing locations due to topographic, weather conditions and the presence of a natural reserve.

The sedimentary column crossed by the study wells is composed of rocks corresponding to Neuquén Group and Rayoso, Centenario Inferior, Centenario Superior Mulichinco and Quintuco formations. Although is known from other neighboring wells that is also composed of the Vaca Muerta, Tordillo and Auquilco formations underneath (Rossello et al. 2002). In the petroleum system, Vaca Muerta formation is the source rock while reservoirs are founded in sandstones of Mulichinco, Centenary Inferior, Centenario Superior and Rayoso formations.

The analysis of well data, vertical seismic profiles and geological background information has allowed us the interpretation of structures and the control they exert together with the magmatism in the reservoir conditions of the Mulichinco Formation, main local oil system reservoir.

Dykes, sills of different sizes and a 100 m thick laccolith hosted in the Mulichinco Formation are the main intrusive bodies founded. The existence of deeper and bigger sills is known by other authors as Longo (2017).

This work shows that borehole imaging and vertical seismic profiles constitutes an essential tool in areas where seismic acquisition is not applicable due to the topography and the high acoustic impedance of the upper basaltic cover.

Based on that borehole imaging (Figure 2), it can be inferred that dykes have the same strike and dip that the previous structures proposed by Cristallini et al (2014) for the structural evolution of the region and the same geometry that a vertical seismic profiling carried out in one of the wells in the work area (Figure 3). This is in accordance with Magee et al (2013) which proposes that several fault zones are used for the propagation of the magma. This compartmentalization of the reservoir rocks is called Box-Work type (Holford et al. 2013). In addition, through the analysis of the fluids behavior hydraulic disconnections were observed between them, which show the presence of faults or dikes that act as barriers. As a result of the structural study focused on the Mulichinco Formation, four blocks that disconnect the fluid in the reservoirs were defined (Figure 1).

The petrophysical conditions of the reservoirs rocks were not altered by metamorphism, but the presence of hydrothermal activity produced a hydrocarbon remigration. Large amounts of gas indicate that the increased heat generated by the intrusion, increased the maturation in source rocks, going to from the oil window to the gas window. The study of the fluids and their interaction with the subsurface structure allows expanding the knowledge of the structural model and to give a greater precision in the development of the oilfield.

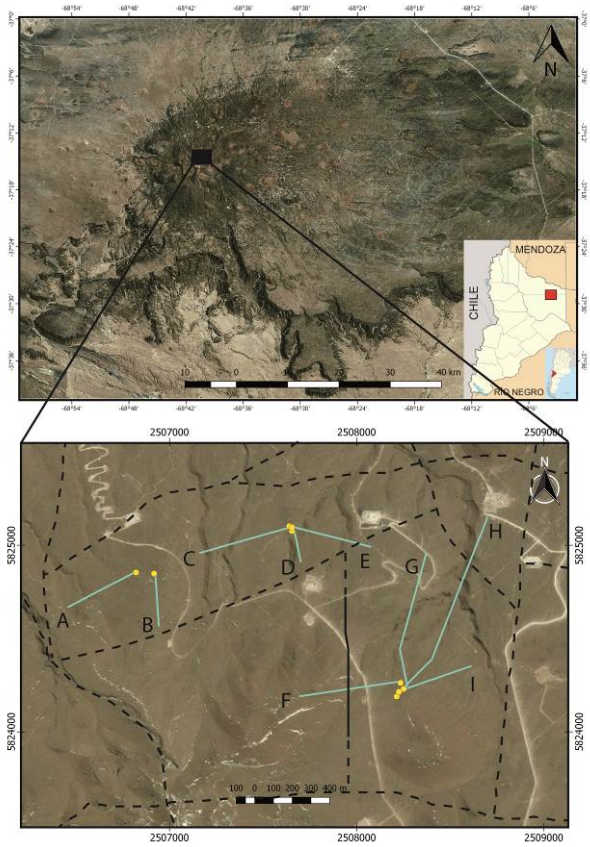

Fig. 1 – Top figure: Auca Mahuida Volcano. The black rectangle represents the study area. Lower figure: Study area with the nine wellheads an tracks. Discontinuous lines represent hydraulics disconnections between wells. Continuous line represents the only structure verified by the vertical seismic profile obtained in F well.

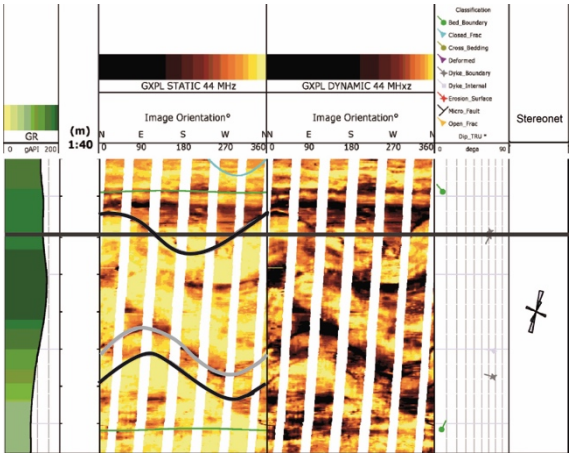

Fig. 2 – Borehole imaging profile showing a dyke (between black lines), its internal banding (in a grey line) and its obtained orientations in the rose diagram.

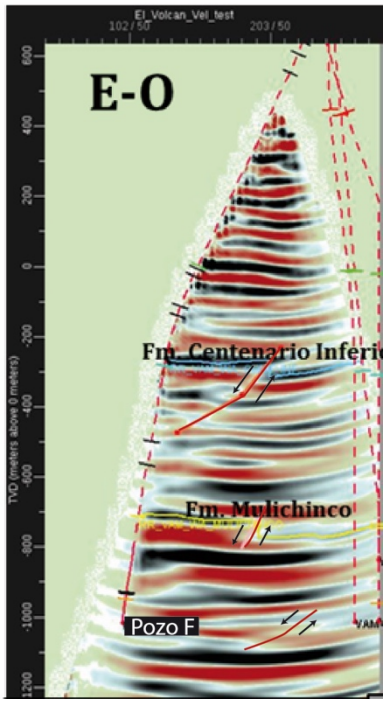

Fig. 3 – A vertical sismic profile obtained in F well. It shows the different N-S faults present in subsurface.

Acknowledgements

I would like to thank to the Universidad Nacional de Río Negro for granting the possibility of carry out this work and YPF S.A. for providing the necessary information.

References

Cristallini, E., R. Tomezzoli, M. A. Mendez, E. Santiago, M. Villar Benvenuto and F. Ghiglione (2014), Caracterización estructural y evolución tectónica de la región de los cerros Auca Mahuida y Bayo (Provincia del Neuquén). *YPF,* Internal report. Pp 48.

Rossello, E. A., P.R. Cobbold, M. Diraison and N. Arnaud (2002), Auca Mahuída (Neuquén basin, Argentina): a quaternary shield volcano on a hydrocarbon-producing substrate. In: *5th international symposium Andean Geodynam Toulouse*, pp 549–552.

Holford, S., N. Schofield, C. Jackson, C. Magee, P. Green and I. Duddy (2013), Impacts of igneous intrusions on source and reservoir potential in prospective sedimentary basins along the western Australian continental margin. *West Australian Basins Symposium*. Pp. 13

Magee, C., C. A. Jackson, and N. Schofield (2013), The influence of normal fault geometry on igneous sill emplacement and morphology. *Geology*, 41(4), 407-410.

Longo, L.M. (2017) Caracterización de la estructura del complejo volcánico Auca Mahuida mediante datos aeromagnéticos y gravimétricos. *Facultad de Ciencias Astronómicas y Geofísica,* Universidad Nacional de La Plata. Pp 185.

Subsurface identification and characterization of volcanic bodies in non-conventional Vaca Muerta reservoir using borehole resistive images, Neuquen Basin, Argentina

Marta D´Angiola[1]

[1] *Weatherford Arg.* – marta.dangiola@weatherford.com

Keywords: intrusive, Vaca Muerta, borehole resistivity image.

The sub-surface identification of concordant and non-concordant subvolcanic bodies of different sources has become a topic of great interest in the oil industry in general and in the development of non-conventional Vaca Muerta reservoir in particular.

They appear with very different mechanical properties and rock qualities compared with their loam host rocks, and their characterization is extremely important, among other reasons, for the design of completion of horizontal wells.

A lot of studies were performed in different scales during the last years regarding Vaca Muerta Formation: its structure, its facies analysis (Crouse et al., 2018) and its organic matter content (Palacio et al., 2018). It was described in detail from cores; electro facies were determined using standard logs and its regional development was interpreted from 3D seismic. However, volcaniclastic and associated products were described as subordinated facies, while mudstones, packstones to grainstones were the main ones. (Kietzmann et al, 2016; Rosemblat et alt, 2016)

This paper is about the use of borehole resistive images in both water-based mud and oil-based muds to better identify volcanic bodies in Vaca Muerta along very long horizontal wells.

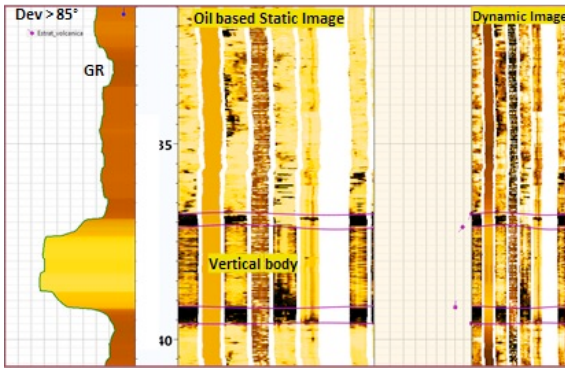

Fig. 1 – Borehole resistivity images showing a vertical volcanic body non-concordant with sub-horizontal bedding of Vaca Muerta formation, in a very long horizontal well drilled with oil based mud.

It is possible to identify textural features (Milicich et al. 208) besides to obtain a precise orientation and spatial relationship referred to host rock.

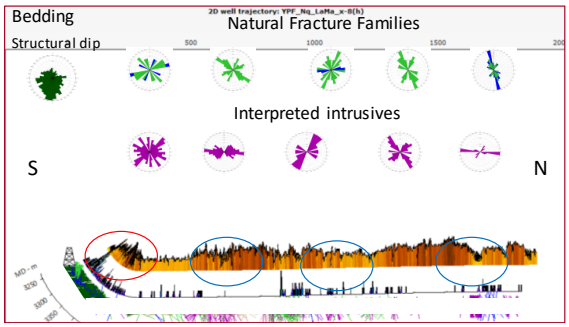

Fig. 2 – Schematic cross section. Borehole image interpretation in a horizontal well in Vaca Muerta. Intrusive bodies, natural fracture system and structural dip are shown in strike plots and azimuth plots respectively.

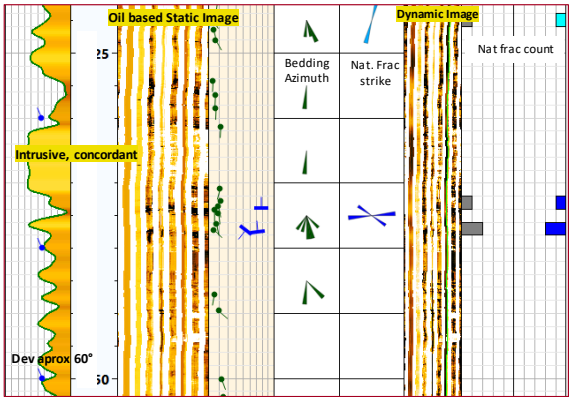

Fig. 3 – Another example of concordant intrusive body, at the top of Vaca Muerta, in the curve of a horizontal very long well.

In addition, they can be characterized combining other available information, such as spectral GR logs and both monopolar and dipolar acoustic logs. This integration would provide vital information regarding both its composition, its mechanical properties as well as its rock quality (Astesiano et al.2008,

This information is validated by several examples and offers strategic importance of having a good and precise characterization of these disruptive bodies, that impact dramatically on the operations.

It is well known that the presence of them may cause damages during drilling, act as barriers for hydraulic fractures growth, with the consequent decrease of stimulated rock volume. On the other hand, TOC values are almost nulls, so they are nonproductive intervals, so the use of their predictive knowledge can critically influence when making decisions in order to avoid invisible costs both during drilling and well completion.

Acknowledgements

All the Authors are kindly thanked Weatherford and YPF for having to allow to present this abstract.

References

Astesiano, D, Whitty C, Chiapello, E., D´Angiola, M. y Lopez, R. (2008). Petrophysic Characterization of a Deep sill in Rio Chico, Integration Data. *VI Congreso Intern.de Explor. Hidrocarburos, Mar del Plata, Argentina*. (Actas)

Crousse, L., Reijenstein, H. Hernández, C. Lanusse Noguera, I., Gonzalez Tomassini, F. (2018) Vaca Muerta Facies Modeling in Loma Campana. Part 1: Electrofacies. *10° Cong. Explor. Y desarrollo, Simpo. Recursos No convencionales*, Mendoza. 523-531.

Kietzmann, D. , Ambrosio, A., Alonso, M. Suriano, J. (2016) Capítulo 20: Puerta Curaco. In: *Transecta Regional de la Formación Vaca Muerta. Integración de sísmica, registros de pozos, coronas y afloramientos. Gonzalez, G., et al Ed.* 219 - 232

Llambías, E.J. (2008) Geología de los cuerpos ígneos. *Asoc. Geol. Arg., 3ra. Ed, S29*.

Milicich. S., Massiot, C., McNamara, D. (2018) Volcanic texture Identification and Influence on Permeability Using a Borehole Resistivity Image Log in the Whakamaru Group ignimbrite, Wairakei Geothermal Field, New Zealand. *Proceedings,* 43rd Workshop on Geothermal Reservoir Engineering, Stanford University, Stanford, CA,

Palacio, J.P., Hryb, E., Gonzalez Tomassini, F. (2018) Predicción de la distribución de beefs en la Formación Vaca Muerta. Un análisis integrado*. 10° Cong. Explor. Y desarrollo, Simp. Recursos No convencionales*, Mendoza. 181-192.

Rosemblat, A., Lanusse Noguera, I. Dominguez, F., Guerberoff, D. Capítulo 12 Bajada de Añelo. In: *Transecta Regional de la Formación Vaca Muerta. Integración de sísmica, registros de pozos, coronas y afloramientos. Gonzalez, G., et al Ed.* 131-142

Vallejo, M.D, Lombardo, E., Crespo, P. Cuervo, S. (2018) Indentificación y caracterización de intrusivos ígneos en la Formación vaca Muerta y su impacto en el diseño de una campaña de exploración. Un caso de estudio: El Trapial, Cuenca Neuquina, Argentina *10° Cong. Explor. Y desarrollo, Simp. Recursos No convencionales*, Mendoza. 557 - 569.

Cajón de los Caballos diabase (Neuquén Basin, Mendoza, Argentina): An atypical hydrocarbon reservoir

de la Cal H.G. [1], Lajoinie M.F. [2, 3], Salvioli M.A. [2, 4], Lanfranchini M.E. [2, 5] and Feinstein E.H. [1]

[1] *ROCH S.A., Avenida Madero 1020, Piso 21, Buenos Aires, Argentina* – hdelacal@roch.com.ar
[2] *Instituto de Recursos Minerales, Facultad de Ciencias Naturales y Museo, Universidad Nacional de La Plata (INREMI-FCNyM-UNLP), Calle 64 N° 3, CP1900, La Plata, Argentina*
[3] *Centro de Investigaciones Viales, Facultad Regional La Plata-Universidad Tecnológica Nacional (LEMaC-FRLP-UTN), Calle 60 y 124, Berisso, Argentina*
[4] *Consejo Nacional de Investigaciones Científicas y Técnicas (CONICET), Godoy Cruz N°2290, Buenos Aires, Argentina*
[5] *Comisión de Investigaciones Científicas de la Provincia de Buenos Aires (CICBA), Calle 532 e/ 10 y 11, La Plata, Argentina*

Keywords: *Neuquén Basin, Malargüe, Sierra de Palauco, Hydrocarbon, Igneous petrography.*

It is well known that in the Valle del Río Grande area, Neuquén Basin, an atypical petroleum system related to magmatism was developed (Garcia et al. 1982, Witte et al. 2012, Alberdi-Genolet 2013, Schiuma and Llambias 2014, Spacapan et al. 2018). This system was often related to the Tertiary magmatism rocks classified as andesites and basaltic-andesites (Nullo 2002, Witte et al. 2012, Alberdi-Genolet 2013, Schiuma and Llambias 2014, Spacapan et al. 2018). In this work, we present new petrographic studies of cutting samples recovered from 4 wells drilled in the past by YPF in the Cajón de los Caballos area. These rocks were initially denominated as augitic basalts and andesites. The aim of this study is to propose a new classification for these rocks and to show that its plutonic equivalents can also form part of this kind of atypical system.

The igneous body (oil-bearing) was identified in well logs (Fig. 1) and has a N-S elongated morphology with at least 8 km^2 in extent, and a maximum recorded length of 120 m. However, there is still no seismic information to delimit the real extent. It is emplaced in Vaca Muerta shales or in the contact between this formation and Chachao limestones.

Petrographic studies were carried out under a binocular loupe and a petro-calcographic microscope Nikon Optiphot-POL in the Instituto de Recursos Minerales, Universidad Nacional de La Plata (INREMI-UNLP).

Studied rock has a heterogeneous color with well differentiated whitish and grayish-green sectors. The mesoscopic observation allowed a porphyroid texture to be identified. The latter is constituted by a plagioclase-biotite matrix and pyroxene and plagioclase phenocrysts of 0.25 - 1.50 mm in size (Fig. 2).

Microscopic analyses show a holocrystalline porphyritic texture. The phenocrysts correspond predominantly to clinopyroxene of augite type and in minor proportion to amphibole (possibly hornblende) and plagioclases (An_{70-80}). The augite crystals have euhedral to subhedral shape and are 1.00 to 1.2 mm in size. In some sectors, these crystals are fractured and replaced by hornblende crowns and by chlorite. Also, few relict olivine crystals were observed. The hornblende and plagioclase phenocrysts are scarce and between 0.5 and 1.00 mm in size. (Fig. 3). The matrix is constituted by plagioclase, biotite, hornblende and opaque minerals up to 0.3mm in size. Epidote and chlorite were also observed as secondary minerals.

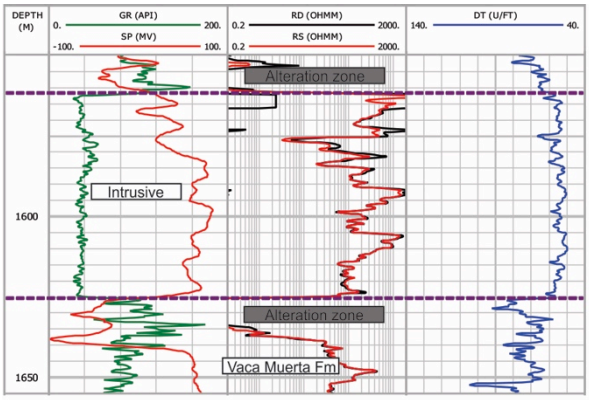

Fig. 1 –Well log of the diabase (Modified from de la Cal et al. 2018).

These petrographic studies allowed this rock to be classified as diabase. Although geochemical analyses and fluid inclusions determinations are currently in process, the crystal size and the mineral association type are enough evidences to support this interpretation.

Plutonic rocks are not described in the bibliography related to the type localities where igneous rocks crop out in contact with the Mendoza Group rocks in the nearby zones (e.g. in the Cuesta del Chihuido). However, similar lithologies were described by Pons et at. (2007) in Cerro de la Minas, eastward of the study area, and by Alberdy-Genolet (2013) in a core recovered from a well within the Valle del Rio Grande area. In addition, current studies on cutting samples recovered from a recently drilled

well in the Agua Botada area show a rock similar to the diabase from the Cajón de los Caballos area.

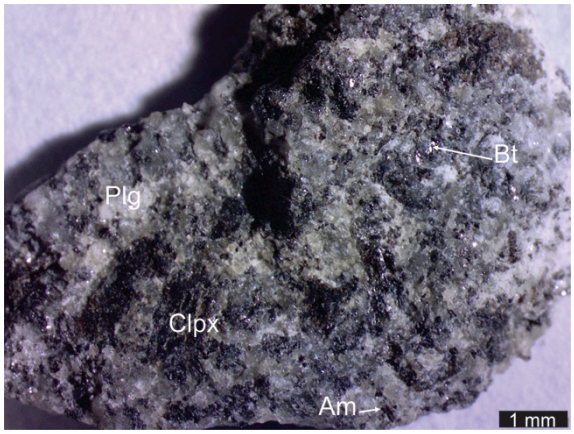

Fig. 2 –Mesoscopic appearance of the cutting samples. Mineral abbreviations according to Kretz (1983).

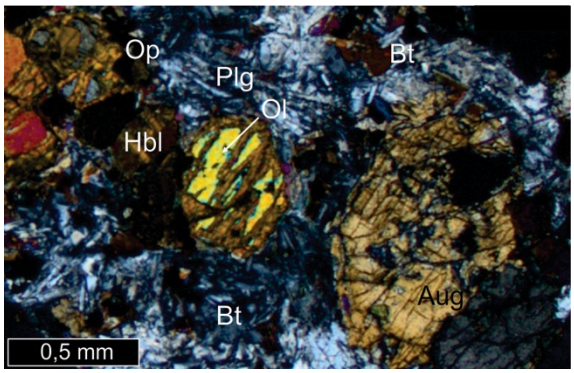

Fig. 3 –Microscopic general view of the cutting samples. Mineral abbreviations according to Kretz (1983).

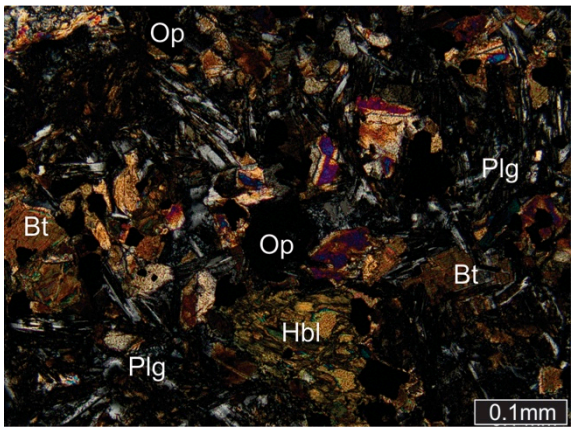

Fig. 4 –Detail of microscopic appearance of matrix. Mineral abbreviations according to Kretz (1983).

Finally, the accurate classification of this type of rocks and the global understanding of their emplacement conditions could be useful to construct a more predictable model to explore oil production from this atypical system. Even more, despite the intrusive bodies have a wide distribution in this part of the basin, oil accumulations related to igneous rocks are mostly concentrated in the Valle del Río Grande area. This low grade of hydrocarbon production outside the Valle del Río Grande area could be due to variations in the emplacement conditions of igneous bodies. In this sense and in order to obtain a genetic model for this atypical oil system, the importance of performing adequate lithological analyzes accompanied by geochronological studies is highlighted.

Acknowledgements

We thank Cajón de los Caballos Consortium to allow us to publish this information.

References

Alberdi-Genolet, M., A. Cavallaro, N. Hernández, D.E. Crosta y L. Martínez (2013), Magmatic events and sour crude oils in the Malargüe area of the Neuquén Basin, Argentina, Marine and Petroleum Geology, 43, p. 48-62.

de la Cal H., E. Feinstein, H. Villar (2018), Origen de los petróleos alojados en rocas ígneas intruidas en la Formación Vaca Muerta del yacimiento Cajón de los Caballos, provincia de Mendoza, Cuenca Neuquina, Argentina, X Congreso de Exploración y Desarrollo de Hidrocarburos, Mendoza, Trabajos Técnicos, p. 315-328.

Garcia C., H. Brocca, R. Martinez, S. Arturi, R. Ferrante, L. Rébori (1982), Importancia de las rocas ígneas intrusivas como reservorio de hidrocarburos en la Cuenca Nequina-Sur Mendocina, I Congreso Nacional de Hidrocarburos Petróleo y Gas, Buenos Aires, T. Exploración, p. 97-114.

Kretz, R. (1983) Symbols for rock-forming minerals. American Mineralogist, 68p, 277-279.

Pons M.F., M.B. Franchini and L. López Escobar (2007), Los cuerpos ígneos neógenos del Cerro de las Minas (35,3°S-69,9°O), Cordillera Principal de los Andes, SO de Mendoza: Geología, Petrografía y Geoquímica, Revista de la Asociacion Geológica Argentina, 62, p. 267-282.

Schiuma, M. F. y E. J. Llambías (2014), Importancia de los sills como reservorios en la Cuenca Neuquina del sur de Mendoza, IX Congreso de Exploración y Desarrollo de Hidrocarburos, IAPG, Trabajos Técnicos I, p. 331-349, Mendoza, Argentina.

Spacapan, J.B., J.O Palma, O. Galland, R. Manceda, E. Rocha, A. D´Odorico y H.A. Leanza (2018), Thermal impact of igneus sill-complexes on organic-rich formations and implications for petroleum systems: A case study in the northern Neuquén Basin, Argentina", Marine and Petroleum Geology, 91, p. 519-531.

Witte, J., M. Bonora, C. Carbone and O. Oncken (2012), Fracture evolution in oil-producing sills of the Rio Grande Valley, norther Nequén Basin, Argentina, AAPG Bulletin, 96, p. 1253-1277.

Volcanic Margin Petroleum Prospectivity - VMAPP

Jerram D.A.[1,2], Planke S.[1,3], Millett J.M.[3] and Myklebust, R.[4]

[1] *Centre for Earth Evolution and Dynamics (CEED), University of Oslo, Norway*
[2] *DougalEARTH Ltd.1, Solihull, UK*
[3] *Volcanic Basin Petroleum Research (VBPR), Oslo Science Park, 0349 Oslo*
[4] *TGS, Asker, Norway.*

Keywords: Volcanic Basin, Training, Volcanic Reservoir.

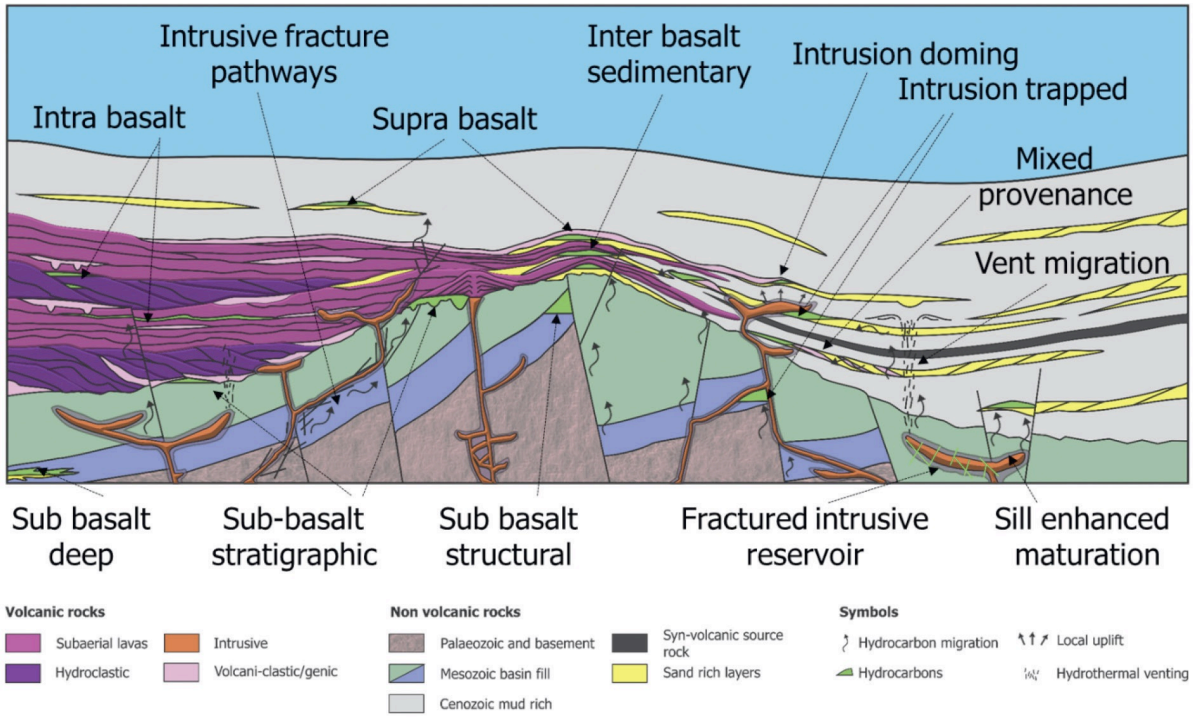

Fig. 1 – Synthesis of the interaction of igneous rocks and the petroleum system (see Senger et al., 2017).

Globally there are a number of examples of hydrocarbon fields and exploration targets where volcanic/igneous rocks play an important role. The Volcanic Margin Petroleum Prospectivity project (VMAPP), is a multi-client funded endeavor which aims to provide a 'state of the art' understanding of volcanic margins and volcanic basins. This contribution outlines the main activities of VMAPP and provides information on how to get involved.

Currently we are in VMAPP phase 2 (2018-2021), with phase 1 being completed in 2016. Our approach is to look at the variety of ways in which the volcanic system, from both extrusive to intrusive settings, interacts with the petroleum system (Fig. 1). The project is funded by a multi-client subscription, providing in-house interaction to sponsors, as well as a number of deliverables.

The project is split up into modules that are produced to address key outcomes. The Core Modules (CM1-5, VMAPP1) provide a training resource to help explorationists from a variety of backgrounds to improve their understanding of the volcanic rocks and their role in the petroleum system. Research Modules (RM 1-5, VMAPP1; RM6-10, VMAPP2), are undertaken to address key issues that need to be studied from all perspectives including seismic, bore-hole data, modelling, outcrop studies etc. The RM outputs are reported within the VMAPP group, and also provide a contribution to our international peer reviewed publication outputs. Basin Modules (BM1-5), place our findings into a regional context providing focused case study material along targeted basins and areas of interest, where volcanic rocks play an important role in the petroleum system.

References

Senger, K., Millett, J., Planke, S., Ogata, K., Eide, C.H., Festøy, M., Galland, O. and Jerram, D.A., 2017. Effects of igneous intrusions on the petroleum system: a review. *First Break*, 35(6), pp.47-56.

Geochemical and mineralogical effects of basic sills on siliciclastic sediments of the Palaeozoic Parnaíba basin: implications for hydrocarbon reservoirs (NE, Brazil)

Lopes, H. A.[1], Santos, R. V.[1] and Cruz, C. E. S.[1], Abreu, J. C.[1]

[1] *Instituto de Geociências, University of Brasília, Brazil* – lopes.henrique04@gmail.com

Keywords: hydrothermalism, reservoir, hydrocarbon

The influence of heat flow and mass transfer associated with igneous intrusions may play significant changes in reservoir rocks as it may cause: (1) the compartmentalization and changes in reservoir quality of reservoir rocks due to authigenic mineralization; (2) the dismigration of previously accumulated hydrocarbons. In the Parnaíba basin, igneous intrusions generate the main trap and seal structures above reservoir rocks in the main petroleum systems associated with commercial accumulations (Miranda et al., 2018). Therefore, understanding the effects of igneous intrusions on reservoir rocks and the processes involved are of great importance to reduce the exploratory and production risks associated with igneous-sedimentary petroleum systems.

This study is based on the BG-1-MA well (337.50m) which crosscut, from the bottom to the top: a thick dolerite sill (>37m), the Longá, Poti and Piauí formations. Petrographic, mineralogical and texture of 75 polished thin sections were analyzed using optical microscopy and QEMScan analysis. Chlorite major element composition of 16 samples were determined using EPMA data that were used to calculate chlorite formation temperature by means of the software WinCcac (Yavuz et al., 2015). Stable isotopic analysis of carbon and oxygen in 15 calcite samples and sulfur in 17 pyrite samples were collected in sedimentary and igneous rocks.

The sedimentary succession presents pervasive cementation and the main diagenetic products were: (1) chemical and mechanical compaction; (2) quartz and feldspar overgrowth and dissolution; (3) authigenic illite, chlorite and pyrite precipitation; (4) carbonatation; (5) oxidation and kaolinization. Intense and pervasive chlorite, pyrite, albite cements preferentially occur within sandstone layers, whereas brittle structures filled by calcite, chlorite occur within mudstone layers. Authigenic chlorite occur in nodular textures, massive cements and filling brittle structures (Fig.1-2). Pyrite occur as euhedral and anhedral isolated crystals, as nodular agglomerates, massive layers and filling veins in sedimentary rocks (Fig.2). In dolerites, pyrite occurs filling amygdules and veins; Authigenic albite occur as overgrowths on detrital K-feldspar grains and with microcrystalline habit replacing mudstone fragments, as cements and associated with aureoles around mudstone-sandstone contact and around veins (Fig.1). Carbonates occur mainly as calcite and occur as veins and filling amygdules in igneous rocks and as cements and filling veins in sedimentary rocks (Fig.1). Brittle structures occur as subvertical veins and horizontal breccias filled by calcite; and as anastomosed and vertically symmetrical discontinuous horizontal structures filled by chlorite and oxides (red bars in Fig.1).

Chlorite temperature of formation varied from 70-342°C based on four empirical methods (Yavuz et al., 2015). Chlorite temperature of formation data plotted on a T (°C) vs. Depth (m) graph cluster around 150 ±49°C and 250 ±37°C temperature values and occur in alternated intervals along the sedimentary succession (Fig.1). $\delta^{13}C_{V\text{-}PDB}$ values varied from -8.58 to -5.12‰ and $\delta^{18}O_{V\text{-}PDB}$ values varied from -21.18 to -6.62‰. Calcite from igneous rocks have $\delta^{18}O_{V\text{-}PDB}$ values varying from -21.01‰ to -6.62‰ and $\delta^{13}C_{V\text{-}PDB}$ values ranging from -6.20‰ to -5.37‰. The $\delta^{13}C_{V\text{-}PDB}$ values of all samples suggest a major mantle carbon source contribution with minor contribution of degradation of organic carbon. The $\delta^{18}O_{V\text{-}PDB}$ values of igneous rocks may vary due to temperature, magma differentiation and degassing processes, whereas in sedimentary rocks they may vary due to water/rock ratio and temperature. The $\delta^{34}S$ values vary from -4.7 to 11.6‰. Pyrite hosted in dolerites present $\delta^{34}S$ ranging between 3.3‰ and 0.9‰. Most pyrite cement in sedimentary rock cluster between +5.0 and +10.0‰, although a few samples have $\delta^{34}S$ values ranging between -5 and 0‰. $\delta^{34}S$ values suggest a major contribution of igneous sulfur and minor sulfur from thermochemical reduction of sulphates and leaching of isotopically heavier previously deposited sulphides and sulphates.

Based on the progressive burial diagenetic conditions of the basin (<3500m of depth; geothermal gradient of 27 °C km^{-1}), normal burial diagenesis products reported in the literature (Góes, 1995), the change in bulk chemical composition of the studied sedimentary succession, we propose that the igneous intrusion have caused a heat flow and hydrothermally induced diagenesis on the studied sediments. The

high chlorite temperature of formation (higher than predicted progressive burial temperatures), sulfur and carbon isotopic composition work as hydrothermal fingerprints. Hydrothermal fluid migration caused dissolution of detrital grains and a pervasive authigenic mineralization, in balance, results in a porosity and permeability loss. The chlorite, albite, pyrite ± sulfides mineralization occurs preferentially along veins and sandstone layers suggesting that the hydrothermal fluid migrated through the most porous and permeable medias limited by fluid baffle layers of low permeability. The brittle structures filled by chlorite or calcite indicate overpressure conditions to form these structures.

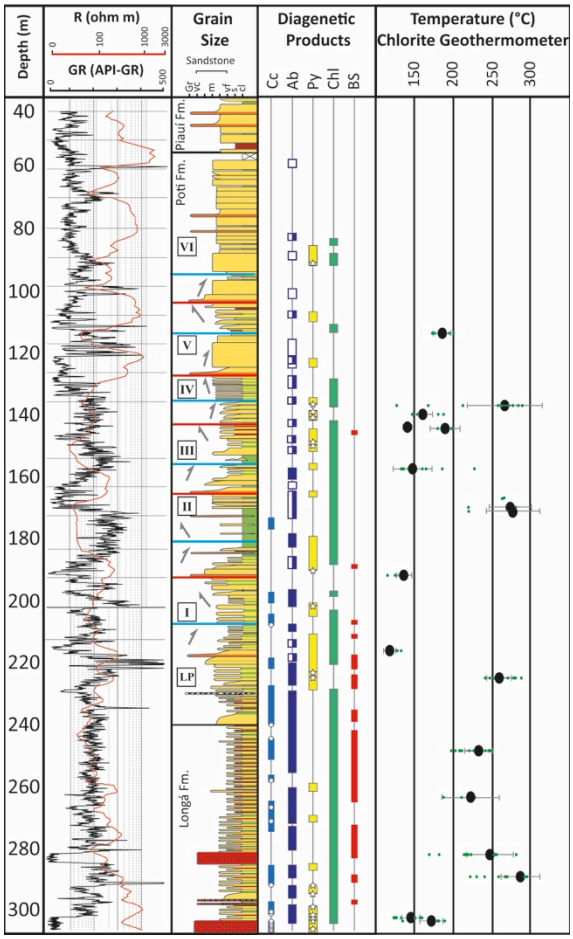

Fig. 1 – Stratigraphic Column of the BG-1-MA well.

The decrease in porosity and permeability of reservoir rocks may cause a decrease reservoir quality and the compartmentalization of reservoir rocks. Both can be favored by the migration of hydrothermal fluid migration through convective cells. Hydrothermal fluid migration through major faults, and within slight tilted stratas support fluid migration through long convective cells and favors the lateral continuity of the hydrothermally induced mineralization. Therefore, these conditions may enhance the probability of reservoir quality decrease and its compartmentalization caused by hydrothermal fluid migration above igneous intrusions.

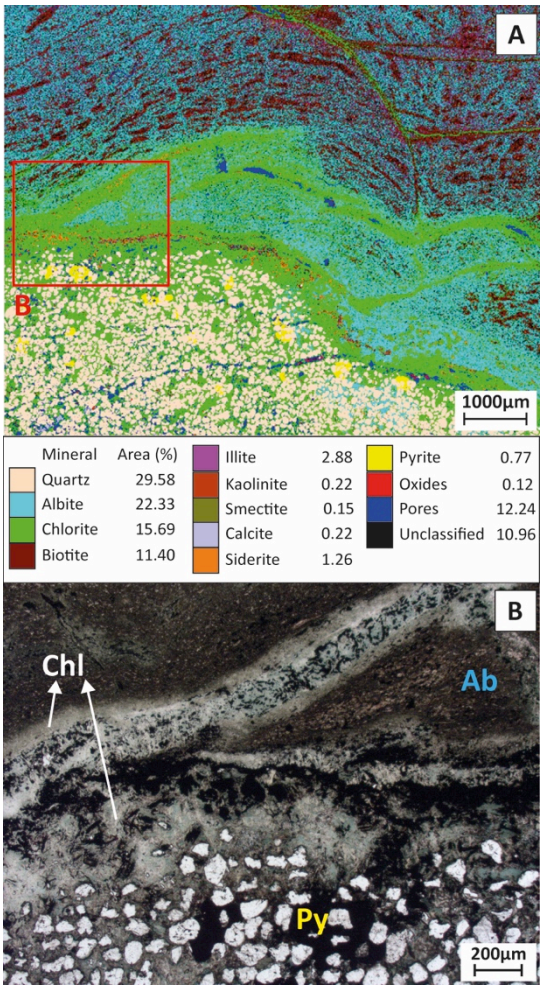

Fig. 2 – A) QEMScan false color map highlighting microcrystalline albite, pyrite and chlorite cementation. B) XPL photomicrograph highlighting a brittle structure filled by chlorite and microcrystalline albite in mudstone; and chlorite and pyrite cementation in sandstone.

Acknowledgements

We thank FINATEC, CAPES and ENEVA for the sponsorship and all the support provided.

References

Góes, A.M., 1995. A Formação Poti (Carbonífero Inferior) da Bacia do Parnaíba. Universidade de São Paulo.

Miranda, F.S.D.E., Vettorazzi, A.N.A.L., Cunha, R.D.A.C., Aragão, F.B., Michelon, D., Caldeira, J.L., Porsche, E., Martins, C., Ribeiro, R.B., Vilela, A.F., Corrêa, J.R., Silveira, L.S., Andreola, K., 2018. Atypical igneous-sedimentary petroleum systems of the Parnaíba Basin , Brazil : seismic , well logs and cores. Geol. Soc. London 472, 341–360.

Yavuz, F., Kumral, M., Karakaya, N., Karakaya, M.T., Yildirim, D.K., 2015. A Windows program for chlorite calculation and classification. Comput. Geosci. 81, 101–113.

Exploration of Serie Tobífera for oil and gas exploration, Austral Basin, Tierra del Fuego, Argentina. Advances in the construction of the Geological Model

Mykietiuk, K.[1], Azpiroz, G.[2], Simonetto, L.[2], Covellone, G.[2] and Petrinovic, I.[3]

[1] *YPF, Buenos Aires, Argentina, karina.mykietiuk@ypf.com*
[2] *YPF, Buenos Aires, Argentina*
3 CONICET, CICTERRA, Córdoba, Argentina
Formal

Keywords: Austral Basin, Serie Tobífera, Graben-Caldera, lava flows, ignimbrites, domes.

The Austral basin, also known as Magallanes, is located on the southwestern end of the South American plate and its southern limit is constituted by the Scotia plate. Basin evolution started in Middle to Upper Jurassic with a regional rifting stage, when grabens and half-grabens were filled with volcanic and volcaniclastic rocks, named "Serie Tobífera", being this unit, historically considered the economic basement of the basin.

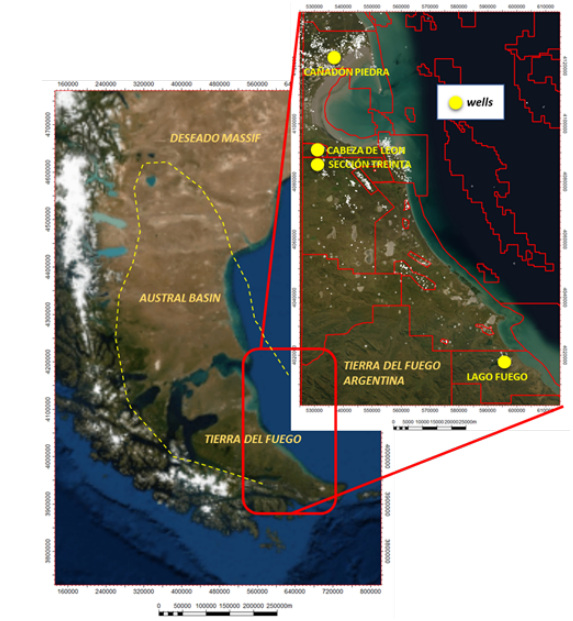

Fig. 1 – Location of the study area.

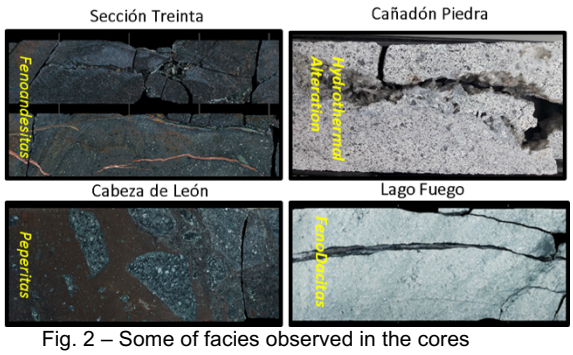

Fig. 2 – Some of facies observed in the cores

Because of its complex nature "Serie Tobífera´s" exploration requested a different methodology compared with the overlaying clastic targets. For this case resulted imperative to understand the volcanic environment and the distribution of volcanic and volcaniclastic facies, in order to minimize the uncertainty in explorations projects.

In recent years, YPF drilled several wells in the Serie Tobífera (as a target), obtaining both positive and negative results in terms of hydrocarbon productivity. The hydrocarbons are housed into fractures (tectonics and cooling), and there is a relationship between the kind of fracture and the volcanic facies; therefore, it is very important to have a solid geological model for the exploration of hydrocarbons in this complex geological setting.

During the last year an integration of the information available was carried out in order to build a Predictive Geological model. Drill cores, side well cores, conventional logs, image logs from and seismic data from the Argentinean wells (Fig.1), were consolidated in one model with previous interpretations of the Chilenean wells (Covellone, 2016; Azpiroz et al., 2018; Atencio et al., 2018).

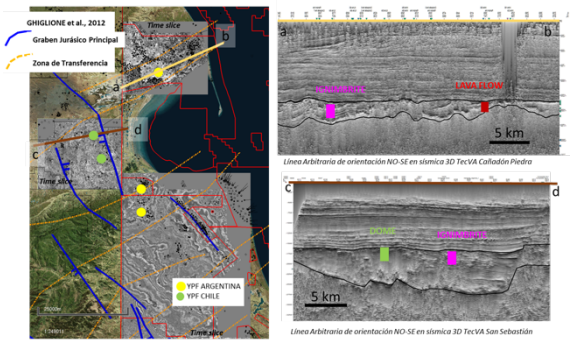

Fig. 3 – Left: Ghiglione et al. (2012) tectonic interpretation, different time slices comparing the Chilenean and Argentinean sides. Right: Arbitrary Seismic 3D line, the black lines represent the interpretation of top and base of Serie Tobífera. In pink color is the well with ignimbrite facies, in red the well with lava flow, and in green the rhyolitic dome.

The facies described in cores (Fig.2) are: i) lava flows, with and without hydrothermal alteration, ii) peperites and iii) block and ash deposits. The petrographic composition of these facies is andesitic to dacitic. From cutting analysis an ignimbrite facies (rhyolitic in composition from petrography) was recognized. On the chilenean side, YPF wells showed rhyolitic domes intruding on ignimbrite deposits (Azpiroz et al., 2018).

Over the interpretation of the available 2D and 3D seismic data, half-graben patterns were detected (Fig.3), coupled with a significant variation in Serie Tobífera thickness.

Through facies correlation using cuttings and cores and seismic interpretation, it was possible to observe that explosive volcanic sequences are located where the half-grabens show greater thicknesses, while effusive sequences tend to be located on the basement shoulders (Fig.3). The lava domes intrude ignimbrite deposits in central parts of halfgrabens, easily recognized in 3D Seismic in Tierra del Fuego Chilean side (Atencio et al., 2018).

Through the analysis of seismic information, it is possible to interpret that the deposition of volcanic rocks is contemporaneous with the formation of the rift (Fig.3). In this sense, our interpretations coincide with those of Navarrete and Márquez (2017) for the Macizo del Deseado, related with Serie Tobífera (Sruoga et al., 2004). In this way, these authors suggest the existence of a graben caldera bounded by extensional faults and involving a piece meal collapse.

In this paper we propose that there is a relationship between volcanic facies with the thickness of graben infill, coherent with a collapse caldera model, founding the ignimbrites facies in the thicker part of the grabens, while lava domes are close to the basement shoulders and extensive fault planes.

Acknowledgements

Authors are kindly thanked to YPF for the authorization of these publication.

References

Covellone, G., 2016; Informe Interno. YPF.

Azpiroz G., G. Covellone, K. Mykietiuk, L. Simonetto, M. Atencio, L. Tórtora, D. Ancheta, V. Meissinger and E. Pedro, 2018. Exploración del Play Serie Tobífera en el ámbito de Tierra del Fuego. Cuenca Austral. Argentina y Chile.X Conexplo 2018.; p-143.

Atencio M., F.G.E. Späth amd G. Azpiroz, 2018. Caracterización sísmica de reservorios complejos: Serie Tobífera. X Conexplo 2018; p-291.

Sruoga, P., N. Rubinstein and G. Hinterwimmer, 2004. Porosity and permeability in volcanic rocks: a case study on the Serie Tobífera, South Patagonia, Argentina. Journal of Volcanology and Geothermal Research 132 (2004), 31-43.,

Ghiglione C., A.T. Navarrete-Rodríguez, M. Gonzalez-Guillot and G. Bujalesky, 2012. The opening of the Magellan Strait and its geodynamic implications. Terra Nova, Vol 00, No.0, 1-8.

Navarrete, C. and M. Márquez, 2017. Caldera del Deseado: una graben caldera multiepisódica jurásica del sector nor-oriental del macizo del deseado. *XX Congreso Geológico Argentino,* 116-123.

The atypical igneous Petroleum System of the Cara Cura range, southern Mendoza province, Argentina

Palma, J. O.[1,2], Spacapan, J. B.[2], Rabbel, O.[3], Galland, O.[3], Ruiz, R.[1], and Leanza, H.[4]

[1] *Y-TEC – CONICET Av. Del Petróleo s/n, Entre 129 y 143, Berisso, Argentina* – octavio.palma@ypftecnologia.com
[2] *Y-TEC Av. Del Petróleo, Argentina s/n, Entre 129 y 143, Berisso, Argentina*
[3] *NJORD Centre, Department of Geosciences, University of Oslo, Norway*
[4] *MACN – CONICET, Museo Argentino de Ciencias Naturales, Av. Angel Gallardo 470, Buenos Aires (1405). Argentina.*

Keywords: *maturation*, *sills-reservoirs, migration*

Hydrocarbon occurrence in or around igneous rocks have been documented in several sedimentary basins worldwide (Schutter, 2003). These systems were defined as igneous petroleum systems by Delpíno and Bermudez (2009). The effects of igneous activity in sedimentary basin and petroleum systems has been reviewed by Senger et al (2017), and include (1) enhancement of source rock maturation, (2) productions of fractures and hydrothermal veins that can be migration pathways, and (3) the igneous rocks themselves could act as reservoirs or seals after cooling. Nevertheless, each of these effects have not been fully quantified. In this contribution, we will analyze a well-exposed outcrop analogue of an igneous petroleum system located in the Neuquén basin to asses how they can promote the maturation of the main source rocks (Vaca Muerta and Agrio formations), their properties as fractured reservoirs, and how associated hydrothermal veins can have major effects on fluid migrations.

The study area is the Cara Cura range, located in the southern part of the Río Grande Valley, southern Mendoza province, Argentina. It belongs to the northern part of the Neuquén basins and is part of the southern limit of the Malargüe Fold and Thrust Belt. In this area, 95% of the boreholes drill through igneous rocks, and 80% of the oil reservoirs are sills (Schiuma and Llambías et al., 2015). Here the igneous petroleum systems are well developed (Spacapan et al., 2018a and 2018b).

The Cara Cura range is formed by two asymmetrical basement anticlines associated with west-verging thrusts. The resulting uplift exposed all the sedimentary units of the Neuquén basin, in which several igneous intrusions are emplaced.

We performed a detailed geological mapping through an W-E transect across the Cara Cura range, sampling of the mains source rocks (Vaca Muerta and Agrio) for pyrolysis analysis and sampling of igneous intrusions and hydrothermal veins for petrographic descriptions. The observed intrusions consist of sills and some laccoliths. The sills are dominantly emplaced in the organic rich levels of Vaca Muerta and Agrio source rocks (Fig. 1 and 2), while laccoliths are emplaced in the continental sandstones of the Neuquén group. Also, a higher number of intrusions was found in the hanging wall than in the foot wall (Fig. 2). The 114 samples analyzed by pyrolysis show that maturation increases close to the intrusions, especially where sills occur in clusters (Fig. 1 and 2). This can be observed in a decrease in Hydrogen Index and S2 peak and an increase in the kerogen Transformation Ratio (TR). These parameters are the best to estimate the size of the thermal aureole. Total Organic Carbon show some increase in the contact with the intrusives, this is due the presence of bitumen in these zones (Fig. 3).

The fractures within sills are filled with bitumen, indicating that these reservoirs were charged (Fig. 3 A). Also, bitumen was identified in thin sections in the matrix of the intrusives, specially where plagioclase was dissolved. Raman spectroscopy confirm the presence of bitumen.

In the contacts with the source rocks, a highly fractured zone is developed, which we call the "damaged zone" (Fig. 3 B). Most of the fractures of this zones are filled with bitumen and carbonate. This zone increases the thickness of the sills fractured reservoirs. Damaged zones were also observed in the contacts of dykes with veins filled with calcite and bitumen (Fig. 3 C).

Hydrothermal veins were found in the contact with the intrusives and crosscutting upwards the stratigraphy. Some veins are filled with anhydrite or gypsums and afterwards intruded by bitumen. Other veins are filled with different cementation pulses, mainly of quartz and calcite cements, and sometimes bitumen. Some of the calcites show fluid inclusions with methane and bitumen indicating that hydrocarbon-bearing fluids migrates through these veins.

A Christmas tree laccolith or stock was found crosscutting upwards the Agrio formation in the hanging wall of the structure (Fig. 4). This intrusion promotes hydraulic connectivity between different unit, acting as a seal bypass system (Cartwright et al., 2006).

The main conclusions of this study are that igneous sills promote maturation of Vaca Muerta and Agrio, evidenced by the pyrolysis data and presence

of bitumen in the damaged zones and host rocks. This effect increases where clustering of sills occurs, specially in the hanging wall of the structure, where a higher number of intrusives were identified. The intrusions are fractured reservoirs with some matrix porosity. Hydrothermal veins are migration pathways which charge upper reservoirs. Finally dykes and discordant intrusives could act as seal bypass system promoting hydraulic connectivity between different units.

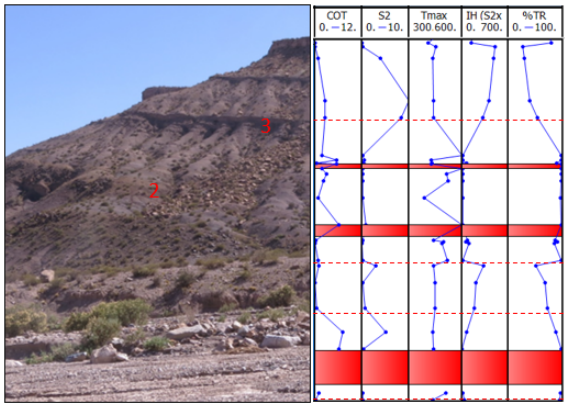

Fig. 1 – Transect through Vaca Muerta Fm. in the foot wall of the structure. Pyrolysis analysis show that IH and TR are the best parameters to identified thermal aureole (dashed red lines).

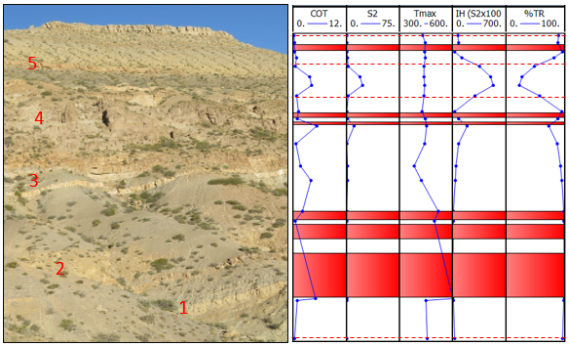

Fig. 2 – Transect through Vaca Muerta Fm. in the hanging wall of the structure. Pyrolysis analysis show that most of the thickness of Vaca Muerta has been transformed.

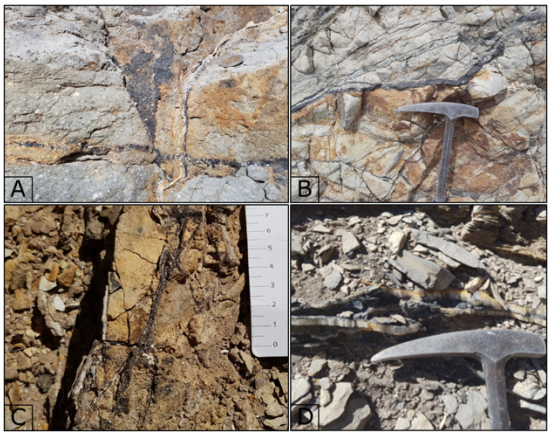

Fig. 3 – A. Sills with fractures filled with bitumen. B. Damaged zoned of a sill with high intensity of fractures filled with bitumen. C. Damaged zone of dike with veins filled with bitumen and calcite. D. Anhydrite vein, of possible hydrothermal origin, intruded by bitumen.

Fig. 4 – Christmas tree laccolith emplaced in Agrio Fm. in the hanging wall of the structure.

Acknowledgements

This project was part of the DIPs project of the University of Oslo, funded by Research Council of Norway. Pyrolysis analysis, Raman spectroscopy and thin sections where performed by Y-TEC Geochemistry and Geology labs.

References

Cartwright, J., Huuse, M., & Aplin, A, 2007, "Seal bypass systems", *AAPG Bulletin, 91, p. 1141–1166.*

Delpino, D. H., y Bermúdez, A. M., 2009, "Petroleum systems including unconventional reservoirs in intrusive igneous rocks (sills and laccoliths)", *The Leading Edge 28, p. 804-811.*

Senger, K., Millett, J., Planke, S., Ogata, K., Eide, C.H., Festøy, M., Galland, O., Jerram, D.A., 2017, "Effects of igneous intrusions on the petroleum system: a review", *First Break, 35(6), p. 47-56.*

Schiuma, M. and Llambías, E., 2014, "Importancia de los sills como reservorios en la Cuenca Neuquina del sur de Mendoza", *9° Congreso de Exploración y Desarrollo de Hidrocarburos, Trabajos técnicos, Tomo 1, p. 331-349, Mendoza.*

Schutter, S.R, 2003, "Occurrences of hydrocarbons in and around igneous rocks", *In: N. Petford, and K. McCaffrey (Eds.), Hydrocarbons in crystalline rocks. Geological Society, London, Special Publications 214, p. 7-33.*

Spacapan, J., Palma, O., Galland, O., Manceda, R., Rocha, E., D'Odorico, A., & Leanza, H, 2018a, "Thermal impact of igneous sill-complexes on organic-rich formations and implications for petroleum systems: A case study in the northern Neuquén Basin, Argentina", *Marine and Petroleum Geology, 91, p. 519–531.*

Spacapan, J. B., Palma, J. O., Rocha, E., Leanza, H. A., D´odorico2, A. Rojas Vera, E., Manceda, R., Galland, O., Medialdea, A. and Cattaneo, D. M., 2018b, "Maduración de las Formaciones Vaca Muerta y Agrio ocasionado por el emplazamiento de un complejo intrusivo magmático en el sector sur mendocino de la Cuenca Neuquina", *Revista de la Asociación Geológica Argentina 75 (2), p. 199-209.*

An Exploratory History of Igneous Reservoirs in the Rio Grande Valley, Malargüe, Argentina

Rébori L.[1], Rapela C.[2], Fantín J.[3] and Medialdea A.[4]

[1] *Searcher Seismic, Argentina* – l.rebori@searcherseismic.com
[2] *CIG-UNLP, Diagonal 113 No. 275, La Plata, Buenos Aires -Argentina*
[3] *YPF , Av. España 955, Capital. Mendoza, Argentina*
[4] *YPF , Jorge Newbery s/n., Malargüe, Mendoza - Argentina*

Keywords: andesite, oil, wells.

The association of igneous rocks with oil seeps has been identified in Argentina since early Spanish colonial times (Yrigoyen, 2007), in the Mendoza province sector of the Neuquén Basin: "Cerro Alquitrán (Mina Los Buitres)" and "Cerro La Brea (Arroyo Las Aucas area)" in San Rafael county and "Cerro Bayo de los Coyihuales (near the Zampal) and "Mina Theys" in Malargüe county.

Also, the teams of YPF - Field Geological Commissions described the potential of the igneous rocks of the El Molle Fm in the Rio Grande Valley as unconventional reservoirs as early as the 1970s, (Bettini – Vasquez, 1978/79).

Although by the late 1970's there was already a history of wells with productive levels of igneous rocks (El Manzano x-1; The Volcanoes is-1), the discovery of unconventional igneous reservoirs in the Rio Grande Valley did not occur until 1980 with the discovery of the Rio Grande field. The well proposal, led by Fernando Bettini, was made based on 2D seismic data and the location of the exploratory wells were based on a structural high, which turned out to be an andesite laccolith. The 2D seismic data quality of the time was insufficient to image and differentiate these igneous bodies.

At that time, a specific operational methodology was developed by the Well Site geologists of the Mendoza Geological Exploration Department of YPF to evaluate these unique reservoirs. Specific mud logging control procedures were developed to ensure consistency both within the company and when the service was outsourced.

While drilling, special attention was paid to the observation of cuttings, bit rate penetration, total gas detection, core samples, drill stem tests and log analysis.

a) **Observation of drilling cuttings** were made using a binocular magnifying glass (10 to 40 X), In addition to recognizing the lithology, the emphasis was oriented to the presence of oil and the appearance of singular details such as vugs, fissures and filling minerals like calcite. The methodology was published early in the work of (García et al, 1982) and form part of this work.

b) Bit rate of penetration was used to identify indications of fractured areas.

c)Total Gas continuous detection was monitored, and it was found that no significant changes were ever observed between the reservoir and the country rock (shales of the Agrio and Vaca Muerta formations). In fact, often the background value of the shales was higher than in the sills, Fig.1.

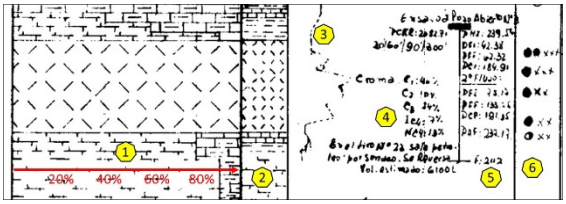

Fig. 1 – Strip-log of one of the discoverer well, showing percentage (1) and interpreted lithology (2), Total Gas (3) curve; chromatographic data (4), data from DST (5) and oil shows (6).

d) Core Samples played a very important role from both a qualitative and quantitative point of view. Cores were used for calibration of the petrophysical evaluation, and for detailed evaluation of the reservoir properties and nature of the porosity and permeability. The presence of pores and micropores (Fig. 2) was analyzed, with many of them found to be filled by biotite (García et al (op cit)).

e) Drill Stem Tests (DSTs) were essential in determining the fundamental characteristics of the reservoir, including the flow rates, formation pressures and fluids contained. DSTs were also a fundamental tool used for the selection of the stimulation method.

Thus, empirically three (3) types of responses were determined:

1) Good flow rates and high closing pressures, corresponding to wells that were naturally flowing. This happened with bodies intruding the Agrio Fm.

2) Regular to poor flow rates with high pressures of rapid recovery. In these cases, it was determined the need to stimulate the well, acidifying first and then performing a hydraulic fracturing operation with sand proppant. This was the case of

the intrusives of the Vaca Muerta Fm in the Los Cavaos field.

3) Low flow rates and low pressures. These levels were determined to be unproductive (García et al (op cit)).

f) Quicklook Log Analysis was performed, and the unique response of the different logs was verified when crossing the intrusive bodies. Low GR values indicated basic composition, high resistivity was observed in the igneous bodies and the inverse, high conductivity was observed in the contacts, due to the presence of sulfide minerals. It was also proven that these intrusive bodies would not erode any part of the sedimentary column, but rather they exert an effect similar to that of a hydraulic device. This effect is discussed in more detail in García et al (op cit).

Shortly after the core were obtained, they were sampled as well as several outcrops to try to define the rocks petrographically and to understand the mechanisms of emplacement. A total of 69 rock samples were taken, 37 from 10 wells and the rest (32) from 17 outcrops (Fig. 2.) These samples were sent to the Exploration Laboratory of YPF in Florencio Varela (province of Buenos Aires). Then these samples were delivered to the Faculty of Natural Sciences and Museum of the National University of La Plata. There Dr. Carlos W. Rapela and his team studied them and created a report, which is still unpublished.

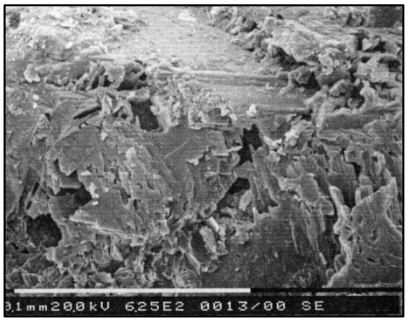

Fig. 2 - SEM Image showing micro and cryptpores with poor connections, “Los Volcanes” field.

There were six main rock types recognized petrographically (Rapela, 1982). They were as follows;

a) Augitic andesites.
b) Andesitic porphyries and hornblendic - augitic andesites.
c) Polymaphytic andesites and basalts.
d) Hypersthenic andesites
e) Leucoandelacites.
f) Olivinic basalts.

The most important conclusions were that the samples of wells corresponding to Río Grande, Loma Atravesada, Los Volcanes, Buta Relvún, Cerro Divisadero, and Sierra Azul Sur, are characterized as being andesites and occasional basalts with augite, hornblende, biotite and altered olivine, which allows characterization of these rocks as belonging to the same igneous event.

No obvious correlation is observed between well samples and outcrop samples, the only similarities observed were between the samples of Agua Botada wells and Bayo de la Batra outcrops, composed of andesite and augitytic-hornblendic porphyries, and surface samples of Cerro Tronquimalal of equal composition.

Fig. 3 – –Augitic Andesite from “Barda de Chachao”.

A unique occurrence is observed in the lime mudstone of the Sierra Azul well, which corresponds to a sparite with prehnite rosettes (confirmed by X-ray diffraction) and as sulfide has been recognized as pyrrhotite possibly linked to hydrothermal activity produced by layer filons housed in limestones.

Geochemical studies of the oils that produced the fields of the Rio Grande Valley were also initiated during 1982, almost simultaneously with the geological characterization of the intrusive reservoirs as described above.

Acknowledgements

With special thanks to YPF for allowing the publication of this paper.

References

Bettini, F. -Vasquez, J. (1978 / 79), Geología de la Sierra Azul-Río Grande, Sector Occidental de la Sierra de Palauco. Distrito Geológico Mendoza YPF. Unpublished.

Garcia C.; Brocca H. Martínez R.; Arturi S.; Ferrante R. and Rébori L. (1982), Importancia de la Rocas Ígneas Intrusivas como Reservorio de Hidrocarburos en la Cuenca Neuquina Sur Mendocina, in 1er. Congreso Nacional de Hidrocarburos; Bs.As, pp. 97-114.

Yrigoyen M.R. (2007) Reseña sobre los conocimientos y la explotación de los hidrocarburos en Argentina antes de 1907, in Petrotecnia, febrero/2007, pp. 16-36.

Rapela C.W: (1982). Informe Petrográfico de las Vulcanitas de la Cuenca Neuquina-Mendocina. Facultad de Ciencias Naturales y Museo de la Universidad Nacional de La Plata. Unpublished.

Presence of hydrocarbon traces in igneous rock-forming minerals from the Colipilli area, central-western sector, Neuquén Basin, Argentina

Salvioli M.A.[1, 2], Lajoinie M.F.[1, 3] Lanfranchini M.E.[1, 4] de la Cal H.G.[5] and Cesaretti N.N.[6]

[1] *Instituto de Recursos Minerales, Facultad de Ciencias Naturales y Museo, Universidad Nacional de La Plata (INREMI-FCNyM-UNLP), Calle 64 N° 3, CP1900, La Plata, Argentina.* Email address: *melisa_salvioli@hotmail.com.ar*

[2] *Consejo Nacional de Investigaciones Científicas y Técnicas (CONICET), Godoy Cruz N°2290, Buenos Aires, Argentina*

[3] *LEMaC, Centro de Investigaciones Viales. Universidad Tecnológica Nacional-Facultad Regional La Plata. Av. 60 y 124, Berisso, Argentina.*

[4] *Comisión de Investigaciones Científicas de La Provincia de Buenos Aires (CICPBA), Calle 532 e/ 10 y 11, La Plata, Argentina*

[5] *ROCH S.A., Avenida Madero 1020, Piso 21, Buenos Aires, Argentina*

[6] *Departamento de Geología, Universidad Nacional del Sur (UNS), San Juan 670, 2° piso, C.P. 8000, Bahía Blanca, Argentina*

Keywords: fluid inclusions, andesites, atypical petroleum system.

The Neuquén Basin, one of the most important hydrocarbon producing basins of Argentina, records an important tectono-magmatic activity mainly in the central-western region, between the Late Mesozoic and Early Cenozoic. In the Colipilli-Naunauco area, magmatic activity is represented by intrusive (Colipilli Fm., Llambías and Rapela, 1989) and extrusive facies (Cayanta Fm., Rapela and Llambías, 1985), both gathered in the Naunauco Group (Zamora Valcarce et al., 2006). This research deals with the identification and characterization of hydrocarbon traces, trapped along with aqueous fluids, into fluid inclusions (FI) hosted in plagioclase and amphibole phenocrysts of the Colipilli Fm. intrusive bodies that crop out in the area.

The rocks and FI studies were performed in a petro-calcographic microscope Nikon Optiphot-POL in the INREMI-UNLP. The fluorescence technique with incident UV light, was carried out in the Laboratorio de Luminiscencia, UNS-Bahía Blanca, in a Nikon Eclipse 50iPOL microscope, working with halogen mercury lamp (100W).

The studied intrusive bodies are andesitic sills (Salvioli, 2017). These rocks have a microporphyritic texture with a holocrystalline mesostasis and, in some sectors, with glomeroporphyritic plagioclase arrangements. Plagioclase (55-60% of the phenocrysts) has andesine to labradorite composition (An46-66), tabular habit, polysynthetic twin and a marked zonation. Some crystals are partially fractured and replaced by sericite and calcite. Hornblende crystals (35-40% of the phenocrysts) show prismatic habit, green to brown pleochroism and are partially replaced by chlorite, biotite and tremolite-actinolite. Also, some crystals show diffuse contours due to the segregation of opaque minerals. The mesostasis is constituted by plagioclase, amphibole, martitized magnetite and scarce limonitized pyrite.

The detailed petrography of FI identified in the plagioclase and amphibole phenocrysts allowed two types of two-phase L+B (liquid + bubble) FI to be recognized: colourless with bright clear liquid which predominates in volumetric proportion over a small vapour or gas bubble, two-phase FI with brown and/or black colours vapour phase and low liquid-vapour proportion. The first ones show high relief, sizes of 15µm on average and tabular shapes while, the second ones are 50µm in size and have low refractive index and ovoid shapes. According to its genesis, the FI, recognized in amphibole phenocrysts are mainly primary with isolated distribution while in plagioclase phenocrysts, are primary and pseudo-secondary, associated to crystalline growth planes (Fig.1a).

In order to identify hydrocarbons into FI, a fluorescence technique with UV light was used, which allowed FI to be separated in two sets, according to its behaviour: a non-fluorescent group which includes two-phase L+B colourless FI and, a fluorescent set, greenish-yellow in tones, composed of two-phase L+B brown and/or black FI. In this sense, the first set point out an aqueous composition; while the second one reveals the presence of organic phases. It is noticeable that, the fluorescence was identified in the vapour phase (Fig.1b).

Although the FI analysis became an important study tool for the petroleum system (Cesaretti et al., 2000; González Sánchez et al., 2009) during the last years, there are few contributions focused on explaining the evolution of magmatism and its relationship with hydrocarbons or focused on estimating the possible migration pathways within a sedimentary basin. On the Colipilli-Naunauco area, the study of primary and pseudo-secondary FI hosted

in plagioclase and amphibole phenocrysts from igneous rocks, allowed the presence of liquid hydrocarbon to be determined, given by the greenish-yellow fluorescence under UV light (Riecker, 1962).

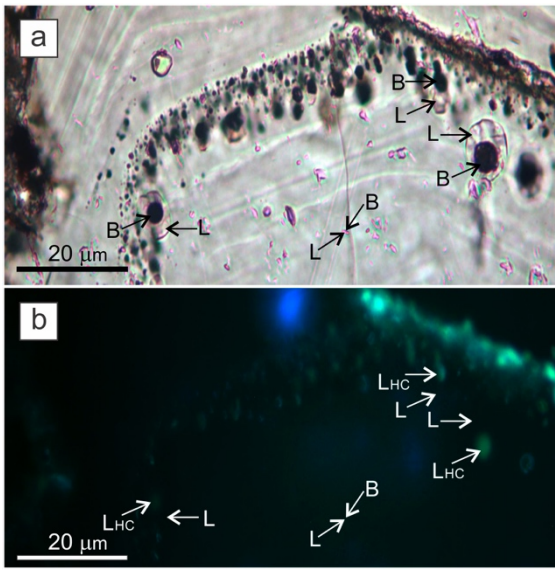

Fig. 1. Two-phase FI, L + B in plagioclase. a) Transmitted light, b) UV light. Fluorescence colours of (B) phases are greenish-yellow. B: bubble, L: liquid, V_{HC}: hydrocarbon vapour (gas).

The petroleum systems that generate hydrocarbons by different processes than maturation by burial are called "atypical" (Maggon and Dow, 1994). This is the case of systems affected by intrusive bodies where the fractured igneous rocks are potential reservoir rocks (Schiuma et al., 2002; Barrionuevo, 2015). During or after igneous rocks emplacement, these ones can interact with the contact rocks while cooling, which becomes of particular interest when the intruded rocks are sedimentary. When sedimentary rocks contain organic matter, a heat addition can transform it, causing its maturation and possible hydrocarbon fluids generation. On the other hand, if the rocks contain previous organic fluid, this one can interact with the igneous rocks during the cooling processes and it can be trapped into the igneous rock. In both cases, igneous rock-organic fluid interaction will be registered as FI inside its constituent minerals.

Several authors (Bodnar, 1990; Stasiuk and Snowdon, 1997) have correlated the fluorescence colour with the API gravimetric coefficient. Based on the greenish-yellow fluorescence colour, the hydrocarbon would present low API values typical of immature hydrocarbon fluids (heavy). In this sense, the emplacement of the igneous rocks from the Colipilli-Naunauco area would have provided the necessary heat to the sedimentary rocks to transform the present organic matter or to generate the circulation of pre-existing organic fluids in the system. At the same time, the phenocrysts of the igneous rocks continued growing and recording the nature of the fluids with which they interacted during their cooling.

FI studies together with fluorescence technique proved to be an important tool to analyse and understand the emplacement processes and its relationship with the crystallization of igneous rock minerals. This type of research also provides a new method for complementary prospecting of atypical petroleum systems associated with intrusive bodies throughout the Neuquén Basin.

Acknowledgements

UNLP and SEG (USA) provided financial support. We thank the institutional support of UNS.

References

Barrionuevo, M.F (2015), Las rocas volcánicas del Grupo Choyoi como reservorio de hidrocarburos. Yacimiento 25 de mayo-Medanito S.E., Cca. Neuquina, Argentina. *Tesis Doctoral,* UNSa. 212 p.

Bodnar, R.J (1990), Petroleum migration in the Miocene Monterey Formation, CA, USA: constraints from FI studies. *Mineralogical Magazine*, 54: 295-304.

Cesaretti, N.N., J. Parnell and E.A. Domínguez (2000), Pore fluid evolution within a hydrocarbon reservoir: Yacoraite Formation (Upper Cretaceous), North west Basin, Argentina. *J. of Petroleum Geol.* 23: 375-398.

González-Sánchez, F., A. Camprubí, E. González-Partida, R. Puente-Solís, C. Canet, E. Centeno-García and V. Atudorei (2009), Regional stratigraphy and distribution of epigenetic stratabound celestine, fluorite, barite and Pb-Zn deposits in the MVT province of northeastern Mexico.*Min.Dep.*44:343-361.

Llambías, E.J. and C.W. Rapela (1989), Las volcanitas de Colipilli, Neuquén (37°S) y su relación con otras unidades paleóg. de la cordillera. *RAGA* 44: 224-236.

Magoon, L.B. and W.G. Dow (1994), The petroleum system. In Magoon and Dow (eds.) *The Petroleum System from Source to Trap*. AAPG, Memoir 60:3-24.

Rapela, C.W. and E.J. Llambías (1985), La secuencia andesítica terciaria de Andacollo, Neuquén, Argentina. *IV Congreso Geológico Chileno*, 4: 458-488.

Riecker, R.E (1962), Hydrocarbon fluorescence and migration of petroleum. *AAPG*, Bulletin 46: 60-75.

Salvioli, M.A (2017), Geología y génesis de los depósitos barítico-polimetálicos (Ba-Fe-Pb-Cu-Zn-Mn) del área de Colipilli, sector centro-occidental de la Cca. Neuquina. *Tesis Doctoral*, UNLP, 298p.

Schiuma, M., G. Hinterwimmer and G. Vergani (2002), Rocas Reservorio de las Cuencas Productivas de la Argentina. *Simposio del V CONEXPLO*. 788 p.

Stasiuk, L.D. and L.R. Snowdon (1997), Fluorescence micro-spectrometry of synthetic and natural hydrocarbon FI: crude oil chemistry, density and application to petroleum migration. *A.G.*12: 229-241.

Zamora Valcarce, G., T.R. Zapata, D. del Pino and A. Ansa (2006), Structural evolution and magmatic characteristics of the Agrio fold-and-thrust belt. In Kay and Ramos (Eds.) *J. Geol. Soc.* 497: 125-145.